



Durham E-Theses

Synthetic, Reactivity and Structural Studies of Pyridyl-N-Phosphinoimines

ALDRED, JOANNA,KRYSTYNA,DOWLING

How to cite:

ALDRED, JOANNA,KRYSTYNA,DOWLING (2017) *Synthetic, Reactivity and Structural Studies of Pyridyl-N-Phosphinoimines*, Durham theses, Durham University. Available at Durham E-Theses Online: <http://etheses.dur.ac.uk/12148/>

Use policy

The full-text may be used and/or reproduced, and given to third parties in any format or medium, without prior permission or charge, for personal research or study, educational, or not-for-profit purposes provided that:

- a full bibliographic reference is made to the original source
- a [link](#) is made to the metadata record in Durham E-Theses
- the full-text is not changed in any way

The full-text must not be sold in any format or medium without the formal permission of the copyright holders.

Please consult the [full Durham E-Theses policy](#) for further details.

Academic Support Office, Durham University, University Office, Old Elvet, Durham DH1 3HP
e-mail: e-theses.admin@dur.ac.uk Tel: +44 0191 334 6107
<http://etheses.dur.ac.uk>

**Synthetic, Reactivity and Structural
Studies of Pyridyl-*N*-
Phosphinoimines**



**Durham
University**

Department of Chemistry, Durham, United Kingdom

Joanna Krystyna Dowling Aldred (née Prentis)

April 2017

*Thesis submitted to Durham University in application for the
degree of Doctor of Philosophy*

Statement

This thesis is based on work conducted by the author, in the Department of Chemistry at Durham University, during the period January 2014 to April 2017.

All the work described in this thesis is original, unless otherwise acknowledged in the text or in the references. None of this work has been submitted for another degree in this or any other University.

Signed: _____

Date: _____

Joanna Krystyna Dowling Aldred (née Prentis)

This thesis is dedicated firstly to my father, Dr Roger Prentis. Your enthusiasm and inquisitiveness did, without a doubt, inspire my decision to pursue the sciences.

Secondly, this thesis is dedicated to my grandfather, Mr Derek Prentis, without whose unfailing support, my studies over the years would not have been possible.

Table of Contents

Statement	ii
Table of Contents.....	iv
Abstract.....	xiv
Acknowledgements.....	xv
Abbreviations.....	xvii
General Abbreviations	xvii
NMR Spectroscopy Abbreviations	xix
Chapter 1 – Introduction	2
1.1 – Interconverting Pyridyl- <i>N</i> -phosphinoimine–Diazaphosphazole Tautomers	2
1.2 – Non-Innocent Ligands (NILs)	4
1.2.1 – i) Redox NILs Acting as Electron Reservoirs	5
1.6.1 – ii) Redox NILs used to Alter the Lewis Acid/Base Properties of a Metal Centre ...	6
1.2.3 – iii) NIL Inducing Radical-Type Reactivity on Substrate-Ligand Complex.....	7
1.2.4 – iv) NILs Facilitating Substrate Bond Breakage/Formation	9
1.3 – Structural Components of the Pyridyl- <i>N</i> -Phosphinoimine – Diazaphosphazole Tautomeric Pairs	10
1.4 – Pyridine	10
1.4.1 – Structure and Properties of Pyridine	10
1.4.2 – Chemical Reactivity of Pyridine	11
1.4.2.1 – Pyridine as a Base.....	13
1.4.2.2 – Electrophilic Reactions of Pyridine	14
1.4.2.3 – Nucleophilic Reactions of Pyridine	15
1.4.2.4 – Pyridine Complexes.....	16
1.4.2.5 – Reaction of Pyridine with Organometallics	16
1.5 – Phosphines	17

1.5.1 – Quantifying the Steric Properties of Phosphines.....	19
1.5.2 – Quantifying the Electronic Properties of Phosphines.....	19
1.5.3 – Aminophosphines	20
1.6 – Nitrogen- and Phosphorus-containing Bidentate Ligands.....	22
1.6.1 – Trans Effect for <i>P,N</i> -Ligands.....	22
1.6.2 – Hemilability of <i>P,N</i> -Ligands	23
1.6.3 – Coordination Behaviour of <i>P,N</i> -Ligands.....	24
1.6.4 – Iminophosphoranes	26
1.6.4.1 – Rearrangements of Iminophosphoranes	27
1.6.4.2 – Cycloaddition Reactions of Iminophosphoranes	28
1.6.4.3 – Coordination Behaviour of Iminophosphoranes	29
1.7 – Investigations into the Interconverting Pyridyl- <i>N</i> -Phosphinoimine – Diazaphosphazole Tautomers.....	30
1.7.1 – Factors Affecting the Position of the “Open”-“Closed” Equilibrium of the Pyridyl- <i>N</i> -Phosphinoimines.....	30
1.7.1.1 – Effect of Temperature on the “Open” and “Closed” Tautomers.....	31
1.7.1.2 – Stereoelectronic Impact of the Phosphorus Substituent Upon the “Open”-“Closed” Equilibrium Position	31
1.7.1.3 – Stereoelectronic Impact of the Pyridine Substituents Upon the “Open”-“Closed” Equilibrium Position	33
1.7.1.4 – Stereoelectronic Impact of the Imine Substituent Upon the “Open”-“Closed” Equilibrium Position	34
1.7.2 – Reactions of the Pyridyl- <i>N</i> -Phosphinoimines with Small Molecules.....	35
1.7.2.1 – Reaction of the Pyridyl- <i>N</i> -Phosphinoimines with Selenium.....	35
1.7.2.2 – Reactions of the Pyridyl- <i>N</i> -Phosphinoimines with Dimethyl Acetylenedicarboxylate (DMAD)	36
1.7.2.3 – Reaction of the Pyridyl- <i>N</i> -Phosphinoimines with $[\{\text{RhCl}(\text{CO})_2\}_2]$	38

1.7.2.4 – Reaction of the Pyridyl- <i>N</i> -Phosphinoimines with AlMe ₃	38
1.7.2.5 – Reaction of Iminophosphorane A with bis(Diisopropylamino)Phosphenium Triflate	39
1.7.3 – Non-Innocent Ligand Behaviour of Pyridyl- <i>N</i> -Phosphinoimines	42
1.8 – Frustrated Lewis Pairs	45
1.8.1 – Reactivity of FLPs	47
1.8.1.1 – Activation of Dihydrogen	47
1.8.1.2 – Activation of Alkenes and Alkynes	48
1.8.1.3 – Activation of Greenhouse Gases	49
1.8.1.4 – Heterolytic CH, NH and CF Activation	50
1.9 – Aims	51
Chapter 1 References	52
Chapter 2 – Pyridyl- <i>N</i> -Phosphinoimine – Diazaphosphazole Valence Tautomerism: Equilibrium Studies	60
2.1 – Introduction	60
2.1.1 – Preparation of Novel Pyridyl- <i>N</i> -Phosphinoimine – Diazaphosphazole Tautomeric Pairs	61
2.2 – Impact of Temperature upon “Open” : “Closed” Equilibrium Position	62
2.3 – Impact of Solvent Polarity Upon “Open” : “Closed” Equilibrium Position	65
2.4 – Effect of Modifying the Pyridine Scaffold upon the Pyridyl- <i>N</i> -Phosphinoimine- Diazaphosphazole Tautomeric Equilibrium Position	67
2.4.1 – Substitution at the 4-Position on the Pyridyl- <i>N</i> -Phosphinoimine Pyridine Ring .	68
2.4.1.1 – Synthesis and Characterisation N,N,N',N'-tetraisopropyl-1-((phenyl(4- phenylpyridin-2-yl)methylene)amino)phosphanediamine (1-Open) / N,N,N',N'- tetraisopropyl-3,5-diphenyl-1H-[1,3,2]diazaphospholo[1,5-a]pyridine-1,1-diamine (1- Closed)	69

2.4.1.2 – Attempted Synthesis of N,N,N',N'-tetraisopropyl-1-((phenyl(4-methylpyridine-2-yl)methylene)amino)phosphanediamine (3-Open)	73
2.4.1.3 – Synthesis and Characterisation of N,N,N',N'-tetraisopropyl-1-((phenyl(4-tbutylpyridin-2-yl)methylene)amino)phosphanediamine (4-Open)/ 4-Closed	75
2.4.1.4 – Synthesis and Characterisation of N,N,N',N'-tetraisopropyl-1-((phenyl(4-dimethylamino-2-yl)methylene)amino)phosphanediamine (5-Open) / (5-Closed)	78
2.4.2 – Substitution of Methyl Groups at the 3- and 5-Positions on the Pyridine Ring of the Pyridyl- <i>N</i> -Phosphinoimine	81
2.4.2.1 – Synthesis and Analysis of N,N,N',N'-tetraisopropyl-1-((phenyl(3,5-dimethylpyridin-2-yl)methylene)amino)phosphanediamine (6-Open) / (6-Closed) ...	81
2.4.2.2 – Attempted Synthesis of N,N,N',N'-tetraisopropyl-1-((phenyl(5-methylpyridin-2-yl)methylene)amino)phosphanediamine (7-Open) / (7-Closed)	83
2.5 – Effect of Modifying the Imine Carbon Substituent upon the Pyridyl- <i>N</i> -Phosphinoimine-Diazaphosphazole Tautomeric Equilibrium Position	84
2.5.1 – Introduction of Aryl Imine Substituents at the Imine Carbon of the “ <i>Open</i> ” Tautomer	84
2.5.1.1 – X-Ray Crystallographic Study of 3-(biphenyl)-N,N,N',N'-tetraisopropyl-115-[1,3,2]diazaphospholo[1,5-a]pyridine-1,1-diamine (2-Closed)	86
2.5.1.2 – Electronic Differences between Imine Substituents on the “ <i>Open</i> ” Tautomers	88
2.5.1.3 – Differences in Steric Bulk Between Imine Substituents on the “ <i>Open</i> ” Tautomers	91
2.5.2 – Attempted Installation of Alkyl Substituents at the Imine Carbon of the Pyridyl- <i>N</i> -Phosphinoimine “ <i>Open</i> ” Tautomer	93
2.5.2.1 – Use of Organolithium reagents: Synthetic Routes 1, 2 and 3	94
2.5.2.2 – Grignard reagents: Synthetic Route 4	98
2.5.2.3 – Ketone-Amine Condensation: Synthetic Route 5	100
2.6 – Summary	101

2.7 – Chapter 2 Experimental Details	103
2.7.1 – Synthesis of bis(Diisopropylamino) chlorophosphine	103
2.7.2 – Synthesis of N,N,N',N'-tetrakisopropyl-1-((phenyl(pyridin-2-yl)methylene)amino)phosphanediamine (A-Open)/ N,N,N',N'-tetrakisopropyl-3-phenyl-115-[1,3,2]diazaphospholo[1,5-a]pyridine-1,1-diamine (A-Closed)	103
2.7.2.1 – Preparation of Compound A Using PhLi	104
2.7.2.2 – Preparation of Compound A Using PhMgBr	104
2.7.2.3 – Attempt to Prepare Compound A from (<i>i</i> Pr ₂ N) ₂ P(NH ₂) and 2-benzoylpyridine.....	105
2.7.3 – Synthesis of bis(Diisopropylamino)(anthracenyl)phosphine Monoselenide.....	106
2.7.4 – Synthesis of N,N,N',N'-tetrakisopropyl-1-((phenyl(4-phenylpyridin-2-yl)methylene)amino)phosphanediamine (1-Open)/ N,N,N',N'-tetrakisopropyl-3,5-diphenyl-115-[1,3,2]diazaphospholo[1,5-a]pyridine-1,1-diamine (1-Closed)	108
2.7.5 – Synthesis of N,N,N',N'-tetrakisopropyl-1-((biphenyl(pyridin-2-yl)methylene)amino)phosphanediamine (2-Open) / 3-(biphenyl)-N,N,N',N'-tetrakisopropyl-115-[1,3,2]diazaphospholo[1,5-a]pyridine-1,1-diamine (2-Closed)	109
2.7.5.1 – Synthesis of 4-biphenyl-bis(Diisopropylamino)phosphine Monoselenide.	110
2.7.6 – Attempted synthesis of N,N,N',N'-tetrakisopropyl-1-((phenyl(4-methyl pyridine-2-yl)methylene)amino)phosphanediamine (3-Open)	111
2.7.7 – Synthesis of N,N,N',N'-tetrakisopropyl-1-((phenyl(4-tbutylpyridin-2-yl)methylene)amino)phosphanediamine (4-Open) / (4-Closed)	112
2.7.8 – Synthesis of N,N,N',N'-tetrakisopropyl-1-((phenyl(4-dimethylamino-2-yl)methylene)amino)phosphanediamine (5-Open) / (5-Closed)	115
2.7.9 – Synthesis of N,N,N',N'-tetrakisopropyl-1-((phenyl(3,5-dimethylpyridin-2-yl)methylene)amino)phosphanediamine (6-Open) / (6-Closed)	117
2.7.10 – Attempted Synthesis of N,N,N',N'-tetrakisopropyl-1-((phenyl(5-methylpyridin-2-yl)methylene)amino)phosphanediamine (7-Open) / (7-Closed)	118

2.7.11 – Synthesis of N,N,N',N'-tetraisopropyl-1-((mesityl(pyridin-2-yl)methylene) amino)phosphanediamine (8-Open) / (8-Closed).....	118
2.7.11.1 – Synthesis of bis(Diisopropylamino)(mesityl)phosphine Selenide.....	119
2.7.12 – Attempted Synthesis of Target Compounds 9 , 10 and 11	121
2.7.12.1 – Attempted Preparation of 9 , 10 and 11 Using Alkylolithium Reagents.....	121
2.7.12.2 – Attempted Preparation of 9 Using LiHDMS.....	122
2.7.12.3 – Attempt to Prepare 9 Using a Grignard Reagent.....	123
Chapter 2 References.....	124
Chapter 3 – Synthesis of a Novel Macrocyclic Pyridyl- <i>N</i> -Phosphinoimine and Intramolecularly Base-Stabilised Phosphenium Salt	128
3.1 – Introduction	128
3.2 – Attempted Preparation of Target Compound Dichlorophosphino-1-((phenyl(6-methyl-pyridin-2-yl)methylene)amino) amine (11-Open) / (11-Closed).....	130
3.2.1 – Structural Elucidation of Products 12 and 13	132
3.2.1.1 – X-Ray Crystallographic Study of Compound 12	132
3.2.1.2 – Computational and Experimental Studies to Identify Compound 13	138
3.2.2 – Proposed Mechanism for the Formation of Compounds 12 and 13	141
3.3 – Probing the Chemical Reactivity of Compounds 12 and 13	143
3.3.1 – Investigating the Lability of the P-Cl Bonds in Compounds 12 and 13	143
3.3.1.1 – Attempted Anion Exchange Reactions of Compound 12	143
3.3.1.2 – Attempted Anion Exchange Reactions of Compound 13	145
3.3.2 – Investigating the ease of Phosphorus(III) Oxidation in Compounds 12 and 13	146
3.3.2.1 – Oxidation of Compounds 12 and 13 by Elemental Se	147
3.3.2.2 – Oxidation of Compounds 12 and 13 by DMF.....	148
3.3.3 – Investigating the Coordination of B(C ₆ F ₅) ₃ to Compounds 12 and 13	152
3.4 – Probing the Coordination of Novel Compounds 12 and 13 to Platinum Centres	154

3.5 – Attempted Preparation of Dichlorophosphino-1-((phenyl(pyridin-2-yl)methylene)amino) amine (18-Open) / (18-Closed)	158
3.6 – Probing the Product(s) of the Reactions Between 2-Cyanopyridine/6-Methyl-2-Cyanopyridine, PhLi and PCl ₅	160
3.7 – Summary	163
3.8 – Chapter 3 Experimental Details	167
3.8.1 – Synthesis of Novel Macrocyclic Compound 12 and Novel Phosphenium Salt 13	167
3.8.2 – Attempted Anion Exchange Reactions of Compounds 12 and 13	168
3.8.3 – Synthesis of the Diselenide Derivative of Compound 12 , 12=Se	169
3.8.4 – Attempted Synthesis of the Mono-Selenide Derivative of Compound 13	169
3.8.5 – Synthesis of the Proposed Product, 14 , from the Reaction of 12 with DMF	170
3.8.6 – Synthesis of the Oxidation Products, 15a and 15b , from the Reaction Between 13 and DMF	170
3.8.7 – Synthesis of the Proposed Adduct from the reaction between B(C ₆ F ₅) ₃ and Compound 12 , 12-B(C₆F₅)₃	171
3.8.8 – Attempted Reaction between Compound 13 and B(C ₆ F ₅) ₃	172
3.8.9 – Attempted Coordination of Compounds 12 and 13 to <i>cis</i> -[PtCl ₂ (PPh ₃) ₂]	172
3.8.10 – Synthesis of <i>cis</i> -[PtCl ₂ (PPh ₂ Me) ₂] and Proposed Complex <i>cis</i> -[PtCl ₂ (12)] (Compound 16) from the Reaction Between 12 and <i>trans</i> -[Pt(PPh ₂ Me)Cl(μ-Cl)] ₂	173
3.8.11 – Synthesis of <i>cis</i> -[PtCl ₂ (PPh ₂ Me)(13)] (Compound 17)	173
3.8.12 – Attempted Synthesis of N-(dichlorophosphanyl)-1-phenyl-1-(pyridin-2-yl)methanimine	174
3.8.13 – Synthesis of Proposed Compounds 19-Open/19-SO (Tetrachlorophosphino-1-((phenyl(6-methyl-pyridin-2-yl)methylene)amino) amine)	175
3.8.14 – Synthesis of Compound 20-Open (Tetrachlorophosphino-1-((phenyl(pyridin-2-yl)methylene) amino) amine)	175

Chapter 3 References.....	177
Chapter 4 – Probing the Reactivity of the Interconverting Pyridyl- <i>N</i> -Phosphinoimine – Diazaphosphazole Tautomers.....	180
4.1 – Introduction	180
4.2 – Reactivity of the Pyridyl- <i>N</i> -Phosphinoimines Towards Elemental Selenium	181
4.3 – Reactivity of Dynamic “ <i>Open</i> ”-“ <i>Closed</i> ” Tautomers Towards Small Molecules.....	184
4.3.1 – Reactivity of the Dynamic “ <i>Open</i> ”-“ <i>Closed</i> ” Tautomers Towards DMAD	185
4.3.2 – Reaction of Compounds A and I with Tris(pentafluorophenyl)borane	189
4.3.3 – Reaction of (<i>i</i> Pr ₂ N) ₂ PCl with B(C ₆ F ₅) ₃	192
4.3.4 – Reaction of Compounds A and I with Nitromethane	196
4.3.5 – Reaction of Compounds A and I with Trimethylsilylazide	201
4.4 – Summary	204
4.5 – Chapter 4 Experimental Details	207
4.5.1 – Synthesis of the “ <i>Open</i> ” P ^V Monoselenides.....	207
4.5.2 – Reaction of Compound 1 with DMAD.....	208
4.5.3 – Synthesis of the B(C ₆ F ₅) ₃ Coordination Complexes of Compounds A , I and (<i>i</i> Pr ₂ N) ₂ PCl	208
4.5.3.1 – Proposed Compound A-B(C₆F₅)₃	208
4.5.3.2 – Compound I-B(C₆F₅)₃	209
4.5.3.3 – Reaction of (<i>i</i> Pr ₂ N) ₂ PCl with B(C ₆ F ₅) ₃	210
4.5.4 – Reactions of Compounds A and I with Nitromethane.....	211
4.5.4.1 – Reaction of Compound A with MeNO ₂	211
4.5.4.2 – Reaction of Compound I with MeNO ₂	212
4.5.5 – Reactions of Compounds A and I with TMSN ₃	212
4.5.5.1 – Reaction of A with TMSN ₃	212
4.5.5.2 – Reaction of I with TMSN ₃	213

Chapter 4 References.....	214
Chapter 5 – Summary, Conclusions and Project Outlook.....	218
5.1 – Thesis Summary	218
5.1.1 – Synthetic, Reactivity and Structural Studies of Novel Pyridyl- <i>N</i> -Phosphinoimine – Diazaphosphazole Tautomers.....	219
5.1.1.1 – Chemical Reactivity of Pyridyl- <i>N</i> -Phosphinoimine – Diazaphosphazole Tatuomeric Pairs	221
5.1.2 – Synthetic, Reactivity and Structural Studies of Macrocyclic, 12 and Phosphenium Salt, 13	223
5.1.2.1 – Chemical Reactivity of Macrocyclic, 12 and Phosphenium Salt, 13	224
5.2 – Conclusions	226
5.3 – Future Project Outlook	226
Chapter 5 References.....	229
Appendix 1 – General Experimental Considerations	231
Appendix 2 – Key NMR Spectra for Chapter 2	233
Appendix 3 – X-Ray Crystallographic Study of 4-Dimethylamino-2-Pyridinecarboxamide...	235
Appendix 4 – X-Ray Crystallographic Study of 4-Dimethylamino-2-Cyanopyridine	237
Appendix 5 – Structural Data for the Macrocyclic Pyridyl- <i>N</i> -Phosphinoimine, Compound 12	239
Appendix 6 – List of Novel Compounds Reported in this Work	242
A6.1 – Novel Pyridyl- <i>N</i> -Phosphinoimine – Diazaphosphazole Species.....	242
A6.2 – Novel Species Prepared from the Reactions the Pyridyl- <i>N</i> -Phosphinoimine - Diazaphosphazole Tautomers with Small Molecules	243
Appendix 7 – X-Ray Crystallographic Parameters.....	244
A7.1 – X-Ray Crystallographic Parameters for Compound 1	244
A7.2 – X-Ray Crystallographic Parameters for Compound 2	245
A7.3 – X-Ray Crystallographic Parameters for Compound 4	246

A7.4 – X-Ray Crystallographic Parameters for Compound 12	247
A7.5 – X-Ray Crystallographic Parameters for Compound 21	248
A7.6 – X-Ray Crystallographic Parameters for 4-Dimethylamino-2-Pyridinecarboxamide	249
A7.7 – X-Ray Crystallographic Parameters for 4-Dimethylamino-2-Cyanopyridine	250
Appendix 8 – Seminars, Conferences and Symposia Attended	251
A8.1 – Seminars Attended	251
A8.2 – Conferences and Symposia Attended	256

Abstract

This thesis reports an extension of the investigations into the factors, both internal and external, which impact upon the equilibrium position of a series of structurally analogous, interconverting pyridyl-*N*-phosphinoimine (“*open*”) - diazaphosphazole (“*closed*”) tautomeric systems. **Chapter 1** presents the basic aspects of the chemistry relevant to the work discussed in this thesis: the structure and chemistry of pyridine, phosphines, phosphorus-nitrogen species, non-innocent ligands and frustrated Lewis pairs.

Chapter 2 describes a study into the position of the dynamic “*open*”-“*closed*” equilibrium as a function of solvent polarity, it was found that polar solvents favour the more polar “*closed*” tautomer. The successful preparation and characterisation of a series of structurally analogous pyridyl-*N*-phosphinoimine – diazaphosphazole tautomeric systems, with varying substituents bound to the central pyridine and phosphinoimine motifs, is reported. The stereoelectronic impact of these substituents upon the position of the reversible “*open*”-“*closed*” equilibrium is discussed.

Chapter 3 reports the unprecedented products of the reaction between 6-methyl-2-cyanopyridine, phenyllithium and phosphorus trichloride: a macrocyclic *P,N*-species and an intramolecularly base-stabilised phosphonium salt which were identified by a combination of experimental and computational techniques. The reactivity of these novel *P,N*-compounds towards Se, B(C₆F₅)₃, DMF and *trans*-[Pt(PPh₂Me)Cl(μ-Cl)]₂ is investigated.

Chapter 4 outlines a study of the behaviour of the pyridyl-*N*-phosphinoimine – diazaphosphazole tautomers towards small molecules *e.g.* MeNO₂ and elemental Se. The *P,N*-species were found to demonstrate some of the characteristic reactivity of their various individual functional components, *i.e.* P^{III}, imine, P=N and dihydropyridine.

Chapter 5 summarises the work reported in chapters 2-4 and discusses the future outlook of work with these interconverting pyridyl-*N*-phosphinoimine – diazaphosphazole tautomers.

Acknowledgements

First and foremost, my thanks go to my supervisor, Dr Phil Dyer, who fought so hard to get funding in order for me to carry out my PhD studies in Durham. Thank you for trusting me to continue Dr Dan Smith's work on the hedgehog project, and for your endless guidance and patience since I arrived in Durham.

Thank you to the analytical services within the Department of Chemistry, especially to Dr Andrei Batsanov who collected all of my crystal data, the solution state NMR staff: Dr Juan Aguilar Malavia, Dr Alan Kenwright, Ms Catherine Heffernan and Ms Raquel Belda-Vidal and the solid-state NMR staff: Dr David Apperley and Mr Fraser Markwell. Huge thanks go to Dr Mark Fox, who ran all the computational analysis reported here, and who generously let me "set up camp" in his outer office whilst I wrote my thesis. The glassblowers within the Department of Chemistry, Aaron Brown and Malcolm Richardson, must also be thanked for fixing the many pieces of glassware that I have broken!

To all the members of the Dyer group and its "extended family" (both past and present), James, Jack, Jas, Jammin', Michael L, Beth, Laura S, LiLi, Michael H, Sarah, Stephen, Alex, Dominikus, Claire and Meera – it has been a pleasure working alongside you all, thank you for your endless support, guidance and friendship throughout my time in Durham. Special thanks go to James, not just for answering my silly chemistry questions, but for being a great friend and keeping my morale up over the last few months. Thank you also to Pippa for your positivity – I will always remember to think and say "smiley face" during the difficult times! Many thanks also to Dr Keith Dillon for his invaluable guidance and advice over the years.

Jas, Beth, Jammin', LiLi, Sarah and Alex – I don't think I would have made it through my PhD without you all. You have never failed to be there for me, you have always boosted my spirits and helped me through the various challenges over the last few years. Whilst I wish I could dedicate a whole page to each of you to express how much you all have, and will continue, to mean to me, I think I must restrict it to this paragraph, and of course, my endless gratitude, friendship and love.

To my family; Mum, Dad, Christopher, Leanne, George, Grandad, Pip and Steve – you have always had never ending faith in me and my abilities, even when I have not, and for that I thank you, thank you for not letting me forget that I can do whatever I set my mind to. Mum and Dad – it has been a very long road to get to this point in my education, you have been my strength and my biggest supporters throughout everything, without you I would not have made it through my A Levels let alone my degree and PhD, I don't think I will ever be able to tell you just how indebted to you I am and how much I love you. Christopher and Leanne, thank you for your words of encouragement and your friendship, and most importantly, for never failing to make me laugh. My darling nephew George, you have brought me infinite joy and happiness over the last three years, from the very moment of your arrival into the world two months into my studies in Durham, your mischievous smile and laugh has never failed to brighten my day.

To Hollie, Katy and Euan – you have been amazing. You have been my escape from Durham, my best friends. Whilst we are all now away from our beloved St Andrews, and living hundreds of miles from each other, you still know me better than I know myself, you have provided me with endless love, encouragement and prosecco, thank you. Hollie – you have soothed my tears and anxieties, you have been by my side every step of the way, both in St Andrews and Durham, without fail. Katy – all those years ago, when I did my summer project in the GJF group, you gave me the confidence that I hadn't been able to find for myself, since then you have been my inspiration, my sense of rationality.

Greg, you told me on our wedding day that I have been your biggest cheerleader and I want you to know that you have been mine too. For years we have known that we make the best team, not only whilst playing board games and pool, but for helping each other get through challenging times. The last 3 years and 3 months have been filled with some of the best times, as well as some very difficult ones, but you have been by my side every step of the way, sharing in both my successes and setbacks. Thank you for everything, I would not be where I am today if I hadn't had you by my side. I am excited for the next chapter of our lives; new places, new jobs, and most importantly, to introduce ourselves as the Drs Aldred!

Abbreviations

General Abbreviations

Abbreviation	Property
ν	Absorbance
μ	Bridging ligand
$^{\circ}\text{C}$	Degrees Celsius
κ	Denticity
Ac	Acyl
Alk	Alkyl
Anth	Anthracenyl
Ar	Aryl
ASAP	Atmospheric solids analysis probe
Az	Aziridinyl
BINAP	2,2'-bis(Diphenylphosphino)-1,1'-binaphthyl
BINOL	1,1'-bi-2-Naphthol
COD	1,5-Cyclooctadiene
Cy	Cyclohexyl
D	Dalton
DABCO	1,4-Diazabicyclo[2.2.2]octane
DCM	Dichloromethane
DMAD	Dimethyl acetylenedicarboxylate
DMAP	4-Dimethylaminopyridine
DME	1,2-Dimethoxyethane
e^{-}	Electron
EDG	Electron donating group
ee	Enantiomeric excess
ESI/EI ⁺	Electron impact
Et	Ethyl
Et ₂ O	Diethyl ether
EWG	Electron withdrawing group
FLP	Frustrated Lewis pair

h	Hour
HDMS	Hexamethyldisilazane
HMPA	Hexamethylphosphoramide
<i>i</i> Pr	<i>Iso</i> -propyl
IR	Infra-red
K	Kelvin
K_a	Acid dissociation constant
kcal	Kilocalorie
LHS	Left-hand side
<i>m</i>	<i>meta</i>
Me	Methyl
MeCN	Acetonitrile
Mes	Mesityl
ml	Millilitre
mmol	Millimole
mol	Mole
MS	Mass spectrometry
NIL	Non-innocent ligand
NMR	Nuclear magnetic resonance
<i>n</i> Pr	<i>n</i> -Propyl
<i>o</i>	<i>ortho</i>
OTf	Trifluoromethanesulfonate
<i>p</i>	<i>para</i>
Ph	Phenyl
pK_a	$-\log_{10}K_a$
(por)	Porphyrins
R	Alkyl/aryl substituent
RHS	Right-hand side
RT	Room temperature
TBABF ₄	<i>tert</i> -Butylammonium tetrafluoroborate
TBP	2,6-Di- <i>tert</i> -butyl-pyridine
<i>t</i> Bu	<i>Tert</i> -butyl
TFAA	Trifluoroacetic anhydride
THF	Tetrahydrofuran

TMEDA	N,N,N',N'-Tetramethylethylenediamine
TOF	Turnover frequency
TOF ₅₀	50% conversion
Tos	Tosyl/ <i>para</i> -CH ₃ (C ₆ H ₄)SO ₂

NMR Spectroscopy Abbreviations

Abbreviation	Property
δ	Chemical shift
COSY	Correlation spectroscopy
d	Doublet
dd	Doublet of doublets
dh	Doublet of heptets
d sept	Doublet of septets
HMBC	Heteronuclear multiple bond coherence
HMQC	Heteronuclear multiple quantum correlation
HSQC	Heteronuclear single quantum coherence
Hz	Hertz
<i>J</i>	Coupling constant
m	Multiplet
ppm	Parts per Million
qC	Quaternary Carbon
s	Singlet
sept	Septet
t	Triplet
$v_{1/2}$	Width at half height

Chapter 1 – Introduction

Chapter 1 – Introduction

This thesis reports a detailed investigation of the synthesis, reactivity and structural studies of a novel class of interconverting pyridyl-*N*-phosphinoimine – diazaphosphazole tautomeric species. **Chapter 1** outlines the literature precedent for the work underpinning this thesis.

1.1 – Interconverting Pyridyl-*N*-phosphinoimine–Diazaphosphazole Tautomers

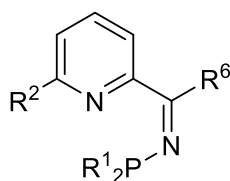
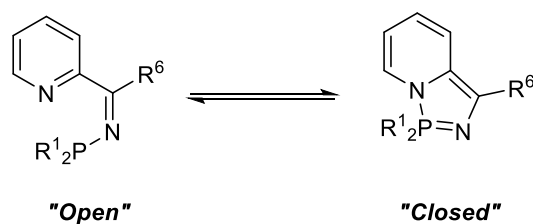


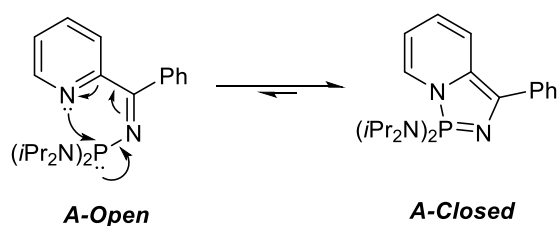
Figure 1 – General structure of the pyridyl-*N*-phosphinoimine species reported by Dyer and co-workers.¹

In 2005 Dyer and co-workers reported the synthesis and chemistry of the first in a series of pyridyl-*N*-phosphinoimine species of the general form shown in Figure 1.^{1,2,3,4} These phosphinoimines have a number of interesting properties: they can coordinate to a metal centre to form a six-membered chelate with unsymmetrical π -acidity and, depending on the nature of the phosphorus substituent, they have the potential to cyclise to form a 5-membered heterocycle and a bicyclic system. It has been shown that this phosphinoimine species (Figure 1) can exist in a dynamic tautomeric equilibrium with a diazaphosphazole form, as shown in Scheme 1; these two species can be regarded as “*open*” and “*closed*” forms, respectively.² DFT studies (at the B3LYP/6-31G** level of theory) have been carried out on the “*open*”-“*closed*” system of compound **A** (Scheme 2) to probe the mechanism of the cyclisation process.² The computational studies on the tautomerism of **A** revealed that the energy barrier to this ring closure is 3 kcal mol⁻¹, and did not identify any transition states for this process, suggesting that there is no kinetic inhibition to the cyclisation of **A-Open** to **A-Closed**. The absence of a kinetic barrier to the interconversion of compounds **A-Open** and **A-Closed** suggests that the ring closure process occurs *via* a concerted *pseudo*-1,5-electrocyclisation mechanism, as denoted in Scheme 2.^{2,3}



Scheme 1 – Dynamic tautomeric equilibrium of the phosphinoimine species.

This *pseudo*-1,5-electrocyclisation process proceeds *via* the attack of the pyridine nitrogen lone pair at an electron deficient phosphorus centre to form a new σ -bond between the pyridine nitrogen and the phosphorus centre. The phosphorus(III) centre in **A-Open** is oxidised to phosphorus(V), and the pyridine ring is dearomatized during the formation of the *pseudo* 10 π -electron heterocyclic system in **A-Closed**. The dynamic nature of this tautomerism has been confirmed using variable temperature ^{31}P NMR spectroscopy.

Scheme 2 – Reversible cyclisation of **A-Open** to **A-Closed**.²

The pyridyl-imine component of the “open” pyridyl-*N*-phosphinoimine species (Figure 2, **b**, *e.g.* **A-Open**) is reminiscent of the α -iminopyridine species reported by Wieghardt and co-workers (Figure 2, **a**).⁵ Such α -iminopyridine species have been shown to demonstrate so-called non-innocent ligand (NIL) behaviour, and have been studied with respect to the coordination behaviour of the different redox states to metal centres (*e.g.* Cr^{II} , Mn^{II} , Fe^{II} and Co^{II}).⁵ In a similar vein, the “open” pyridyl-*N*-phosphinoimine species can be regarded as organic analogues to the systems reported by Wieghardt and co-workers (Figure 2, **a**),⁵ *i.e.* $\text{R}' = \text{PR}^1_2$. The potential for reversible single electron reductions at the iminopyridine motif in the “open” pyridyl-*N*-phosphinoimine, and therefore NIL behaviour, makes these species of interest to explore further, and hence a brief overview of NIL chemistry will be given in section **1.2**.

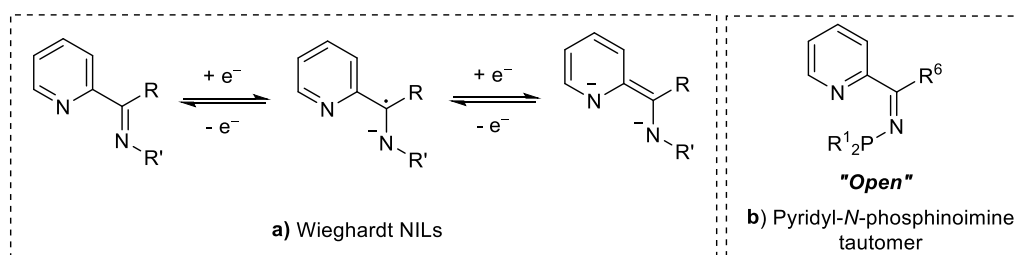


Figure 2 – a) Redox states of α -iminopyridine ligands reported by Wieghardt.⁵ b) General pyridyl-*N*-phosphinoimine reported by Dyer and co-workers.

1.2 – Non-Innocent Ligands (NILs)

“Non-innocent ligand” (NIL) is a term first used by Jørgensen in 1966 in reference to metal-ligand combinations that undergo redox changes at a position remote from the metal centre.⁶ NILs are of potential great importance in coordination chemistry, notably in catalysis, due to their varied electrochemical, magnetic and biochemical properties.^{7,8} The definition of NIL has now been broadened to encompass redox-inactive systems, where external influences result in the modification of the ligand structure and/or bonding mode, causing disruption to the metal’s coordination sphere.^{9,10,11}

In a “classical” redox catalytic system, ligands are chosen for the steric and electronic impact they have upon a metal centre; it is the metal centre of the complex that undergoes the electronic change required to facilitate a catalytic process, leaving the ligand itself unchanged. Ligands that play a much more active role in the catalytic cycle, by participation in the redox process, are referred to as “redox non-innocent” or “redox active” ligands.^{12,13,14,15} NIL species have been the focus of much attention over the past ten years due to their potential to engender new catalytic reactions, as a consequence of their ability to alter the reactivity of a catalytic species.

In general, redox NILs participate in a catalytic process in one of two ways: a) by acting as an electron donor/acceptor, or, b) by interacting with a substrate causing bond breakage and/or formation.¹⁶ These generalised modes of action, a) and b), can each be subdivided into two different mechanisms, which are shown in Figure 3. Approaches **i)** and **ii)** proceed by the ligands acting as an electron donor/acceptor, whereas in **iii)** and **iv)**, the ligand interacts with

the substrate causing bond breakage and/or formation. The four modes of action of NILs shown in Figure 3 will now be discussed.

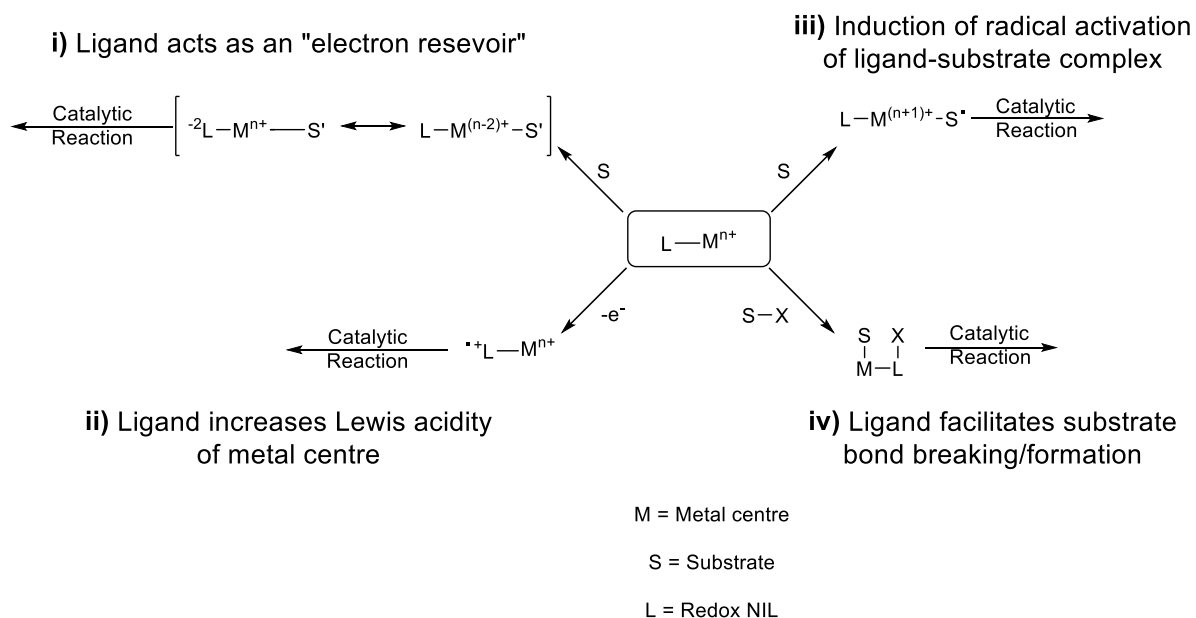
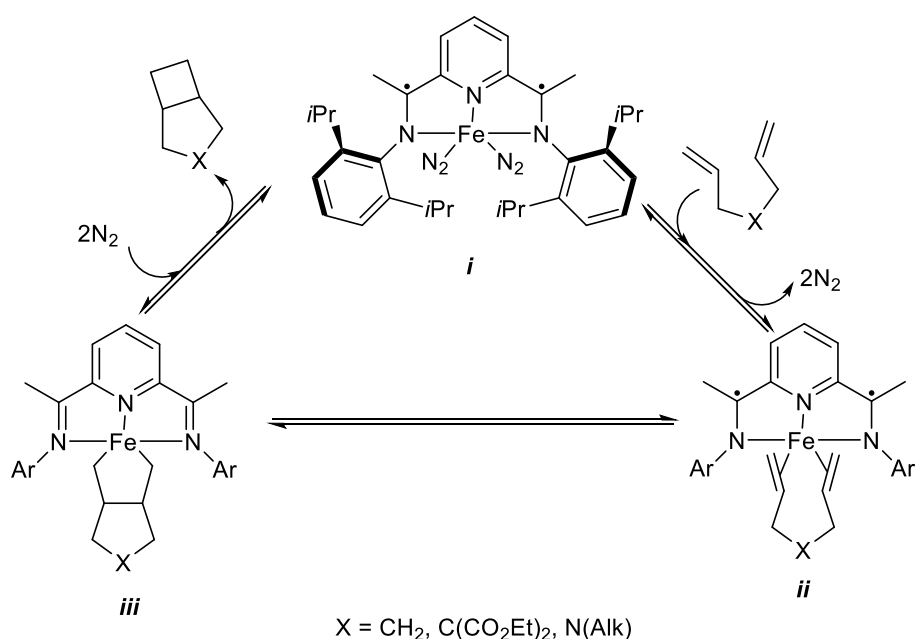


Figure 3 - Methods by which NILs participate in catalytic processes. i) and ii) proceed by the ligand acting as an electron donor/acceptor, iii) and iv) proceed by the ligand interacting with the substrate causing bond breakage and/or formation.¹⁶

1.2.1 – i) Redox NILs Acting as Electron Reservoirs

Wieghardt-type NILs⁸ have found extensive application in bis-pyridyl-imines, especially in homogeneous catalysis. In homogeneous catalytic processes, the transfer of multiple electrons from a metal to an activated substrate is common, but can require the metal centre to adopt an uncommon and undesirable oxidation state. For metals such as Pt, Pd and Rh, these transformations and oxidation states are readily achieved, however, for cheaper, more readily available first row transition metals, they are much harder.¹⁶ Ligands that can act as electron reservoirs and facilitate multi-electron storage and transfer, such as redox NILs, allow first row transition metals to undergo multielectron transformations without the need for the metal centre to adopt an undesirable oxidation state.^{17,18} By way of example, the catalytic cycle in Scheme 3 demonstrates how a redox NIL can be employed in Fe^{II}-catalysed cycloaddition ring-closures.^{19,20} The initial Fe^{II} complex, *i*, undergoes complexation to a diene, causing displacement of the two N₂ ligands to yield *ii*, which exists in equilibrium with *iii*. The

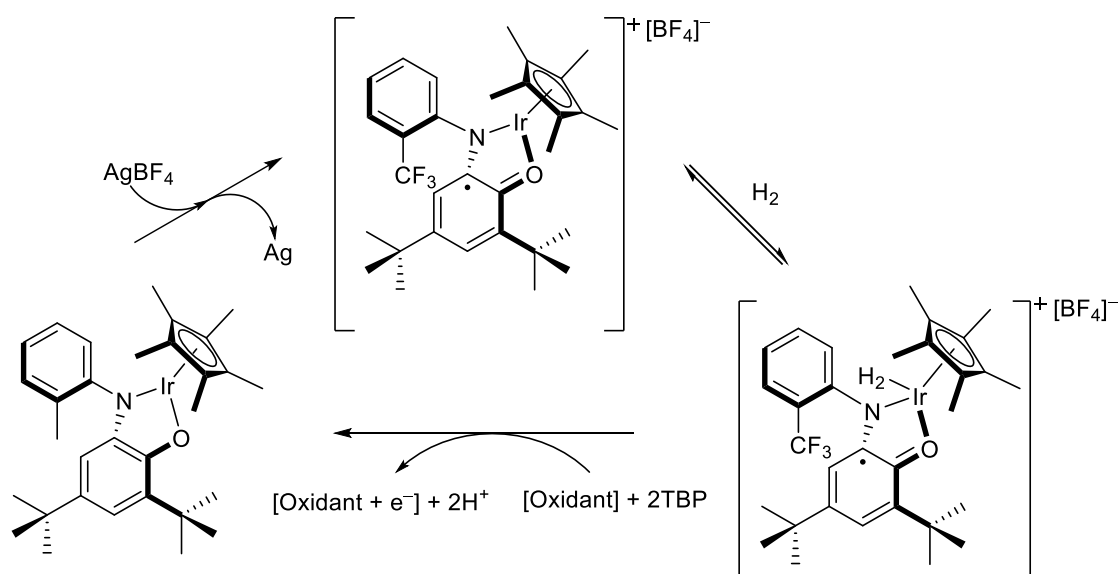
tridentate *N,N,N*-ligand in *i* and *ii* is the redox active ligand, and can be regarded as the dianionic reduced form of 2,6-di-iminopyridine.^{21,22} The equilibrium transformation between *ii* and *iii* is a two-electron process, with the electrons originating from the reduced 2,6-di-iminopyridine ligand, not the metal centre, so avoiding the need for the Fe^{II} centre to oxidise, and adopt the energetically unfavourable 4+ oxidation state. The *pseudo* [2+2] cycloaddition product is yielded from *iii* in a two-electron reductive elimination, generating *i*. The 2,6-di-iminopyridine ligand facilitates this reductive elimination, allowing the iron centre to retain its 2+ oxidation state instead of adopting another energetically unfavourable oxidation state, in this case, 0.



Scheme 3 - NIL acting as an electron reservoir for iron catalysed [2+2] cycloaddition reactions.^{19,20}

1.6.1 – *ii*) Redox NILs used to Alter the Lewis Acid/Base Properties of a Metal Centre

Scheme 4^{23,24} demonstrates how the oxidation/reduction of a ligand can change the Lewis acid/base character of the metal centre to which it is bound, without changing its steric environment. The particular example shown in Scheme 4 shows the oxidation of the ligand by AgBF₄ to form a radical species in order to increase the Lewis acidity of the iridium centre and allow addition, and subsequent oxidation, of dihydrogen by either Ag⁺ or the cationic metallic species.^{23,24} Dihydrogen reduces the oxidised form of the NIL, meaning that the NIL also acts as an electron reservoir.



Scheme 4 - Oxidation of a NIL to increase the Lewis acidity of a metal centre to enable a catalytic process.^{23,24}

To facilitate a catalytic process, an increase in the Lewis basicity of the metal centre may also be required. In the alkene hydrogenation reactions catalysed by the Rh^I-diphosphinoferrocene species shown in Figure 4, the rate of olefin hydrogenation can be increased by alteration of the R substituent bound to the phosphorus atoms from phenyl to more electron donating alkyl groups, such as *t*Bu.²⁵ The diphosphinoferrocene ligand exhibits NIL behaviour by the electron donating phosphine R groups increasing the Lewis basicity of the rhodium centre, which aids in the oxidative addition of dihydrogen (which is often the rate-determining step).^{16,25}

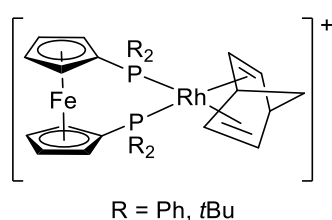
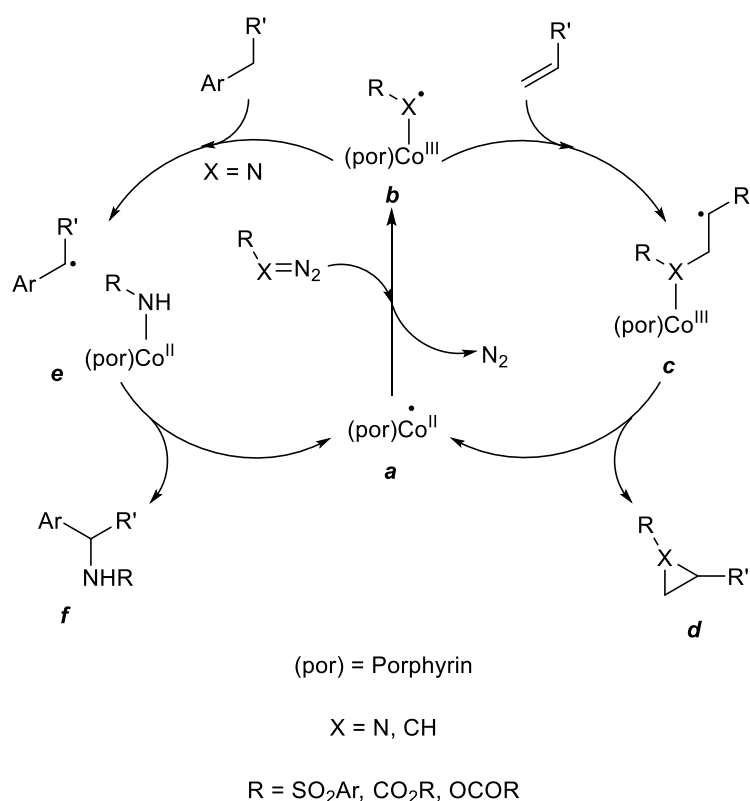


Figure 4 - Rh^I-diphosphinoferrocene species employed in olefin hydrogenation.²⁵

1.2.3 – iii) NIL Inducing Radical-Type Reactivity on Substrate-Ligand Complex

The redox non-innocent character of a substrate itself can be profited from. The use of these properties in a ligand-substrate complex enables the transfer of electrons to or from the substrate, giving rise to radical-like reactivity of the ligand-substrate complex.¹⁶ The radical-

type species generated yield dramatically different reactivities and selectivities, compared to their neutral analogues. The exploitation of the redox non-innocent properties of substrates is demonstrated in Scheme 5 for nitrene and carbene transfer reactions catalysed by cobalt(II)-porphyrin species.¹⁶ The processes shown in Scheme 5 start with the reaction of the cobalt(II)-porphyrin catalyst (**a**) with an azido- or diazo-species to give the reactive radical-type species, **b**. This process is accompanied by the loss of dinitrogen - after the release of N₂, a single electron transfer occurs from the cobalt(II) centre to the carbene/nitrene ligand, creating the radical species **b**.



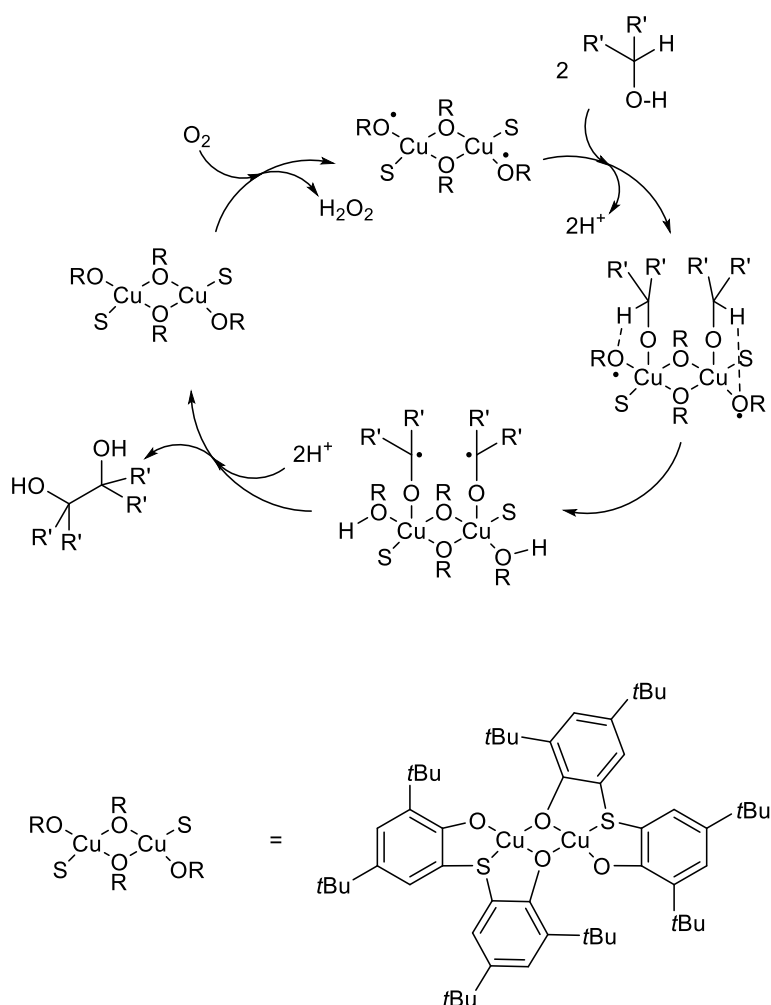
Scheme 5 - Use of radical-like ligand-substrate complexes in catalytic carbene and nitrene transfer reactions.¹⁶

The radical **b** (Scheme 5) can undergo reactions with alkenes to form the radical species **c**, which then cyclises to form cyclopropanes or aziridines (**d**). The advantages of employing redox NILs for the cyclopropanation reactions (*i.e.* X = C, Scheme 5) is the ability to be able to incorporate electron withdrawing R' substituents, as there is only a low risk of carbene dimerization,¹⁶ an unwanted consequence of using closed-shell copper(I), rhodium(II) and ruthenium(II) catalysts for the cyclopropanation of electron-poor alkenes.¹⁶ When X = N for **b** (Scheme 5), however, these species can undergo insertions into C-H bonds (both allylic^{26,27}

and benzylic^{28,29}) to give amines. The allylic/benzylic hydrogen is abstracted to yield **e**, which then breaks down to form the desired amine product, **f**.

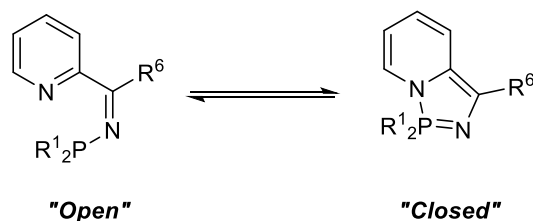
1.2.4 – iv) NILs Facilitating Substrate Bond Breakage/Formation

NILs can play an active role in catalytic processes by facilitating bond activation. This direct participation of NILs is used by many enzymes, including oxidases such as galactose oxidase in the oxidation of D-galactose into D-galactohexodialdose and hydrogen peroxide.^{16,30,31} Scheme 6 shows another catalytic process that makes use of bond activation by NILs, this time for the dimerization of secondary alcohols in the presence of oxygen.³² The cycle starts with the oxidation of the copper(II) complex by oxygen to give a biradical, followed by the coordination of two deprotonated alcohol motifs. These alkoxides then undergo α -hydrogen transfer to the radical ligands. The final step consists of radical combination and diol elimination.³³



Scheme 6 –An example of the use of NILs to facilitate bond breakage/formation in a catalytic cycle.³²

1.3 – Structural Components of the Pyridyl-*N*-Phosphinoimine – Diazaphosphazole Tautomeric Pairs



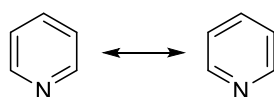
Scheme 7 - Dynamic tautomeric equilibrium of the phosphinoimine species.

As stated in section **1.1**, the interconverting “open” and “closed” species shown in Scheme 7 are of interest to explore as a consequence of the potential for NIL behaviour. The pyridyl-imine motif in these “open” phosphinoimines is reminiscent of the α -iminopyridine motif in Wieghardt’s NILs (discussed in section **1.2**).⁸ It is not just the potential non-innocent character of the “open” phosphinoimine species that is of interest to explore, but their ability to cyclise. The various structural components of the “open” and “closed” species (*i.e.* the pyridine ring, imine bond, P^{III} centre, iminophosphorane, dihydropyridine) and their associated chemistry are therefore of particular interest to examine. The basic aspects of the pyridyl, phosphine and iminophosphorane functionalities present in the “open” and “closed” *P,N*-compounds will now be discussed in sections **1.4**, **1.5** and **1.6**.

1.4 – Pyridine

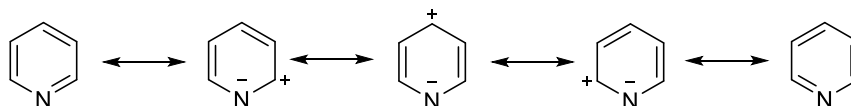
Pyridine is a key component of an array of compounds in modern day chemistry, from pharmaceuticals (*e.g.* esomeprazole and amlodipine) to agrochemicals (*e.g.* chlorpyrifos).³⁴ The chemistry of pyridine is of interest because of its similarities and differences to that of benzene.³⁵

1.4.1 – Structure and Properties of Pyridine



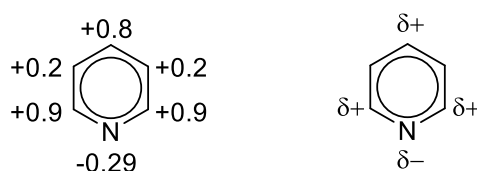
Scheme 8 - Kekulé structures of pyridine.

Pyridine is an organic, aromatic heterocycle with 6 π -electrons that is structurally related to benzene. The structure of pyridine, initially proposed concurrently by Körner³⁶ and Dewar,³⁷ is most commonly described by using a resonance approach (Scheme 8), *i.e.* by which it is shown as a hybrid of its corresponding resonance structures shown in Scheme 9.³⁸

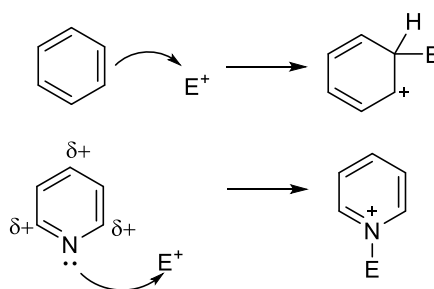


Scheme 9 – Resonance structures of pyridine.

1.4.2 – Chemical Reactivity of Pyridine

Figure 5 – Calculated charge distribution in pyridine.^{39,40}

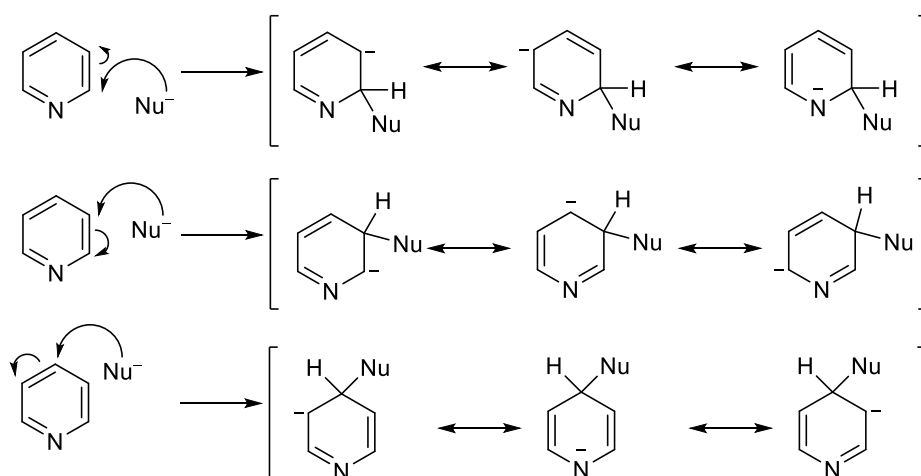
The presence of the heteroatom in pyridine, C_5H_5N , gives rise to an uneven charge distribution (dipole moment = 2.23 D, Figure 5) which benzene, C_6H_6 , does not have.^{39,40} This difference in charge distribution between pyridine and benzene contributes to the contrasting chemical reactivity of these aromatic species.

Scheme 10 – Contrasting reactivity of benzene and pyridine with an electrophile (E^+).

Benzene, for example, is more prone to undergoing electrophilic substitution reactions than pyridine, as the partial positive charges at the 2- and 4-positions on pyridine (Figure 5) results in an unfavourable interaction of the π -electrons within the ring with electrophiles (E^+). Instead of the interaction of the π electrons in the pyridine ring with an electrophile, the lone pair of electrons at the nitrogen centre interacts in such a way that the formation of a formal

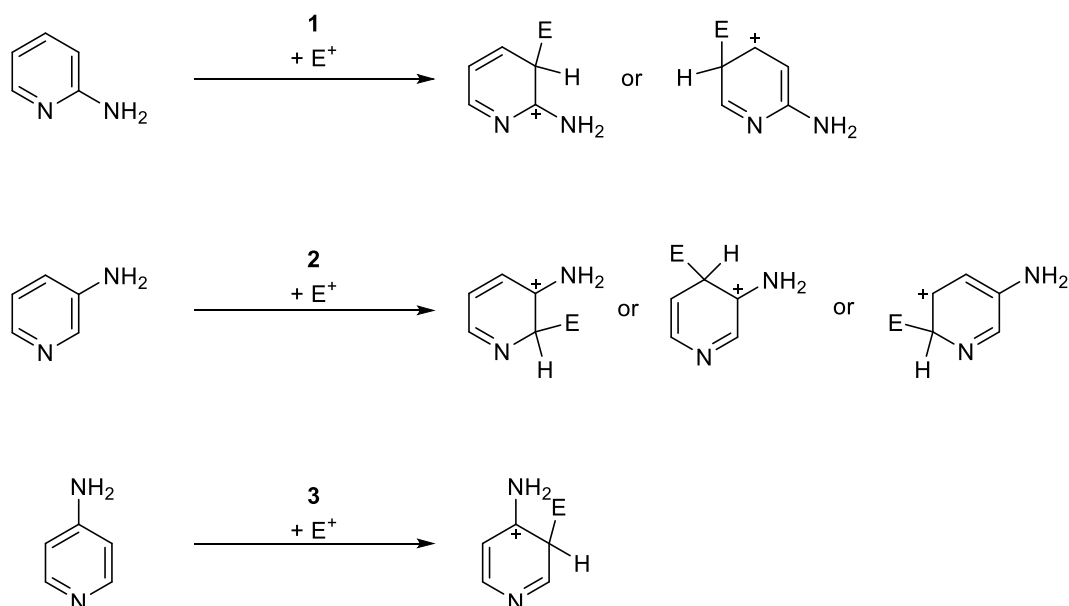
positive charge results (Scheme 10).³⁸ The partial positive charge in the pyridine ring, however, does favour the approach of nucleophiles, and therefore nucleophilic attack.

Nucleophilic attack at a pyridine ring can occur at either the 2-, 3- or 4-positions, the resonance structures for each of the corresponding transition states can be drawn as shown in Scheme 11. The favourable stabilisation of the negative charge on the nitrogen centre renders nucleophilic attack at the 2- and 4- positions to be more favourable than at the 3-position.³⁸



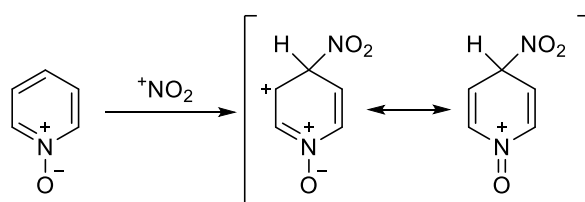
Scheme 11 – Nucleophilic (Nu^-) attack at the 2-, 3- and 4-positions of the pyridine ring, and resonance structures of the associated transition states.³⁸

As with benzene, the presence of substituents on a pyridine ring has the effect of modifying the position at which a substitution reaction occurs. Electron donating groups (EDG, *e.g.* OH, NR_2) direct electrophilic attack to positions *ortho* and *para* to them. The activation of the *ortho* and *para* positions to electrophilic attack arises from the ability of the electron donating group to resonance stabilise the positive charge generated in the transition states depicted in Scheme 12.³⁸



Scheme 12 – Possible transition states generated by attack of an electrophile (E^+) at an electron donating group substituted pyridine.³⁸

The substitution of an electron donating group at the nitrogen centre of a pyridine ring, for example an oxygen atom, can also act to direct electrophilic substitution *para* to the nitrogen atom, again, due to the ability of the nitrogen substituent to stabilise the positive charge generated during the reaction (Scheme 13).



Scheme 13 – Resonance-stabilised transition states generated from electrophilic attack of an electrophile on pyridine-*N*-oxide.

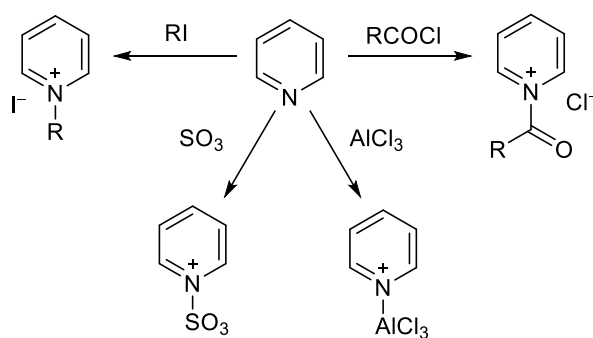
1.4.2.1 - Pyridine as a Base

The lone pair of electrons at the pyridine nitrogen centre resides in an sp^2 hybrid orbital orientated in the plane of the ring, which is unable to form a part of the delocalised aromatic π -electron system. The availability of the nitrogen lone pair results in the nitrogen centre being able to act as an electron donor, thus giving pyridine a pK_a of 5.2.⁴¹ The basicity of

pyridine varies depending on the electron donor-acceptor characteristics of substituents bound to the ring.

It has been demonstrated that the substitution of an alkyl group at the 2-, 3- or 4-position on a pyridine ring can increase the basicity of the species by 0.5-0.8 pK_a units, *e.g.* 2-picoline, $pK_a = 5.97$; 2-ethylpyridine, $pK_a = 5.92$.^{42,43} The impact of the alkyl group upon the pK_a of the pyridine derivative is primarily electronic, the alkyl groups increase the electron density at the nitrogen centre, either inductively, or by hyperconjugation into the σ -electron system of the ring. Substitution at the 4-position has a more marked impact upon the pK_a of the alkylpyridine than when substitution of the alkyl group is made at the 3-position.³⁸ When the size of the 2-substituent increases, for example for 2-substituted pyridines, steric factors come into play as the groups crowd the pyridine nitrogen centre and lone pair, serving to decrease the basicity of the species: $pK_a = 5.97$ (Me), 5.92 (Et), 5.83 (*i*Pr), 5.76 (*t*Bu).⁴³ The substitution of an electron withdrawing group on the pyridine scaffold has the effect of decreasing the pK_a of the species, for example, pyridine-3-carboxamide ($pK_a = 4.77$) and pyridine-4-carboxamide ($pK_a = 4.90$).⁴¹

1.4.2.2 – Electrophilic Reactions of Pyridine

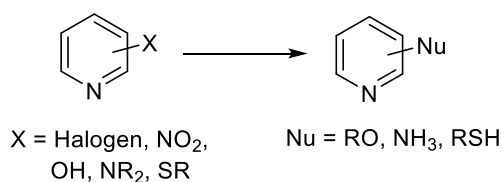


Scheme 14 – Electrophilic reactions of pyridine at the nitrogen centre.³⁸

Unsubstituted pyridine undergoes electrophilic reactions at the electron-rich nitrogen centre, as is demonstrated by the selected reactions shown in Scheme 14.³⁸ Electrophilic substitution at the pyridine carbon centres is much more difficult to achieve than at the nitrogen centre, as a result of the partial positive charge at the 2- and 4-positions (Scheme 9). To force electrophilic substitution at a pyridine carbon centre, harsh reaction conditions are required

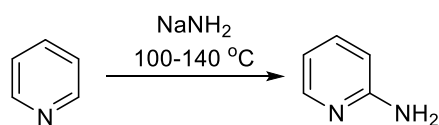
and only give low yields. The nitration of pyridine, for example, requires the use of concentrated nitric and sulfuric acids, a temperature of 350 °C and an extended reaction time of 24 hours to give a < 10 % yield of nitropyridines.³⁸

1.4.2.3 – Nucleophilic Reactions of Pyridine



Scheme 15 – Nucleophilic substitution reactions of substituted pyridine.

As has already been discussed in section **1.4.2**, unsubstituted pyridine can undergo nucleophilic substitution at the 2- and 4-positions (Scheme 11). For nucleophilic substitution to occur on pyridine, the mechanism requires the attack of the ring by a negatively charged species, followed by the subsequent elimination of a high-energy hydride ion. The high energy associated with the hydride ion means that this type of elimination rarely occurs, nucleophilic substitution typically occurs *via* the elimination of a more stable anion, as shown in Scheme 15.³⁸ The Chichibabin reaction, shown in Scheme 16, is an example of a nucleophilic substitution reaction of pyridine that proceeds *via* the elimination of a hydride ion to generate a 2-aminopyridine..⁴⁴



Scheme 16 – Chichibabin reaction for the preparation of 2-aminopyridines.⁴⁴

The ease of nucleophilic substitution varies depending on the position of the X substituent (Scheme 15), with the rate being fastest when groups are present at the 2- and 4-positions, than when at the 3-position, due to the ability of the pyridine nitrogen to stabilise the negative charge present in the transition states (Scheme 11).

1.4.2.4 – Pyridine Complexes

When presented with an electron deficient metal centre, a pyridine moiety can readily coordinate to the metal as a consequence the electron donor character of the heterocycle (discussed in **1.4.2.1**). Pyridine forms tetrahedral complexes with aluminium trihalides *via* the donation of the nitrogen lone pair into a vacant *p* orbital on the aluminium centre, an example of which is shown in Figure 6.⁴⁵ Pyridine can also form similar complexes with beryllium, boron and magnesium, 2-substituted pyridines can also coordinate to boron trihalides.⁴⁶ The complexation ability of a 2-substituted pyridine species decreases as the size of the 2-substituent increases.⁴⁷ As well as tetrahedral complexes, pyridine can also form square planar complexes as shown by the selected gold(III)⁴⁸ and copper(II)⁴⁹ complexes shown in Figure 6.

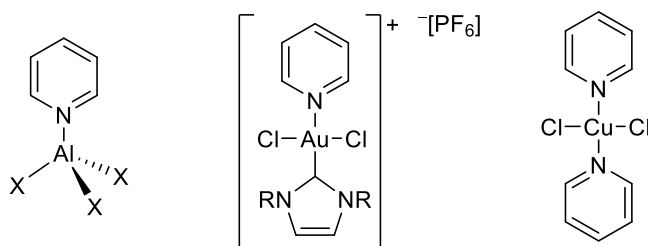
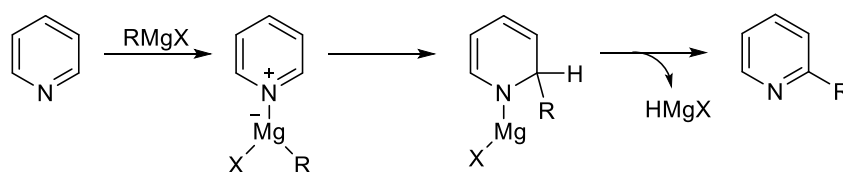


Figure 6 – Examples of aluminium, gold and copper complexes of pyridine.⁴⁵

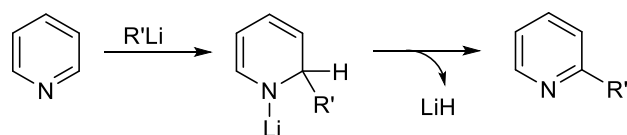
1.4.2.5 – Reaction of Pyridine with Organometallics

The installation of an alkyl-/aryl-substituent at the 2-position on pyridine cannot be achieved by a Friedel-Crafts reaction (*i.e.* electrophilic aromatic substitution) for the reasons explained in section **1.4.2.2**. Organolithium and Grignard reagents, however, can be employed to achieve this.³⁸ The reaction between pyridine and Grignard reagents proceeds *via* the pathway shown in Scheme 17.³⁸



Scheme 17 – General reaction of Grignard reagents (RMgX) with pyridine.³⁸

However, the yields of 2-substituted pyridines from the reaction of pyridine with a Grignard reagent are typically low, as a result of the difficulty associated with the elimination of HMgX , and the consequent rearomatisation of the pyridine motif (Scheme 17).³⁸ Organolithium reagents, however, are able to generate higher yields of 2-substituted pyridines, and proceed *via* the pathway shown in Scheme 18 to readily liberate LiH .⁵⁰

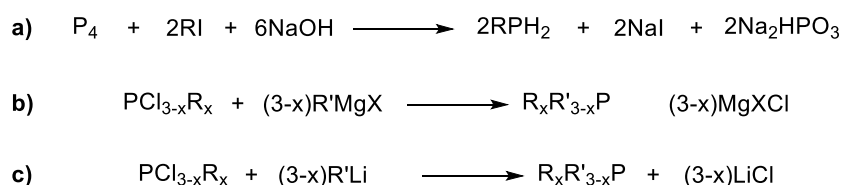


Scheme 18 - Reaction of organolithium reagents ($\text{R}'\text{Li}$) with pyridine.

1.5 – Phosphines

Phosphines, PR_3 , are a key class of phosphorus compound that adopt a pyramidal geometry, and can be thought of as derivatives of phosphine, PH_3 , itself.^{54,52} Phosphorus chemistry is both diverse and rich, and has been pursued extensively due to the variety of applications of organophosphorus compounds in the synthesis of, for example, pesticides, insecticides, fertilizers, detergents, pharmaceuticals, phosphoric acid, animal feedstuffs and catalysts.^{53,54,55,56}

The preparation of phosphines has been extensively reviewed in the literature, for example by Maier in 1972⁵⁷ and Elsner in 1982,⁵⁸ and comprehensive summaries of organophosphorus chemistry in the literature are published annually by the Royal Society of Chemistry as Specialist Periodical Reports.⁵⁹ There is a whole library of methods for the preparation of PR_3 compounds, including from elemental phosphorus (such as *via* route **a**, Scheme 19), which can be obtained *via* the electrothermal reduction of calcium phosphate rock.^{56,60} Organolithium and Grignard reagents can also be employed to prepare both symmetric and asymmetric phosphines from $\text{PCl}_{3-x}\text{R}'_x$, examples are shown in Scheme 19 (routes **b** (Grignard reagents) and **c** (organolithium reagents)).⁵⁶

Scheme 19 – Selected reactions for the preparation of phosphines.⁵⁶

Reactions possible at a phosphorus(III) centre are wide and varied because of the ambivalent character of phosphorus. Phosphorus (electronic ground state configuration of $[\text{Ne}] 3s^2 3p_x^1 3p_y^1 3p_z^1$) can be either tri- or penta-valent, and can readily switch between these oxidation states. When a phosphorus centre is in its +3 oxidation state, it possesses a lone pair of electrons, which has two key impacts on the P^{III} species: its stereochemistry and its ability to act as a nucleophile.⁵⁶ Phosphorus, whilst its valence electrons lie in its $3s$ and $3p$ orbitals, has the ability to make use of its comparatively low-lying $3d$ orbitals to enable it to stabilise high bond energies, such as in phosphonium ylides and phosphine oxides.⁶¹

Organic synthesis, organometallic chemistry and catalysis all make extensive use of phosphines. Phosphines are readily available and make attractive ligands as their steric and electronic properties can be altered in a systematic fashion by varying the groups bound to the phosphorus centre. Similarly, the donor-acceptor character of phosphine ligands depends on the nature of its substituents – some phosphines are very strong σ -donors, whilst others can exhibit strong π -acceptor properties like CO.^{62,63,64,67} The ease of tunability of the electronic and steric properties of phosphines makes them excellent ligands for catalysis as the environment about the metal centre can be altered depending on the requirements at the metal centre. Metal complexes with strongly electron donating phosphines have been key in the development of catalytic processes such as C-H bond activation⁶⁵ and the hydroformylation of alkenes,⁶⁶ which both have a requirement for an electron rich metal centre. The steric and electronic properties of a phosphine are not only readily tuned, but also easily quantified.

1.5.1 – Quantifying the Steric Properties of Phosphines

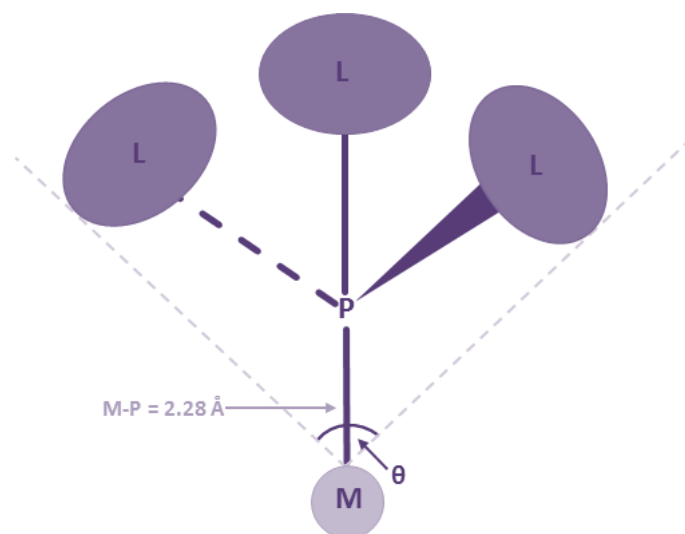


Figure 7 - Pictorial representation of the Tolman cone angle. M = metal, θ = cone angle, ellipsoids = van der Waals radii of substituents at phosphorus.⁶⁷

The steric bulk of a phosphine species can be measured by using the Tolman cone angle, θ , as shown in Figure 7.⁶⁷ This cone angle is used to describe the amount of space a phosphine ligand occupies when bound to a metal centre (Tolman used Ni as the metal to define a standard metal-phosphine distance of 2.28 Å, and used van der Waals radii of the P substituents to define the boundary of the space occupied by the ligand).⁶⁷ The cone angle is determined by rotating the phosphine ligand about the metal-phosphorus bond, this creates a cone in space that the ligand occupies (as depicted by the dashed lines in Figure 7) creating the Tolman cone angle, θ . The larger the phosphorus substituent, the greater the cone angle and space it occupies about the metal centre.

1.5.2 – Quantifying the Electronic Properties of Phosphines

The electronic donor-acceptor properties of a phosphine can be readily quantified by two methods:

- Measuring the A_1 carbonyl stretching frequency of a $\text{Ni}(\text{CO})_3(\text{PR}_3)$ complex. The greater the electron donor character of a phosphine, the greater the electron density on the Ni centre, and therefore back donation into the π^* orbital on the CO ligands.

This increased back donation has the effect of weakening the CO bond, and consequently decreasing the frequency of the carbonyl stretch.⁶⁸

- Measuring the $|^1J_{\text{PSe}}|$ coupling constant for $[\text{Se}=\text{PR}_3 \leftrightarrow \text{Se}^{-+}\text{PR}_3]$ species by the use of ^{31}P NMR spectroscopy.⁶⁹ When a phosphine is a poor σ -donor, the phosphorus-selenium bond is primarily of s character, which increases the $|^1J_{\text{PSe}}|$ coupling constant (e.g. $\text{P}(\text{OMe})_3$, $|^1J_{\text{PSe}}| = 963$ Hz; $\text{P}(\text{NMe}_2)_3$, $|^1J_{\text{PSe}}| = 805$ Hz).^{69,70,71} The reverse of this, i.e. a good σ -donor phosphine, will give a smaller $|^1J_{\text{PSe}}|$ coupling constant (e.g. PPh_3 , $|^1J_{\text{PSe}}| = 732$ Hz; PMe_3 , $|^1J_{\text{PSe}}| = 684$ Hz).^{69,70,71}

1.5.3 – Aminophosphines

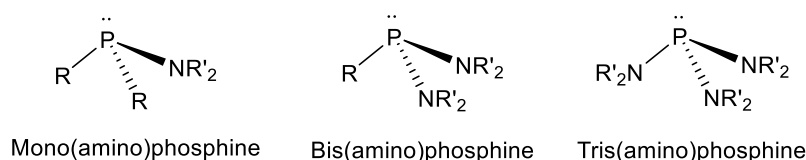


Figure 8 - Mono-, bis- and tris-(amino)phosphines.

Aminophosphines are a class of phosphine compound which take the form $\text{R}_x\text{P}(\text{NR}'_2)_{3-x}$, the first examples of which were reported by Michaelis in 1903.⁷² Aminophosphines consist of a trivalent P^{III} centre singly bonded to at least one trivalent N^{III} centre. A wide variety of aminophosphines have been prepared, including simple mono-, bis- and tris-(amino) variants, as shown in Figure 8, as well as cyclic, cage and polymeric species, some examples of which are shown in Figure 9.⁵¹ Other aminophosphines, with specific functionalities bound to the nitrogen and/or phosphorus atom(s), also exist, for example, phosphonamidites where the trivalent phosphorus centre is bonded to a trivalent nitrogen centre, an oxygen centre and a carbon centre.

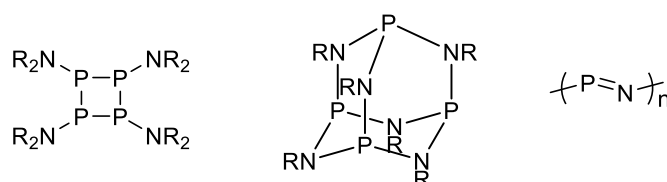


Figure 9- Examples of cyclic, cage and polymeric aminophosphines.⁵¹

X-Ray crystallographic studies of tris(alkylamino)phosphines show that two of the P-N bonds are shorter than the third, and that the nitrogen atoms involved in the shorter bonds adopt a planar geometry, whereas the other adopts a pyramidal geometry.^{73,80} The differences in P-N bond distance arise from only two of the nitrogen lone pairs being able to undergo π -donation towards the phosphorus due to orbital availability at the phosphorus centre.⁵⁵ Each of the three nitrogen atoms pull electron density away from the more electropositive phosphorus centre in a σ -interaction (Figure 10), with one nitrogen centre acting purely as an electron withdrawing moiety, unable to contribute to the π -interaction with the phosphorus atom. In tris(alkylamino)phosphines, the high basicity of the phosphorus centre is as a result of negative hyperconjugation of the nitrogen lone pairs towards the phosphorus centre in a π -interaction (Figure 10).⁸⁰

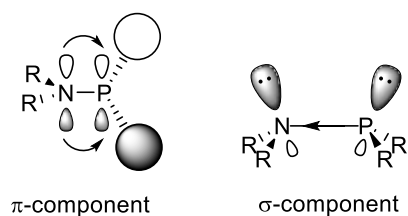
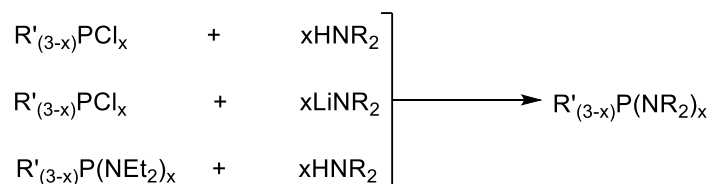


Figure 10 – π - and σ -components of P-N bonding in aminophosphines.⁷⁸

Aminophosphines are readily accessed from primary phosphines *via* a variety of synthetic routes, such as those shown in Scheme 20.^{51,55,80} This ease of tunability of the stereoelectronic nature of the nitrogen and phosphorus centres in aminophosphines (and other *P,N*-ligand species), similarly to phosphines, makes them potentially valuable ligands for asymmetric catalysis.



Scheme 20 – Selected synthetic routes towards aminophosphines.^{49,53,78}

1.6 – Nitrogen- and Phosphorus-containing Bidentate Ligands

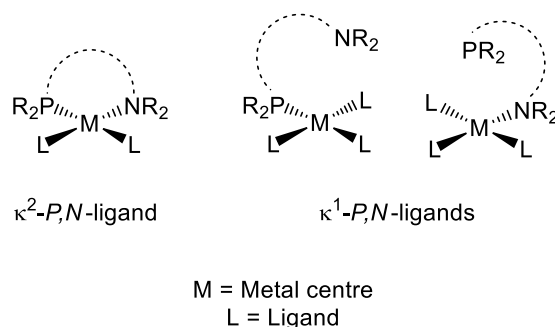


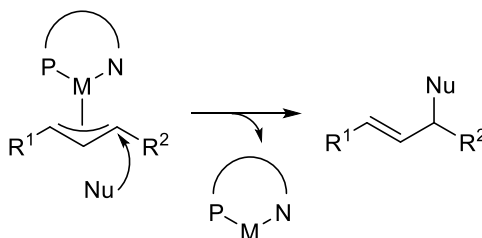
Figure 11 - Representation of κ^2 - and κ^1 -*P,N*-ligands coordinated to a metal centre.

Both κ^1 - and κ^2 -ligands containing a nitrogen and a phosphorus centre, *P,N*-ligands (Figure 11), have been widely investigated in inorganic chemistry, and been found to be of key importance in catalysis. Heteroditopic *P,N*-ligands possess two electronically different donor atoms; these donor centres can be readily tuned to provide the steric and electronic environment at a metal centre that is required for a given process.

1.6.1 – *Trans* Effect for *P,N*-Ligands

Heteroditopic *P,N*-ligands exhibit a kinetic property known as the *trans* effect; this enables these ligands to introduce regioselectivity into reactions occurring at a metal centre and, potentially, in any catalytic processes mediated by that metal complex.^{74,75} In a square planar ligand-metal complex, the lability and reactivity of a ligand is directly influenced by the ligand coordinated *trans* to it, *i.e.* the ligand that shares the same metal *d* orbital.⁷⁶ The rate of ligand substitution is increased by strong σ -donors and strong π -acceptors. Strong π -acceptors draw electron density away from the metal centre *via* a *d* orbital, thus increasing the electrophilicity of the species bound *trans* to it, making it more susceptible to nucleophilic attack and increasing its rate of exchange. However, the donation of electron density into a *d* orbital on a metal centre by a σ -donor causes weakening of the M-L bonding of the species coordinated *trans* to it, so increasing the rate at which the *trans* ligand can be exchanged. The *trans* effect for a phosphine (PR_3) ligand is greater than that of an amine (NR_3) species, therefore, the rate of exchange for a ligand coordinated *trans* to a phosphine will be greater than that of a ligand *trans* to an amine.⁸⁴ This difference in *trans* effect can be made use of in asymmetric catalytic

processes in order to exhibit a control on the site of coordination/reaction of a substrate. An example of this type of control is for nucleophilic substitution of a metal-allyl complex, where nucleophilic substitution will occur preferentially at the more electrophilic allylic terminus, the terminus coordinated *trans* to the phosphorus atom, as shown in Scheme 21.⁸⁴



Scheme 21 – The impact of the differing *trans* influences of N vs P donors on the nucleophilic attack at a metal allyl complex.⁸⁴

1.6.2 – Hemilability of P,N-Ligands

Within a *P,N*-ligand, the nitrogen and phosphorus donor groups provide different electronic contributions to the metal-ligand complex: phosphorus is electronically soft and can exhibit both π -acceptor and σ -donor behaviour, whereas the nitrogen atom is electronically hard and can exhibit only σ -donor properties. When a *P,N*-ligand adopts a κ^2 -*P,N* coordination mode, the amalgamation of the donor-acceptor properties of both centres, and the ability of these ligands to chelate, leads to the lowering of the energy of *d* orbitals at the metal centre. The lowering of the metal centre energy by the κ^2 -*P,N* ligand coordination during a catalytic cycle is achieved *via* the stabilisation of low oxidation states of the metal centre, whilst making the metal centre more prone to oxidative attack.⁸⁴ As a direct consequence of the electronic differences between the nitrogen and phosphorus centres, the harder nitrogen donor will form stronger bonds to hard metal centres (such as Li and Ti), whereas the softer phosphorus donor will show a bonding preference towards soft metal centres (such as Pt, Rh and Ag).⁷⁷ It follows, therefore, that when a *P,N*-ligand is bound to a given metal centre, one donor atom will bind more strongly than the other (*e.g.* in a Pd complex, the softer phosphorus will bind more strongly to the soft metal centre than the electronically harder nitrogen atom) leaving the other donor atom as potentially hemilabile, and able to reversibly dissociate from the metal centre (whilst the other donor remains bound) to provide a vacant coordination site on the metal (Figure 12).⁷⁸ *P,N*-Ligands, therefore, exhibit the advantages of both mono- and bi-

dentate ligands by possessing the ability to provide vacant coordination sites required in catalysis, whilst stabilising reactive metal species.⁷⁴

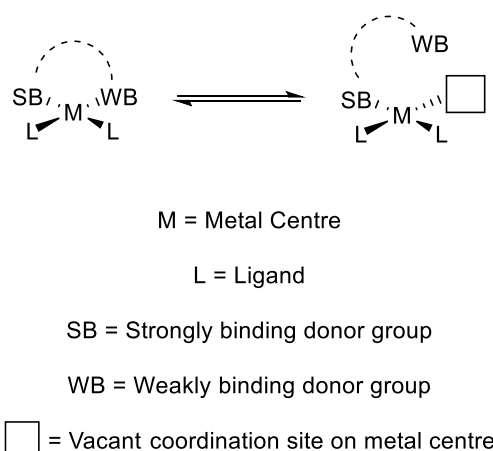


Figure 12 - Proposed hemilability of a heteroditopic ligand on a metal complex.

1.6.3 – Coordination Behaviour of *P,N*-Ligands

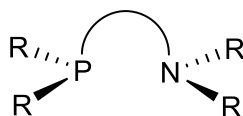


Figure 13 – *P,N*-ligand with a spacer group.

Heteroditopic *P,N*-compounds (Figure 13) have an assortment of applications, including as components of chemotherapeutic and antimicrobial agents, for example.^{51,79} One of the most important use of *P,N*-ligands is in asymmetric catalysis due to their ability to coordinate in either a mono- or bi-dentate fashion (Figure 11), depending on the hard-soft nature of the metal centre.⁸⁴

P,N-ligands of the form $PR_{3-x}(NR_2)_x$ (aminophosphines) readily coordinate to metal centres, preferentially through the phosphorus atom - a range of phosphorus bound examples have been prepared by Dyer and co-workers.⁸⁰ Favoured coordination of $PR_{3-x}(NR_2)_x$ species to a metal *via* the phosphorus centre, instead of through the nitrogen, is attributed to the negative hyperconjugation of the nitrogen lone pair(s) to the phosphorus centre, rendering them “less available” than the phosphorus lone pair.⁸¹ Coordination *via* both the phosphorus and an

adjacent nitrogen atom is seen less often due to high strain in the three-membered P-N-metal systems formed.⁸²

P,N-ligands containing a spacer group between the amine and phosphine functionalities (Figure 13) are of key importance in catalysis and, if the ligand itself is chiral, in asymmetric catalysis. Asymmetric catalysis is achieved by controlling the stereochemical outcome of a process; this is often facilitated by the ligands bound to a metal which can modify the electronic and steric environment about the metal centre to direct how a substrate binds and reacts. Both symmetric (*i.e.* with two equivalent coordinating atoms, *e.g.* BINAP (a diphosphine) and BINOL (a diol))⁸³ and asymmetric (*i.e.* with two inequivalent coordinating atoms, *e.g.* *P,N*-ligands) chiral ligands can be used in metal mediated asymmetric processes. The use of symmetric ligands, however, is advantageous as they reduce the number of reaction pathways and number of substrate-catalyst species that can form. The chelating ability of asymmetric bidentate ligands can facilitate the retention of substrate chirality in order to achieve a desired stereochemical outcome.⁸⁴ Asymmetric bidentate ligands can aid in chirality retention by controlling the orientation of the substrate when in the coordination sphere of the metal centre. *P,N*-Ligands can be used for a wide range of catalytic transformations, three of which are outlined in Table 1.

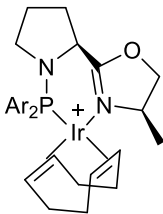
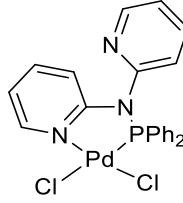
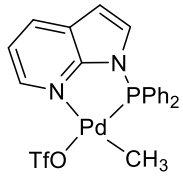
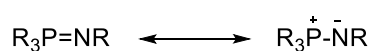
Catalytic Process	Procatalyst	Catalytic Process	Procatalyst
Allylic substitution ⁸⁵		C-C coupling ⁸⁶	
CO/C ₂ H ₄ polymerisation ⁸⁷			

Table 1 – Three examples of procatalysts that incorporate *P,N*-ligands.

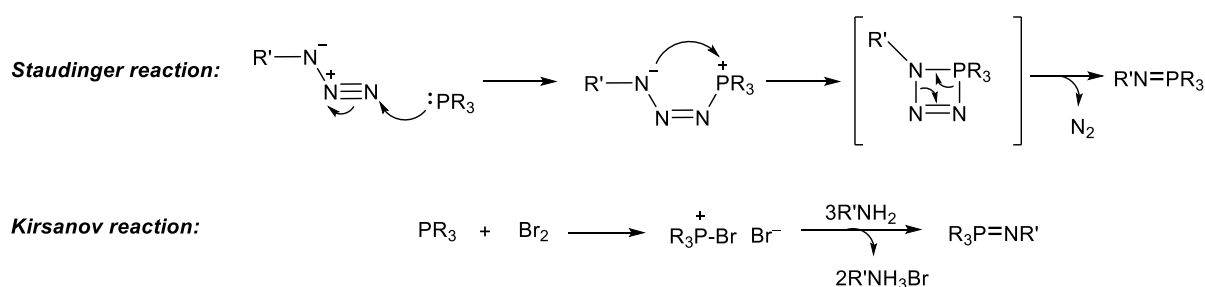
1.6.4 – Iminophosphoranes

Iminophosphoranes are phosphorus- and nitrogen-containing species with the general formula $R_3P=NR$, that can also be described as phosphoranimines, phosphinimines or phosphazenes.⁸⁸ The structure of iminophosphoranes can be interpreted as being a resonance hybrid of the two canonical forms shown in Scheme 22. Iminophosphoranes have a wide and varied number of applications, for example as *aza*-analogues to Wittig reagents ($R_3P=C(R^1)R^2$) for use in *aza*-Wittig reactions,⁸⁹ as building blocks for *P,N*-polymers,⁹⁰ as super bases,⁹¹ and in catalysis.⁸⁸



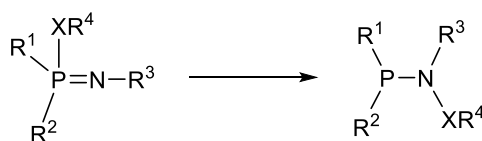
Scheme 22 - Resonance structures of Iminophosphoranes.

Iminophosphoranes are most commonly prepared from phosphines, PR_3 , *via* Staudinger and Kirsanov reactions (Scheme 23).⁹⁰ The Staudinger reaction involves oxidation of a phosphine by an organo-azide,⁹² whereas the Kirsanov reaction proceeds *via* the initial bromination of the phosphine to give a phosphonium salt, followed by treatment with an amine in the presence of a base.⁹³ The chemistry of iminophosphoranes is rich, they are known to undergo a variety of different reactions including hydrolysis, insertion, substitution, oxidation, reduction, rearrangement, cyclisation, cycloaddition and alkylation, the latter four will now be discussed.¹⁰⁵



Scheme 23 - Staudinger and Kirsanov reactions for the preparation of iminophosphoranes.^{92,93}

1.6.4.1 – Rearrangements of Iminophosphoranes



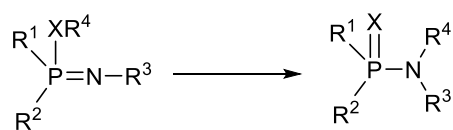
R^{1-4} = Alkyl/Aryl

X = Heteroatom

Scheme 24 – General 1,2-migration of Iminophosphoranes.¹⁰⁵

Iminophosphoranes can readily undergo several different types of intramolecular rearrangement processes.¹⁰⁵ Iminophosphorane species with one or more heteroatoms (*e.g.* O, P, Si or S)^{94,95,96,97} singly bonded to the phosphorus centre are particularly prone to rearrangement reactions. The liability of such species to undergo rearrangements is often believed to be as a consequence of the comparatively weak phosphorus-heteroatom bond being susceptible to cleavage. 1,2-migrations (Scheme 24) are examples of iminophosphorane rearrangements where the phosphorus-heteroatom bond is cleaved, followed by migration of the heteroatom group to the iminophosphorane nitrogen centre, accompanied by the reduction of a P^V to a P^{III} centre.^{95,105}

Iminophosphoranes containing a phosphorus-heteroatom bond can also undergo rearrangement reactions *via* the formation of a more energetically favourable phosphorus-heteroatom double bond. An example of this type of rearrangement is the general 1,3-rearrangement shown in Scheme 25.^{97,105}

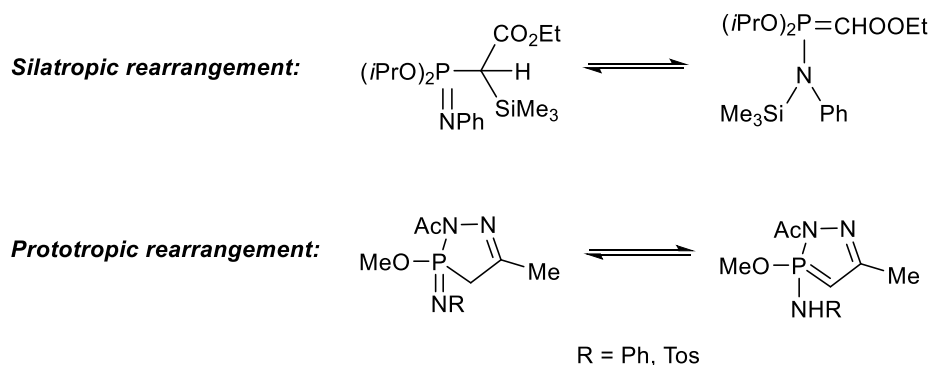


R^{1-4} = Alkyl/Aryl

X = S, O

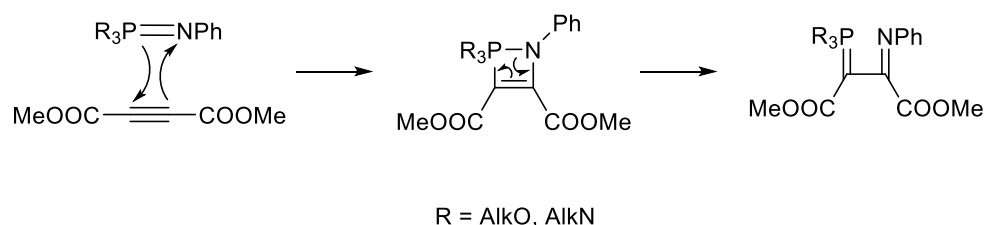
Scheme 25 - General iminophosphorane 1,3-migration.^{97,105}

Iminophosphoranes which possess a C–P=N moiety can undergo rearrangements leading to the formation of a C=P–N motif. This type of process can involve the movement of either a silicon group (silatropic) or a proton (prototropic) as shown in Scheme 26.^{98,105}

Scheme 26 – Silatropic and prototropic iminophosphorane rearrangements.^{98,105}

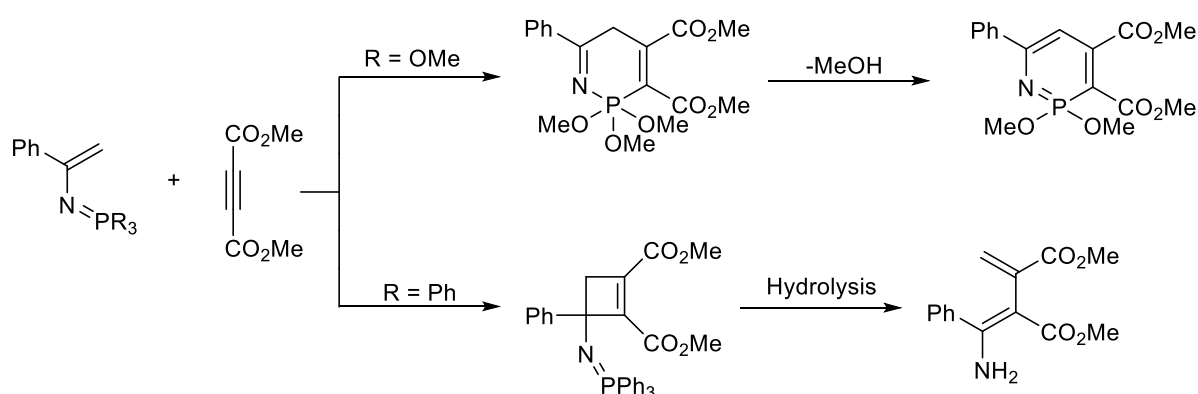
1.6.4.2 – Cycloaddition Reactions of Iminophosphoranes

Iminophosphoranes can readily undergo *pseudo* [2+2] cycloaddition reactions with other unsaturated species due to the presence of the unsaturated phosphorus-nitrogen double bond. The reaction shown in Scheme 27 shows how an iminophosphorane undergoes cycloaddition with the alkyne dimethyl acetylenedicarboxylate (DMAD), to initially form the expected four-membered heterocycle, followed by the breakdown of the four-membered ring to yield a phosphorus ylide.^{101,102}

Scheme 27 – *Pseudo* [2+2] cycloaddition of an iminophosphorane to DMAD.^{101,102}

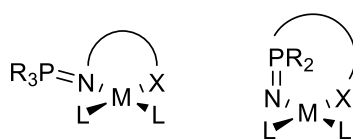
Iminophosphoranes with a C=C bond elsewhere in the structure can readily undergo cycloaddition reactions with other unsaturated species. These cycloaddition reactions can either be *pseudo* [2+2] (with the C=C bond acting as the ene) or [4+2] (with the iminophosphorane acting as the diene); examples of each of these types of cycloadditions are shown in Scheme 28.¹⁰³ The upper route shown in Scheme 28 (R = OMe) shows the [4+2] cycloaddition, which is succeeded by a rearrangement to yield the more stable aromatic species. The lower route in Scheme 28 (R = Ph) shows a *pseudo* [2+2] cycloaddition – the four-

membered ring species formed from the cycloaddition reaction can be hydrolysed to give an unstrained ring-open compound.¹⁰³



Scheme 28 - Cycloaddition reactions of an iminophosphorane containing a C=C bond.¹⁰³

1.6.4.3 – Coordination Behaviour of Iminophosphoranes



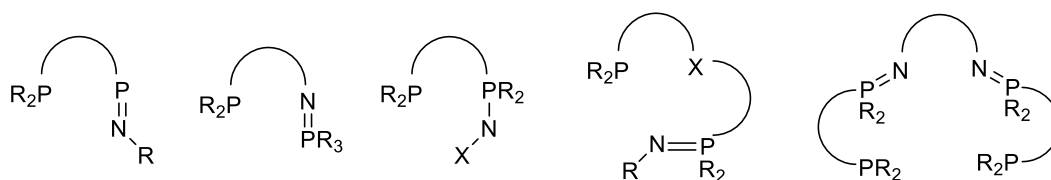
X = N, P, O, As or C

M = metal centre

L = ligand

Figure 14 – Coordination of iminophosphorane scaffolds containing other donor groups.⁸⁸

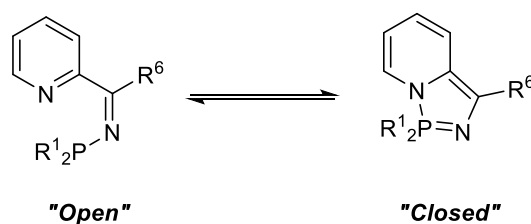
Iminophosphoranes can coordinate to a metal centre *via* the lone pair of electrons on the nitrogen atom. Iminophosphorane scaffolds containing other donor groups (*e.g.* N-, P-, O-, As- or C-groups) within their structure give the ligand the ability to coordinate to a metal centre in a polydentate fashion (Figure 14).⁸⁸ κ^2 -Coordination of a ligand increases the stabilisation of the metal centre relative to the κ^1 -coordination of the ligand.⁸⁸ Iminophosphorane-phosphine ligands, which can coordinate in either a mono- or bi-dentate fashion, have been found to have many uses in homogeneous catalysis. The structures of iminophosphorane-phosphine species are varied and can contain more than just iminophosphorane and phosphine donor groups, some examples of the general types of ligands employed in homogeneous catalysis are shown in Figure 15.⁸⁸



X = CH₂, NH, O or S

Figure 15 - Some iminophosphorane-phosphine ligand types used in homogeneous catalysis.⁸⁸

1.7 – Investigations into the Interconverting Pyridyl-*N*-Phosphinoimine – Diazaphosphazole Tautomers



Scheme 29 - Dynamic tautomeric equilibrium of the "open"-*"closed"* P,N-species.

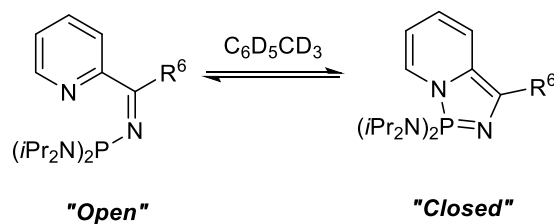
In order to exploit the potential non-innocence of the "open" pyridyl-*N*-phosphinoimine species (Scheme 29), a full understanding of the factors that impact upon the tendency of these phosphinoimines to cyclise (to form a "closed" diazaphosphazole, Scheme 29) is essential. Once understood, this opens the way to gaining an insight into the chemical reactivity of both *P,N*-tautomers shown in Scheme 29. Hence, the following sections (**1.7.1**, **1.7.2** and **1.7.3**) will examine the structural and chemical reactivity studies previously reported by Dyer and co-workers.

1.7.1 – Factors Affecting the Position of the "Open"-*"Closed"* Equilibrium of the Pyridyl-*N*-Phosphinoimines

In order to probe the factors affecting the position of the "open"-*"closed"* equilibrium (Scheme 29), Dyer and co-workers investigated the stereoelectronic impact of groups R¹, R² and R⁶ (Figure 1).^{2,3} A series of phosphinoimines were studied, and the ratio of "open":*"closed"* tautomers determined by ³¹P NMR spectroscopy at 298 K. The "open" and "closed" tautomers were found to give rise to distinct resonances in ³¹P NMR spectra; the

“open” form displays a singlet resonance around $\delta_P \sim +70$ ppm, consistent with *N*-bis(dialkylamino)phosphinoimines, and the “closed” tautomer a singlet resonance around $\delta_P \sim +40$ ppm, in agreement with anellated σ^4 - $1\lambda^5$ -[1,3,2]diazaphospholes.^{2,99}

1.7.1.1 – Effect of Temperature on the “Open” and “Closed” Tautomers



Compound	R ⁶	% "Closed" tautomer		
		223 K	298 K	363 K
A	Ph	98	95	75
B	Anthracenyl	-	45	20

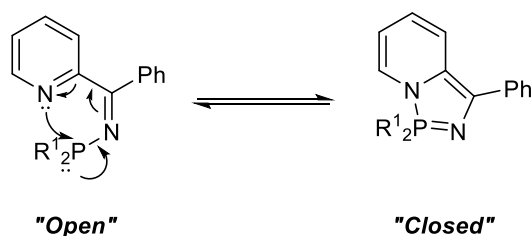
Figure 16 – Variable temperature NMR results for compounds **A** and **B**.^{2,3}

Variable temperature ³¹P NMR spectroscopic studies were carried out to investigate how the position of the “open”-“closed” equilibrium (Scheme 29) changes with temperature; the results for compounds **A** and **B** are shown in Figure 16.^{2,3} Examination of the data presented in Figure 16 shows not only that the tautomerism is dynamic, but that an increase in temperature decreases the relative amount of “closed” tautomer observed. This decrease in percentage “closed” tautomer with an increase in temperature indicates that the “closed” species is the kinetic tautomer.

1.7.1.2 – Stereoelectronic Impact of the Phosphorus Substituent Upon the “Open”-“Closed” Equilibrium Position

The proposed *pseudo*-1,5-electrocyclisation mechanism for the cyclisation of the “open” phosphinoimine species described in Scheme 2 shows the attack of the pyridine nitrogen lone pair at the phosphorus centre. For this nitrogen-phosphorus interaction to be favourable, the

phosphorus centre must be electrophilic, and must therefore possess electron withdrawing substituents. This requirement for an electron deficient phosphorus centre in order for ring closure to occur is readily apparent from the examination of the “open”：“closed” ratios for reported species **A** and **C-H** shown in Figure 17.^{1,2,3}



Compound	R ¹ Substituent	"Open"：“Closed" (in C ₆ D ₆ at 298 K)
A	NiPr ₂	5:95
C	½ OC ₂ H ₄ O	0:100
D	½ MeNC ₂ H ₄ NMe	0:100
E	Ph	100:0
F	<i>i</i> Pr	100:0
G	<i>t</i> Bu	100:0
H	Cy	100:0

Figure 17 – “Open”：“closed” ratios for compounds **A-H**.^{1,2,3}

Alkyl/aryl phosphorus substituents (as for compounds **E-H**, Figure 17) give rise to the iminophosphorane species existing exclusively in the “open” form, whereas σ -electron withdrawing substituents, such as NiPr₂ (**A**), lead to electron deficient phosphorus centres, and therefore favour its attack by the pyridine nitrogen lone pair.^{1,2,3} These observations are consistent with the *pseudo*-1,5-electrocyclisation process proposed as a result of DFT studies on the mechanism (Figure 17).

Upon closer examination of compounds **A** and **D** (Figure 17), it can be seen that, although their R¹ substituents are both dialkylamino groups, and therefore electronically comparable, **D** exists solely as its “closed” form, whereas **A** exists in both “open” and “closed” forms. This difference in equilibrium position between compounds **A** and **D** can be attributed to the size difference between the R¹ substituents, with the larger NiPr₂ groups sterically hindering

cyclisation of **A-Open** to **A-Closed**, whereas the MeNC₂H₄NMe moiety does not impose the same steric constraints.

1.7.1.3 – Stereoelectronic Impact of the Pyridine Substituents Upon the “Open”-“Closed” Equilibrium Position

The substitution of groups onto a pyridine ring inductively changes the electronics of the system, notably the nitrogen centre (section 1.4.2). When an alkyl substituent is introduced at the 2-position of the pyridine ring, for example for 2-substituted pyridines, an increase in size of the substituent decreases the basicity of the pyridine species as a result of steric blocking of the nitrogen lone pair (section 1.4.2.1). It follows, therefore, that substitution on the pyridine moiety of the pyridyl-*N*-phosphinoimine will impact upon the extent of its cyclisation, as can be seen by the comparison of compounds **A** and **I**, Figure 18.²

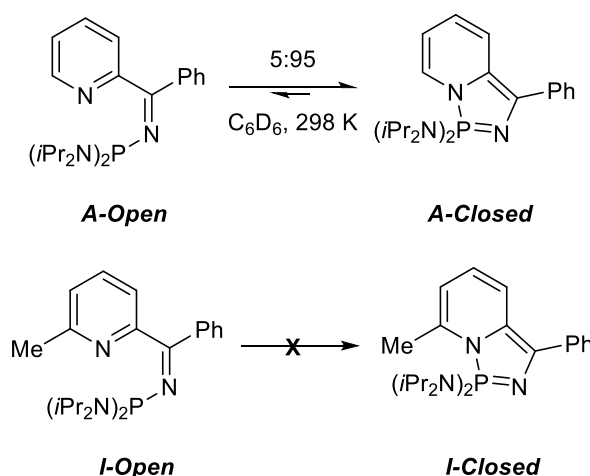
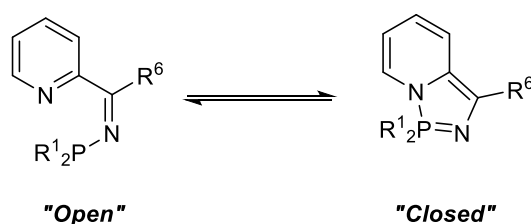


Figure 18 – “Open”-“closed” equilibrium for **A** and **I**.²

Compound **I-Open** does not undergo ring closure, even after prolonged heating at 365 K, this contrasts with what is observed for compound **A**, which exists primarily in its “closed” form (Figure 18). The apparent inability of **I-Open** to cyclise to form **I-Closed** is attributed to an unfavourable steric interaction between the methyl substituent on the pyridine ring and (N*i*Pr₂) groups at the phosphorus centre (Figure 19). Computational studies carried out (at the B3LYP/6-31G** level of theory) into the energy difference between compounds **I-Open** and **I-Closed** revealed that **I-Closed** is 20.2 kcal mol⁻¹ higher in energy than **I-Open**, an energy

1.7.2 – Reactions of the Pyridyl-*N*-Phosphinoimines with Small Molecules

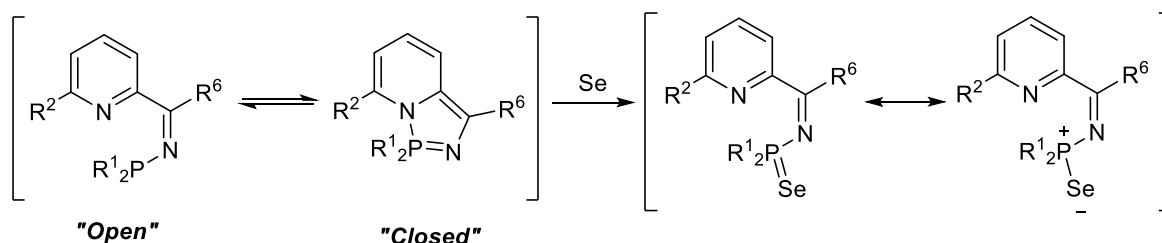


Scheme 30 - Dynamic tautomeric equilibrium of the *P,N*- species.

The interconverting *"open"* and *"closed"* species shown in Scheme 30 can be regarded as phosphinoimines and iminophosphoranes, respectively. The different functionalities present in the *"open"* and *"closed"* species, as well as the reversible, dynamic interconversion between the two, poses the question of how an equilibrium mixture of these tautomers react. The following sections (1.7.2.1-1.7.2.5) will outline the reactivity of these dynamic tautomers with small molecules.

1.7.2.1 – Reaction of the Pyridyl-*N*-Phosphinoimines with Selenium

The reaction of an equilibrium mixture of the pyridyl-*N*-phosphinoimine species with elemental selenium yields the phosphorus(V) monoselenide of the *"open"* tautomer, which takes the form shown in Scheme 31.^{1,2,3} For all the monoselenides prepared (including those of compounds **A-E**, Figure 17), no reaction between grey selenium and the *"closed"* tautomer occurs.³



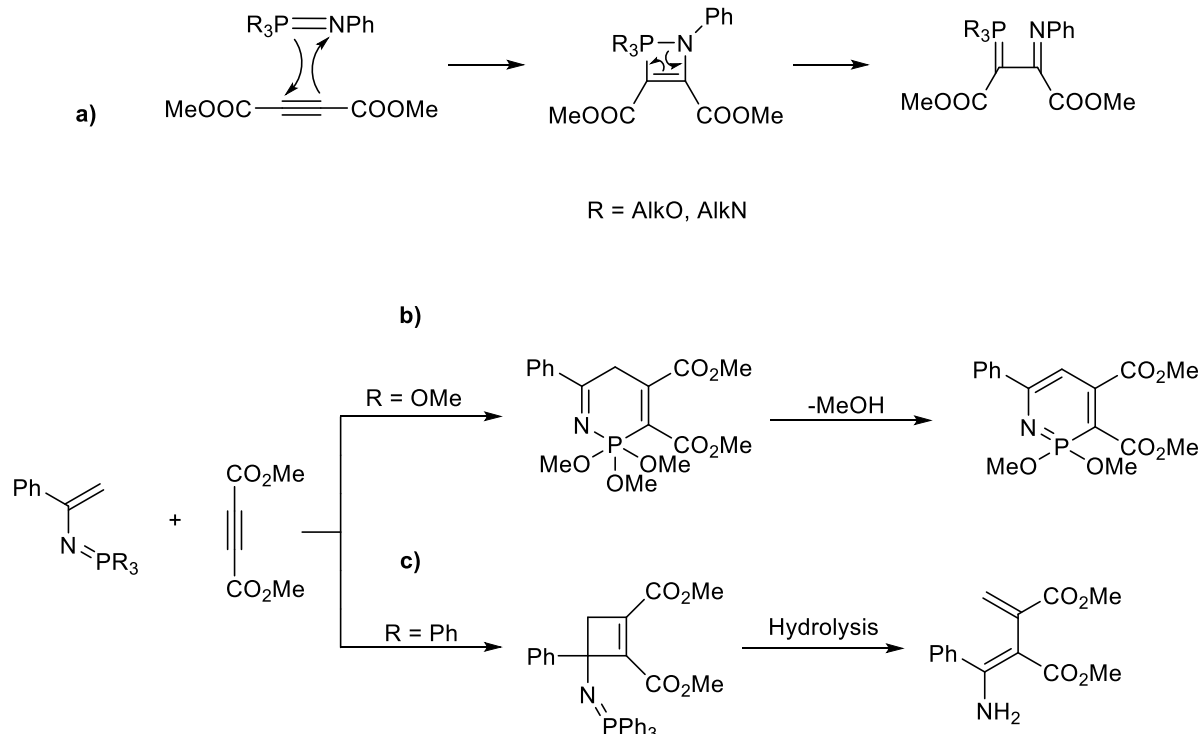
Scheme 31 – Synthesis of the *"open"* phosphorus(V) monoselenides.^{1,2,3}

The formation of the *"open"* monoselenides of compounds **A**, **C** and **D** (Figure 17) is particularly noteworthy as **A**, **C** and **D** exist between 95%-100% in their *"closed"* forms (by ³¹P NMR spectroscopic analysis).³ For the *"open"* monoselenides of **C** and **D** (100% *"closed"*) to

form, these species must exist, to some extent, however negligible, in their “open” forms. The “open” forms of compounds **C** and **D** must be present in concentrations below the ^{31}P NMR spectroscopic detection limit.¹⁰⁰

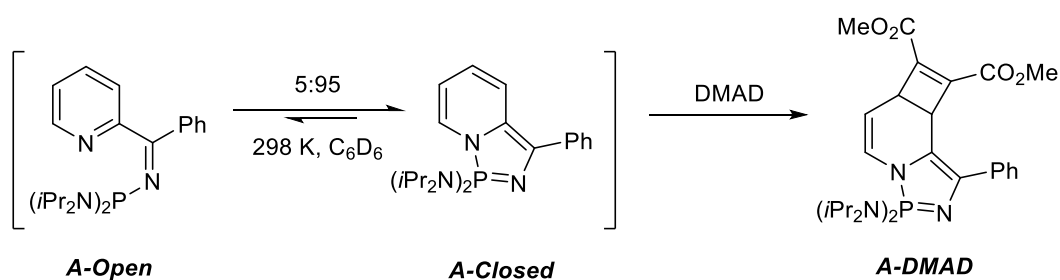
1.7.2.2 – Reactions of the Pyridyl-*N*-Phosphinoimines with Dimethyl Acetylenedicarboxylate (DMAD)

The reaction of compound **A** with dimethyl acetylenedicarboxylate (DMAD) was investigated in order to probe the multifunctional reactivity of **A**.² Iminophosphoranes are known to undergo *pseudo* [2+2] cycloaddition reactions with the electron-deficient alkyne, DMAD, as shown in Scheme 32 (route **a**).^{101,102} Reactions **b** and **c**, Scheme 32, show how iminophosphoranes with a C=C group elsewhere within the structure can undergo two different cycloaddition reactions with DMAD, depending on the nature of the groups bound to the phosphorus centre – *pseudo* [2+2] cycloaddition at the C=C double bond and also a [4+2] cycloaddition with the unsaturated iminophosphorane acting as the diene.¹⁰³

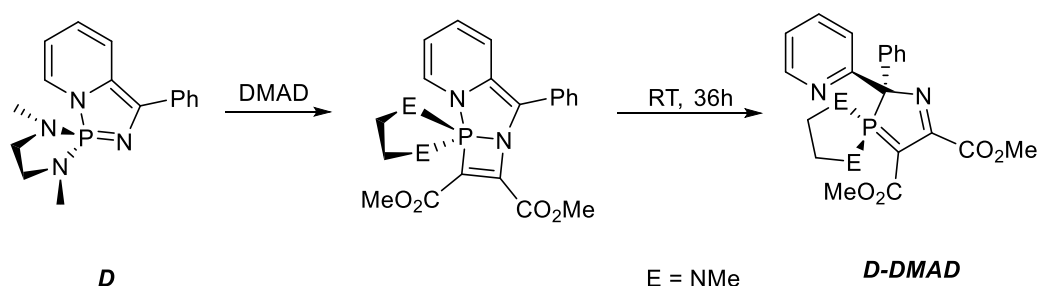


Scheme 32 – *Pseudo* [2+2] cycloaddition of DMAD with an iminophosphorane.^{101,102,103}

When the reaction between DMAD and compound **A** was carried out, neither a *pseudo* [2+2] cycloaddition at the P=N double bond (likely prevented by steric hindrance at the phosphorus centre), nor a [4+2] cycloaddition with the dienic fragment of the de-aromatised pyridine motif, was observed. Instead, a *pseudo* [2+2] cycloaddition at one of the de-aromatised dihydropyridine ring C=C double bonds took place to yield the species shown in Scheme 33.² This type of reactivity towards DMAD is consistent with that of *N*-substituted dihydropyridines, which act as enamines to yield cyclobuta[*b*]pyridines.¹⁰⁴

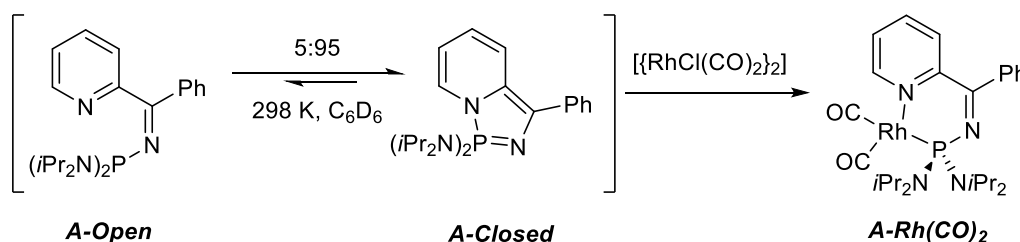
Scheme 33 - Reaction of **A** with DMAD.²

For diazaphosphazole species where the degree of steric bulk about the phosphorus centre is less, such as compounds **C** and **D** (Figure 17), the *pseudo* [2+2] cycloaddition between DMAD and the P=N double bond occurs (Scheme 34), as generally anticipated for iminophosphoranes.^{3,101,102} Interestingly, upon leaving the cycloaddition product from the reaction between **D** and DMAD at room temperature for 36 hours, an unprecedented rearrangement occurs to form a spiro-species (*via* a ring expansion of the initial *pseudo* [2+2] cycloaddition product), Scheme 34.

Scheme 34 - Reaction of DMAD with **D**.³

1.7.2.3 – Reaction of the Pyridyl-*N*-Phosphinoimines with $[\{\text{RhCl}(\text{CO})_2\}_2]$

The coordination of compound **A** to a soft Lewis acidic rhodium centre was probed by carrying out its reaction with $[\{\text{RhCl}(\text{CO})_2\}_2]$. The ^{31}P NMR spectrum of the reaction mixture revealed the formation of a single species (Scheme 35), a rhodium metal complex whereby *P,N*-ligand **A** coordinates to the rhodium centre *via* the phosphorus and pyridine nitrogen centres.² Complete conversion to the rhodium complex **A-Rh(CO)₂** is achieved.

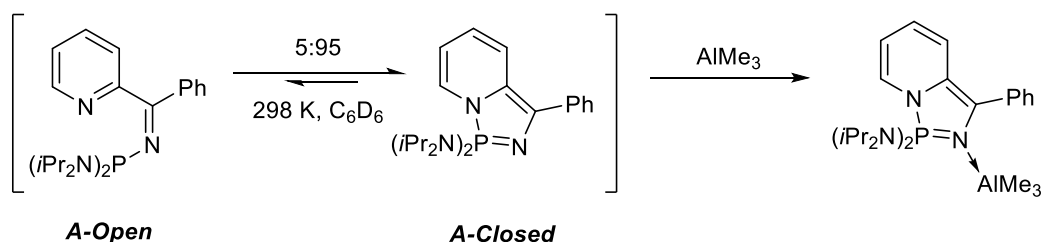


Scheme 35 - Reaction between **A** and $[\{\text{RhCl}(\text{CO})_2\}_2]$.²

The κ^2 -*P,N* coordination mode of compound **A** results from the favourable interaction of the soft phosphorus centre with the soft rhodium centre, and the formation of a favourable six-membered chelate by the coordination of the hard nitrogen centre.² The coordination of the “open” form causes a shift in the “open”-“closed” equilibrium to the “open” form in accordance with Le Chatelier’s Principle. Coordination of the “closed” tautomer, which possesses an available lone pair on the hard-iminophosphorane nitrogen centre, does not occur as the lone pair on the phosphorus(V) centre is unavailable, and therefore favourable soft(P)-soft(Rh) interaction cannot occur.

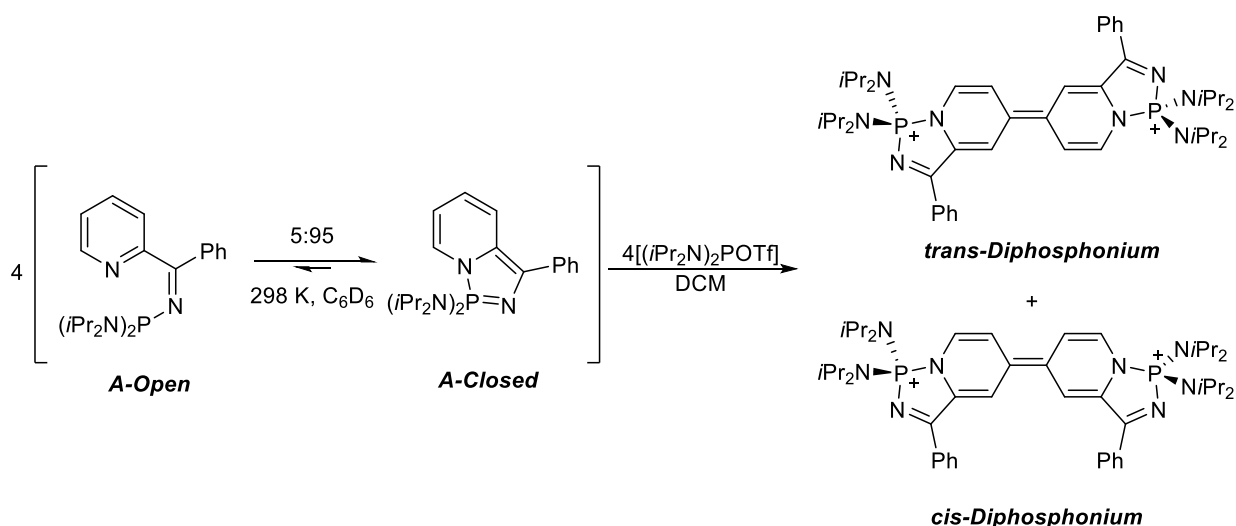
1.7.2.4 – Reaction of the Pyridyl-*N*-Phosphinoimines with AlMe_3

Compound **A** was reacted with AlMe_3 to yield a single species, in which **A-Closed** coordinates to the hard Lewis acidic aluminium centre *via* the hard nitrogen centre of the P=N bond, as shown in Scheme 36. The observed coordination of **A-Closed** to AlMe_3 is concordant with what is seen more generally when iminophosphoranes react with hard Lewis acids, *e.g.* the $\text{N} \rightarrow \text{Al}$ coordination in $[(\text{Et})_2(\text{Cl})\text{P}=\text{NPh}](\text{AlCl}_3)$.^{105,106}

Scheme 36 - Reaction of **A** with AlMe_3 .²

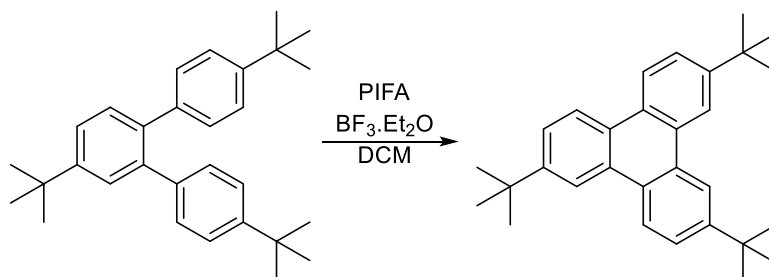
1.7.2.5 – Reaction of Iminophosphorane **A** with bis(Diisopropylamino)Phosphenium Triflate

Phosphenium cations, $[\text{R}_2\text{P}^+]$, are considered to be isolobal to carbenes, $[\text{R}_2\text{C}]$, and can be stabilised by the presence of amino groups.¹⁰⁷ The σ -electron withdrawing amino groups in the $[(i\text{Pr}_2\text{N})_2\text{P}]^+$ cation, for example, acts to stabilise the cationic phosphorus centre by withdrawal of the phosphorus lone pair electron density and the donation of nitrogen lone pair electron density into the vacant p -orbitals on the phosphorus centre.¹⁰⁷ Phosphenium cations are ambiphilic, and can therefore act as either Lewis acids or Lewis bases.

Scheme 37 – Reaction of **A** with bis(diisopropylamino)phosphenium triflate.¹⁰⁸

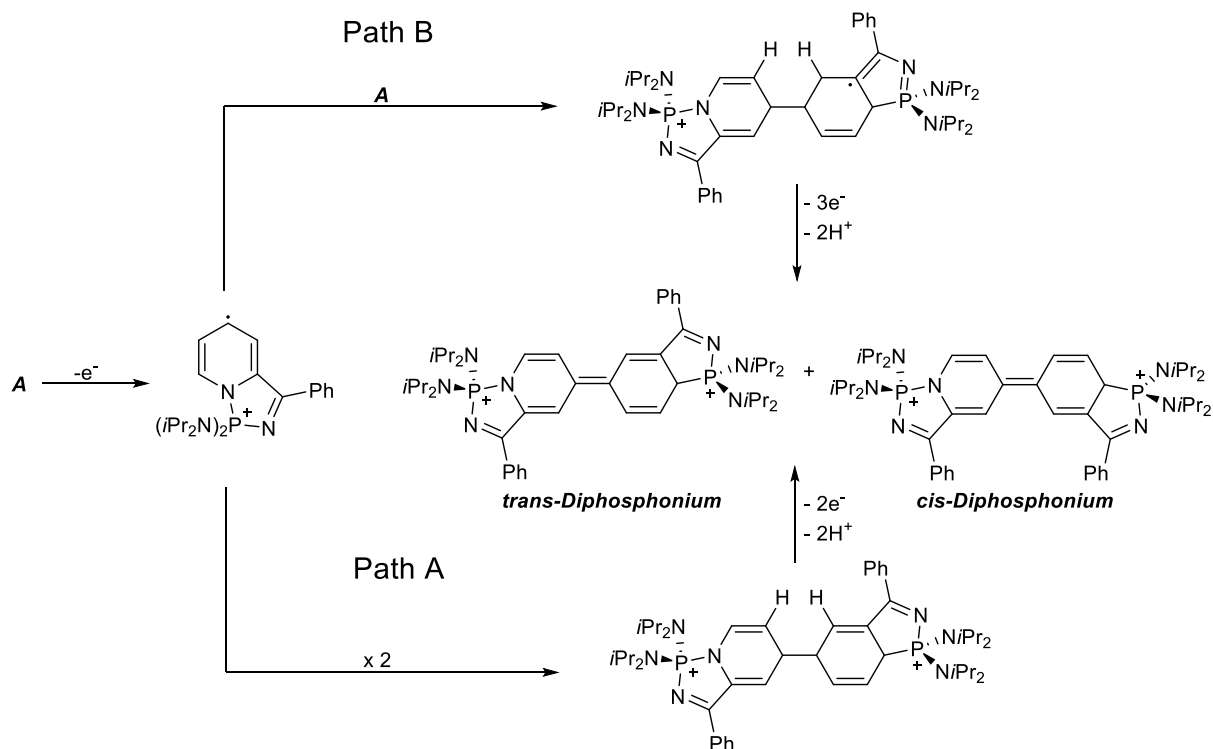
The reactivity of compound **A** towards the ambiphilic phosphenium salt $[(i\text{Pr}_2\text{N})_2\text{P}][\text{OTf}]$ was probed, and found to yield two products, **cis-Diphosphenium** and **trans-Diphosphenium** (Scheme 37), in a 1:1 ratio.¹⁰⁸ The **cis-Diphosphenium** and **trans-Diphosphenium** products possess a planar $1H,1'H-4,4'$ -bipyridylidene scaffold with a $\sigma^4\text{-}\lambda^4\text{-}[1,3,2]$ diazaphosphole group

at each end. The mechanism for the reaction shown in Scheme 37 is proposed to proceed *via* a radical mechanism that can be likened to Scholl reaction (Scheme 38).¹⁰⁹



Scheme 38 – Example of a Scholl coupling reaction reported by King and co-workers.¹⁰⁹ PIFA = phenyliodine bis(trifluoroacetate).

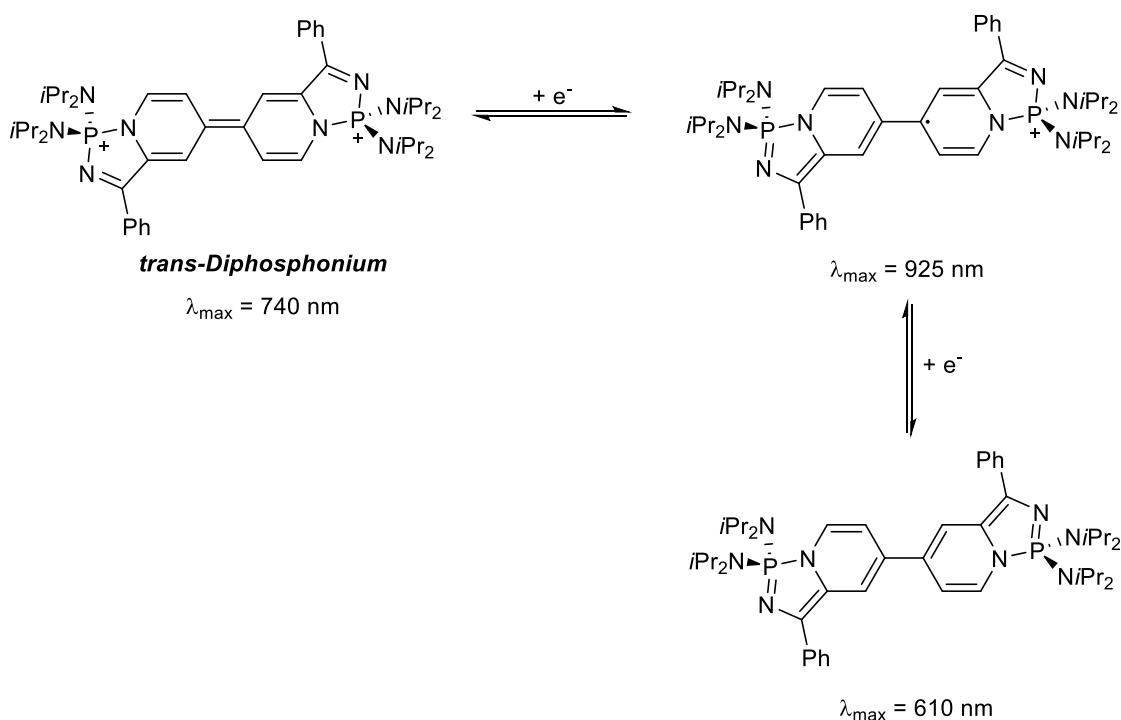
Based on the formation of small quantities of $[\text{iPr}_2\text{NH}_2][\text{OTf}]$ (as a result of the generation of acid from the reaction between compound **A** and $[(\text{iPr}_2\text{N})_2\text{P}][\text{OTf}]$), as well as the 1:1 ratio of *cis-Diphosphonium*:*trans-Diphosphonium* observed, two mechanisms for the formation of *cis-Diphosphonium* and *trans-Diphosphonium* have been proposed, which both start with the formation of a radical cation (Scheme 39). The radical cation can take one of two pathways to yield *cis-Diphosphonium* and *trans-Diphosphonium*: Path A (Scheme 39), where the coupling between two equivalents of the radical cation occurs followed by the loss of two protons; Path B (Scheme 39), where the radical cation reacts with a second equivalent of compound **A**, then undergoes a double deprotonation and oxidation.¹⁰⁸



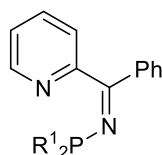
Scheme 39 - Proposed mechanisms for the formation of *cis-Diphosphonium* and *trans-Diphosphonium*.¹⁰⁸

The structures of *cis-Diphosphonium* and *trans-Diphosphonium* are reminiscent of the dication of the doubly reduced viologen, *N,N'*-dimethyl-4,4'-bipyridinium.¹¹⁰ TD-DFT studies (at the B3LYP-6-31G* level of theory) carried out on *cis-Diphosphonium* and *trans-Diphosphonium* showed a number of electronic similarities with the doubly reduced *N,N'*-dimethyl-4,4'-bipyridinium cation, including that the π -electron density is conjugated across the 4,4'-bipyridylidene core as well as the imine groups.¹⁰⁸ Viologens are of particular interest due to their electrochromic properties, which are responsible for their varied applications, such as in electron relays and redox mediators.^{110,111}

A more in depth study of the electronic properties of *cis-Diphosphonium* and *trans-Diphosphonium* revealed that they could readily undergo two reversible one-electron reductions (as shown for *trans-Diphosphonium* in Scheme 40).¹⁰⁸ The first of these single-electron reductions gives rise to a monocationic radical, which subsequently undergoes a second reduction to form a neutral bis(benzannulated diazaphosphazole). These single-electron reductions are each accompanied by a change in λ_{\max} , as shown in Scheme 40 for *trans-Diphosphonium*.¹⁰⁸ The tunability of the extended π -conjugated *cis-Diphosphonium/trans-Diphosphonium* systems, and the associated changes in their photochemistry, make them of particular interest for potential use in OLEDs.^{112,113}



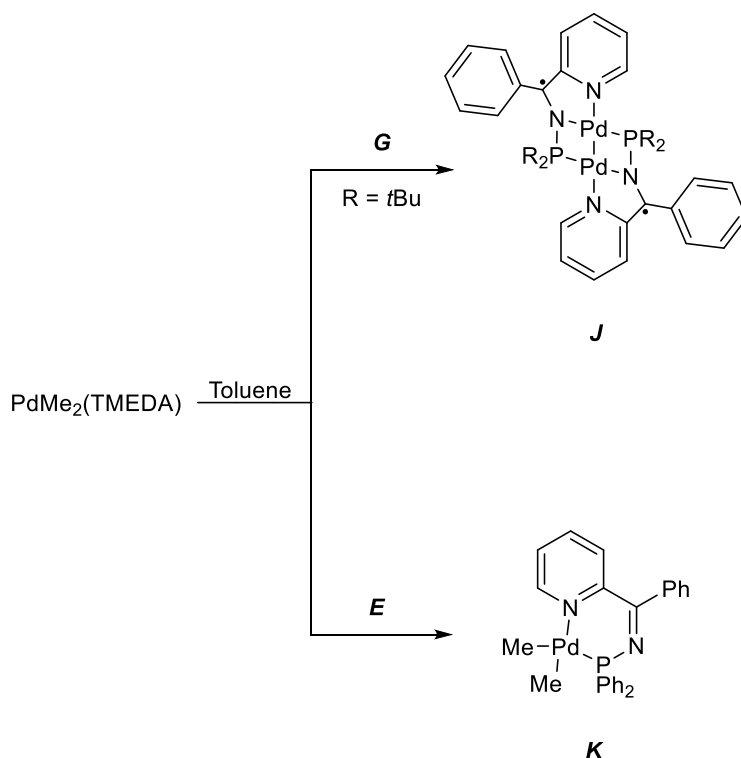
Scheme 40 – Redox properties of *cis/trans-Diphosphonium* – λ_{\max} values recorded in DCM.¹⁰⁸

1.7.3 – Non-Innocent Ligand Behaviour of Pyridyl-*N*-Phosphinoimines

$R^1 = iPr_2N$ (**A-Open**), Ph (**E**), *t*Bu (**G**)

Figure 21 – Compounds **A**, **E** and **G**.⁴

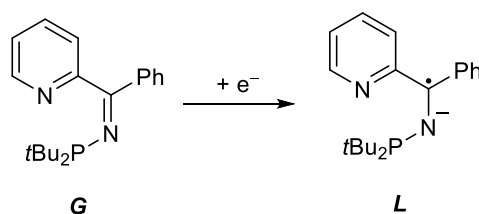
The chemistry of non-innocent ligands (NILs) has been discussed at length in section 1.2, the studies carried out by Dyer and co-workers into the non-innocent properties of compounds **A**, **E** and **G** (Figure 21), which are reminiscent of Wieghardt's NILs,⁸ will now be discussed. The use of NILs in palladium catalysis is a field that has received surprisingly little attention despite the potential for NILs to meet the contrasting steric and electronic requirements of oxidative addition and reductive elimination. Consequently, Dyer and co-workers investigated how NILs **A-Open**, **E** and **G** (Figure 21) behave when bound to a palladium centre.⁴



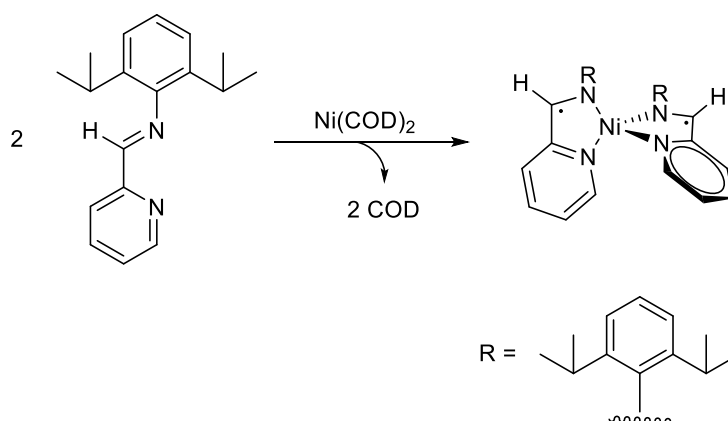
Scheme 41 - Synthesis of complexes **J** and **K**.⁴

Compound **A**, which exists in a dynamic tautomeric equilibrium between an “open” (**A-Open**) and “closed” (**A-Closed**) form (Scheme 30), exhibits interesting redox activity and can behave as a κ^1-N or κ^2-P,N ligand, depending on the nature of the metal centre to which it

coordinates.^{2,3,4} Neither compounds **E** nor **G**, however, are observed to undergo ring closure, they exist solely in their “open” form and behave as κ^2 -*P,N* ligands.^{1,2,4} Unsaturated palladium(0) species display heightened activity in cross-coupling reactions, and their formation can be promoted by the presence of bulky ligands at the metal centre (such as *t*Bu) which provide the steric crowding required for the generation of low coordinate platinum(0) species.¹¹⁴ Based on the evidence reported in the literature, compound **G**, which possesses *t*Bu groups at the phosphorus centre, fulfils the structural requirement of ligands in Pd(0) species that encourage cross-coupling reactions. In order to explore the potential use of compound **G** in cross coupling reactions, complex **J** was prepared from PdMe₂(TMEDA) and **G** (Scheme 41).^{4,115}

Scheme 42 - Redox conversion of **G** to **L**.⁴

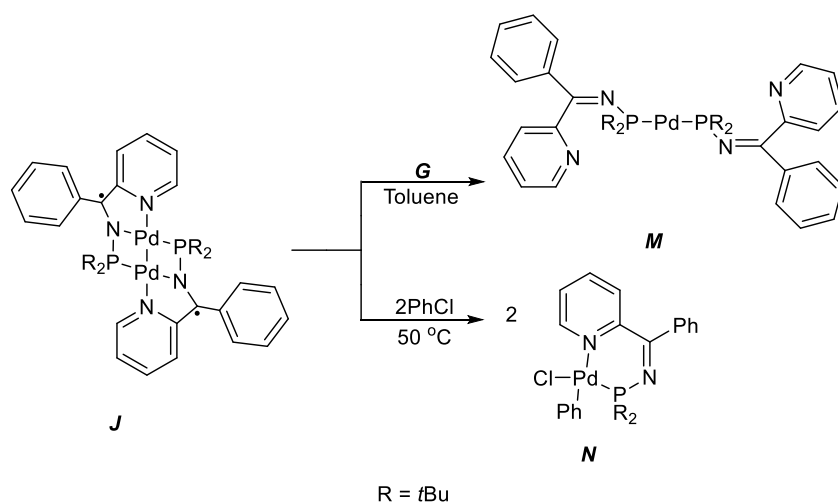
The crystallographic data for complex **J** suggest that, during its formation, **G** has undergone a single electron reduction to give a monoanionic radical species, **L** (Scheme 42), which then coordinates to the palladium(0) centre. This single electron reduction **G**, followed by coordination to a metal centre, is reminiscent of the formation of the nickel complex reported by Wieghardt and co-workers shown in Scheme 43.⁵

Scheme 43 – Nickel complex reported by Wieghardt and co-workers.⁵

The reaction to prepare the analogous complex to **J** from compound **E** and PdMe₂(TMEDA) was unsuccessful, and only yielded species **K** (Scheme 41).⁴ No reaction was observed

between compound **A** and PdMe₂(TMEDA), something that has been tentatively attributed to the chelating TMEDA ligand being unable to be displaced by the weakly Lewis acidic phosphine group.⁴

The chemistry of complex **J** was investigated in order to probe the effect of disrupting the coordination sphere of the palladium centre. The role of the bridging phosphorus ligands was first investigated. It was found that, upon disruption of the κ^1 -P bridging interaction by using 2 equivalents of PPh₃, [Pd⁰(PPh₃)(**G**)] was formed.⁴ Secondly, the stable species **M** was prepared *via* the reaction of **J** with **G** (Scheme 44). The observed κ^1 -P coordination (in preference to κ^2 -P,N coordination) of ligand **G** in compound **M**, has also been seen in other comparable species, and the coordination preference is attributed to the soft nature of the palladium centre.^{4,116} These two reactions of complex **J** demonstrate how modification of the binding mode of the phosphorus species leads to the oxidation of **J** and reduction of the palladium centre.⁴

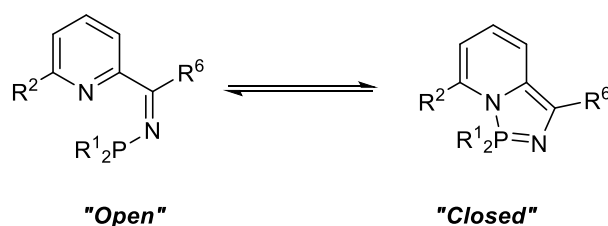


Scheme 44 - Reactions of complex **J**.⁴

Cleavage of the palladium-palladium bond in complex **J** can also be achieved by its treatment with two equivalents of chlorobenzene and heating at 50 °C, this yields complex **N** (analogous to **K**, Scheme 41).⁴ The incorporation of both the chloro and organic moiety into complex **N** is indicative of the reaction proceeding by a redox-dissociation step to give a palladium(0) intermediate, which undergoes oxidative addition to give **N** – not *via* a binuclear process.

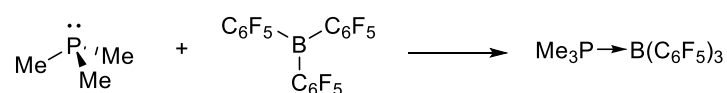
1.8 – Frustrated Lewis Pairs

Section 1.1 details the valence tautomerism of a series of pyridyl-*N*-phosphinoimines of the general form shown in Scheme 45.^{2,3,4} The position of this dynamic tautomeric equilibrium has been shown to be dependent on temperature and the stereoelectronic nature of groups R¹, R² and R⁶ (Scheme 45).^{2,3,4}



Scheme 45 – Valence tautomer of iminophosphorane species reported by Dyer and co-workers.

The “*open*” tautomer (Scheme 45) can be regarded as an intramolecular FLP, with a Lewis basic pyridine nitrogen centre and a Lewis acidic phosphorus centre. Dyer and co-workers have shown that the formation of the Lewis adduct (“*closed*” tautomer) can be precluded by tuning groups R¹, R² and R⁶, for example, by the installation of a bulky electron donating substituent (*e.g.* *t*Bu) at the P centre. In light of this FLP-type character of the “*open*” species, the following section of this thesis (section 1.8) will outline some of the rich chemistry and applications of FLPs, some of which will be explored in **Chapter 4** of this thesis.

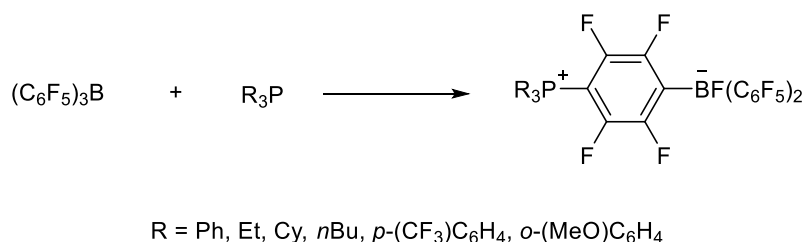


Scheme 46 – Classical Lewis acid-base adduct formation.

The terms Lewis acid and Lewis base were first coined in 1923 to describe species that act as electron pair acceptors and electron pair donors, respectively.¹¹⁷ Lewis acids, such as B(C₆F₅)₃, have low lying LUMOs that can readily accept electron density from the high-energy HOMOs of Lewis bases, such as PMe₃, to form a classical Lewis acid-base adduct, as shown in Scheme 46.

In 1942 Brown and co-workers reported that 2,6-dimethylpyridine and triphenylphosphine did not combine to form the expected Lewis adduct, this unexpected result was not fully

understood at the time, and was attributed to the steric crowding about the P and B centres.¹¹⁸ The emergence in the literature of many more examples of Lewis acids and bases that do not combine to form the Lewis adduct has occurred since 1942, and such systems are referred to as “frustrated Lewis pairs” (FLPs).¹¹⁹ One key example, that was first reported by Stephan and co-workers, shows the reaction between a series of sterically hindered phosphines and $B(C_6F_5)_3$ to give the zwitterionic species (in preference to a Lewis adduct) shown in Scheme 47.^{120,121}



Scheme 47 – Reactions of sterically hindered phosphines with $B(C_6F_5)_3$.^{120,121}

FLPs can form in an intermolecular manner (such as the species shown in Scheme 47), as well as in an intramolecular fashion, as shown in Figure 22.^{122,123} The $PMes_2-B(C_6F_5)_2$ FLP shown in Figure 22 is a weakly interacting FLP, with a P-B distance of 2.2 Å. DFT studies reveal that the $PMes_2-B(C_6F_5)_2$ FLP can exist in two conformers, one where the terminus groups angle gauche to each other, and the other where the groups are anti-periplanar.¹²² Vicinal and geminal FLPs are also known, an example of each is shown in Figure 22.¹²³ The geometric constraint imposed by the double bond in the vicinal species prevents any interaction between the P and B centres, and DFT studies show no interaction between these centres in the geminal analogue.¹²³

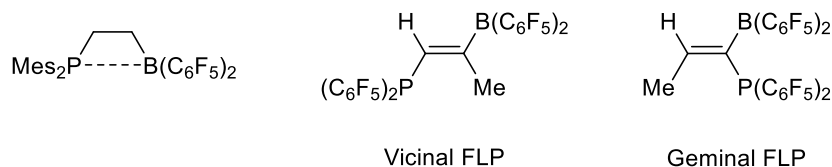
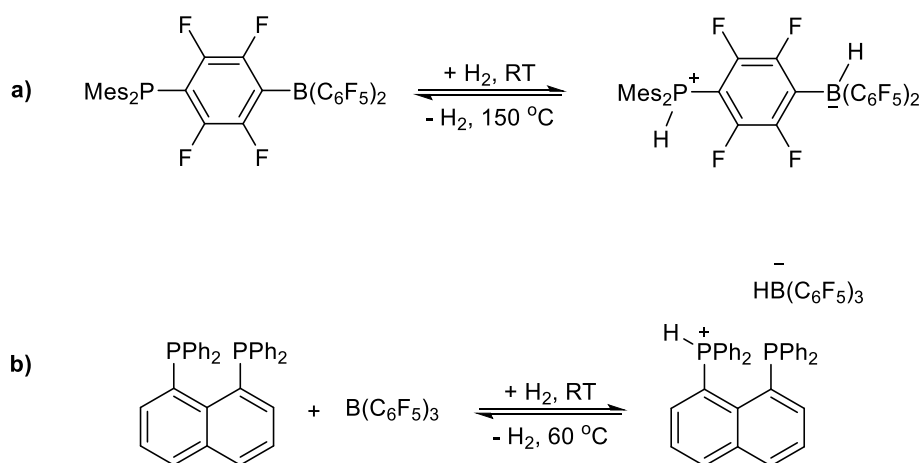


Figure 22 – Examples of intramolecular FLPs.^{122,123}

1.8.1 – Reactivity of FLPs

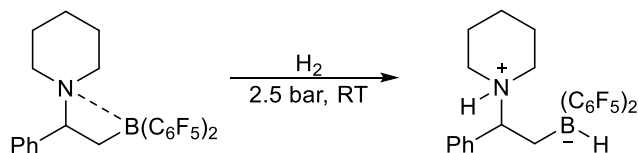
The plethora of FLPs reported in the literature¹²⁴ demonstrate how the steric congestion about a Lewis acid/base centre can preclude the formation of a classical Lewis adduct, and instead give rise to combinations that retain the Lewis acidic/basic character of the individual components. The reactivity of FLPs towards small molecules has been extensively studied, some examples are listed in sections **1.8.1.1-1.8.1.4**.

1.8.1.1 – Activation of Dihydrogen

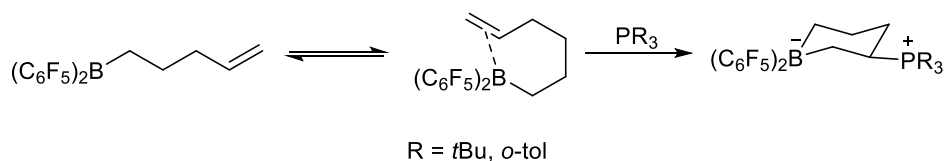


Scheme 48 – H₂ activation by a) an intramolecular and b) an intermolecular phosphine-boron intermolecular FLP.^{124,125}

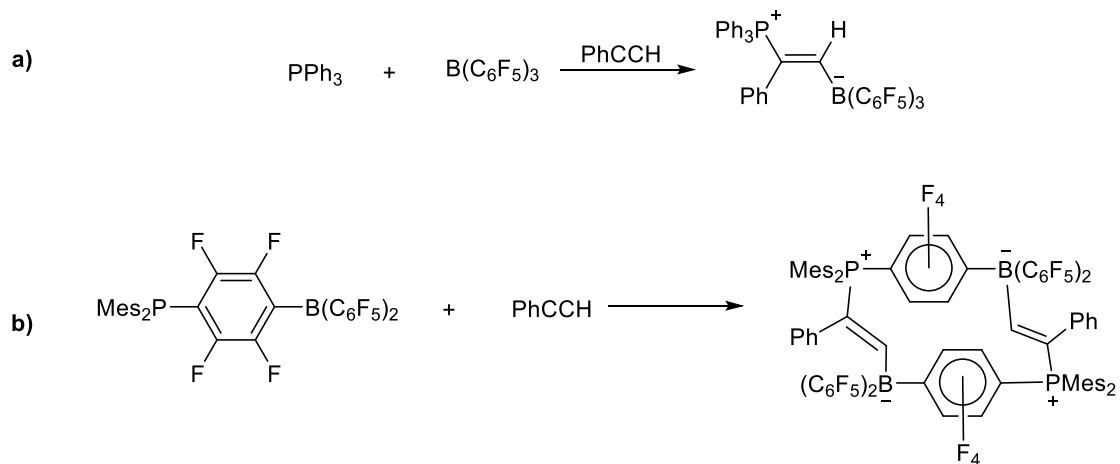
Two examples of the heterolytic splitting of dihydrogen by FLPs are shown in Scheme 48.^{124,125} Reaction **a** (Scheme 48) shows how the intramolecular FLP splits the molecule of dihydrogen to give a zwitterionic species which possesses both a protic and hydridic component.¹²⁴ For scheme **b** (Scheme 48), the phosphorus components of the starting 1,8-bisphosphinonaphthalene behave as bases, and, upon splitting of H₂, a proton binds to one of these two equivalent phosphorus centres (and can subsequently undergo a rapid exchange between the two), and the Lewis acidic boron centre forms a hydridoborate anion.¹²⁵ The hydrogen uptake can be readily reversed by heating the zwitterion (**a**) and phosphonium hydridoborate salt (**b**) to 150 and 60 °C, respectively.^{124,125} Intramolecular FLPs can also activate dihydrogen, as is seen by the irreversible process described in Scheme 49 to form an ammonium/hydridoborate zwitterion.¹²⁶

Scheme 49 – Irreversible dihydrogen activation using an intramolecular FLP.¹²⁶

1.8.1.2 – Activation of Alkenes and Alkynes

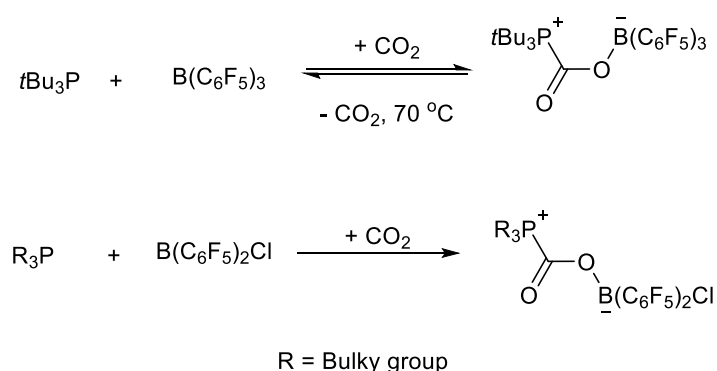
Scheme 50 – Olefin activation by an intermolecular FLP.^{127,128}

Intermolecular FLPs activate olefins in as shown in Scheme 50.^{127,128} The activation begins with a van der Waals interaction between the alkene and boron motif, followed by the formation of a phosphonium cyclic borate species. The reaction of FLPs with alkynes is similar to their behaviour towards alkenes. Two alkyne activation reactions are shown in Scheme 51, the products taking the form of those from a *pseudo* [2+2]-type reaction.¹²⁹

Scheme 51 – Activation of alkynes by FLPs.¹²⁹

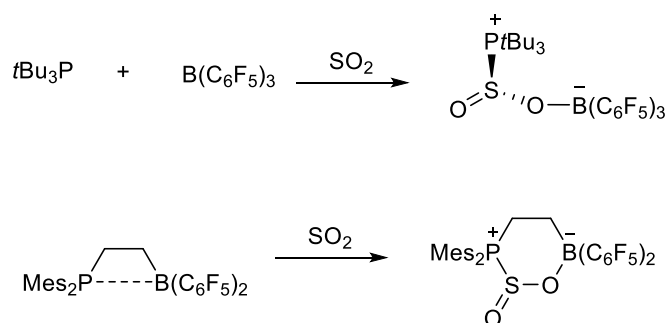
1.8.1.3 – Activation of Greenhouse Gases

The reactions of FLPs towards small molecules, *e.g.* H₂ and alkenes, prompted investigations into how these species interact with CO₂, N₂O and SO₂, three greenhouse gases. These gases pose much danger to the environment, and alternative methods for capture, or even further reactivity, are continually being sought. Carbon dioxide has received a large amount of attention in the press concerning its detrimental effect upon the ozone layer, therefore its sequestration an attractive proposition. The capture of CO₂ can either be a reversible or an irreversible process as shown in Scheme 52.^{130,131}



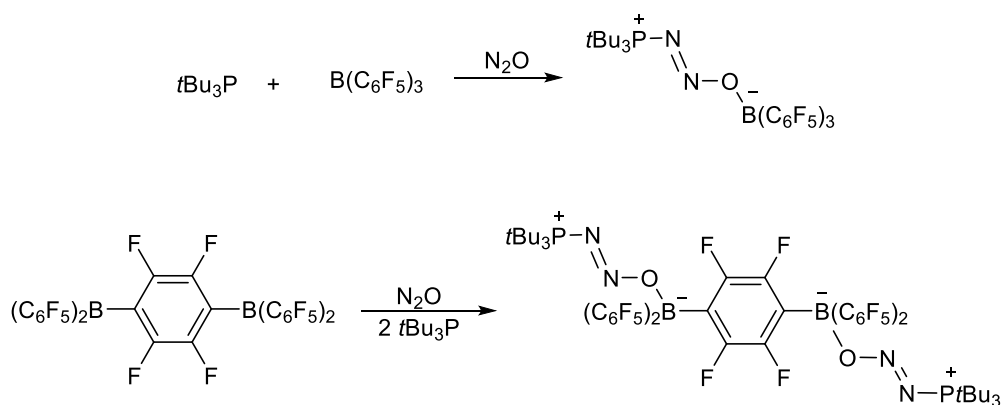
Scheme 52 – Reversible and irreversible CO₂ capture.^{130,131}

The activation of SO₂ by FLPs occurs *via* a similar process to the activation of CO₂. The products of SO₂ capture take a zwitterionic form (Scheme 53), comparable to the zwitterionic species in Scheme 52.¹³²



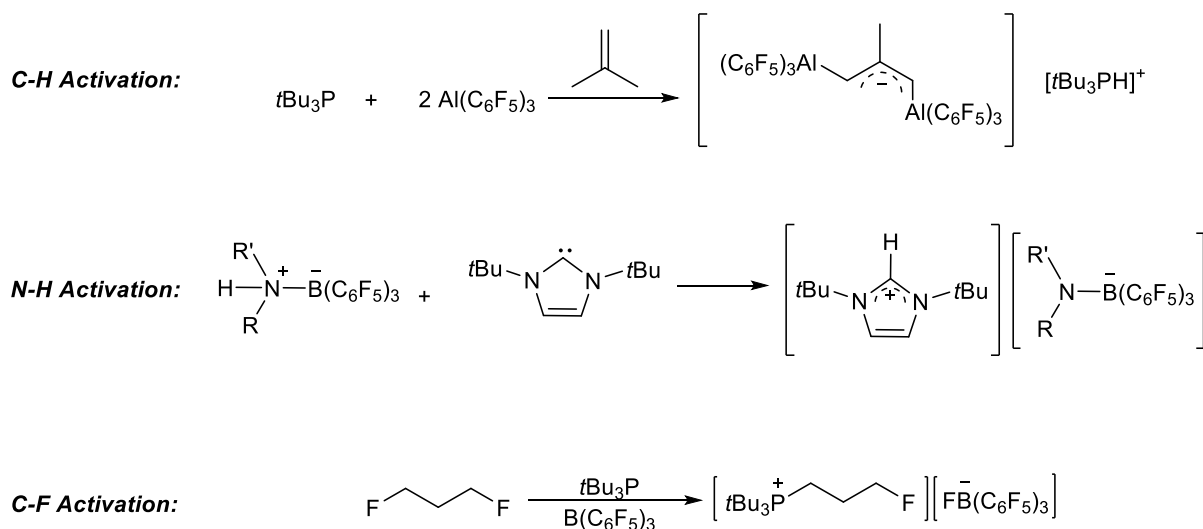
Scheme 53 – Products of FLP activation of SO₂.¹³²

N₂O is a greenhouse gas that is 300 times more damaging than CO₂. As with CO₂, FLPs can capture N₂O, examples are shown in Scheme 54.^{133,134}

Scheme 54 – N₂O activation by FLPs.^{133,134}

1.8.1.4 – Heterolytic CH, NH and CF Activation

FLPs can activate C-H,¹³⁵ N-H¹³⁶ and C-F¹³⁷ bonds, examples of each of these activation/bond-cleavage processes are shown in Scheme 55. The C-H, N-H and C-F bond activation by FLPs make up some of the few reported examples of these processes which proceed in the absence of a transition metal centre.

Scheme 55 – C-H, N-H and C-F activation by FLPs.^{135,136,137}

1.9 – Aims

Section **1.8.1** has highlighted some of the wide variety of the chemistry that can be carried out by FLPs. The latent value of FLP mediated processes, from both a synthetic and environmental standpoint, makes the potential FLP reactivity of the “open” pyridyl-*N*-phosphinoimines (described in section **1.1**), combined with their Wiegardt-type NIL behaviour, of interest to explore. It is of key importance, however, to have a full, fundamental understanding of how modifications to the central pyridine-phosphinoimine scaffold, as well as external factors (*e.g.* solvent), impact upon the ability of these “open” species to cyclise, prior to probing their FLP and NIL character.

Chapter 2 (Pyridyl-*N*-Phosphinoimine – Diazaphosphazole Valence Tautomerism: Equilibrium Studies) of this thesis explores the effect of the variation of temperature, solvent polarity and modifications to the pyridine and imine components of the “open” pyridyl-*N*-phosphinoimines upon the extent of Lewis adduct (“closed” diazaphosphazole) formation. The impact of installing chloro substituents (good leaving groups) at the phosphorus centre is outlined in **Chapter 3**. The preliminary results of an investigation into the reactivity of the “open” and “closed” tautomers towards selected small molecules is reported in **Chapter 4**, and reaction outcomes compared and contrasted with known systems, including FLPs.

This thesis is broken down into three results chapters (chapters 2-4), each of which begins with a brief introduction, followed by a discussion of the results obtained, and ends with a summary and the relevant experimental methods (**Appendix 1** outlines general experimental procedures used throughout). A summary of the work discussed in chapters 2-4, as well as a discussion of the outlook for the future prospects of this work can be found in **Chapter 5**.

Chapter 1 References

- ¹ P. W. Dyer, J. Fawcett and M. J. Hanton, *J. Organomet. Chem.*, 2005, **690**, 5264-5281.
- ² D. A. Smith, A. S. Batsanov, K. Miqueu, J. –M. Sotiropoulos, D. C. Apperley, J. A. K. Howard and P. W. Dyer, *Angew. Chem. Int. Ed.*, 2008, **47**, 8674-8677.
- ³ D. A. Smith, PhD Thesis, Durham University, 2009.
- ⁴ D. A. Smith, A. S. Batsanov, K. Costuas, E. Edge, D. C. Apperley, D. Collison, J. –F. Halet, J. A. K. Howard and P. W. Dyer, *Angew. Chem. Int. Ed.*, 2010, **49**, 7040-7044.
- ⁵ C. C. Lu, E. Bill, T. Weyhermüller, E. Bothe and K. Wieghardt, *J. Am. Chem. Soc.*, 2008, **130**, 3181-3197.
- ⁶ C. K. Jørgensen in *Structure and Bonding*, 1966, Springer.
- ⁷ J. Stubbe and W. A. van der Donk, *Chem. Rev.*, 1998, **98**, 705-762.
- ⁸ K. Ray, T. Petrenko, K. Wieghardt and F. Nesse, *Dalton Trans.*, 2007, 1552-1566.
- ⁹ C. Amatore and A. Jutand, *Coord. Chem. Rev.*, 1998, **178**, 511-528.
- ¹⁰ S. C. F. Kui, N. Zhu and M. C W. Chan, *Angew. Int. Ed.*, 2003, **42**, 1628-1632.
- ¹¹ C. E. Anderson, D. C. Apperly, A. S. Bastinov, P. W. Dyer and J. A. K. Howard, *Dalton Trans.*, 2006, 4134-4145.
- ¹² H. Grützmacher, *Angew. Chem. Int. Ed.*, 2008, **47**, 1814-1818.
- ¹³ J. L. van der Vlugt and J. N. H. Reek, *Angew. Chem. Int. Ed.*, 2009, **48**, 8832-8846.
- ¹⁴ W. Kaim and B. Schwederski, *Coord. Chem. Rev.*, 2010, **254**, 1580-1588.
- ¹⁵ W. Kaim, *Coord. Chem. Rev.*, 1987, **76**, 187-235.
- ¹⁶ V. Lyaskovskyy and B. de Bruin, *ACS Catal.*, 2012, **2**, 270-279.
- ¹⁷ J. I. van der Vlugt, *Eur. J. Inorg. Chem.*, 2012, **3**, 363-375.
- ¹⁸ W. I. Dzik, J. I. van der Vlugt, J. N. H. Reek and B. de Bruin, *Angew. Chem. Int. Ed.*, 2011, **50**, 3356-2258.
- ¹⁹ P. J. Chirik and K. Wieghardt, *Science*, 2010, **327**, 794-795.
- ²⁰ M. W. Bouwkamp, A. C. Bowman, E. Lobkovsky and P. J. Chirik, *J. Am. Chem. Soc.*, 2006, **128**, 13340-13341.
- ²¹ B. de Bruin, E. Bill, E. Bothe, T. Weyhermueller and K. Wieghardt, *Inorg. Chem.*, 2000, **39**, 2936-2947.
- ²² P. H. M. Budzelaar, B. de Bruin, A. W. Gal, K. E. Wieghardt and J. H. van Lethe, *Inorg. Chem.*, 2001, **40**, 4649-4655.

- ²³ M. R. Ringenberg, S. L. Kokatam, Z. M. Heiden and T. B. Rauchfuss, *J. Am. Chem. Soc.*, 2008, **130**, 788-789.
- ²⁴ M. R. Ringenberg, and T. B. Rauchfuss, *Eur. J. Inorg. Chem.*, 2012, **3**, 490-495.
- ²⁵ W. R. Cullen, T. J. Kim, F. W. B. Einstein and T. Jones, *Organometallics*, 1983, **2**, 714-719.
- ²⁶ A. Caselli, E. Gallo, S. Fantauzzi, S. Morlacchi, F. Ragaini and F. Cenini, *Eur. J. Inorg. Chem.*, 2008, 3009-3019.
- ²⁷ K. H. Hopmann and A. Ghosh, *ACS Catal.*, 2011, **1**, 597-600.
- ²⁸ S. Fantauzzi, A. Caseli and E. Gallo, *Dalton Trans.*, 2009, 5434-5443.
- ²⁹ V. Lyaskovskyy, A. I. Olivos Suarez, H. Lu, H. Jiang, X. P. Zhang and B. de Bruin, *J. Am. Chem. Soc.*, 2011, **133**, 12264-12273.
- ³⁰ L. Que and W. B. Wolman, *Nature*, 2008, **455**, 333-340.
- ³¹ J. W. Whittaker, *Chem. Rev.*, 2003, **103**, 2347-2363.
- ³² P. Chaudhuri, M. Hess, U. Flörke and K. Wieghardt, *Angew. Chem. Int. Ed.*, 1998, **37**, 2217-2220.
- ³³ P. Chaudhuri, K. Wieghardt, T. Weyhermüller, T. K. Paine, S. Mukherjee and C. Mukherjee, *C. Biol. Chem.*, 2005, **386**, 1023-1033.
- ³⁴ J. A. Bull, J. J. Mousseau, G. Pelletier and A. B. Charette, *Chem. Rev.*, 2012, **112**, 2642-2713.
- ³⁵ A. R. Katritzky and R. Taylor in *Advances in Heterocyclic Chemistry Volume 47: Electrophilic Substitution of Heterocycles Quantitative Aspects*, 1990, Academic Press.
- ³⁶ W. G. Körner, *Giornale di Scienze Naturali ed Economiche*, 1869, **5**, 111-114.
- ³⁷ J. Dewar, *Chem. News*, 1871, **23**, 38-41.
- ³⁸ R. A. Barnes in *Heterocyclic Compounds: Pyridine and its Derivatives Part One*, 1960, Wiley-Interscience.
- ³⁹ H. C. Longuet-Higgins and C. A. Coulson, *Trans. Faraday Soc.*, 1947, **43**, 87-94.
- ⁴⁰ L. E. Orgel, T. L. Cottrell, W. Dick and L. E. Sutton, *Trans. Faraday Soc.*, 1951, **47**, 113-119.
- ⁴¹ R. K. Bansal in *Heterocyclic Chemistry Third Edition*, 2005, New Age International (P) Ltd.
- ⁴² H. Brown and X. Mihm, *J. Am. Chem. Soc.*, 1955, **77**, 1723-1726.
- ⁴³ H. Brown and B. Kanner, *J. Am. Chem. Soc.*, 1966, **88**, 986-992.
- ⁴⁴ A. E. Chichibabin and O. A. Zeide, *Zhur. Russ. Fiz. Khim. Obshch*, 1914, **46**, 1216-1236.
- ⁴⁵ D. D. Eley and H. Watts, *J. Chem. Soc.*, 1952, 1914-1918.
- ⁴⁶ R. Fricke and F. Ruschhaupt, *Z. Anorg. u. allegm. Chem.*, 1925, **146**, 103-120.

- ⁴⁷ H. C. Brown and R. H. Horowitz, *J. Am. Chem. Soc.*, 1955, **77**, 1730-1733.
- ⁴⁸ S. Orbisaglia, B. Jacques, P. Braunstein, D. Hueber, P. Pale, A. Blanc and P. de Frémont, *Organometallics*, 2013, **32**, 4153-4164.
- ⁴⁹ E. G. Cox, E. Sharratt, K. C. Webster and W. Wardlaw, *J. Chem. Soc.*, 1936, 129-133.
- ⁵⁰ G. Fraenkel and J. C. Cooper, *Tetrahedron Lett.*, 1968, **15**, 1825-1830.
- ⁵¹ J. Gopalakrishnan, *Appl. Organometal., Chem.*, 2009, **23**, 291-318.
- ⁵² D. G. Gilheany in *The Chemistry of Organophosphorus Compounds Volume 1 Primary, secondary and tertiary phosphines, polyphosphines and heterocyclic organophosphorus (III) compounds*, 1990, Wiley-Interscience.
- ⁵³ R. Derache in *Organophosphorus Pesticides: Criteria for Organophosphorus Pesticides*, 1977, Pergamon Press.
- ⁵⁴ A. D. F. Troy and E. N. Walsh in *Phosphorus Chemistry in Everyday Living, 2nd Edition*, 1987, American Chemical Society.
- ⁵⁵ M. L. Clarke, G. L. Holliday, A. M. Z. Slawin and J. D. Woollins, *J. Chem. Soc. Dalton Trans.*, 2002, 1093-1103.
- ⁵⁶ F. R. Hartley in *The Chemistry of Organophosphorus Compounds Volume 1 Primary, secondary and tertiary phosphines, polyphosphines and heterocyclic organophosphorus (III) compounds*, 1990, Wiley-Interscience.
- ⁵⁷ L. Maier in *Organic Phosphorus Compounds Volume 1*, 1972, Wiley-Interscience.
- ⁵⁸ G. Elsner in *Methoden der Organischen Chemie Organische Phosphor-Verbindungen 1*, 1982, Georg Thieme.
- ⁵⁹ All books in the Organophosphorus Specialist Periodical Report series can be found here:
<http://pubs.rsc.org/bookshop/collections/series?issn=0306-0713>
- ⁶⁰ R. Thompson in *The Modern Inorganic Chemicals Industry Chemical Society Special Publication No. 31*, 1977, Chemical Society.
- ⁶¹ F. A. Cotton and G. Wilkinson in *Advanced Inorganic Chemistry 4th edition*, 1980, Wiley-Interscience.
- ⁶² M. M. Rahman, H. -Y. lie, K. Eriks, A. Prock and W. P. Giering, *Organometallics*, 1989, **8**, 1-7.
- ⁶³ K. G. Moloy and J. L. Petersen, *J. Am. Chem. Soc.*, 1995, **117**, 7696-7710.
- ⁶⁴ M. F. Ernst and D. M. Roddick, *Inorg. Chem.*, 1989, **28**, 1624-1627.

- ⁶⁵ T. Sakakura, T. Sodeyama, K. Sasaki, K. Wada and M. Tanaka, *J. Am. Chem. Soc.*, 1990, **112**, 7221-7229.
- ⁶⁶ J. K. MacDougall, M. C. Simpson, M. J. Green and D. J. Cole-Hamilton, *J. Chem. Soc. Dalton Trans.*, 1996, 1161-1170.
- ⁶⁷ C. A. Tolman, *Chem. Rev.*, 1977, **77**, 313-348.
- ⁶⁸ C. A. Tolman, *J. Am. Chem. Soc.*, 1970, **92**, 2956-2965.
- ⁶⁹ D. W. Allen and B. F. Taylor, *Dalton Trans.*, 1982, 51.
- ⁷⁰ D. G. Gilheany, *Chem. Rev.*, 1994, **94**, 1339-1374.
- ⁷¹ W. McFarlane and D. S. Rycroft, *Dalton Trans.*, 1973, 2162-2166.
- ⁷² A. Michaelis, *Ann. Chem.*, 1903, **326**, 129-258.
- ⁷³ A. H. Cowley, M. Lattman, P. M. Stricklen and J. G. Verkade, *Inorg. Chem.*, 1982, **21**, 543-549. C. Romming and J. Songstad, *Acta Chem. Scand., Ser. A*, 1978, **31**, 689. C. Romming and J. Songstad, *Acta Chem. Scand., Ser. A*, 1979, **33**, 187. C. Romming and J. Songstad, *Acta Chem. Scand., Ser. A*, 1982, **36**, 665.
- ⁷⁴ B. J. Coe and S. J. Glenwright, *Coord. Chem. Rev.*, 2002, **203**, 5-80.
- ⁷⁵ K. M. Anderson and A. G. Orpen, *Chem. Comm.*, 2001, 2682-2683.
- ⁷⁶ D. F. Shriver and P. W. Atkins in *Inorganic Chemistry 3rd edition*, 1999, Oxford University Press.
- ⁷⁷ P. Espinet and K. Soulantica, *Coord. Chem. Rev.*, 1999, **293**, 499-556.
- ⁷⁸ P. Braunstein and F. Naud, *Angew. Chem. Int. Ed.*, 2001, **40**, 680-699.
- ⁷⁹ N. R. Price and J. Chambers in *The Chemistry of Organophosphorus Compounds*, 1991, Wiley-Interscience.
- ⁸⁰ P. W. Dyer, J. Fawcett, M. J. Hanton, R. D. W. Kemmitt, R. Padma and N. Singh, *Dalton Trans.*, 2003, 104-113.
- ⁸¹ C. C. Brown and D. W. Stephan, *Dalton Trans.*, 2012, **41**, 9431-9438.
- ⁸² M. S. Balakrishna, T. K. Prakasha, S. S. Krishnamurthy, U. Siriwardane and N. S. Hosmane, *J. Organomet. Chem.*, 1990, **390**, 203-216.
- ⁸³ G. Helmchen and A. Pfaltz, *Acc. Chem. Res.*, 2000, **33**, 336-345.
- ⁸⁴ M. P. Carroll and P. J. Guiry, *Chem. Soc. Rev.*, 2014, **43**, 819-833.
- ⁸⁵ G. Xu and S. R. Gilbertson, *Tetrahedron Lett.*, 2003, **44**, 953-955.

- ⁸⁶ R. Schareina and R. Kempe, *Angew. Chem. Int. Ed.*, 2002, **41**, 1521-1523.
- ⁸⁷ A. D. Burrows, M. F. Mahon and M. Varrone, *Dalton Trans.*, 2003, 4718-4730.
- ⁸⁸ J. García-Álvarez, S. E. García-Garrido and V. Cadierno, *J. Organomet. Chem.*, 2014, **751**, 792-808.
- ⁸⁹ A. W. Johnson in *Ylides and Imines of Phosphorus*, 1993, Wiley-Interscience.
- ⁹⁰ H. R. Allock in *Chemistry and Applications of Polyphosphazenes*, 2003, John Wiley and Sons.
- ⁹¹ P. Ilankumar, G. Zhang and J. G. Verkade, *Heteroatom Chem.*, 2000, **11**, 251-253.
- ⁹² H. Staudinger and J. Meyer, *Helv. Chem. Acta.*, 1919, **2**, 635-646.
- ⁹³ A. V. Kirsanov, *Isv. Akad. Nauk. SSSR, Ser. Khim.*, 1950, 426-437.
- ⁹⁴ V. A. Gilyarov, N. A. Tikhonina, T. M. Shcherbina and M. I. Kabachnik, *Zh. Obshch. fiim.*, 1980, **50**, 1438-1442.
- ⁹⁵ Y. G. Gololobov, E. A. Suvalova and T. I. Chudakova, *Zh. Obshch. Khim.*, 1981, **51**, 1433-1434.
- ⁹⁶ O. I. Kolodyazhnyi, V. N. Yakovlev, V. P. Kukhar', *Zh. Obshch. Khim.*, 1979, **49**, 2458.
- ⁹⁷ M. N. Danchenko and A. D. Sinitsa, *Zh. Obshch. Khim.*, 1986, **56**, 1773-1776.
- ⁹⁸ B. A. Arbuzov and E. N. Dianova, *Dokl. Akad. Nauk SSSR*, 1980, **225**, 1117.
- ⁹⁹ A. Maraval, K. Owsianik, D. Arquier, A. Igau, Y. Coppel, B. Donnadieu, M. Zablocka and J. -P. Majoral, *Eur. J. Inorg. Chem.*, 2003, 960-968.
- ¹⁰⁰ J. A. Iggo in *NMR Spectroscopy in Inorganic Chemistry*, 2008, Oxford University Press.
- ¹⁰¹ J. Bellan, M. R. Marre, M. Sanchez and R. Wolf, *Phosphorus and Sulfur*, 1981, **12**, 11-18.
- ¹⁰² J. Bellan, M. Sanchez, M. R. Marre-Mazières and A. Murillo Beltran, *Bull. Soc. Chim. Fr.*, 1985, 491-495.
- ¹⁰³ T. Kobayashi and M. Nitta, *Chem. Lett.*, 1985, 1459-1552.
- ¹⁰⁴ R. M. Acheson, G. Paglietti and P. A. Tasker, *J. Chem. Soc. Perkin Trans.*, 1974, **1**, 2496-2500.
- ¹⁰⁵ Y. G. Gololobov and L. F. Kasukhin, *Tetrahedron*, 1992, **48**, 1353-1406.
- ¹⁰⁶ N. Burford, R. E. v H. Spence and J. F. Richardson, *J. Chem. Soc. Dalton Trans.*, 1991, 1615-1619.
- ¹⁰⁷ A. H. Cowley and R. A. Kemp, *Chem. Rev.*, 1985, **85**, 367-382.
- ¹⁰⁸ D. A. Smith, A. S. Batsanov, M. A. Fox, A. Beeby, D. C. Apperley, J. A. K. Howard and P. W. Dyer, *Angew. Chem.*, 2009, **121**, 9273-9277.
- ¹⁰⁹ B. T. King, J. Kroulík, C. R. Robertson, P. Rempala, C. L. Hilton, J. D. Korinek and L. M. Gortari,

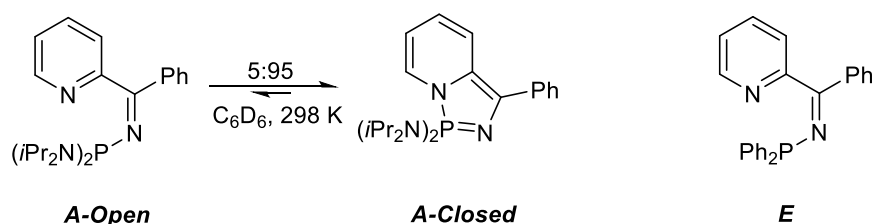
- J. Org. Chem.*, 2007, **72**, 2279-2288.
- ¹¹⁰ P. M. S. Monk in *The Viologens: Physicochemical Properties, Synthesis and Applications of 4,4'-Bipyridine*, 2001, Wiley-Interscience.
- ¹¹¹ C. L. Bird and A. T. Kuhn, *Chem. Soc. Rev.*, 1981, **10**, 49-80.
- ¹¹² C. Fave, T. Y. Cho, M. Hissler, C. W. Chen, T. Y. Luh, C. -C. Wu and R. Réau, *J. Am. Chem. Soc.*, 2003, **125**, 9254-9255.
- ¹¹³ K. Rurack, M. Kollmannsberger and J. Daub, *New J. Chem.*, 2001, **25**, 289-292.
- ¹¹⁴ J. F. Hartwig, M. Kawatsure, S. I. Huack, K. H. Shaughnessy and L. M. Alcatraz-Roman, *J. Org. Chem.*, 1999, **64**, 5575-5580.
- ¹¹⁵ S. M. Reid, J. T. Mague and M. J. Fink, *J. Am. Chem. Soc.*, 2001, **123**, 4081-4082.
- ¹¹⁶ Z. Weng, S. Teo, L. L. Koh and T. S. A. Hor, *Organometallics*, 2004, **23**, 4342-4345.
- ¹¹⁷ G. N. Lewis in *Valence and the Structure of Atoms and Molecules*, 1923, Chemical Catalogue Company.
- ¹¹⁸ H. C. Brown, H. I. Schlesinger and S. Z. Cardon, *J. Am. Chem. Soc.*, 1942, **64**(2), 325-329.
- ¹¹⁹ G. Wittig and E. Benz, *Chem. Ber.*, 1959, **92**, 1999-2013. G. Wittig G and A. Ruckert, *Liebigs Ann. Chem.*, 1950, **566**, 101-113. W. Tochtermann, *Angew. Chem. Int. Ed.*, 1966, **5**, 351-371. R. Damico and C. D. Broaddus, *J. Org. Chem.*, 1966, **31**, 1607-1612. H. Lankamp, W. T. Nauta and C. Maclean, *Tetrahedron Lett.*, 1968, **2**, 249-254. Y. Okamoto and Y. Shimakaw, *J. Org. Chem.*, 1970, **35**, 3752-3756. S. Doering, G. Erker, R. Fröhlich, O. Meyer and K. Bergander, *Organometallics*, 1998, **17**, 2183-2187.
- ¹²⁰ G. C. Welch, T. Holtrichter-Roessmann and D. W. Stephan, *Inorg. Chem.*, 2008, **47**, 1904-1906.
- ¹²¹ G. C. Welch, R. Prieto, M. A. Dureen, A. J. Lough, O. A. Labeodan, T. Holtrichter-Rossmann and D. W. Stephan, *Dalton Trans.*, 2009, 1559-1570.
- ¹²² P. Spies, G. Erker, G. Kehr, K. Bergander, R. Fröhlich, S. Grimme and D. W. Stephan, *Chem. Comm.*, 2007, **43**, 5072-5074.
- ¹²³ C. Rosorius, G. Kehr, R. Fröhlich, S. Grimme and G. Erker, *Organometallics*, 2011, **30**, 4211-4219.
- ¹²⁴ D. W. Stephan and G. Erker, *Angew. Chem. Int. Ed.*, 2010, **49**, 46-76.
- ¹²⁵ R. D. Jackson, S. James, A. G. Orpen and P. G. Pringle, *J. Organomet. Chem.*, 1993, **458**, 1-2.

- ¹²⁶ D. Chen, Y. Wang and J. Klankermayer, *Angew. Chem. Int. Ed.*, 2010, **49**, 9475-9478.
- ¹²⁷ X. Zhao and D. W. Stephan, *J. Am. Chem. Soc.*, 2011, **133**, 12448-12450.
- ¹²⁸ B. -H. Xu, R. A. Adler Yanez, H. Nakatsuka, M. Kitamura, R. Fröhlich, G. Kehr and G. Erker, *Chem. Asian J.*, 2012, **7**, 1347-1356.
- ¹²⁹ M. A. Dureen and D. W. Stephan, *Organometallics*, 2010, **29**, 6594-6607.
- ¹³⁰ C. M. Mömning, E. Otten, G. Kehr, R. Fröhlich, S. Grimme, D. W. Stephan and G. Erker, *Angew. Chem. Int. Ed.*, 2009, **48**, 6643-6646.
- ¹³¹ I. Peuser, R. C. Neu, X. Zhao, M. Ulrich, B. Schirmer, J. A. Tannert, G. Kehr, R. Fröhlich, S. Grimme, G. Erker G and D. W. Stephan, *Chem. Eur. J.*, 2011, **17**, 9640-9650.
- ¹³² M. Sajid, A. Klose, B. Birkmann, L. Liang, B. Schirmer, T. Wiegand, H. Eckert, A. J. Lough, R. Fröhlich, C. G. Daniliuc, S. Grimme, D. W. Stephan, G. Kehr and G. Erker, *Chem. Sci.*, 2013, **4**, 213-219
- ¹³³ E. Otten, R. C. Neu and D. W. Stephan, *J. Am. Chem. Soc.*, 2009, **131**, 9918-9919.
- ¹³⁴ R. C. Neu, E. Otten, A. Lough and D. W. Stephan, *Chem. Sci.*, 2011, **2**, 170-176.
- ¹³⁵ G. Ménard and D. W. Stephan, *Angew. Chem. Int. Ed.*, 2012, **51**, 8272-8275.
- ¹³⁶ P. A. Chase and D. W. Stephan, *Angew. Chem. Int. Ed.*, 2008, **47**, 7433-7437. P. A. Chase, A. L. Gille, T. M. Gilbert and D. W. Stephan, *Dalton Trans.*, 2009, 7179-7188.
- ¹³⁷ C. B. Caputo and D. W. Stephan, *Organometallics*, 2012, **31**, 27-30.

Chapter 2 - Pyridyl-*N*-
Phosphinoimine – Diazaphosphazole
Valence Tautomerism: Equilibrium
Studies

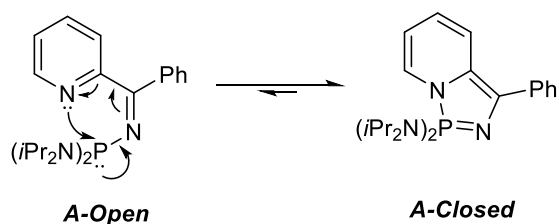
Chapter 2 – Pyridyl-*N*-Phosphinoimine – Diazaphosphazole Valence Tautomerism: Equilibrium Studies

2.1 – Introduction



Scheme 1 - Compounds *A* and *E*.

In 2005, Dyer and co-workers reported the first of several pyridyl-*N*-phosphinoimine compounds, compound *E* (Scheme 1).¹ A study probing the chemical reactivity of compound *E* revealed that it could act as a bidentate κ^2 -*P,N* ligand in Pd(II) complexes, providing the metal with a mixed pyridine/phosphine donor environment, and a relatively flexible six-membered P-N tether backbone. The observed κ^2 -*P,N* coordination of compound *E* to palladium was key to the development of highly regio- and chemo-selective initiators for ethylene/CO co-oligomerisation that, for example, in a medium of methanol produce a single organic product, 4-oxo-hexanoic acid methyl ester.¹ The unprecedented selectivity towards this product (in preference to a distribution of product chain lengths)² is linked to the nature of the *P,N*-ligand, *E*, and its ability to allow the palladium centre to adopt, and switch between, a square planar and trigonal bipyramidal geometry.¹ This behaviour of ligand *E* prompted an investigation into replacing the aryl groups at the phosphorus centre with various different substituents, including σ -withdrawing dialkyl amino groups. The introduction of (*NiPr*₂) groups led to the discovery that such compounds with an electrophilic phosphorus centre can undergo a reversible cyclisation, as shown for compound *A* in Scheme 1.³

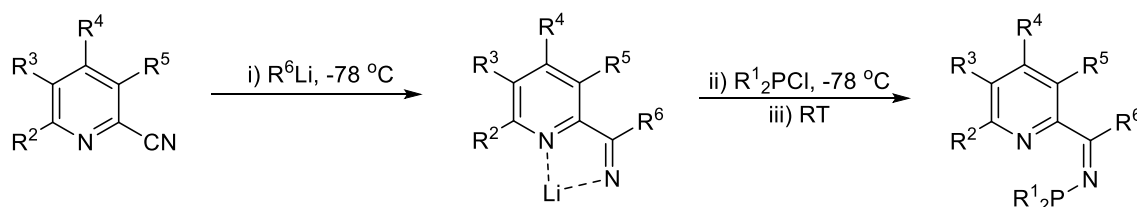


Scheme 2 – *Pseudo*-1,5-electrocyclisation of *A*.³

For the cyclisation of **A-Open** to **A-Closed** (Scheme 2), Dyer and co-workers initially proposed two mechanisms: a step-wise and a concerted cyclisation.⁴ The step-wise mechanism was postulated to proceed *via* the nucleophilic attack of the pyridine nitrogen lone pair at the phosphorus LUMO, followed by inversion at the phosphorus centre to yield the diazaphosphazole, **A-Closed**.⁴ The concerted mechanism proposed is believed to proceed *via* a *pseudo*-1,5-electrocyclisation (Scheme 2) that leads to the formation of a new P-N σ -bond. DFT studies carried out (at the B3LYP/6-31G** level of theory) on the reversible tautomerism of **A-Open** and **A-Closed** did not reveal any intermediates for this process. The absence of any intermediates states for this valence tautomerism led Dyer and co-workers to conclude that the cyclisation process is likely to proceed *via* a concerted *pseudo*-1,5-electrocyclisation-type pathway.^{3,4}

The emergence of this tautomeric equilibrium between pyridyl-phosphine **A-Open** and benzannulated diazaphosphazole **A-Closed** prompted a detailed study into how the steric and electronic nature of the substituents about the central scaffold (R^1 - R^6 , Scheme 3), as well as a variation in temperature, impact upon the position of the “open”-“closed” equilibrium. The following reports the synthesis of structural analogues of compounds **A** and **E**, and examines how minor changes to the pyridyl-imine framework, as well as alterations in temperature and solvent polarity, influence the extent of Lewis adduct (“closed”) formation.

2.1.1 – Preparation of Novel Pyridyl-*N*-Phosphinoimine – Diazaphosphazole Tautomeric Pairs



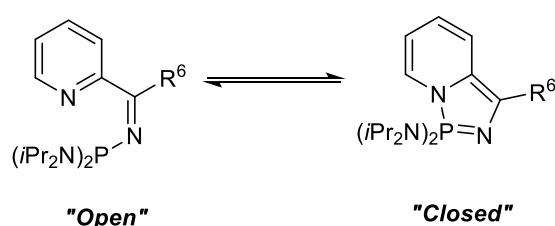
Scheme 3 – General synthesis of pyridyl-*N*-phosphinoimines.³

The pyridyl-*N*-phosphinoimines described in this chapter were synthesised using variations upon the synthetic methodology reported previously for the preparation of compound **A**

(Scheme 3).³ The required organolithium was added to a solution of the selected 2-cyanopyridine (in DME), followed by the quenching of the intermediate *N*-lithiopyridylimine by the addition of the desired chlorophosphine. Solution state ³¹P NMR spectroscopic analysis was used to determine the ratio of “open” : “closed” tautomers. All of the “open” tautomers show a singlet resonance at around $\delta_P \sim +70$ ppm, a shift consistent with that of bis(dialkylamino)phosphinoimines, while the “closed”, anellated σ^4 - $1\lambda^5$ -[1,3,2] diazaphosphole tautomers, give rise to a singlet resonance at around $\delta_P \sim +40$ ppm.⁵

2.2 – Impact of Temperature upon “Open” : “Closed” Equilibrium Position

Variable temperature (VT) ³¹P NMR spectroscopic studies have been employed previously by Dyer and co-workers to demonstrate the reversibility of the dynamic tautomeric equilibrium that exists between the pyridyl-*N*-phosphinoimines and diazaphosphazoles, as shown for the two previously reported species (**A** and **B**) in Table 1.^{3,4} The results from these VT NMR spectroscopic studies show that, for both derivatives **A** and **B**, the “open” tautomer is the thermodynamic product. Determination of the thermodynamic parameters associated with the dynamic tautomeric systems **A** and **B** revealed that **A-Open** and **B-Open** are more entropically favourable than their respective “closed” tautomers, which is consistent with the greater degree of rotation available to the “open” tautomers.⁴



% “Closed” tautomer observed by solution state ³¹P{¹H} NMR spectroscopic analysis^a

Compound	R ⁶	223 K	298 K	303 K	333 K	363 K
A	Ph	98	95	-	75	-
B	Anthracenyl	-	36	31	25	18

Table 1 – % “Closed” tautomer as a function of temperature: variable temperature ³¹P NMR spectroscopic results for compounds **A** and **B**. ^aSpectra were recorded C₆D₅CD₃.^{3,4}

Two novel compounds, **1** (Figure 2) and **2** (Figure 3), structural analogues of **A** and **B**, have been prepared in this work and studied by VT $^{31}\text{P}\{^1\text{H}\}$ NMR spectroscopy (see **Appendix 2** for spectra). These tautomeric systems display a negative correlation between temperature and the percentage of “closed” tautomer observed. The corresponding thermodynamic parameters for the tautomeric systems of **1** and **2** have been calculated using equations Eq. 1 – Eq. 4 shown in Figure 1 and drawing plots of $\ln K$ against $1/T$ (Figure 2 and Figure 3).

$$\Delta G = -RT \ln K \quad \text{Eq. 1}$$

$$\Delta G = \Delta H - T\Delta S \quad \text{Eq. 2}$$

$$-RT \ln K = \Delta H - T\Delta S \quad \text{Eq. 3}$$

$$\ln K = \frac{\Delta S}{R} - \frac{\Delta H}{RT} \quad \text{Eq. 4}$$

Figure 1 – Thermodynamic equations. K = equilibrium constant, G = Gibbs free energy, H = enthalpy, S = entropy, R = gas constant, T = temperature (K).

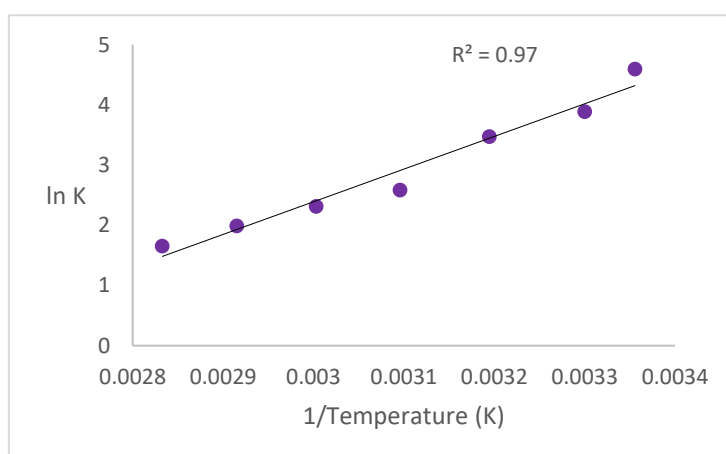
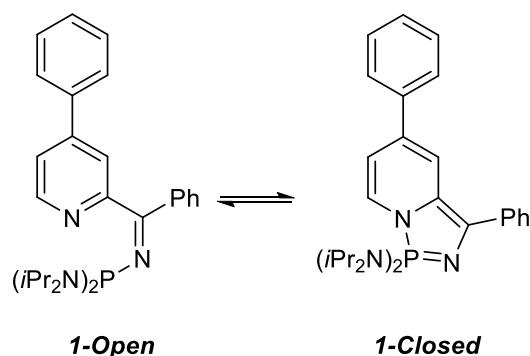


Figure 2 – Plot of $\ln K$ against $1/\text{Temperature}$ for compound **1**. Trend line generated by Microsoft Excel.

Chapter 2 - Pyridyl-*N*-Phosphinoimine – Diazaphosphazole Valence Tautomerism:
Equilibrium Studies

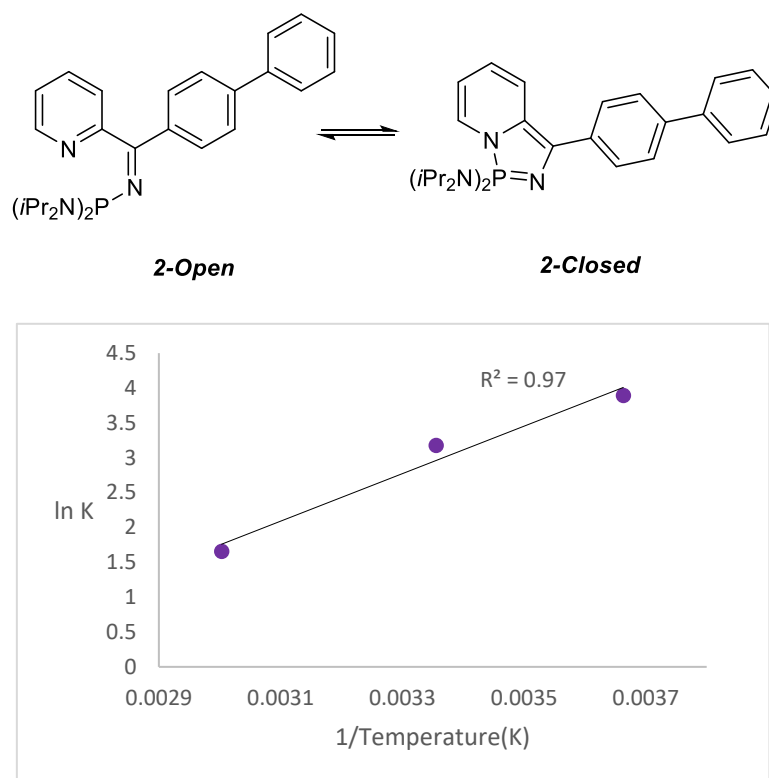
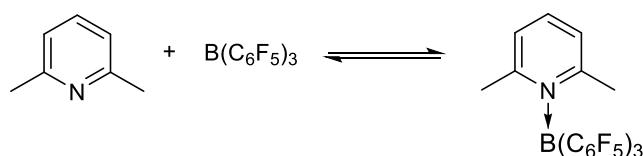


Figure 3 – Plot of $\ln K$ against $1/\text{Temperature}$ for compound **2**. Trend line generated by Microsoft Excel.

Compound	ΔS $J mol^{-1} K^{-1}$	ΔH $kJ mol^{-1}$
1	-115.4	-54.2
2	-70.4	-34.1

Table 2 – Experimentally calculated ΔS and ΔH values for compounds **1** and **2**.

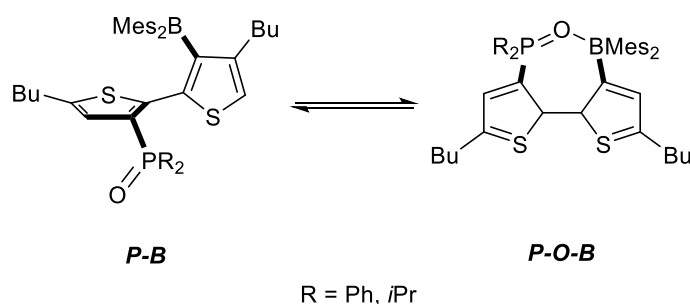
The ΔS and ΔH values calculated for compounds **1** and **2** (Table 2) are consistent with those reported for **A** and **B**.^{3,4} The cyclisation processes of **1-Open** and **2-Open** to form **1-Closed** and **2-Closed**, respectively, both possess a negative ΔS value. The ΔG values for the cyclisation of **1-Open** and **2-Open**, which are temperature dependent, can be readily calculated using Eq. 2 (Figure 1), and therefore the equilibrium position can be determined for any temperature by using Eq. 3/eq.4 (Figure 1).



Scheme 4 – Reversible Lewis adduct formation studied by Stephan and co-workers.^{6,7}

For the pyridine-phosphine systems of compounds **A**, **B**, **1** and **2**, the preference for the formation of the Lewis adduct (“closed” tautomer) over the “open” pyridyl-*N*-iminophosphine species at lower temperatures is comparable to what is observed for the association/dissociation of the pyridine-borane system (Scheme 4) studied by Stephan and co-workers.^{6,7} Stephan and co-workers investigated the equilibrium shown in Scheme 4 as a function of temperature using VT ¹⁹F NMR spectroscopy. Broad signals for a 1:1 ratio of 2,6-lutidine:B(C₆F₅)₃ were observed in the ¹⁹F NMR spectrum at 298 K, suggesting an equilibrium between free Lewis acid and base and the classical Lewis adduct.^{6,7} Cooling to 264 K saw a sharpening of the signals in the ¹⁹F NMR spectrum and a shift in the equilibrium position in favour of the Lewis adduct, as was seen for compounds **A**, **B**, **1** and **2**. The Δ*S* associated with the formation of the pyridine-borane Lewis adduct in Scheme 4 is negative (−131(5) J mol^{−1} K^{−1}), indicating that the Lewis adduct is the kinetic product, as for compounds **A**, **B**, **1** and **2**.^{6,7} The magnitude of the Δ*S* value for Stephan’s bimolecular system is greater than the magnitude of the Δ*S* values observed for the unimolecular systems of compounds **A**, **B**, **1** and **2** – this is consistent for the comparison between a bimolecular Lewis acid-base pair vs a unimolecular pair.^{6,7}

2.3 – Impact of Solvent Polarity Upon “Open”：“Closed” Equilibrium Position



Scheme 5 – Reversible Lewis adduct formation.⁸

The unimolecular Lewis pair system shown in Scheme 5 is an example of a system reported in the literature where the formation of the Lewis adduct (**P-O-B**) can be controlled by altering the solvent.⁸ The formation of the Lewis adduct can be prevented by strongly hydrogen-bonding solvents, such as methanol, due to the ability of the solvent to stabilise the free P=O bond in **P-B**, and to destabilise the O-B interaction in **P-O-B**. Solvents can preclude the

formation of a Lewis adduct, not just as a result of their polarity, but also by their ability to coordinate to the Lewis acid, and consequently crowd the acidic centre, preventing the formation of the Lewis adduct, this is known as “solvent-assisted frustration”.⁹ An example of a “solvent-assisted” FLP is the Me_3P and AlCl_3 system.⁹ The formation of the weakly bound $\text{Me}_3\text{P} \rightarrow \text{AlCl}_3$ pair is prevented in bromobenzene, which coordinates to the free AlCl_3 Lewis acid *via* a $\text{Br} \rightarrow \text{Al}$ interaction.⁹

The literature precedent outlined above, which shows the impact of solvent upon the formation of a Lewis adduct, prompted an investigation into the impact of the solvent on the extent of Lewis adduct (“closed”) formation for the pyridyl-*N*-phosphinoimine-diazaphosphazole system. A series of commonly available solvents, with different dielectric constants (ϵ)/polarity,¹⁰ were selected for this study and approximately 20 mg of compound **A** was dissolved in 0.8 ml of solvent, and the equilibrium position determined by ^{31}P NMR spectroscopy, results of this solvent study are shown in Figure 4 (see **Appendix 2** for NMR spectra).

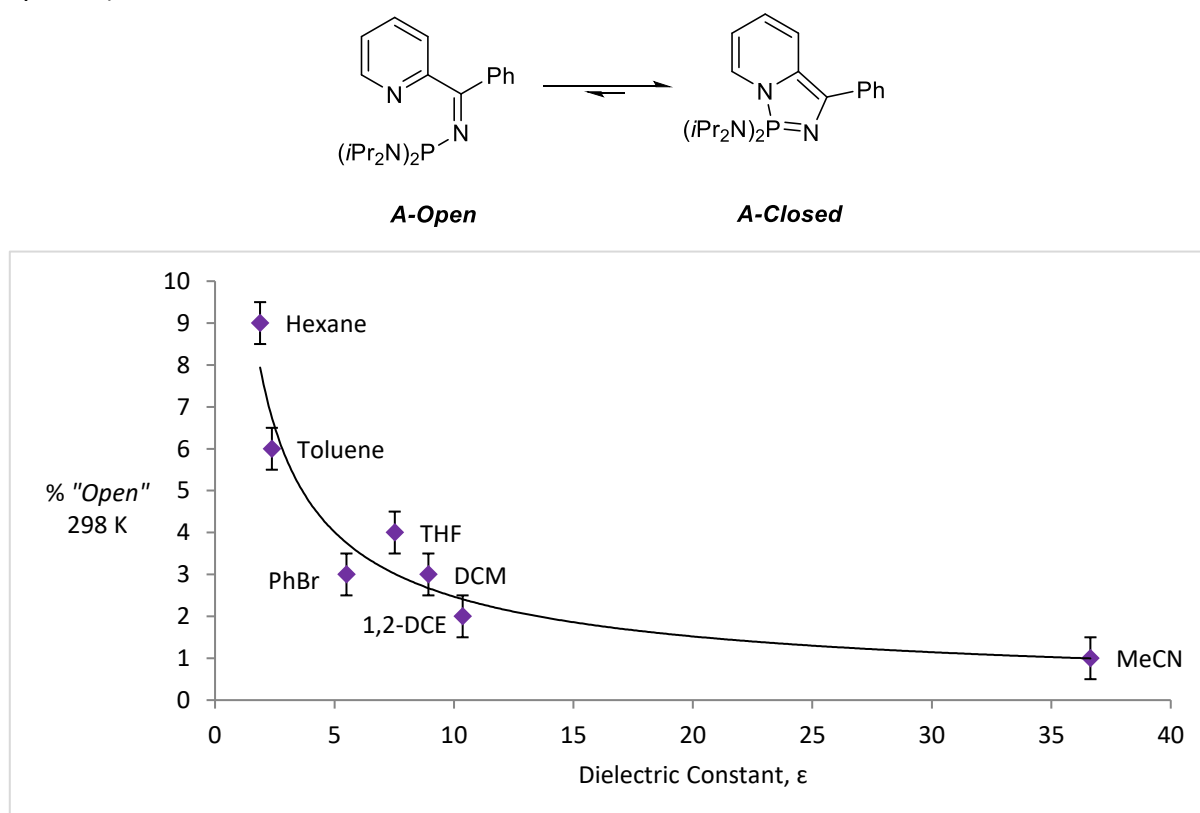
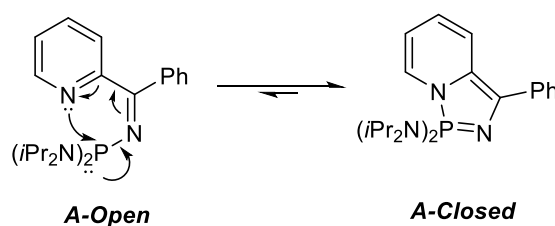


Figure 4 – Plot showing the relationship between the polarity of solvent¹⁰ and the % of *A-Open* observed. Trend line generated by Microsoft Excel. Error bars for % “open” determined by experimental solution state ^{31}P NMR spectroscopy and fixed at 0.5 %.

The plot of relative percentage **A-Open** (at 298 K) against the dielectric constant (Figure 4) shows that with an increase in solvent polarity (increase in ϵ), a decrease in the percentage of **A-Open** (and therefore an increase in the amount of **A-Closed**) is observed by ^{31}P NMR spectroscopic analysis. Whilst the changes in the relative amount of **A-Open** are minimal, its relationship with solvent polarity is nevertheless evident from Figure 4. The shift of the **A-Open-A-Closed** equilibrium towards **A-Closed** in more polar solvents suggests that the diazaphosphazole (“closed”) form of **A** is more polar than the “open” pyridyl-*N*-phosphinoimine tautomer. A computational study was carried out (at the B3LYP/6-31G** level of theory)* and revealed **A-Closed** (dipole moment = 5.39 D) to be more polar than **A-Open** (dipole moment = 2.34 D) – results consistent with the experimental observations shown in Figure 4.

2.4 – Effect of Modifying the Pyridine Scaffold upon the Pyridyl-*N*-Phosphinoimine-Diazaphosphazole Tautomeric Equilibrium Position



Scheme 6 – Pseudo-1,5-electrocyclisation of **A-Open**.

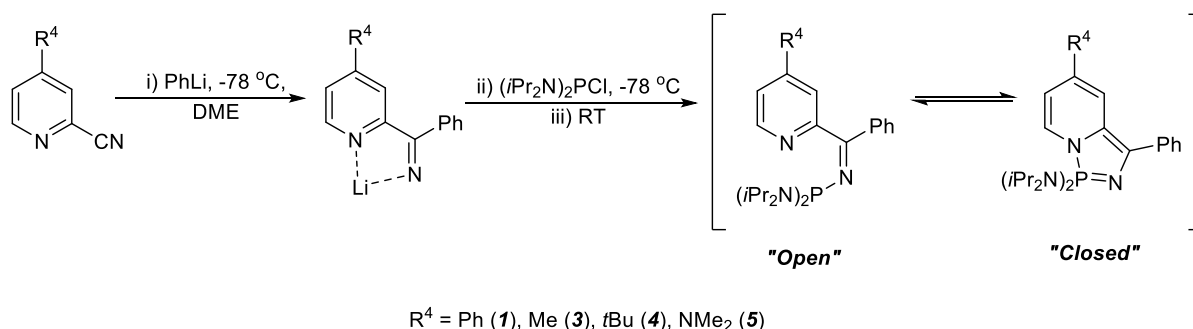
As has been discussed previously, computational studies suggest that the cyclisation of pyridyl-*N*-phosphinoimines occurs *via* a concerted *pseudo*-1,5-electrocyclisation, as is shown in Scheme 6 for compound **A**.³ For cyclisation to occur (*i.e.* favourable attack of the pyridine nitrogen lone pair at the phosphorus centre), there is an electronic requirement for the phosphorus centre to be electron deficient, as has been evidenced in the literature.^{3,4,11} It has been previously reported for systems that possess electron donating phosphorus substituents, *e.g.* Ph (**E**), *i*Pr (**F**) and *t*Bu (**G**), that no cyclisation is observed, whereas when the phosphorus substituents are electron withdrawing *e.g.* (*Ni*Pr₂) (**A**), OC₂H₄O (**C**) and

* Computational studies carried out by Dr Mark A. Fox, Durham University.

MeNC₂H₄NMe (**D**), cyclisation takes place and the position of the “open”-“closed” equilibrium lies in favour of the “closed” tautomer.⁴ It would follow, therefore, that an increase in nucleophilicity of the pyridine nitrogen centre would also promote the formation of the Lewis adduct (“closed” tautomer).

As has been discussed in **Chapter 1**, the nitrogen lone pair, which resides in an *exo*-cyclic *sp*² hybrid orbital orientated in the plane of the ring, and therefore cannot conjugate into the aromatic π -system, enables pyridine to act as a base.¹² The electron donor-acceptor characteristics of substituents bound to a pyridine ring can increase the basicity of the a substituted pyridine by 0.5-0.8 p*K*_a units.^{13,14} Installation of an electron donating substituent, such as an alkyl or aryl group, at the 2- or 4-position on a pyridine ring increases the electron density at the nitrogen centre, either inductively, mesomerically (*via* the overlap of the *p*-orbital(s) of the substituent with the *p*-orbitals of the pyridine ring) or by hyperconjugation (*via* the σ -electron system of the ring or by electron delocalisation in an extended π -system).¹⁵ The following will outline attempts to prepare pyridyl-*N*-phosphinoimine – diazaphosphazole systems with electron donating substituents (\neq H) at various positions on the pyridine ring in order to probe the impact of pyridine basicity upon the position of the “open”-“closed” equilibrium.

2.4.1 – Substitution at the 4-Position on the Pyridyl-*N*-Phosphinoimine Pyridine Ring



Scheme 7 – Proposed synthetic route to prepare target compounds **1**, **3**, **4** and **5**.

To probe the effect of nucleophilicity of the pyridine nitrogen centre upon the extent of Lewis adduct (“closed”) formation, a series of 4-substituted-2-cyanopyridines with different nucleophilicities of the heterocyclic nitrogen atoms were selected as reagents for the proposed synthetic procedure for the preparation of the necessary pyridyl-imines shown in Scheme 7. The synthesis of target compounds **1**, **3**, **4** and **5** was chosen due to the ease of accessibility of the starting cyanopyridines (either commercially or synthetically) and the range of pK_a values of the parent 4-substituted pyridines (Figure 5). Across the series of target pyridines, an increase in pK_a , relative to unsubstituted pyridine, with the introduction of a Ph < Me < *t*Bu < NMe₂ group at the *para*-position is observed (Figure 5).^{12,15,16} Target compounds **1**, **3**, **4** and **5** will now be discussed in order of increasing pK_a of their parent 4-substituted pyridines.

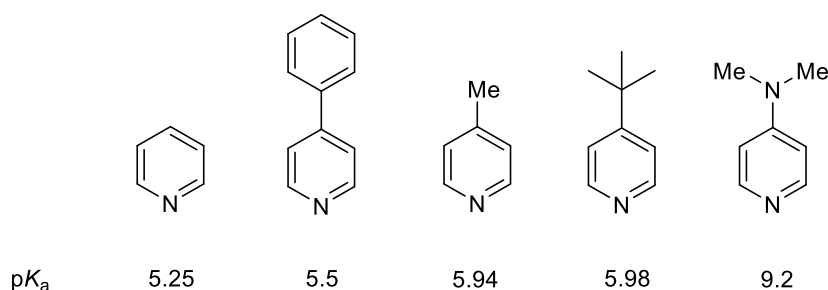
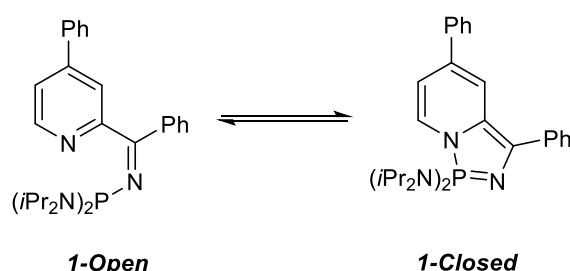


Figure 5 – pK_a values of the parent 4-substituted pyridines for 3-6.^{12,15,16}

2.4.1.1 – Synthesis and Characterisation *N,N,N',N'*-tetraisopropyl-1-((phenyl(4-phenylpyridin-2-yl)methylene)amino)phosphanediamine (1-Open)/ *N,N,N',N'*-tetraisopropyl-3,5-diphenyl-1*H*-[1,3,2]diazaphospholo[1,5-*a*]pyridine-1,1-diamine (1-Closed)

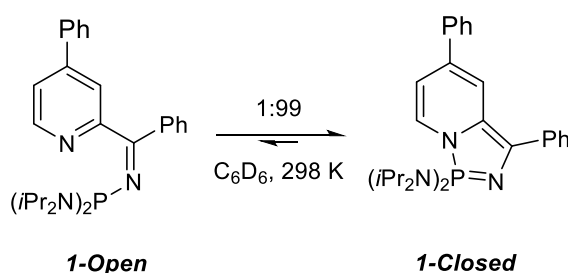


Scheme 8 – Target compound 1.

Pyridyl-imine compound **1** (Scheme 8) possesses a phenyl substituent bound at the position *para* to the pyridine nitrogen centre. The phenyl substituent at the 4-position can exhibit either a positive or a negative mesomeric effect on the pyridine ring through delocalisation

of its *p*-electron density into the conjugated system, something that is dependent on its orientation relative to the pyridine ring itself.¹⁵ Compound **1** was successfully synthesised using a modification of the procedure laid out by Dyer and co-workers for the preparation of compound **A**³ (*i.e.* Scheme 7) using commercially available 4-phenyl-2-cyanopyridine.

Solution state ³¹P{¹H} NMR spectroscopic analysis of product **1** (isolated by extraction with hexane from the crude reaction residue) showed that compound **1** exists as both **1-Open** and **1-Closed** tautomers (Scheme 9) in a 1:99 ratio, respectively, in C₆D₆ at 298 K. Singlet resonances were observed for each tautomer: **1-Open** at δ_P = +70.3 ppm and **1-Closed** at δ_P = +41.0 ppm, chemical shifts consistent with those observed for **A-Open** and **A-Closed**.³ A comparison of the ratio of “open” and “closed” tautomers for compound **A** (5:95 in C₆D₆ at 298 K)³ and compound **1** (1:99 in C₆D₆ at 298 K) indicates that the substitution of the aromatic phenyl substituent at the 4-position on the pyridine ring pushes the tautomeric equilibrium towards the “closed” tautomer. This experimental observation is consistent with an extension of the conjugated π-system in compound **1**, and the higher basicity of the 4-phenylpyridine motif compared to pyridine (in **A**), which together increase the favourability of Lewis adduct (**1-Closed**) formation relative to the situation for compound **A**, the unsubstituted analogue **1** with a H atom at the 4-position on the pyridine ring.



Scheme 9 – Tautomeric equilibrium between **1-Open** and **1-Closed**.

Following recrystallization of compound **1** from hexane at –30 °C, deep purple crystals suitable for an X-ray diffraction study were obtained. The resulting molecular structure obtained is shown in Figure 6 and selected structural data are reported in Table 3. The crystals of compound **1** obtained at –30 °C from a saturated hexane solution are of **1-Closed**, rather than **1-Open**, as low temperatures favour the kinetic “closed” tautomer (section 2.2). Solution state ³¹P{¹H} NMR spectroscopic analysis of crystals of **1-Closed** redissolved in C₆D₆ at 298 K confirmed the dynamic tautomeric equilibrium between **1-Open** and **1-Closed** and the 1:99

ratio observed by solution state $^{31}\text{P}\{^1\text{H}\}$ NMR spectroscopic analysis of the reaction residue in C_6D_6 at 298 K. The X-ray crystallographic analysis of compound **1-Closed** reveals an anellated $\sigma^4\text{-}1\lambda^5\text{-}[1,3,2]$ diazaphosphole structure, this is consistent with its characteristic singlet resonance observed by solution state $^{31}\text{P}\{^1\text{H}\}$ spectroscopic NMR analysis ($\delta_{\text{P}} = +41.0$ ppm). Compound **1** is seen to have a planar, fused heterocyclic motif (small dihedral angle (C6-N2...C2-C2) of $4.0(2)^\circ$, see Figure 6 for atom labels), comparable to that observed for **A-Closed**. Within the fused heterocyclic motif of **1-Closed**, the bond lengths and angles are concurrent with those in compound **A-Closed** (Table 4 and Figure 7), suggesting that the introduction of a phenyl substituent at the 4-position does not significantly impact the bonding within the five-membered heterocycle, something consistent with the small perturbation of the “open”-“closed” equilibrium position compared with compound **A**. The P-N4 and P-N3 bond distances in **1-Closed** are characteristic of single bonds,¹⁷ with the bond distances within the five-membered heterocycle indicating the ring is made up of localised single and double bonds.¹⁷

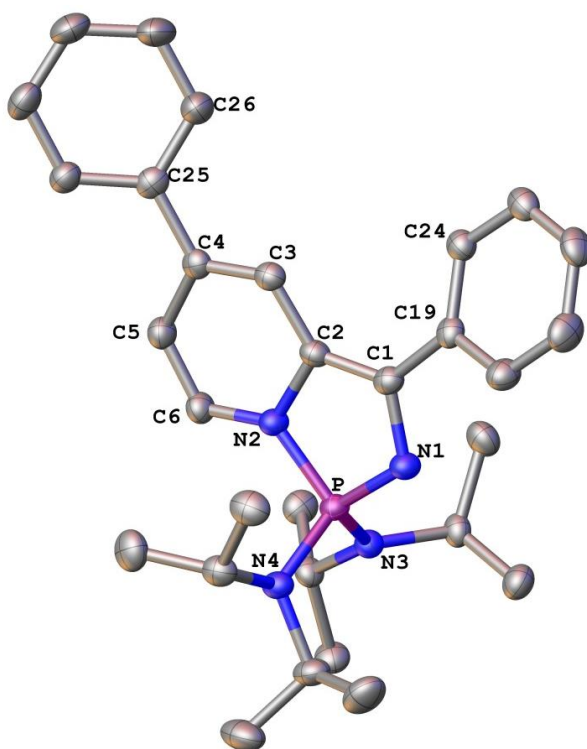


Figure 6 - X-Ray molecular structure of **1-Closed**. Key atoms are labelled and hydrogen atoms have been omitted for clarity. Thermal ellipsoids are drawn at the 50% probability level.

Bond Distances (Å)		Angles (°)		Angles (°)	
C25-C4	1.480(3)	C5-C4-C25	120.1(2)	C19-C1-N1	117.1(2)
C4-C3	1.353(3)	C5-C4-C3	118.5(2)	N4-P-N1	119.56(9)
C3-C2	1.425(3)	C4-C3-C2	123.2(2)	N4-P-N2	109.07(9)
C2-N2	1.449(3)	C3-C2-N2	115.9(2)	N4-P-N3	103.66(9)
N2-C6	1.393(3)	C2-N2-C6	119.9(2)	N3-P-N2	113.51(9)
C6-C5	1.341(3)	N2-C6-C5	121.8(2)	N3-P-N1	113.89(9)
C5-C4	1.453(3)	C6-C5-C4	120.2(2)	Dihedral Angles (°)	
C2-C1	1.373(3)	N2-C2-C1	110.0(2)		
C1-C19	1.465(3)	C2-C1-N1	114.4(2)	C26-C25...C4-C3	32.4(3)
C1-N1	1.402(3)	C1-N1-P	110.3(2)	C3-C2...C1-C19	6.6(4)
N2-P	1.676(2)	N1-P-N2	97.42(9)	C2-C1...C19-C24	25.4(3)
P-N1	1.581(2)	P-N2-C2	107.8(1)	C6-N2...C2-C1	176.0(2)
P-N3	1.643(2)	C2-C1-C19	128.6(2)		
P-N4	1.655(2)	C25-C4-C3	121.4(2)		

Table 3 - Selected structural data for compound *1-Closed*. Estimated standard deviations shown in brackets. See Figure 6 for atom labels.

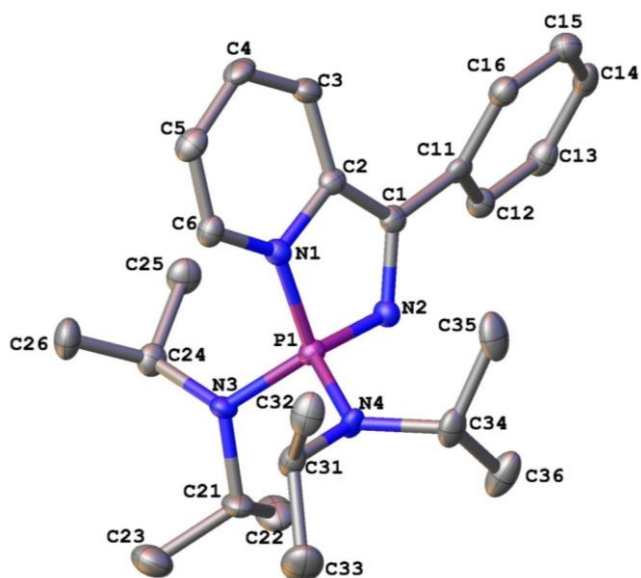


Figure 7 - X-Ray molecular structure of *A-Closed*. Atoms are labelled and hydrogen atoms have been omitted for clarity. Thermal ellipsoids are drawn at the 50% probability level.³

Bond Distances (Å)		Angles (°)	
P1-N1	1.681(3)	PN1-P1-N2	97.41(14)
P1-N2	1.598(3)	P1-N2-C1	109.6(2)
P1-N3	1.653(3)	P1-N1-C2	108.0(2)
P1-N4	1.647(3)		
N2-C1	1.399(4)	Dihedral Angle (°)	
C1-C2	1.376(4)	C2-C1...C11-C26	35.1(5)
C3-C4	1.353(3)		
C5-C6	1.336(4)		
C1-C11	1.466(4)		

Table 4 - Selected structural data for compound *A-Closed*. Estimated standard deviations shown in brackets. See Figure 7 for atom labels.³

Examination of the solution state ^1H NMR spectrum of the redissolved single crystals of **1-Closed** revealed broad peaks in the aromatic region of the spectrum (Figure 8). This broadening of lines has been attributed to the hindered rotation of both the phenyl substituent bound to the pyridine ring and that bound adjacent to the pyridine ring, this restricted rotation has been confirmed by a NOESY NMR experiment.

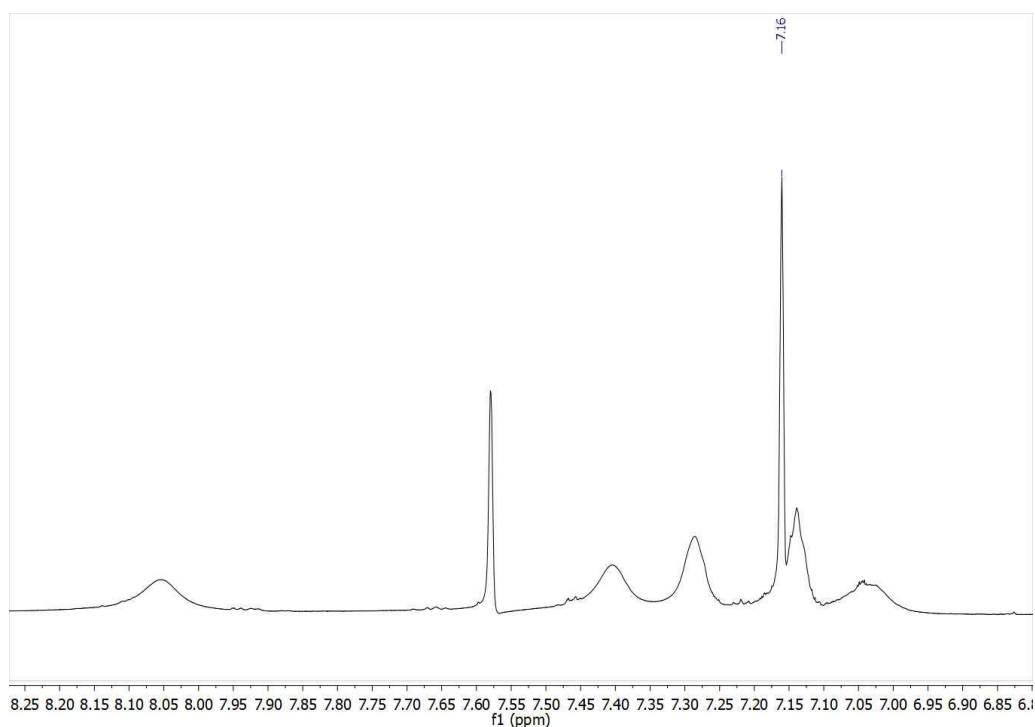


Figure 8 - Aromatic region of the solution state ^1H NMR spectrum of **1-Closed** (run in C_6D_6 at a frequency of 699.73 MHz).

2.4.1.2 – Attempted Synthesis of *N,N,N',N'*-tetraisopropyl-1-((phenyl(4-methyl pyridine-2-yl)methylene)amino)phosphanediamine (**3-Open**)

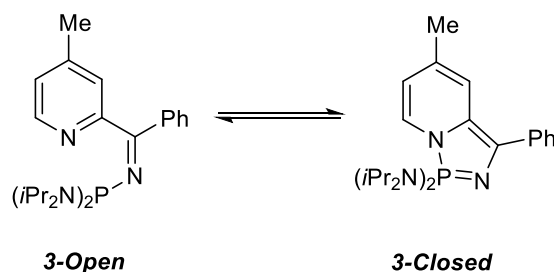


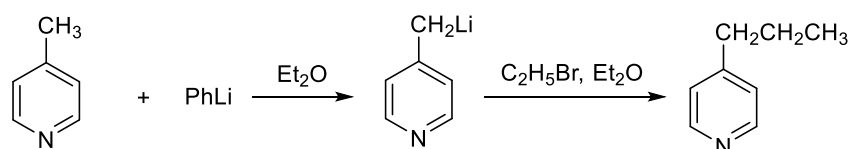
Figure 9 – Target compound **3**.

The introduction of a phenyl substituent at the 4-position on the pyridine ring (compound **1**) has been shown to shift the position of the “open”-“closed” equilibrium towards the “closed”

tautomer, relative to its unsubstituted analogue, compound **A**. Consequently, attempts were made to prepare a more basic structural analogue to compound **1**, with a methyl substituent at the 4-position (4-methylpyridine $pK_a = 5.94 > 4$ -phenylpyridine $pK_a = 5.5$).¹⁶ The target compound, **3**, is shown in Figure 9. Attempts were made to access this species from commercially available 4-methyl-2-cyanopyridine in accordance with the procedure laid out by Dyer and co-workers for the synthesis of compound **A** (Scheme 3).³

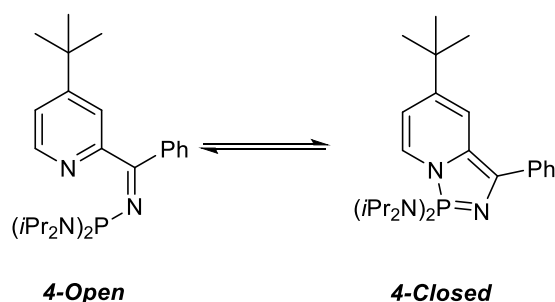
Analysis of the crude reaction mixture from the reaction between 4-methyl-2-cyanopyridine, PhLi and $(iPr_2N)_2PCl$ by solution state ^{31}P NMR spectroscopy revealed the presence of several phosphorus-containing species. Singlet resonances in the regions consistent with **3-Open** (at $\delta_P = +70.8$ and $+70.3$ ppm) and **3-Closed** (at $\delta_P = +47.5$, $+40.2$ and $+40.1$ ppm) were observed alongside several singlet resonances in the $+50$ and $+10$ ppm regions of the ^{31}P NMR spectrum. All attempts (by solvent extraction and recrystallization) to isolate a single phosphorus-containing product were unsuccessful, therefore the reaction was discontinued. The presence of multiple phosphorus-containing products is suggestive that more than one reaction pathway is in operation for the reaction between 4-methyl-2-cyanopyridine, PhLi and $(iPr_2N)_2PCl$.

The complexity of the reaction product mixture has been attributed to the presence of acidic CH_3 protons in the starting 4-methyl-2-cyanopyridine. PhLi is a strong base, pK_a of PhH = 43,¹⁵ and thus can deprotonate the methyl substituent of the 4-methyl-2-cyanopyridine, as well as attack at the cyano group. The resulting alkyllithium species are highly reactive towards electrophiles, and can react with $(iPr_2N)_2PCl$ to form products other than the desired **3-Open** and **3-Closed** (Figure 9). Indeed, it has been reported previously that the methyl substituent in 4-methylpyridine is deprotonated by PhLi, and the high reactivity of the resulting alkyllithium towards RX species (X = halogen) has been demonstrated using bromoethane (Scheme 10).¹⁸



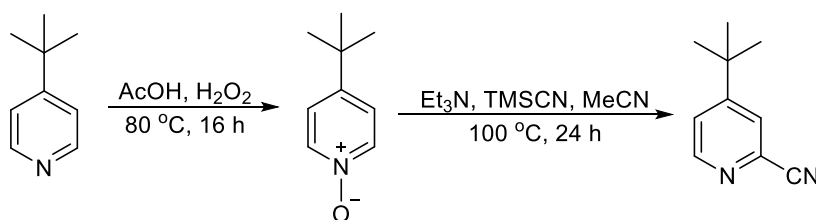
Scheme 10 – Reaction of 4-methylpyridine with PhLi followed by quenching with EtBr.¹⁸

2.4.1.3 – Synthesis and Characterisation of *N,N,N',N'*-tetraisopropyl-1-((phenyl(4-*tert*-butylpyridin-2-yl)methylene)amino)phosphanediamine (4-Open)/4-Closed



Scheme 11 – Target compound **4**.

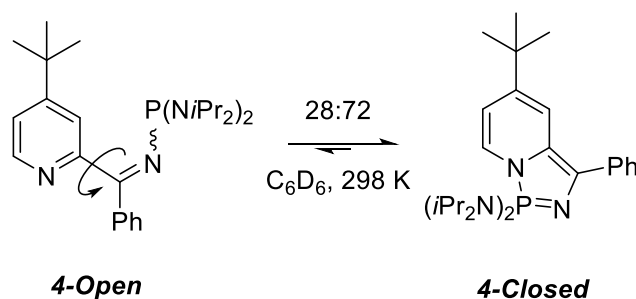
The next compound successfully prepared possesses an electron donating *t*Bu substituent at the 4-position on the pyridine ring, compound **4** (Scheme 11); the pK_a of its parent 4-*tert*-butylpyridine (5.98)¹⁶ is similar to that of 2-methylpyridine (5.94)¹⁶, the parent pyridine for target compound **3**. In contrast to the 4-Me substituent in 4-methyl-2-cyanopyridine, the *t*Bu substituent in 4-*tert*-butylpyridine, does not possess any acidic protons that would be susceptible to deprotonation by PhLi. The 4-*tert*-butyl-2-cyanopyridine precursor, required for the synthesis of **4** (Scheme 11), was prepared from 4-*tert*-butylpyridine using a modified literature procedure (Scheme 12),¹⁹ and the subsequent synthetic steps laid out by Dyer and co-workers for the preparation of compound **A**³ used to prepare compound **4**.



Scheme 12 – Preparation of 4-*tert*-butyl-2-cyanopyridine.

Solution state $^{31}\text{P}\{^1\text{H}\}$ NMR spectroscopic analysis of the reaction product (isolated by extraction with hexane from the crude reaction residue) showed that compound **4** exists as both **4-Open** and **4-Closed** forms, in a 28:72 ratio, respectively, at 298 K in C_6D_6 . Singlet resonances were observed for each tautomer: **4-Open** at $\delta_{\text{P}} = +69.9$ ppm and **4-Closed** at $\delta_{\text{P}} = +40.3$ ppm, resonances consistent with those observed for **A-Open** and **A-Closed**.³ The “open”-“closed” equilibrium for compound **4** lies further towards the “open” tautomer than

that for the 4-phenyl compound **1** (1:99 in C₆D₆ at 298 K), this is not consistent with the initial postulate that the higher the pK_a of the parent 4-substituted pyridine (pK_a for 4-*tert*-butylpyridine (**4**) > 4-phenylpyridine (**1**)), the further the “open”-“closed” equilibrium should lie towards the “closed” tautomer. For compounds **1** and **4**, this inconsistency between their equilibrium positions and the basicity of the pyridine nitrogen centres is instead attributed to an unfavourable steric interaction between the phenyl substituent bound to the imine carbon and the 4-substituent on the pyridine ring, which increases as the steric bulk of the latter increases.

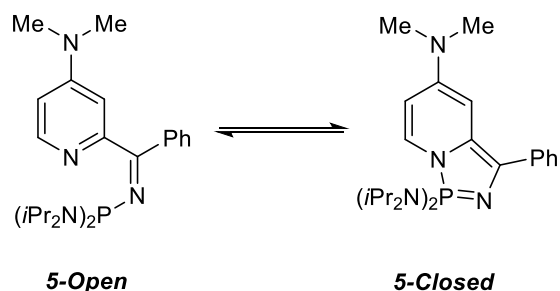


Scheme 13 – Tautomeric equilibrium position for **4-Open** and **4-Closed**.

Solution state ¹H NMR spectroscopic analysis of reaction product (which contains a mixture of **4-Open** and **4-Closed**) reveals two distinct sets of signals for both **4-Open** and **4-Closed**, which could be distinguished from one another by use of 2D NMR spectroscopic experiments. Analysis of the ¹H NMR spectrum of the interconverting mixture of **4-Open** and **4-Closed** revealed broad resonances for **4-Closed** (ν_{1/2} = 24 Hz), something that is likely to result from restricted rotation of the *t*Bu pyridine substituent and the phenyl group bound adjacent to the pyridine ring. The 2D NMR spectroscopic analysis of compound **4** suggests that **4-Open** exists as the rotamer shown in Scheme 13 (the NOESY NMR spectrum shows no interaction through space between the phenyl and pyridyl protons). The rotamer of **4-Open** in Scheme 13 demonstrates how the *t*Bu and Ph substituents are preferentially orientated away from each other in order to avoid an unfavourable steric interaction, in this conformation cyclisation cannot occur. Concerted cyclisation of **4-Open** can be achieved as rotation at the position shown in Scheme 13 is possible. The *cis/trans* geometry about the imine bond in **4-Open** cannot be determined from the magnitude of the |³J_{CP}| coupling constant as the signal for the quarternary imine carbon was not observed by ¹³C{¹H} NMR spectroscopic analysis (due to the long relaxation times associated with quarternary carbon centres).

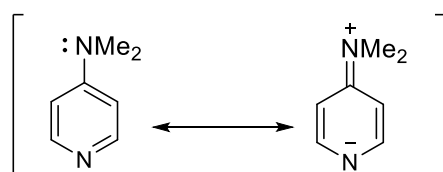
Following recrystallization from hexane at $-30\text{ }^{\circ}\text{C}$, deep red crystals of compound **4**, suitable for an X-ray crystallographic study, were obtained. The resulting molecular structure is shown in Figure 10 and key structural data are shown in Table 5. The crystals isolated for compound **4** at $-30\text{ }^{\circ}\text{C}$ correspond to the anellated $\sigma^4\text{-}1\lambda^5\text{-}[1,3,2]$ diazaphosphole **4-Closed**, the kinetic tautomer. The planarity of the fused bicyclic skeleton of **4-Closed**, which comprises of a five-membered heterocycle with alternating double and single bonds, is demonstrated by its small C3-C2...C1-C11 dihedral angle of 5.69 ° , consistent with the planar bicyclic motifs in **A-Open** and **1-Open**.^{3,17} The key bond lengths and angles in **4-Closed** (Table 5) are in good agreement with those observed for **A-Closed** (Table 4)³ and **1-Closed** (Table 3). The $^{31}\text{P}\{^1\text{H}\}$ NMR shift of **4-Closed** ($\delta_{\text{P}} = +40.3\text{ ppm}$) is consistent with the structure revealed by the X-ray crystallographic study and the data obtained for **A-Closed** and **1-Closed**.³

2.4.1.4 – Synthesis and Characterisation of *N,N,N',N'*-tetraisopropyl-1-((phenyl(4-dimethylamino-2-yl)methylene)amino)phosphanediamine (**5-Open**) / (**5-Closed**)



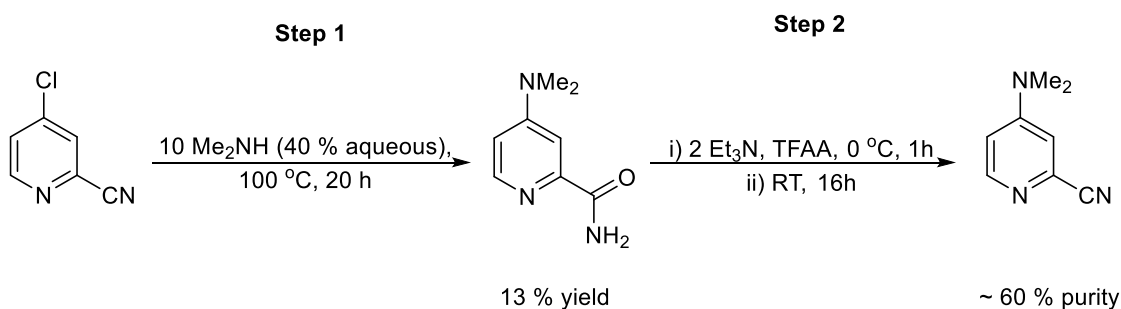
Scheme 14 – Target compound 5.

Target compound **5** (Scheme 14), a 4-substituted analogue of compound **A**, was of interest to prepare because of the high $\text{p}K_{\text{a}}$ value of 4-*N,N*-dimethylaminopyridine (DMAP, $\text{p}K_{\text{a}} = 9.2$).¹⁵ The strong nucleophilic character of the pyridine nitrogen centre in DMAP originates from the ability of the amine lone pair to donate into the aromatic ring (Scheme 15).^{15,20} It was of interest to probe the impact (if any) that the conjugating lone pair has upon the “open”-“closed” equilibrium of the pyridyl-*N*-phosphinoimine – diazaphosphazole tautomers.



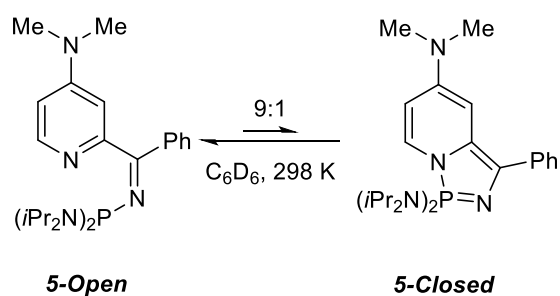
Scheme 15 – Resonance structures of DMAP.

In order to prepare the target compound **5** (Scheme 14), 4-*N,N*-dimethylamino-2-cyanopyridine was synthesised using modified literature procedures,^{21,22} as shown in Scheme 16. The high cost of the commercially available 4-chloro-2-cyanopyridine, combined with the poor yield associated with **Step 1** (Scheme 16) and the challenges of purifying the product of **Step 2**, meant that only 100 mg of material was isolated from **Step 2**. The material isolated from **Step 2** was found to comprise of ~ 60 % 4-dimethylamino-2-cyanopyridine (by ¹H NMR spectroscopic analysis) alongside unidentifiable contaminants, this material was unable to be purified further and used as-was for the preparation of compound **5**.



Scheme 16 – Synthesis of 4-dimethylamino-2-cyanopyridine.

The reaction between 4-dimethylamino-2-cyanopyridine, PhLi and (*i*Pr₂N)₂PCl was carried out in accordance with the procedure laid out by Dyer and co-workers for the preparation of compound **A**.³ Solution state ³¹P NMR spectroscopic analysis of the redissolved crude reaction mixture revealed the presence of a complex mixture of phosphorus-containing species, suggesting that the reaction did not proceed cleanly. The sample of 4-dimethylamino-2-cyanopyridine used in the reaction with PhLi and (*i*Pr₂N)₂PCl was not pure (by ¹H and ¹³C{¹H} NMR spectroscopic analysis), the impurities were unable to be removed and are likely to have undergone reaction(s) with PhLi and (*i*Pr₂N)₂PCl, resulting in the complex mixture of phosphorus-containing species observed. Singlet resonances in the solution state ³¹P NMR spectrum recorded for the crude reaction mixture, that have been attributed to **5-Open** (at δ_P = +70.4 ppm) and **5-Closed** (at δ_P = +44.9 ppm) were observed; the inability to isolate these species hindered further NMR spectroscopic analysis.



Scheme 17 - Tautomeric equilibrium for compound 5.

$^{31}\text{P}\{^1\text{H}\}$ NMR spectroscopic analysis of the crude mixture obtained from the reaction between 4-dimethylamino-2-cyanopyridine, PhLi and $(i\text{Pr}_2\text{N})_2\text{PCL}$ revealed the presence of both **5-Open** and **5-Closed**, in a 9:1 ratio, respectively (in C_6D_6 at 298 K (Scheme 17), by integration of the ^{31}P NMR spectroscopic signals). 4-Dimethylaminopyridine (DMAP) has a high $\text{p}K_{\text{a}}$ value of 9.2,¹⁵ far greater than the parent 4-substituted pyridines for compounds **1** and **A** (4-phenylpyridine (5.5)¹⁵ and pyridine (5.25),¹⁵ respectively), the 9:1 ratio of **5-Open:5-Closed** (in C_6D_6 at 298 K) is not consistent with the $\text{p}K_{\text{a}}$ of DMAP and the “open”：“closed” ratios of 5:95 and 1:99 (in C_6D_6 at 298 K) observed for tautomeric species **A** and **1**, respectively.

There is ample evidence in the literature that DMAP ($\text{p}K_{\text{a}} = 9.2$)¹⁵ is a more powerful nucleophile and organocatalyst than pyridine ($\text{p}K_{\text{a}} = 5.25$),¹⁵ as well as other amine bases with similar, or even greater, $\text{p}K_{\text{a}}$ values, notably Et_3N that has a $\text{p}K_{\text{a}}$ of 10.65.²⁰ The nucleophilic potency of DMAP is attributed to the ability of the lone pair on the amine nitrogen centre to donate into the aromatic pyridine ring. Despite the high $\text{p}K_{\text{a}}$ and nucleophilicity of the DMAP motif, and the expectation that these factors would lead to a greater degree of cyclisation of **5-Open** to form **5-Closed** than was observed for compounds **A** and **1**, this is not what has been observed experimentally for compound **5** (**5-Open:5-Closed**, 9:1 in C_6D_6 at 298 K). The rationale behind this result is not clear at this time, however, steric constraints imposed by the NMe_2 substituent on the pyridine ring may contribute to hindering the cyclisation of **5-Open**, as was seen for the *t*Bu group in compound **4**.

2.4.2 – Substitution of Methyl Groups at the 3- and 5-Positions on the Pyridine Ring of the Pyridyl-*N*-Phosphinoimine

Section 2.4.1 details how the stereoelectronic nature of the *para*-substituent on the pyridine ring impacts the “open”-“closed” equilibrium position of the pyridyl-*N*-phosphinoimine – diazaphosphazole tautomeric pairs (**1**, **3**, **4** and **5**). This section (2.4.2) will now address attempts to prepare target compounds **6** and **7** (Figure 11), which possess methyl substituent(s) at the *meta*-position(s) on the pyridine ring.

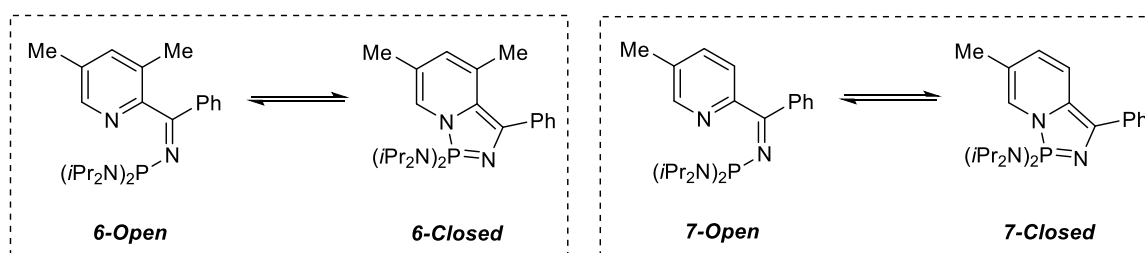
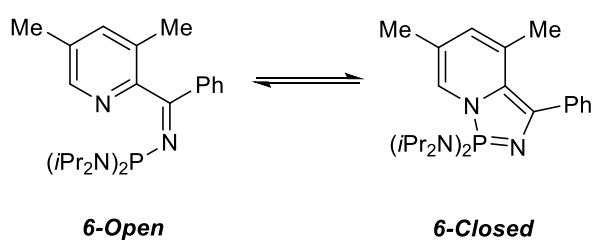


Figure 11 – Target compounds **6** and **7**.

2.4.2.1 – Synthesis and Analysis of *N,N,N',N'*-tetraisopropyl-1-((phenyl(3,5-dimethylpyridin-2-yl)methylene)amino)phosphanediamine (6-Open) / (6-Closed)



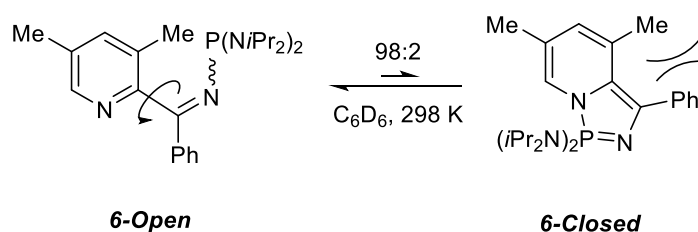
Scheme 18 – Target compound **6**.

The disubstituted pyridyl-imine compound **6** (Scheme 18) was chosen as a target because of the higher pK_a value of 3,5-dimethylpyridine ($pK_a = 6.13$)²⁴ relative to the pyridine motifs present in compounds **A** (pyridine, $pK_a = 5.25$),¹⁵ **1** (4-phenylpyridine, $pK_a = 5.5$),¹⁵ and **4** (4-*tert*-butylpyridine, $pK_a = 5.98$).¹⁶ The higher pK_a of the pyridine motif in compound **6** could result in the “open”-“closed” ratio for **6** being similar to, if not greater than, that observed for compounds **A**, **1** and **4**.

Although 3,5-dimethylpyridine possesses two sets of acidic CH₃ protons that are susceptible to nucleophilic attack by PhLi, in 3,5-dimethyl-2-cyanopyridine (precursor to target compound **6**), the 5-methyl substituent *para* to the 2-cyano group has the effect of activating the CN functionality towards nucleophilic attack as a result of inductive effects. Consequently, attack at the cyano group in 3,5-dimethyl-2-cyanopyridine by PhLi is kinetically favourable over attack at the 3- or 5-methyl substituents. This kinetic preference for reaction at the cyano group was evidenced experimentally by the successful preparation of compound **6** from commercially available 3,5-dimethyl-2-cyanopyridine, PhLi and (*i*Pr₂N)₂PCl. Solution state ³¹P{¹H} NMR spectroscopic analysis of the crude reaction mixture and the redissolved reaction residue revealed that **6** exists in a tautomeric equilibrium between **6-Open** and **6-Closed**, which are present in a ratio of 98:2 in C₆D₆ at 298 K. The ¹H and ¹³C{¹H} NMR spectra recorded for the reaction product show signals consistent with **6-Open**, notably the CH carbon centre *ortho* to the pyridine nitrogen is observed as a singlet (δ_c = 146.9 ppm), indicative of there being no N(pyridine)-P bond. A signal at δ_c = 164.7 ppm in the ¹³C{¹H} NMR spectrum is observed, a chemical shift that is consistent with the presence of an imine carbon.

The ratio of **6-Open:6-Closed** observed in C₆D₆ at 298 K, 98:2, contrasts with the ratio observed for compounds **A** (**A-Open:A-Closed**, 5:95 in C₆D₆ at 298 K) and **1** (**1-Open:1-Closed**, 1:99 in C₆D₆ at 298 K), despite the core substituted pyridine motif having a greater pK_a. This equilibrium position for compound **6** suggests that there is a steric barrier to the cyclisation of **6-Open** (as was observed for **4-Open**). When **6-Open** adopts the conformation shown in Scheme 18 (conformation required for cyclisation), the methyl substituent at the 3-position on the pyridine ring lies in close proximity to the phenyl substituent bound to the imine carbon centre, which gives rise to an unfavourable steric interaction. Examination of the solution state 2D NMR spectra recorded for the interconverting mixture of **6-Open** and **6-Closed** indicated that **6-Open** exists as the rotamer shown in Scheme 19 (the NOESY NMR spectrum shows no interaction through space between the phenyl and 3-methyl protons), whereby the imine-phenyl and 3-methyl groups are angled away from each other to reduce their unfavourable steric interaction. When **6-Open** adopts the conformation shown in Scheme 19, the attack of the pyridine nitrogen lone pair at the phosphorus centre, and therefore cyclisation, cannot occur. Concerted cyclisation can occur as rotation at the position shown in Scheme 19 is possible. A greater proportion of **4-Closed** (section 2.4.1.3) is observed

experimentally than for **6-Closed**, despite both experiencing unfavourable steric interactions between pyridine and imine substituents when in their “open” tautomeric forms, this difference is attributed to the closer proximity of the 3-methyl substituent to the imine-phenyl group in **6-Open** than for the 4-*tert*-butyl moiety in **4-Open**.



Scheme 19 – **6-Open** and **6-Closed** tautomeric equilibrium showing the conformation of **6-Open**.

2.4.2.2 – Attempted Synthesis of *N,N,N',N'*-tetraisopropyl-1-((phenyl(5-methylpyridin-2-yl)methylene)amino)phosphanediamine (**7-Open**) / (**7-Closed**)

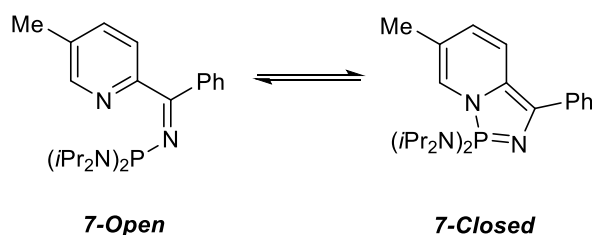
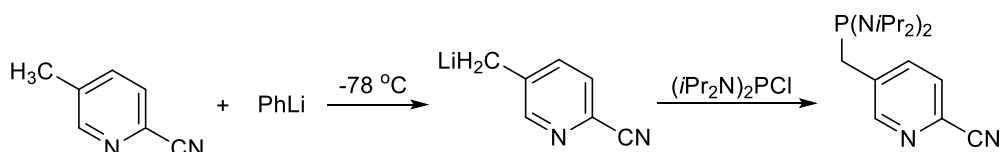


Figure 12 – Target compound **7**.

The successful preparation of compound **6** revealed that the presence of the methyl substituent at the 3-position on the pyridine ring is very likely to sterically hinder cyclisation, despite the high nucleophilicity of the pyridine nitrogen centre (3,5-dimethylpyridine $pK_a = 6.13$).²³ Consequently, attempts were made to prepare the target 5-methyl derivative, compound **7** (Figure 12), in order to probe the impact of an electron donating substituent at the 5-position (5-methylpyridine, $pK_a = 5.68$)²⁴ on the pyridine ring upon the position of the “open”-“closed” tautomeric equilibrium. The preparation of compound **7** was explored, starting from commercially available 5-methyl-2-cyanopyridine. All attempts to synthesise compound **7** from 5-methyl-2-cyanopyridine, PhLi and $(iPr_2N)_2PCl$, however, were unsuccessful. In contrast to 3,5-dimethyl-2-cyanopyridine, 5-methyl-2-cyanopyridine does not possess an activating methyl substituent *para* to the cyano group which acts to direct

nucleophilic attack at the CN moiety in 3,5-dimethyl-2-cyanopyridine. The acidic methyl protons in 5-methyl-2-cyanopyridine are more susceptible to nucleophilic attack by PhLi than its cyano group, and, whilst no reports in the literature of the reaction between 3-methylpyridine and PhLi can be found, it is highly likely that the methyl group in 5-methyl-2-cyanopyridine is deprotonated by PhLi (as is seen for 4- and 2-methylpyridine)¹⁸ to form an alkyllithium species, which is then quenched by the chlorophosphine (Scheme 20). The preparation of target compound **7** was subsequently discontinued.



Scheme 20 – Proposed deprotonation of 3-methyl-2-cyanopyridine by PhLi and subsequent quenching by $(iPr_2N)_2PCl$.

2.5 – Effect of Modifying the Imine Carbon Substituent upon the Pyridyl-*N*-Phosphinoimine-Diazaphosphazole Tautomeric Equilibrium Position

2.5.1 – Introduction of Aryl Imine Substituents at the Imine Carbon of the “Open” Tautomer

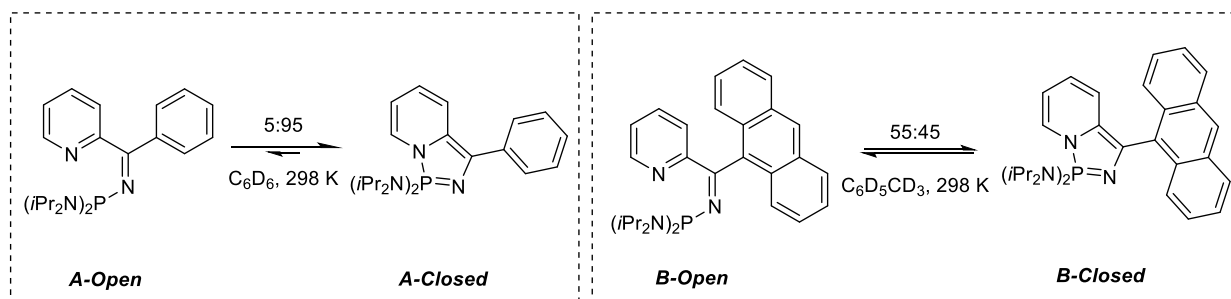
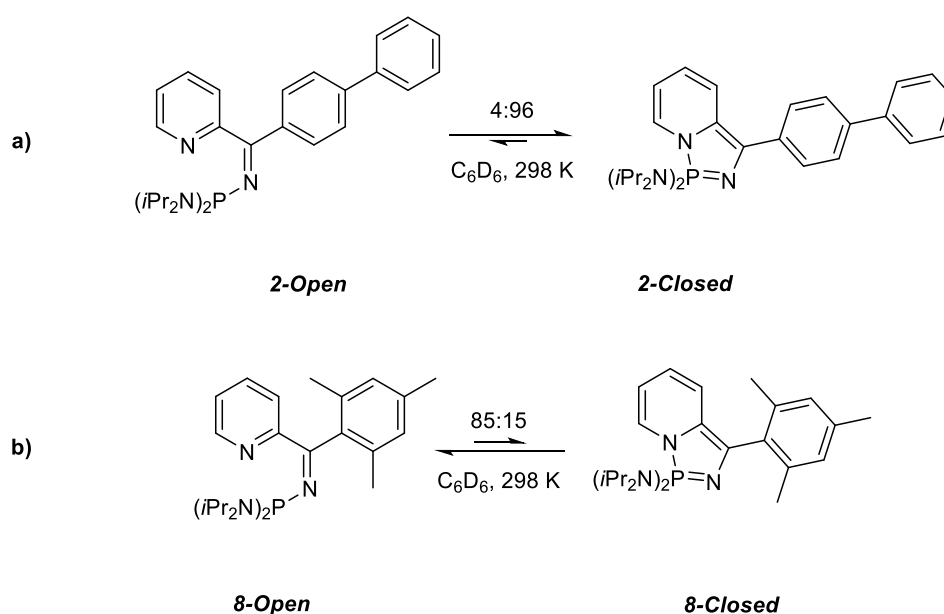


Figure 13 – Structural analogues compounds **A** and **B**, previously reported by Dyer and co-workers.^{3,4}

As was discussed in **Chapter 1**, Dyer and co-workers have previously reported the synthesis and structural analysis of compounds **A** and **B** (Figure 13), which differ from each other in the stereoelectronic nature of their imine substituents (phenyl vs anthracenyl), something that results in notably different ratios of “open”：“closed” tautomers.^{3,4} This section will report the successful synthesis of compounds **2** and **8** (Scheme 21), which differ structurally from compounds **A** and **B** in their imine substituents (**2** = 4,4'-biphenyl, **8** = Mes). The preparation

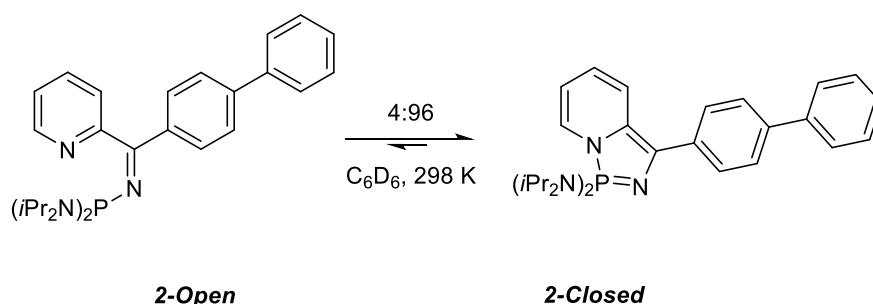
of compound **2** was chosen as it possesses a 4,4'-biphenyl group at the imine carbon, this extends the π -system that exists between the imine substituent and imine C=N double bond, as well as the size of the group relative to phenyl substituent in **A**. Compound **8** was targeted as it possesses a mesityl group at the imine carbon, Mes is a bulkier group than the Ph substituent in **A**, it comprises of a single phenyl moiety which is more electron rich than unsubstituted phenyl as a consequence of the three methyl groups bound to it.

Compounds **2** and **8** (Scheme 21) were prepared in accordance with the synthetic procedure laid out by Dyer and co-workers for the preparation of compound **A**.³ 4,4'-Biphenyllithium and mesityllithium were prepared using a modified literature procedure,²⁵ and used *in situ* for the preparation of compounds **2** and **8**, respectively. Subsequent ³¹P NMR spectroscopic analyses revealed that compounds **2** and **8** both exist as “open” and “closed” tautomers, in ratios of 4:96 and 85:15, respectively (in C₆D₆ at 298 K). By solution state ³¹P{¹H} NMR spectroscopic analysis, compounds **2-Open** and **8-Open** give rise to singlet resonances at $\delta_P = +70.4$ and $+67.9$ ppm, respectively, and compounds **2-Closed** and **8-Closed** to singlet resonances at $\delta_P = +41.2$ and $+39.0$ ppm, respectively. The ³¹P{¹H} NMR chemical shifts observed for compounds **2** and **8** are consistent with those of their structural analogues, **A** and **B**.^{3,4} The electronic and steric differences between the R⁶ substituents in compounds **A**, **B**, **2** and **8** will be considered in order to rationalise the differing tautomeric equilibrium positions.



Scheme 21 – Tautomeric equilibrium positions for compounds a) **2** and b) **8**.

2.5.1.1 – X-Ray Crystallographic Study of 3-(biphenyl)-*N,N,N',N'*-tetraisopropyl-115-[1,3,2]diazaphospholo[1,5-*a*]pyridine-1,1-diamine (2-Closed)

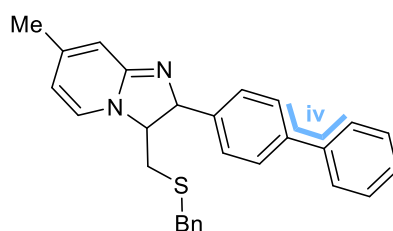


Scheme 22 – Experimentally observed equilibrium position for compound **2**.

Following recrystallization of compound **2** from hexane at $-30\text{ }^\circ\text{C}$, deep-red crystals of **2-Closed** (Scheme 22) suitable for an X-ray crystallographic study were obtained. The X-ray molecular structure for compound **2**, which corresponds to **2-Closed**, is shown in Figure 15 and selected structural data are shown in Table 6.

The structural data for anellated $\sigma^4\text{-}1\lambda^5\text{-}[1,3,2]$ diazaphosphole, **2-Closed**, are consistent with its multinuclear NMR spectroscopic data, notably its solution state ^{31}P NMR shift at $\delta_{\text{P}} = +41.2$ ppm, a chemical shift that is comparable to those observed for **A-Closed**, **B-Closed** and **8-Closed**. The key structural data obtained for **2-Closed** (Table 6) are consistent with those observed experimentally for its structural analogues **A-Closed**,³ **1-Closed** and **4-Closed** (section 2.4.1.3). It is of interest to compare the dihedral angle *i* in **A-Closed** and *ii* in **2-Closed** (Figure 14), which take the values of $35.1(5)^\circ$ and $23.4(2)^\circ$, respectively. These two dihedral angles, *i* and *ii*, differ noticeably from each other (by $11.7(5)^\circ$), indicating that the stereoelectronically different phenyl and 4,4'-biphenyl groups orientate themselves differently with respect to the planar fused bicyclic system. The C1-C11 bond length in **A-Closed** ($1.466(4)\text{ \AA}$, Figure 7) and the C1-C19 bond length in **2-Closed** ($1.458(2)\text{ \AA}$, Figure 15), *i.e.* the C(imine)-C(R^6) bond lengths, are statistically identical, and lie in the region between the average pure C(sp^3)-C(sp^3) (1.54 \AA) and pure C(sp^2)-C(sp^2) (1.33 \AA) bond lengths.²⁶ These bond lengths are indicative of the C(imine)-C(R^6) bond in compounds **A-Closed** and **2-Closed** possessing partial double character and conjugation of the imine substituent π -electron density with the rest of the molecule.

The second dihedral angle for **2-Closed**, **iii** (Figure 14), measures 16.5(2) °, indicating that the two rings in the 4,4'-biphenyl moiety are not coplanar as they are in free biphenyl.³⁷ The distortion of the normally coplanar 4,4'-biphenyl motif is further seen by the C22-C25 bond length in **2-Closed** (1.4823(2) Å), which is shorter than the C(*sp*²)-C(*sp*²) bond length in free biphenyl (1.5074 Å).³⁶ The **iv** torsional angle (35.1(5) °) in the species shown in Figure 16, which possesses a 4,4'-biphenyl motif bound to a fused heterocycle, and its C(*sp*²)-C(*sp*²) bond length (1.480(2) Å) are consistent with the corresponding dihedral angle/bond length in compound **2-Closed**.²⁷

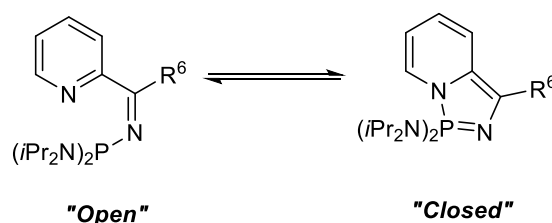


$$\text{iv} = 35.1(5)^\circ$$

Figure 16 – Dihedral angle **iv** of the non-coplanar 4,4'-biphenyl moiety bound to a fused heterocyclic system.²⁷

2.5.1.2 – Electronic Differences between Imine Substituents on the “Open”

Tautomers



	R ⁶	% “Open” ^a	% “Closed” ^a	Δ _p (ppm) of “Open”/“Closed” ^a	R ⁶ NICS(0) [†]	R ⁶ NICS(1) [‡]
A	Ph	5	95	+70.3 / +42.3 ^b	-8.03	-10.2
B	Anth	55	45	+68.9 / +40.5 ^c	-11.47 [§]	-13.06 [§]
2	4,4-Biphenyl	85	15	+70.4 / +41.2 ^b	-7.54	-9.63
8	Mes	4	96	+67.9 / +39.0 ^b	-9.78	-9.54

Figure 17 – “Open”：“closed” ratios for **A**, **B**, **2** and **8** and the NICS(0) and NICS(1) values for the R⁶ group.²⁸ ^a At 298 K.

^b Spectrum recorded in C₆D₆. ^c Spectrum recorded in C₆D₅CD₃.

[†] NICS(0) measured at the ring centre at the RB3LYP/6-31+G** level of theory.

[‡] NICS(1) measured 1 Å above the ring centre at the RB3LYP/6-31+G** level of theory.

[§] NICS(0) and NICS(1) values for central ring in anthracenyl moiety.

The imine substituents present in compounds **A**, **B**, **2** and **8** differ from each other in their stereoelectronic nature, the differences in the extent of aromaticity between these groups will be explored first. Aromaticity is of interest to examine as the R⁶ groups, which can rotate about the C(imine)-C(R⁶) bond, can enter into (and out of) conjugation with the imine C=N bond when their respective π-systems lie coplanar to each other. The ability of the R⁶ substituent to enter into and out of conjugation with the imine C=N bond will have an impact upon the electron distribution within the exocyclic component of the “open” species and, consequentially, could affect the extent of cyclisation of the “open” species. The data presented in Figure 16 summarise the tautomeric equilibrium positions for compounds **A**,³ **B**,⁴ **2** and **8**, as well as the computationally-derived nuclear-independent chemical shift (NICS) values for their R⁶ substituents.²⁸ NICS values are being used here as a parameter to quantify the extent of aromaticity of a compound. NICS values are defined as the computed negative magnetic shielding value calculated for a given point in a molecule.²⁸ Figure 16 shows two NICS values for each R⁶ group: NICS(0), measured at the ring centre, and NICS(1), measured 1 Å above the ring centre.²⁸ Schleyer²⁹ has suggested that NICS(1) indices are better descriptors for delocalised π-electron density than NICS(0) values, as they eliminate contributions from the σ-framework, NICS(1) values will therefore be used here. Figure 18 shows a plot of the percentage of “closed” tautomer observed for compounds **A**, **B**, **2** and **8** (at 298 K) against the NICS(1) value of their respective R⁶ substituent. It is evident from the data presented in Figure 18 that there is no correlation between the R⁶ NICS(1) values (*i.e.* extent of R⁶ aromaticity) and the percentage “closed” tautomer observed.

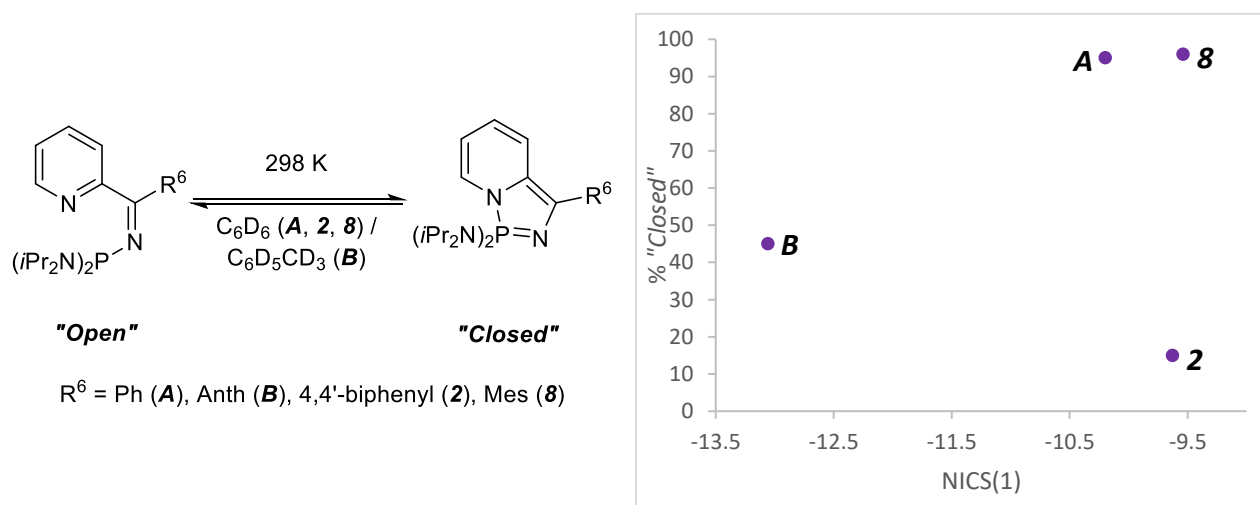


Figure 18 – Plot of % “closed” tautomer (at 298 K in C₆D₆ (**A**, **2**, **8**)/C₆D₅CD₃ (**B**)) against NICS(1) values for **A**, **B**, **2** and **8**. Error for % “closed” determined by experimental solution state ³¹P{¹H} NMR spectroscopy and fixed at 0.5 %.

The R⁶ substituents for compounds **A**, **B**, **2** and **8** differ from each other electronically, not just in terms of their aromaticity, but also in their electron donating/accepting character. Multiple methods are available for the quantification of the electronic character of the R⁶ group, for example, by the preparation of the Ni(CO)₃(PR₂R⁶) complexes and subsequent measurement of the A₁ carbonyl stretching frequency.³⁰ For the purposes of this investigation, the electronic effect associated with the R⁶ moieties was probed by ³¹P NMR spectroscopic analysis of the readily accessed P^V mono-selenides of the corresponding (iPr₂N)₂PR⁶ phosphines. As was discussed in **Chapter 1**, the |¹J_{PSe}| coupling constant for Se=PR₃ species is a quantitative indication of σ-donor ability of a phosphorus centre.^{31,32,33} As substituents bound to a phosphorus centre directly determine its donor ability, comparing the monoselenides of (iPr₂N)₂PR⁶ phosphines will allow a crude, but direct, comparison of the relative electronic character of the R⁶ substituents, phenyl, anthrathenyl, 4,4'-biphenyl and mesityl. It should be noted, however, that this approach does not take into account the steric impact of the substituents bound to the phosphorus centre. Bulky substituents bound to a phosphorus centre have been reported perturb |¹J_{PSe}| values, the reason for this, however, is not fully understood.³⁴ This steric effect is believed to be minimal for the substituents of interest to this thesis.

Compound	R ⁶	δ _P (ppm)	¹ J _{PSe} (Hz)	Corresponding iminophosphorane	"Open": "Closed" of corresponding iminophosphorane (298 K)
A-PSe	Ph	+70.2 ^a	759 ^a	A	5:95 ^d
B-PSe	Anth	+75.8 ^b	750 ^b	B	55:45 ^e
2-PSe	4,4'-Biphenyl	+69.7 ^c	760 ^c	2	4:96 ^d
8-PSe	Mes	+76.1 ^c	746 ^c	8	85:15 ^d

Figure 19 - |¹J_{PSe}| values for the monoselenides of (iPr₂N)₂PR⁶. ^a 101.3 MHz, CDCl₃. ^b 283.3 MHz, CDCl₃. ^c 162.0 MHz, CDCl₃. ^d In C₆D₆. ^e In C₆D₅CD₃.

The (iPr₂N)₂PR⁶ phosphines (Figure 19) were synthesised from the reaction of (iPr₂N)₂PCl with the respective R⁶Li lithium reagent (themselves prepared and used *in situ*),²⁵ then reacted with elemental selenium to give the desired monoselenide species. ³¹P{¹H} NMR spectroscopic analysis was used to determine the |¹J_{PSe}| values shown in Figure 19. The |¹J_{PSe}| values for **A-PSe**, **B-PSe**, **2-PSe** and **8-PSe**, and therefore the electronic character of

phenyl, anthracenyl, 4,4'-biphenyl and mesityl groups, respectively, are all very similar (Figure 19), whereas the position of the “open”：“closed” equilibrium for compounds **A**, **B**, **2** and **8**, respectively, vary widely. This suggests that the electronic character of the R⁶ substituent has little impact upon the extent of “closed” formation.

2.5.1.3 – Differences in Steric Bulk Between Imine Substituents on the “Open” Tautomers

Comparison of the electronic character of the imine substituents in compounds **A**, **B**, **2** and **8** (Figure 19) suggests that these electronic differences do not impact upon the position of the “open”-“closed” equilibrium. Consequently, the differences in the steric bulk of the R⁶ substituents will now be examined to explore their potential impact.

The volume of space occupied by the R⁶ substituents about the imine carbon centre, defined as the “R⁶ cone angle” θ (Figure 20), has been calculated using a similar premise to that used by Tolman (see **Chapter 1**)³⁵ to determine the amount of space a phosphine ligand occupies when bound to a metal centre (so-called Tolman cone angle). A representative example of the parameters used to calculate the “R⁶ cone angle” is shown for the mesityl R⁶ group in Figure 20. For this purpose, the C(imine)-C(R⁶) bond length, **C-C** (Figure 20), has been defined as 1.46 Å, a value that (within error) is representative of the C(imine)-C(R⁶) bond lengths for all the analogous species reported in this work, and previously, which have been studied by X-ray crystallographic methods.^{3,4} The Van der Waals radii of the R⁶ protons have been used to represent the boundary of the R⁶ group, to give the distance **X** (Figure 20), **X** values have been determined by analysis of previously reported experimental X-ray crystallographic data for molecules of benzene,³⁶ biphenyl,³⁷ anthracene^{38,**} and mesitylene.^{39,††} A summary of the **X** and θ values are shown in Table 7. Examination of a plot of the percentage of the “closed” tautomer observed for **A**, **B**, **2** and **8** (by ³¹P NMR spectroscopic analysis at 298 K) against the

** The molecule of anthracene studied co-crystallised alongside 1,1'-bi-3,5-dichloro-4-oxo-hexa-2,5-dienylidene and is treated here as an independent entity.

†† The molecule of mesitylene studied co-crystallised alongside (2R,5R,8R,11R)-1,4,7,10-Tetrabenzyl-2,5,8,11-tetraethyl-1,4,7,10-tetra-azacyclododecane and treated here as an independent entity.

calculated R^6 cone angle for the corresponding R^6 substituent (Figure 21), it is evident from these data that there is no correlation between the two factors.

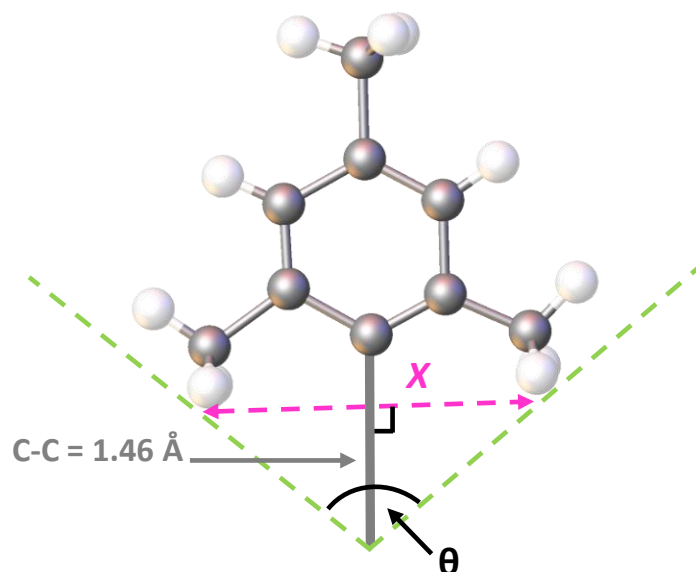


Figure 20 – R^6 cone angle parameters for the mesityl group. The proton at the 1-position has been omitted to show the point of connection to the imine carbon centre, C-C.

R^6	X (Å)	θ (°)	"Open": "Closed" (Tautomeric pair), 298 K
Benzene	4.0096	107	5:95 (A) ^a
Anthracene	9.146	144	55:45 (B) ^b
4,4-Biphenyl	4.1803	110	4:96 (2) ^a
Mesitylene	5.003	119	85:15 (8) ^a

Table 7 – X values for benzene,³⁶ biphenyl,³⁷ mesitylene³⁸ and anthracene³⁶ and the calculated R^6 cone angles. ^a In C_6D_6 . ^b In $C_6D_5CD_3$.

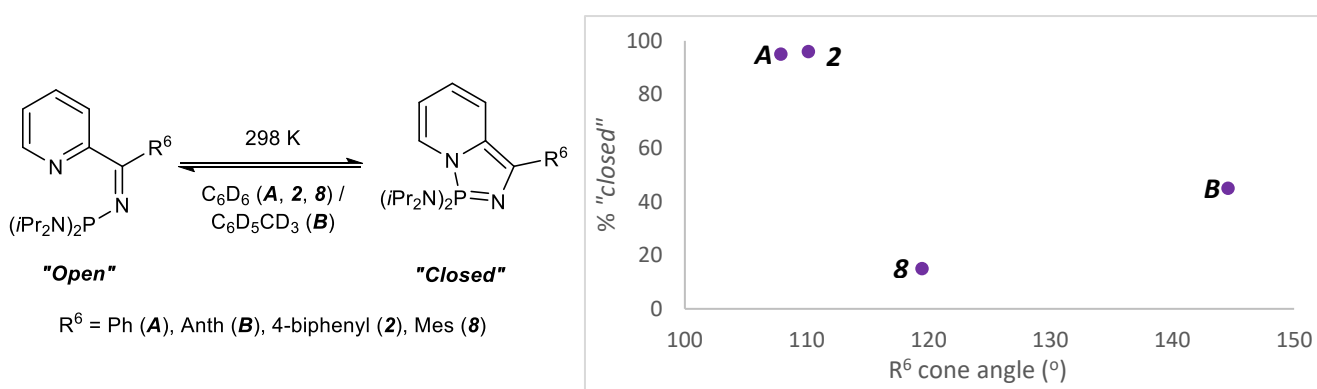
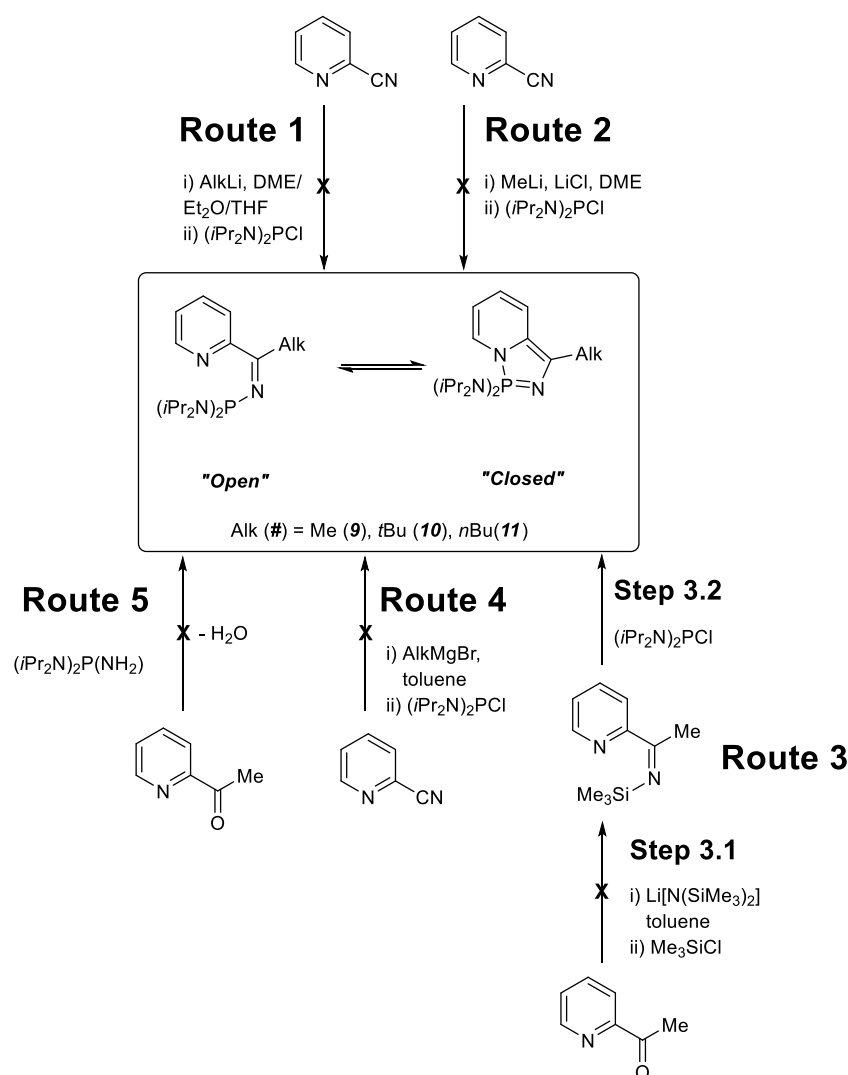


Figure 21 – Plot of percentage "closed" observed for **A**, **B**, **2** and **8** (by $^{31}P\{^1H\}$ NMR spectroscopic analysis at 298 K in C_6D_6 (**A**, **2**, **8**)/ $C_6D_5CD_3$ (**B**)) against the " R^6 cone angle". Error for % "closed" determined by experimental solution state $^{31}P\{^1H\}$ NMR spectroscopy and fixed at 0.5 %.

The comparative studies outlined thus far in this section (**2.5**) have not revealed any correlation between the marked differences in extent of cyclisation observed for compounds **A**, **B**, **2** and **8** (i.e. the relative amounts of the “open” vs “closed” tautomers) and the variations in steric (“R⁶ cone angle”) and electronic (donor-acceptor character and extent of aromaticity) character of their respective imine substituents. It must be concluded, therefore, that the relationship between the nature of the R⁶ imine substituent and the position of the “open”-“closed” equilibrium is as a consequence of a mixture of both subtle steric and electronic effects.

2.5.2 – Attempted Installation of Alkyl Substituents at the Imine Carbon of the Pyridyl-*N*-Phosphinoimine “Open” Tautomer

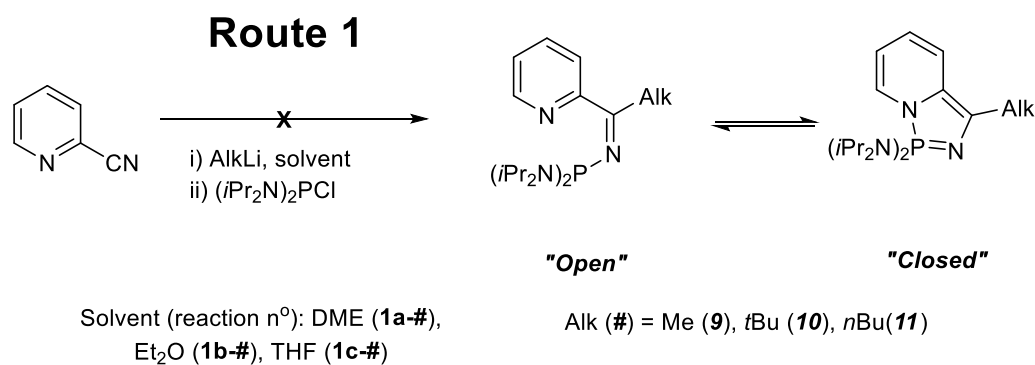


Scheme 23 - Synthetic routes probed whilst attempting to prepare target compounds **9**, **10** and **11**.

Section **2.5.1** described the synthesis and comparison of pyridyl-*N*-phosphinoimine - diazaphosphazole species with aryl substituents bound to the imine carbon. It was of interest to prepare analogous species with electron donating alkyl substituents bound to the imine carbon in order to probe the impact of a non-aromatic substituent, which cannot enter into π -conjugation with the imine bond, upon the position of the “open”-“closed” equilibrium. To this end, a range of synthetic approaches to such compounds were considered (Scheme 23).

2.5.2.1 – Use of Organolithium reagents: Synthetic Routes 1, 2 and 3

The synthetic route reported by Dyer and co-workers in 2008 for the preparation of compound **A** and its analogues^{3,4} makes use of organolithium species to introduce a substituent at the cyano group of a starting 2-cyanopyridine. Indeed, the use of organolithium reagents has proved effective for aryllithium species, *i.e.* these reactions have been found to proceed cleanly, and give reasonable yields of product(s). The use of this same synthetic approach, **1a** (Scheme 24), to prepare target compounds **9**, **10** and **11** (using MeLi, *t*BuLi and *n*BuLi, respectively) did not yield the desired products. ³¹P NMR spectroscopic analysis of the crude reaction mixtures resulting from reactions **1a-9**, **1a-10** and **1a-11** (Scheme 24) for the preparation of target compounds **9**, **10** and **11**, respectively, revealed significant proportions of starting (*i*Pr₂N)₂PCl as well as several other (mostly) unidentifiable phosphorus-containing species, even after extended reaction times and applying heat. Among the phosphorus-containing species generated by reactions **1a-9**, **1a-10** and **1a-11**, resonances in the ³¹P NMR spectra in the ~ +70 ppm region, characteristic of other “open” pyridyl-*N*-phosphinoimine species, were seen (+74.0 and +66.3 ppm (**1a-9**), +66.6 ppm (**1a-10**), +65.6 ppm (**1a-11**)). However, all attempts to isolate and identify these species were unsuccessful. These spectroscopic results are indicative that the reaction mechanism is more complex than expected, likely as a result of the high basicity of the alkyllithium reagents used.



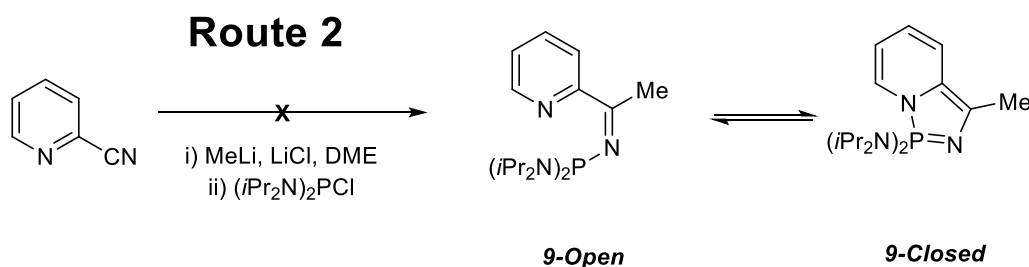
Scheme 24 – Synthetic procedures carried out in attempts to prepare target compounds **9**, **10** and **11** using AlkLi reagents.

When using organolithium species, the solvent used for the reaction must be considered due to the aggregated cage structures organolithium species (RLi) adopt in solution (as well as in the solid state).^{40,41} Here, the degree of aggregation of organolithium species is intimately linked to the nature of the organo-substituent, and coordinating solvents are required to break up the aggregation of the organolithium and allow it to react.⁴¹ Reaction **1a** (Scheme 24) used DME as the reaction solvent; in order to probe the role of solvent in synthetic **Route 1**, this approach was repeated using different solvents: **1b** – Et₂O and **1c** – THF.

MeLi is an unusually strongly-aggregated species, and there are no reports in the literature of a solvent that can fully disrupt this aggregation to form the solvated monomer, however, the solvated tetramer can be obtained in Et₂O.⁴² Synthetic route **1b-9** (Scheme 24), which uses Et₂O as the reaction solvent, was therefore attempted. Solution state ³¹P NMR spectroscopic analysis of the crude reaction residue from reaction **1b-9** revealed a mixture of unidentifiable, inseparable phosphorus-containing species of a similar composition to that observed for reaction **1a-9**.

The aggregation of *t*BuLi can be disrupted in Et₂O to give the solvated dimer,⁴³ and the solvated monomer in THF.⁴⁴ Two further attempts, therefore, were made to prepare target compound **10**, by reaction **1b-10** (Scheme 24) which used Et₂O as the reaction solvent, and reaction **1c-10** (Scheme 24) which used THF as the solvent. Synthetic route **1b-10** yielded a complex mixture of mostly unidentifiable phosphorus-containing species, including starting (iPr₂N)₂PCl. Reaction **1c-10**, however, gave a mixture of products, and saw full consumption of the starting (iPr₂N)₂PCl suggesting that the THF solvent altered the course of the reaction,

however, the reaction did not proceed cleanly and the resulting mixture of phosphorus-containing products could not be purified.

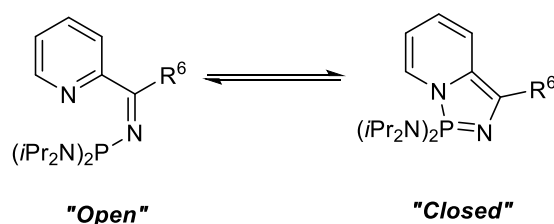


Scheme 25 – Synthetic procedure carried out in an attempt to prepare target compound **9** using MeLi and LiCl.

The reactivity of an organolithium species can be modified by the introduction of other aggregate species to form mixed aggregates.⁴¹ Organolithium solutions that are commercially available are known to contain impurities that can form mixed aggregates. MeLi, for example, can contain impurities of MeI (used in its preparation), that result in the formation of a mixed aggregate of (MeLi)₃·(LiI) and (MeLi)₄, that can interfere with the reactivity of the “MeLi”.⁴² Since the variation of the solvent medium used in the attempted preparation of target compounds **9**, **10** and **11** using synthetic **Route 1** (Scheme 24) proved unsuccessful, the use of LiCl, to deliberately form a solvated dimeric mixed aggregate (which is known to modify the solubility and reactivity of MeLi),⁴⁵ as well as the required alkyllithium, was probed. Synthetic **Route 2** (Scheme 25) was carried out without success – incomplete consumption of the starting (iPr₂N)₂PCl was observed, alongside the formation of several other phosphorus-containing species, which could not be isolated or identified.

The basicity of the alkyllithium species used in the attempted preparation (by synthetic **Route 1** and **Route 2**) of target compounds **A**, **9** and **10** are shown in Figure 22; it can be seen that MeLi and *t*BuLi are significantly more basic than PhLi.⁴¹ Based on the above evidence, the formation of the complex reaction mixtures when 2-cyanopyridine is treated with an alkyllithium reagent (synthetic **Route 1** and **Route 2**, Scheme 24 and Scheme 25) has been attributed to the high basicity of the lithium species.

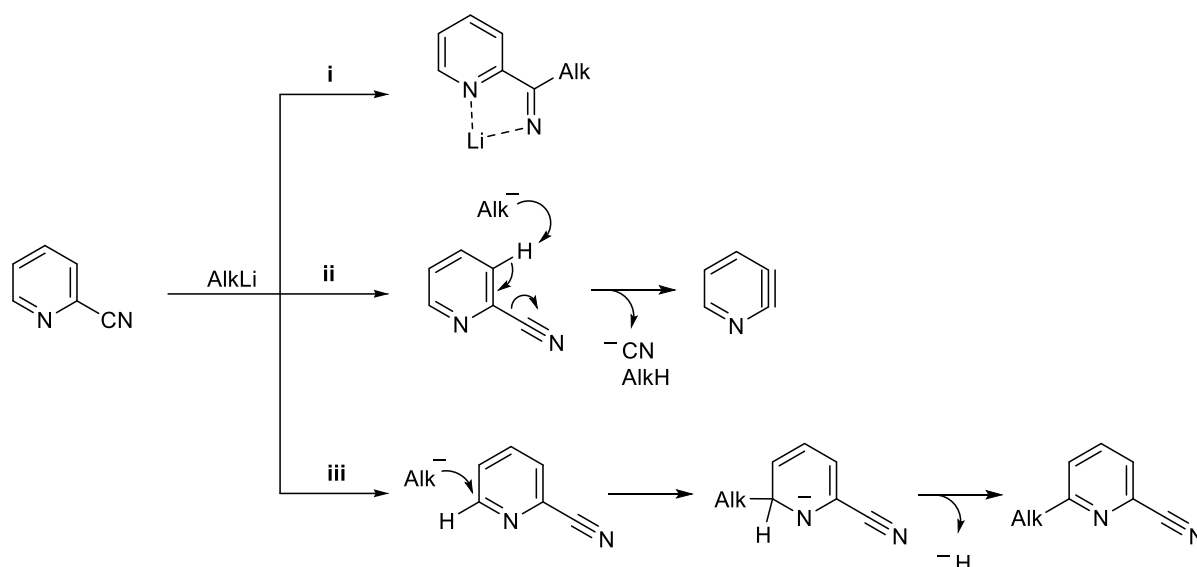
Chapter 2 - Pyridyl-*N*-Phosphinoimine – Diazaphosphazole Valence Tautomerism:
Equilibrium Studies



Compound	R ⁶	pK _a of R ⁶ H
A	Ph	43
9	Me	48
10	<i>t</i> Bu	53

Figure 22 – pK_a values of the alkyllithium species required for the synthesis of target compounds **A**, **9** and **10**.¹⁵

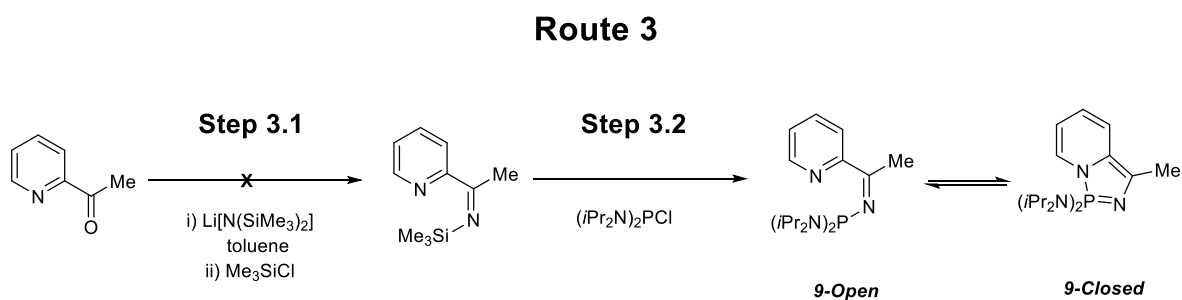
The high basicity of *alkyllithium* relative to *aryllithium* reagents can lead to their attacking the 2-cyanopyridine at a position other than at the cyano group as desired (reaction **i**, Scheme 26). The potential reaction pathways, competing against desired reaction **i**, between alkyllithium species and 2-cyanopyridine are shown in Scheme 26; reactions **ii** and **iii** yield undesired pyridyne and substituted pyridine, respectively.



Scheme 26 – Potential competing reactions between 2-cyanopyridine and AlkLi species.

All attempts to prepare target compounds **9**, **10** and **11** from 2-cyanopyridine using AlkLi reagents proved unsuccessful, and were therefore discontinued. Using a different strategy, Rawson and co-workers have previously reported the successful preparation (full conversion over 2 steps) of an analogue to target compounds **9-10**, namely trimethyl silyl (phenyl

pyridine-2-yl methylene) amine, starting from 2-benzoylpyridine.⁴⁶ Consequently, a related approach was adopted such that the conditions laid out by Rawson and co-workers were replicated, using 2-acetylpyridine in place of 2-benzoylpyridine (synthetic **Route 3**, Scheme 27), in an attempt to prepare target compound **9**.



Scheme 27 - Synthetic procedure carried out in an attempt to prepare target compound **9** from 2-acetylpyridine.

Upon analysis of the crude reaction mixture from **Step 3.1** by solution state ¹H NMR spectroscopy, a mixture of products was observed which proved inseparable, indicating that **Step 3.1** was not suitable for the clean preparation of the desired product, trimethyl silyl (methyl pyridine-2-yl methylene) amine. It is proposed that the primary difference between **Step 3.1** (Scheme 27) being successful, when using 2-benzoylpyridine, and unsuccessful, when using 2-acetylpyridine, is the presence of acidic methyl protons α to the carbonyl group in 2-acetylpyridine (but not in 2-benzoylpyridine), which are prone to deprotonation as well as the carbonyl.

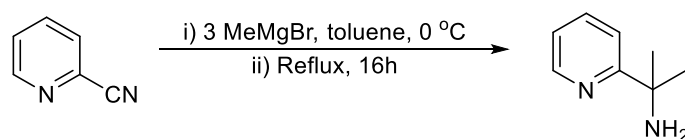
2.5.2.2 – Grignard reagents: Synthetic Route 4



Scheme 28 – Composition of a Grignard reagent in solution – Schlenk Equilibrium.⁴⁷

As has been demonstrated in section **2.5.2.1**, alkyllithium reagents have proved unsuitable for the preparation of target compounds **9**, **10** and **11** from 2-cyanopyridine due to their high reactivity. Focus turned next to using Grignard reagents. Grignard reagents are considered less reactive than organolithium species due to the high association of the former in solution.⁴⁷ A Grignard reagent exists as the equilibrium shown in Scheme 28 when in solution (the Schlenk equilibrium) - RMgX and MgX₂ are strongly associated, something that results in

the decreased reactivity of the RMgX species.⁴⁷ It was hoped that the lower reactivity of Grignard reagents, compared to their lithium analogues, would eliminate the possibility of competing side reactions occurring, and therefore other products forming (such as those shown in Scheme 26).

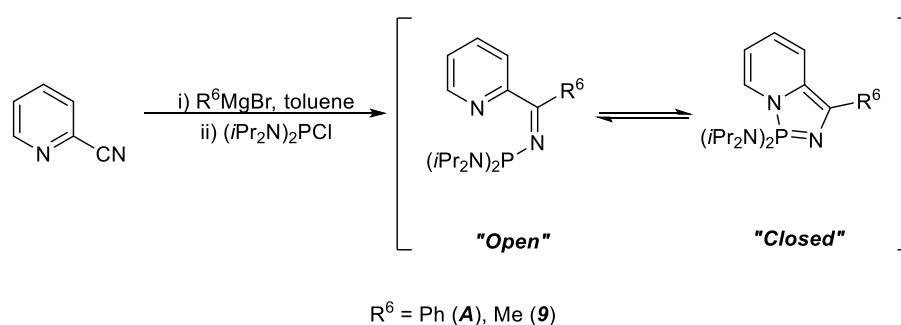


Scheme 29 – Successful reaction between 2-cyanopyridine and MeMgBr (3 eq.).⁴⁸

Shi and co-workers have previously reported the successful introduction of a methyl substituent at the cyano group of 2-cyanopyridine using the Grignard reagent MeMgBr (Scheme 29).⁴⁸ Shi and co-workers reported the quenching of the reaction shown in Scheme 29 with NH₄Cl, followed by treatment of the aqueous phase with HCl, then NaOH and finally extraction of the (pyridin-2-yl)isopropyl amine product using DCM.⁴⁸

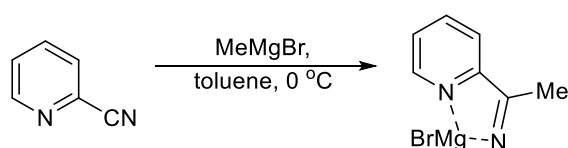
A modified version of the synthetic procedure reported by Shi and co-workers (excluding the aqueous work-up step)⁴⁸ was used to prepare compound **A** (which has been successfully prepared previously from 2-cyanopyridine using PhLi and (*i*Pr₂N)₂PCl), synthetic **Route 4** (Scheme 30). Whilst synthetic **Route 4** did indeed yield **A-Open** and **A-Closed**, the reaction (even after extended reaction times and heating under reflux) only proceeded to 22 % conversion of starting material, in contrast to the 100 % conversion observed after 24 hours at room temperature when the more reactive PhLi is used in place of PhMgBr.

Route 4



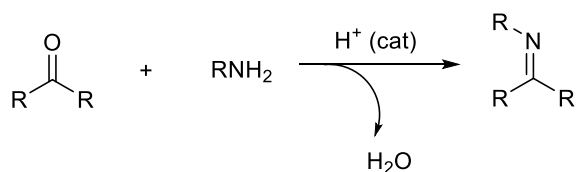
Scheme 30 – Synthetic procedure carried out in an attempt to prepare compounds **A** and **9** using a Grignard reagent.

Having established that Grignard reagents can be successfully used to prepare compound **A**, albeit in a poor yield, an attempt to synthesise target compound **9** ($R^6 = \text{Me}$) *via* synthetic **Route 4**, using MeMgBr (Scheme 30), was made. ^{31}P NMR spectroscopic analysis of the crude reaction mixture revealed that there was no conversion of the starting $(i\text{Pr}_2\text{N})_2\text{PCl}$. The failure of any reaction to occur between the proposed magnesium species generated from the reaction between 2-cyanopyridine and MeMgBr (Scheme 31) and $(i\text{Pr}_2\text{N})_2\text{PCl}$ is attributed to the low reactivity of the magnesium intermediate towards the chlorophosphine. Synthetic **Route 4** was not pursued further.



Scheme 31 – Proposed magnesium species generated from the reaction between 2-cyanopyridine and MeMgBr.

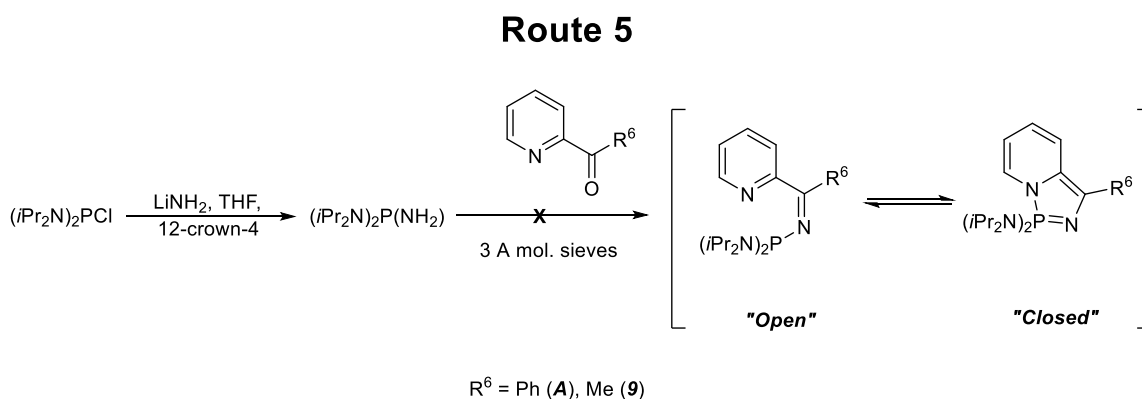
2.5.2.3 – Ketone-Amine Condensation: Synthetic Route 5



Scheme 32 – Imine synthesis *via* a condensation reaction.⁴⁹

It is well established that imines can be readily prepared from the condensation reaction between an amine and a ketone/aldehyde, typically in an acid-catalysed process, Scheme 32.⁴⁹ An analogous imine formation reaction, *i.e.* synthetic **Route 5** (Scheme 33), was first tested for the preparation of known compound **A** from 2-benzoylpyridine and $(i\text{Pr}_2\text{N})_2\text{P}(\text{NH}_2)$. An attempt to prepare the tertiary phosphine, $(i\text{Pr}_2\text{N})_2\text{P}(\text{NH}_2)$, in accordance with a literature procedure⁵⁰ was made using LiNH_2 , THF (solvent) and $\text{NH}_3(\text{l})$, however, the work-up step proved a challenge due to the need to remove all unreacted ammonia and solvent from the low boiling product (boiling point = 43 °C - 45 °C).⁵⁰ A second procedure, using 12-crown-4⁵¹ to solubilise the LiNH_2 (instead of $\text{NH}_3(\text{l})$), was found to yield $(i\text{Pr}_2\text{N})_2\text{P}(\text{NH}_2)$, albeit in a relatively low yield, 35 %, $\delta_{\text{P}} = +74.5$ ppm (a chemical shift consistent with that reported in the literature).⁵⁰

The reaction between 2-benzoylpyridine and $(iPr_2N)_2P(NH_2)$ (**Route 5**, Scheme 33) requires the presence of a desiccant (activated 3 Å molecular sieves were chosen) to remove the water generated by the condensation reaction *in situ*, to prevent it from reacting with the moisture-sensitive tertiary phosphine. Despite the presence of the activated 3 Å molecular sieves to remove the water by-product, hydrolysis of **A-Open** and **A-Closed** was observed by ^{31}P NMR spectroscopic analysis almost straight away. A suitable alternative to molecular sieves to remove water from the reaction could not be formulated, therefore synthetic **Route 5** was discontinued. In light of the failure to prepare target compounds **9-10** by the methods outlined in this section (**2.5.2**), no further attempts were made to prepare these target compounds.



Scheme 33 – Proposed synthesis of compounds **A** and **9** *via* condensation reaction.

2.6 – Summary

A fundamental study into the factors controlling the position of the tautomeric equilibrium between a series of structurally analogous pyridyl-*N*-phosphinoimines and diazaphosphazoles has been carried out. Variable temperature ^{31}P NMR spectroscopic studies have revealed that the “closed” diazaphosphazole tautomer is entropically and enthalpically disfavoured over the pyridyl-*N*-phosphinoimine “open” tautomer, and that this tautomerism is dynamic. A study into the relationship between the “open”-“closed” equilibrium position in solution, and the polarity of solvent shows that as you increase the polarity of the solvent, the equilibrium position shifts in favour of the more polar “closed” tautomer. It must be recognised that the change in equilibrium position is minimal, but nonetheless evident.

An investigation into the variation of the substituents bound to the pyridine scaffold and imine functionality has been carried out in order to probe the stereoelectronic impact of these groups upon the extent of Lewis adduct (“*closed*” tautomer) formation. Modification of the pyridine ring substituents demonstrated that, as the electron density at the pyridine nitrogen is increased *via* substitution of an electron donating substituent *para* to the nitrogen, such as Ph (**1**), cyclisation *via* the proposed *pseudo*-1,5-electrocyclisation becomes increasingly favourable. Substitution of a bulky, electron donating group at the 4-position on the pyridine ring, such as *t*Bu (**4**), imposes a steric barrier to cyclisation of the “*open*” tautomer. A similar steric barrier to cyclisation is also observed upon introducing a methyl substituent at the 3-position on the pyridine ring (**6**). The introduction of an electron donating NMe₂ moiety at the 4-position (**5**) on the pyridine ring shifts the position of the “*open*”-“*closed*” equilibrium in favour of the “*open*” tautomer, at this time it is unclear why this shift in equilibrium position occurs. Synthesis of the desired “*open*” and “*closed*” species cannot be achieved when there are acidic CH₃ protons present in the starting substituted 2-cyanopyridine (**3**, **7**) as these open a new reactivity pathway – nucleophilic attack at these acidic protons by PhLi – in addition to the desired attack at the cyano group.

Aryl substituents bound to the imine carbon have been varied in terms of their steric bulk and the extent of their aromaticity – Ph (**A**), Anth (**B**), 4,4'-biphenyl (**2**), Mes (**8**). It has been found that there is no direct correlation between the position of the “*open*”-“*closed*” tautomeric equilibrium and either the electronic character (extent of aromaticity, σ -donor ability) or steric bulk of the imine substituents. It is most likely that the relationship between the nature of the imine substituent and the “*open*”-“*closed*” ratio is as a result of a combination of steric and electronic factors.

All attempts to prepare pyridyl-*N*-phosphinoimine species with electron donating alkyl substituents at the imine carbon have been unsuccessful. The high basicity of alkyllithium species is proposed to result in the attack of these species at positions other than the cyano group (as desired) on 2-cyanopyridine. AlkMgBr reagents were found to be unsuitable for the preparation of the pyridyl-*N*-phosphinoimine species as their reactivity is too low. Attempts at devising a new pathway to prepare target compounds **9**, **10** and **11** have all been unsuccessful.

2.7 – Chapter 2 Experimental Details

Standard preparative methods were used throughout, see **Appendix 1** for general experimental considerations.

2.7.1 – Synthesis of bis(Diisopropylamino) chlorophosphine

The chlorophosphine, $(iPr_2N)_2PCl$, was prepared using a modification of a known procedure.⁵² A stirred solution of PCl_3 (3.5 ml, 0.04 moles) in toluene (25 ml) was cooled to 0 °C and iPr_2NH (22.5 ml, 0.16 moles) in toluene (25 ml) added dropwise over one hour. The mixture was then heated under reflux for 18 hours to yield a white solid in an orange solution. The solution was isolated by filtration and the residual solid washed with toluene (3 x 25 ml); the washings were combined with the orange solution and the solvent removed under reduced pressure to give a yellow/orange solid. The resulting solid was recrystallized from acetonitrile, isolated by filtration and dried *in vacuo* to yield bis(diisopropylamino)chlorophosphine as a white crystalline solid (4.782 g, 0.0179 moles, 45 %). The identity and purity of the product were confirmed by 1H and $^{31}P\{^1H\}$ NMR spectroscopy and found to be consistent with data reported in the literature.⁵²

$^{31}P\{^1H\}$ NMR (162.0 MHz, C_6D_6): δ (ppm) = +140.8 (s, $(iPr_2N)_2PCl$). 1H NMR (400.1 MHz, $CDCl_3$): δ (ppm) = 3.56 (4H, sept d, $^3J_{HH} = 6.7$ Hz, $^3J_{PH} = 5.7$ Hz, $CH(CH_3)_2$), 1.16 (24H, dd, $^3J_{HH} = 6.7$ Hz, $^4J_{PH} = 22.0$ Hz, CH_3).

2.7.2 – Synthesis of *N,N,N',N'*-tetraisopropyl-1-((phenyl(pyridin-2-yl)methylene)amino)phosphanediamine (A-Open)/ *N,N,N',N'*-tetraisopropyl-3-phenyl-1*l*5-[1,3,2]diazaphospholo[1,5-*a*]pyridine-1,1-diamine (A-Closed)

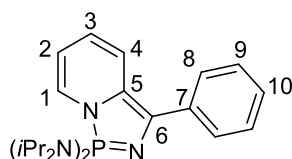


Figure 23 – A-Closed showing NMR spectroscopic assignment numbering scheme.

2.7.2.1 – Preparation of Compound A Using PhLi

Compound **A** was prepared from 2-cyanopyridine using phenyllithium according to a modification of a literature method.³ Phenyllithium (1.8 M in dibutylether, 5.4 ml, 9.6 mmol) was added to a solution of 2-cyanopyridine (1.000 g, 9.6 mmol) in DME (50 ml) at $-78\text{ }^{\circ}\text{C}$ and the mixture stirred for 1 hour at this temperature. A solution of $(i\text{Pr}_2\text{N})_2\text{PCl}$ (2.560 g, 9.6 mmol) in DME (70 ml) was added to the deep red solution. The mixture was allowed to attain room temperature and then stirred for 22 hours. The volatile components were removed *in vacuo* and the product extracted using hexane (400 ml). Upon cooling this hexane solution to $-30\text{ }^{\circ}\text{C}$, dark red cuboidal crystals formed, which were isolated by filtration and dried under reduced pressure. Further concentration of the hexane filtrate and subsequent cooling to $-30\text{ }^{\circ}\text{C}$ yielded another crop of crystals (2.330 g, 5.65 mmol, 59 %). The identity and purity of the product were confirmed by ^1H , $^{13}\text{C}\{^1\text{H}\}$ and $^{31}\text{P}\{^1\text{H}\}$ NMR spectroscopy, and found to be consistent with data reported in the literature.³

$^{31}\text{P}\{^1\text{H}\}$ NMR (161.9 MHz, C_6D_6): δ (ppm) = +71.0 (s, **A-open**), +42.3 (s, **A-closed**). **A-closed data:** ^1H NMR (699.7 MHz, C_6D_6): δ (ppm) = 8.01 (2H, d, $^3J_{\text{HH}} = 7.6\text{ Hz}$, CH^8), 7.29 (2H, t, $^3J_{\text{HH}} = 7.6\text{ Hz}$, CH^9), 7.14 (1H, d, $^3J_{\text{HH}} = 9.8\text{ Hz}$, CH^4), 7.05 (1H, t, $^3J_{\text{HH}} = 7.0\text{ Hz}$, CH^{10}), 6.06 (1H, dd, $^3J_{\text{HH}} = 7.5\text{ Hz}$, $^3J_{\text{PH}} = 5.6\text{ Hz}$, CH^1), 5.32 (1H, dd, $^3J_{\text{HH}} = 10.5\text{ Hz}$, $^3J_{\text{HH}} = 5.0\text{ Hz}$, CH^3), 5.22 (1H, t, $^3J_{\text{HH}} = 6.3\text{ Hz}$, CH^2), 3.30-3.45 (4H, m, CHCH_3), 1.20 (12H, d, $^3J_{\text{HH}} = 6.4\text{ Hz}$, CH_3), 0.97 (12H, d, $^3J_{\text{HH}} = 6.4\text{ Hz}$, CH_3). $^{13}\text{C}\{^1\text{H}\}$ NMR (125.7 MHz, C_6D_6): δ (ppm) = 158.5 (d, $^2J_{\text{PC}} = 7.7\text{ Hz}$, C^6), 140.5 (d, $^3J_{\text{PC}} = 24.9\text{ Hz}$, C^7), 128.8 (s, C^9), 127.2 (s, C^8), 126.5 (d, $^2J_{\text{PC}} = 1.5\text{ Hz}$, C^1), 125.2 (s, C^{10}), 123.2 (d, $^3J_{\text{PC}} = 9.2\text{ Hz}$, C^4), 123.1 (d, $^3J_{\text{PC}} = 34.1\text{ Hz}$, C^5), 112.9 (d, $^4J_{\text{PC}} = 1.3\text{ Hz}$, C^3), 107.3 (d, $^3J_{\text{PC}} = 5.8\text{ Hz}$, C^2), 48.2 (d, $^2J_{\text{PC}} = 3.8\text{ Hz}$, $\text{CH}(\text{CH}_3)_2$), 23.4 (d, $^3J_{\text{PC}} = 2.4\text{ Hz}$, CH_3), 22.9 (d, $^3J_{\text{PC}} = 1.3\text{ Hz}$, CH_3).

2.7.2.2 – Preparation of Compound A Using PhMgBr

Preparation of PhMgBr

A solution of bromobenzene (14.0 ml, 0.139 moles) in THF (100 ml) was added dropwise to a mixture of magnesium turnings (5.786 g, 0.238 moles) and a single crystal of iodine in THF (100 ml) at $0\text{ }^{\circ}\text{C}$. The reaction was allowed to attain room temperature and then stirred for 16 hours. Excess magnesium turnings were removed by filtration from the grey-yellow Grignard

solution. The concentration of the phenylmagnesium bromide solution was estimated by a titration of an aqueous solution of Grignard against 0.05 M hydrochloric acid using bromothymol blue as the indicator, and found to be 0.475 M (in THF).

Preparation of A

Compound **A** was synthesised from 2-cyanopyridine using phenylmagnesium bromide by a modification of a known procedure.⁴⁸ Phenylmagnesium bromide (0.467 M in THF, 3.9 ml, 1.87 mmol) was added dropwise to a solution of 2-cyanopyridine (0.2 ml, 1.87 mmol) in toluene (30 ml) at 0 °C. The mixture was allowed to attain room temperature and then heated under reflux for 16 hours. The deep green solution was allowed to cool to room temperature, and then cooled further to 0 °C. A solution of (*i*Pr₂N)₂PCl (0.500 g, 1.87 mmol) in toluene (40 ml) was then added to the mixture at 0 °C. The mixture was allowed to attain room temperature and stirred for 48 hours. The volatile components were removed under reduced pressure from the deep red solution to give a deep red solid. Compound **A** was extracted, using hexane, from the crude reaction product. The hexane solution was concentrated and cooled to –30 °C and found to yield deep red crystals of **A**, which were isolated by filtration and dried *in vacuo* (0.170 g, 0.411 mmol, 22 %).

³¹P{¹H} NMR (161.9 MHz, C₆D₆): δ (ppm) = +71.0 (s, **A-open**), +42.3 (s, **A-closed**).

2.7.2.3 – Attempt to Prepare Compound A from (*i*Pr₂N)₂P(NH₂) and 2-benzoylpyridine

*Preparation of (*i*Pr₂N)₂P(NH₂)*

To a stirred solution of LiNH₂ (0.172 g, 7.49 mmol) and 12-crown-4 ether (0.198 g, 1.124 mmol) in THF (15 ml), a solution of (*i*Pr₂N)₂NPCl (2.000 g, 7.49 mmol) in THF (20 ml) was added dropwise and the mixture stirred at room temperature for 4 days. The solvent was removed under reduced pressure and hexane (20 ml) added to the residue. The pale-yellow solution was isolated from the white solid by filtration and the solvent removed *in vacuo* to yield (*i*Pr₂N)₂P(NH₂) as a pale-yellow oil (1.002 g, 4.05 mmol, 35 %). The identity and purity of the product was confirmed by ¹H and ³¹P{¹H} NMR spectroscopy and found to be consistent with data reported in the literature.⁵⁰

$^{31}\text{P}\{^1\text{H}\}$ NMR (162.0 MHz, C_6D_6): δ (ppm) = +74.5 (s, $(i\text{Pr}_2\text{N})_2\text{P}(\text{NH}_2)$). ^1H NMR (400.1 MHz, C_6D_6): δ (ppm) = 2.85-2.70 (4H, m, CH_3), 0.95 (24H, d, $^3J_{\text{HH}} = 6.7$ Hz, $\text{CH}(\text{CH}_3)_2$). The amine protons were not observed here in the ^1H NMR spectrum due to the rapid exchange of these protons with the deuterated solvent.

Reaction of $(i\text{Pr}_2\text{N})_2\text{P}(\text{NH}_2)$ with 2-benzoylpyridine

A modified literature procedure was used in an attempt to prepare **A** from 2-benzoylpyridine and $(i\text{Pr}_2\text{N})_2\text{P}(\text{NH}_2)$.⁵³ A Young's NMR tube was charged with a C_6D_6 lock tube, two 3 Å molecular sieves, 2-benzoylpyridine (0.020 g, 0.11 mmol) and $(i\text{Pr}_2\text{N})_2\text{P}(\text{NH}_2)$ (0.031 g, 0.12 mmol) and toluene (1 ml) was added. The reaction mixture was sonicated once a day and heated at 60 °C for 7 days. Analysis by ^{31}P NMR spectroscopy revealed complete consumption of the starting phosphine and several unidentifiable phosphorus containing species including those in the region of +10 ppm consistent with phosphorus(V) hydrolysis species.⁵⁴

2.7.3 – Synthesis of bis(Diisopropylamino)(anthracenyl)phosphine Monoselenide

Preparation of bis(Diisopropylamino)(anthracenyl)phosphine

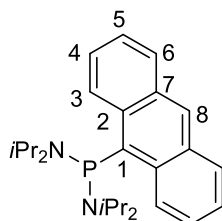


Figure 24 – $(i\text{Pr}_2\text{N})_2\text{P}(\text{Anth})$ showing NMR spectroscopic assignment numbering scheme.

To a cooled (-78 °C) solution of 9-bromoanthracene (1.000 g, 3.89 mmol) in hexane (20 ml), *n*-butyllithium (2.5 M in hexane, 1.6 ml, 3.89 mmol) was added dropwise. The reaction was stirred at -78 °C for 1 hour and then allowed to attain room temperature. A solution of $(i\text{Pr}_2\text{N})_2\text{PCl}$ (1.038 g, 3.889 mmol) in THF (20 ml) was added to the as-prepared solution of anthracenyllithium, and the mixture stirred at room temperature for 16 hours to yield an orange solution. The volatile species were removed under reduced pressure to yield orange solid bis(diisopropylamino)(anthracenyl)phosphine (1.080 g, 2.64 mmol, 68 %). MS (ASAP) m/z : 409.3 ($[\text{MH}]^+$).

$^{31}\text{P}\{^1\text{H}\}$ NMR (283.3 MHz, C_6D_6): δ (ppm) = +72.5 (s, $\text{P}(\text{Anth})(\text{NiPr}_2)_2$). ^1H NMR (699.7 MHz, C_6D_6): δ (ppm) = 9.93-9.84 (2H, m, CH^3), 8.18 (1H, s, CH^8), 7.77 (2H, dd, $^5J_{\text{HH}} = 1.5$ Hz, $^4J_{\text{HH}} = 8.3$ Hz, CH^6), 7.35 (2H, ddd, $^5J_{\text{HH}} = 1.5$ Hz, $^3J_{\text{HH}} = 6.4$ Hz, $^3J_{\text{HH}} = 9.1$ Hz, CH^4), 7.24 (2H, ddd, $^4J_{\text{HH}} = 1.1$ Hz, $^3J_{\text{HH}} = 6.3$ Hz, $^4J_{\text{HH}} = 8.4$ Hz, CH^5), 3.73-3.61 (4H, m, $\text{CH}(\text{CH}_3)_2$), 1.27 (12H, d, $^3J_{\text{HH}} = 6.7$ Hz, CH_3), 0.83 (12H, d, $^3J_{\text{HH}} = 6.7$ Hz, CH_3). $^{13}\text{C}\{^1\text{H}\}$ NMR (76.0 MHz, C_6D_6): δ (ppm) = 135.1 (d, $^4J_{\text{CP}} = 2.3$ Hz, C^8), 129.0 (d, $^4J_{\text{CP}} = 1.1$ Hz, C^6), 127.9 (s, C^3), 124.6 (d, $^4J_{\text{CP}} = 3.5$ Hz, C^4), 124.0 (d, $^5J_{\text{CP}} = 3.5$ Hz, C^5), 47.5 (d, $^2J_{\text{CP}} = 15.2$ Hz, $\text{CH}(\text{CH}_3)_2$), 23.9 (d, $^3J_{\text{CP}} = 6.1$ Hz, CH_3), 23.2 (d, $^3J_{\text{CP}} = 6.9$ Hz, CH_3). The quaternary carbons were not observed in the $^{13}\text{C}\{^1\text{H}\}$ NMR spectrum due to the long relaxation times associated with quaternary carbon centres.

Preparation of bis(Diisopropylamino) (anthracenyl)phosphine Monoselenide

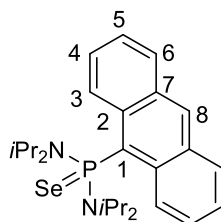


Figure 25 – $(i\text{Pr}_2\text{N})_2\text{PSe}(\text{Anth})$ showing NMR spectroscopic assignment numbering scheme.

To a solution of $\text{AnthP}(\text{NiPr}_2)_2$ (20 mg, 0.05 mmol) in CDCl_3 (1 ml) in a Young's NMR tube was added elemental selenium (7.1 mg, 0.09 mmol) and the solution left to stand for 24 hours until full conversion of the starting tertiary phosphine was observed by solution state $^{31}\text{P}\{^1\text{H}\}$ NMR spectroscopy. MS (EI^+) m/z : 487.8 (M^+).

$^{31}\text{P}\{^1\text{H}\}$ NMR (283.3 MHz, CDCl_3): δ (ppm) = +75.8 (s, with satellites $^1J_{\text{PSe}} = 750$ Hz, $\text{P}(\text{NiPr}_2)_2(\text{Anth})(\text{Se})$). ^1H NMR (699.7 MHz, C_6D_6): δ (ppm) = 9.34-9.28 (2H, m, CH^3), 8.55-8.49 (1H, m, CH^8), 7.97-7.92 (2H, m, CH^6), 7.48-7.45 (2H, m, CH^4), 7.44-7.40 (2H, m, CH^5), 4.47-4.38 (4H, m, $\text{CH}(\text{CH}_3)_2$), 1.39 (12H, d, $^3J_{\text{HH}} = 7.0$ Hz, CH_3), 1.33 (12H, d, $^3J_{\text{HH}} = 6.9$ Hz, CH_3). $^{13}\text{C}\{^1\text{H}\}$ NMR (76.0 MHz, C_6D_6): δ (ppm) = 133.1 (d $^4J_{\text{CP}} = 4.0$ Hz, C^8), 128.7 (d, $^3J_{\text{CP}} = 7.5$, C^3), 128.5 (d, $^4J_{\text{CP}} = 1.0$ Hz, C^6), 125.2 (d, $^4J_{\text{CP}} = 1.0$ Hz, C^4), 124.0 (d, $^5J_{\text{CP}} = 1.0$ Hz, C^5), 50.2 (d, $^2J_{\text{CP}} = 7.0$ Hz, $\text{CH}(\text{CH}_3)_2$), 24.7 (d, $^3J_{\text{CP}} = 3.2$ Hz, CH_3), 24.5 (d, $^3J_{\text{CP}} = 5.1$ Hz, CH_3). The quaternary carbons were not observed in the $^{13}\text{C}\{^1\text{H}\}$ NMR spectrum due to the long relaxation times associated with quaternary carbon centres.

2.7.4 – Synthesis of *N,N,N',N'*-tetraisopropyl-1-((phenyl(4-phenylpyridin-2-yl)methylene)amino)phosphanediamine (1-Open)/ *N,N,N',N'*-tetraisopropyl-3,5-diphenyl-1*H*-[1,3,2]diazaphospholo[1,5-*a*]pyridine-1,1-diamine (1-Closed)

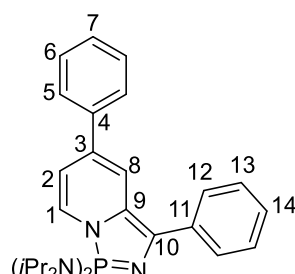


Figure 26 – **1-Closed** showing NMR spectroscopic assignment numbering scheme.

Phenyllithium (1.8 M in dibutyl ether, 1.5 ml, 2.77 mmol) was added dropwise to a stirred solution of 4-phenyl-2-cyanopyridine (0.500 g, 2.77 mmol) in DME (25 ml) at $-78\text{ }^{\circ}\text{C}$, then the mixture stirred for 1 hour at $-78\text{ }^{\circ}\text{C}$. A mixture of $(i\text{Pr}_2\text{N})_2\text{PCl}$ (0.740 g, 2.77 mmol) in DME (35 ml) was added and the mixture then allowed to attain room temperature and stirred for 3 days. Volatile species were removed under reduced pressure, then hexane (100 ml) added to the residue and the resulting mixture filtered. The deep purple solution was then cooled to $-30\text{ }^{\circ}\text{C}$ and yielded deep purple crystals of **1** after 24 hours. These crystals were isolated by filtration and dried *in vacuo*; the crystals were suitable for single crystal X-ray diffraction analysis (0.357 g, 0.887 mmol, 32 %). MS (ASAP) m/z : 488.3 (M^+). *Anal.* Found C, 73.97 %; H, 8.66 %; N, 11.20 %. Calc. C, 73.47 %; H, 8.46 %; N 11.47 %.

$^{31}\text{P}\{^1\text{H}\}$ NMR (283.3 MHz, C_6D_6): δ (ppm) = +70.3 (s, **1-open**), +41.0 (s, **2-closed**). $^{31}\text{P}\{^1\text{H}\}$ NMR (202.3 MHz, $\text{C}_6\text{D}_5\text{CD}_3$): (298 K) δ (ppm) = +71.4 (s, **1-Open**, 1 %), +42.0 (s, **1-Closed**, 99 %). (303 K) δ (ppm) = +71.5 (s, **1-Open**, 2 %), +42.0 (s, **1-Closed**, 98 %). (313 K) δ (ppm) = +71.7 (s, **1-Open**, 3 %), +41.7 (s, **1-Closed**, 97 %). (323 K) δ (ppm) = +72.1 (s, **1-Open**, 7 %), +42.0 (s, **1-Closed**, 93 %). (333 K) δ (ppm) = +72.4 (s, **1-Open**, 9 %), +41.8 (s, **1-Closed**, 91 %). (343 K) δ (ppm) = +72.7 (s, **1-Open**, 12 %), +41.7 (s, **1-Closed**, 88 %). (353 K) δ (ppm) = +73.0 (s, **1-Open**, 16 %), +41.8 (s, **1-Closed**, 84 %). **1-Closed data:** ^1H NMR (499.6 MHz, $\text{C}_6\text{D}_5\text{CD}_3$): δ (ppm) = 8.00 (1H, d, $^3J_{\text{HH}} = 7.8\text{ Hz}$, CH^8), 7.53 (1H, s, CH^4), 7.40 – 7.34 (2H, m, aromatic H), 7.32 – 7.24 (2H, m, aromatic H), 7.18 – 7.10 (2H, m, aromatic H), 7.09 – 6.98 (2H, m, aromatic H), 6.22 (1H, s, CH^1), 7.56 (1H, s, CH^2), 3.54 – 3.35 (4H, m, $\text{CH}(\text{CH}_3)_2$), 1.24 (12H, d, $^3J_{\text{HH}} = 6.8\text{ Hz}$, CH_3), 1.05

(12H, d, $^3J_{\text{HH}} = 6.8$ Hz, CH₃). Due to the broad nature of the resonances in the ^1H and 2D NMR spectra, the $^{13}\text{C}\{^1\text{H}\}$ NMR spectrum could not be assigned.

2.7.5 – Synthesis of *N,N,N',N'*-tetraisopropyl-1-((biphenyl(pyridin-2-yl)methylene)amino)phosphanediamine (2-Open) / 3-(biphenyl)-*N,N,N',N'*-tetraisopropyl-1*H*-[1,3,2]diazaphospholo[1,5-*a*]pyridine-1,1-diamine (2-Closed)

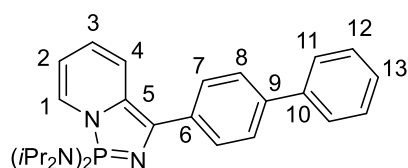


Figure 27 – 2-Closed showing NMR spectroscopic assignment numbering scheme.

Preparation of 4,4'-biphenyllithium *in situ*

To a solution of 4-biphenylbromide (1.120 g, 4.80 mmol) in THF (30 ml) at -78 °C, *n*-butyllithium (2.5 M in hexane, 2.4 ml, 4.80 mmol) was added dropwise. The reaction was stirred at -78 °C for 2 hours and the resulting product used without isolation or further purification.

Preparation of **2**

2-Cyanopyridine (0.5 ml, 4.80 mmol) was added to a THF solution of 4,4'-biphenyllithium (as-prepared above) at -78 °C and the solution stirred for 1 hour at -78 °C. A solution of $(i\text{Pr}_2\text{N})_2\text{PCl}$ (1.281 g, 4.80 mmol) in DME (30 ml) was added to the purple solution at -78 °C then the mixture was allowed to attain room temperature and stirred for 16 hours. Volatile species were removed under reduced pressure. The product was extracted using hexane (50 ml), the solution concentrated and cooled to -30 °C. Deep red crystals suitable for a single crystal X-ray diffraction study were obtained after 3 days at -30 °C. (1.009 g, 2.06 mmol, 43 %). MS (ASAP) m/z : 488.2 (M^+), 489.3 ($[\text{MH}]^+$).

$^{31}\text{P}\{^1\text{H}\}$ NMR (283.3 MHz, C_6D_6): δ (ppm) = +70.4 (s, **2-Open**), +41.2 (s, **2-Closed**). $^{31}\text{P}\{^1\text{H}\}$ NMR (202.3 MHz, $\text{C}_6\text{D}_5\text{CD}_3$): (215 K) δ (ppm) = +72.6 (s, **2-Open**, 16 %), +41.4 (s, **2-Closed**, 84 %). (298 K) δ (ppm) = +72.5 (s, **2-Open**, 4 %), +42.1 (s, **2-Closed**, 96 %). (273 K) δ (ppm) = +71.0 (s, **2-Open**, 2 %), +42.2 (s, **2-Closed**, 98 %). (253 K) δ (ppm) = +42.3 (s, **2-Closed**, 100 %). (233 K)

δ (ppm) = +42.5 (s, **2-Closed**, 100 %). (213 K) δ (ppm) = +42.6 (s, **2-Closed**, 100 %). **2-Closed data:** ^1H NMR (699.7 MHz, C_6D_6): δ (ppm) = 8.23-7.33 (8H, m, aromatic *H*), 7.22-7.12 (3H, m, aromatic *H*), 7.09-6.98 (2H, m, aromatic *H*), 3.44-3.27 (4H, m, $\text{CH}(\text{CH}_3)_2$), 1.18 (12H, d, $^3J_{\text{HH}} = 6.8$ Hz, CH_3), 0.94 (12H, d, $^3J_{\text{HH}} = 6.8$ Hz, CH_3). Due to the broad nature of the resonances in the ^1H and 2D NMR spectra, the $^{13}\text{C}\{^1\text{H}\}$ NMR spectrum could not be assigned.

2.7.5.1 – Synthesis of 4-biphenyl-bis(Diisopropylamino)phosphine Monoselenide

Preparation of 4,4'-biphenyl-bis(diisopropylamino)phosphine

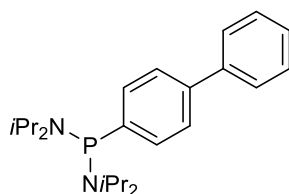


Figure 28 - 4,4'-Biphenyl-bis(diisopropylamino)phosphine.

To a cooled (-78 °C) solution of 4,4'-biphenylbromide (1.00 g, 4.29 mmol) in THF (20 ml), *n*-butyllithium (2.5 M in hexane, 1.7 ml, 4.29 mmol,) was added dropwise. The reaction was allowed to stir at -78 °C for 2 hours. A solution of $(i\text{Pr}_2\text{N})_2\text{PCl}$ (1.145 g, 4.29 mmol) in THF (20 ml) was added dropwise to the as-prepared solution of 4,4'-biphenyllithium at -78 °C and the mixture allowed to attain room temperature. The reaction was allowed to stir at room temperature for 2 days and yielded a pale-yellow solution. Volatile species were removed under reduced pressure and the product extracted from the residue using hexane (30 ml). The volatile species were removed *in vacuo* to yield the product as a pale-yellow solid (0.942 g, 2.45 mmol, 57 %) of only 66 % purity (by $^{31}\text{P}\{^1\text{H}\}$ NMR) – further attempts at purification were unsuccessful and prevented the successful assignment of the ^1H and $^{13}\text{C}\{^1\text{H}\}$ NMR spectra. $^{31}\text{P}\{^1\text{H}\}$ NMR (283.3 MHz, C_6D_6): δ (ppm) = +59.5 (s, $\text{P}(\text{N}i\text{Pr}_2)_2(4'4\text{-biphenyl})$).

Preparation of 4-biphenyl-bis(diisopropylamino)phosphine monoselenide

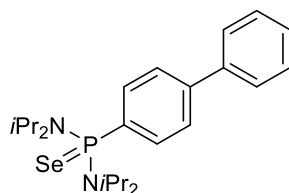


Figure 29 – 4,4'-Biphenyl-bis(diisopropylamino)phosphine monoselenide

To a solution of the as-prepared 4,4'-biphenyl-bis(diisopropylamino)phosphine (20 mg, 0.05 mmol) in CDCl₃ (1 ml) in a Young's NMR tube was added elemental selenium (7.11 mg, 0.09 mmol) and the solution left to stand for 24 hours until full conversion of the starting tertiary phosphine was observed by ³¹P{¹H} NMR spectroscopic analysis.

³¹P {¹H} NMR (283.3 MHz, CDCl₃): δ (ppm) = +69.7 (s, with satellites ¹J_{PSe} = 751 Hz, P(NiPr₂)₂(4,4'-biphenyl)(Se)).

2.7.6 – Attempted synthesis of *N,N,N',N'*-tetraisopropyl-1-((phenyl(4-methylpyridine-2-yl)methylene)amino)phosphanediamine (3-Open)

Phenyllithium (1.9 M in dibutylether, 0.5 ml, 0.846 mmol) was added to a solution of 4-methyl-2-cyanopyridine (0.100 g, 0.846 mmol) in DME (20 ml) at -78 °C and the mixture stirred for 1 hour at this temperature. A solution of (iPr₂N)₂PCl (0.226 g, 0.846 mmol) in DME (20 ml) was added to the deep red solution at -78 °C. The solution was allowed to attain room temperature and stirred for 24 hours. ³¹P NMR spectroscopic analysis of the reaction mixture revealed a mixture of phosphorus-containing species, most of which could not be identified. Resonances at δ_P = +70.8 ppm, +70.3 ppm and +47.5 ppm, +40.2 ppm, +40.1 ppm were seen, some of which could potentially correspond to target compounds **3-Open** and **3-Closed**, respectively (Figure 9). All attempts to isolate these species were unsuccessful. This reaction was discontinued in light of this, and previous, failed attempts.⁴

2.7.7 – Synthesis of *N,N,N',N'*-tetraisopropyl-1-((phenyl(4-*tert*-butylpyridin-2-yl)methylene)amino)phosphanediamine (4-Open) / (4-Closed)

Preparation of 4-*tert*-butyl-pyridine-*N*-oxide

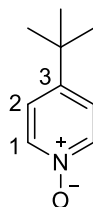


Figure 30 – 4-*tert*-Butyl-pyridine-*N*-oxide showing NMR spectroscopic assignment numbering scheme.

4-*tert*-Butyl-pyridine-*N*-oxide was synthesised using a modification of a known procedure.⁵⁵ To a solution of 4-*tert*-butylpyridine (7.6 ml, 0.052 mol) in glacial acetic acid (25 ml), a mixture of glacial acetic acid (26.0 ml) and hydrogen peroxide (3 % aqueous solution, 2.9 ml) was added dropwise then the reaction heated for 3 hours at 80 °C. A further portion of glacial acetic acid (26.0 ml) and hydrogen peroxide (3 % aqueous solution, 2.9 ml) was added to the reaction dropwise before the mixture was then heated for a further 16 hours at 80 °C. The reaction was allowed to attain room temperature and the volatile species removed under reduced pressure to yield a yellow oil, which was neutralised using aqueous sodium hydroxide. Crude 4-*tert*-butyl-pyridine-*N*-oxide was extracted using dichloromethane (3 x 20 ml) and the combined organic extracts dried over magnesium sulfate. The yellow organic solution was isolated by filtration and the volatile components removed *in vacuo*. The resulting solid was dried under reduced pressure for 3 hours to yield 4-*tert*-butyl-pyridine-*N*-oxide as a cream solid (2.376 g, 0.156 mol, 30 %). Spectroscopic data were found to be consistent with those reported in the literature.⁵⁵

¹H NMR (400.1 MHz, CDCl₃): δ (ppm) = 8.12 (2H, d, ³J_{HH} = 7.0 Hz, H¹), 7.24 (2H, d, ³J_{HH} = 7.0 Hz, H²), 1.30 (9H, s, (CH₃)₃).

Preparation of 4-*tert*-butyl-2-cyanopyridine

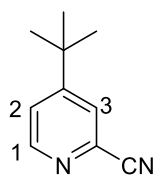
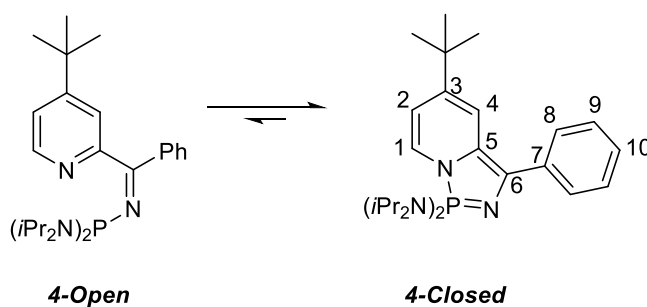


Figure 31 – 4-*tert*-Butyl-2-cyanopyridine showing NMR spectroscopic assignment numbering scheme.

4-*tert*-Butyl-2-cyanopyridine was synthesised using a modification of a known method.⁵⁵ Trimethylsilylcyanide (4.9 ml, 0.039 mol) was added to a solution of 4-*tert*-butyl-pyridine-*N*-oxide (2.000 g, 0.013 moles) and triethylamine (3.7 ml, 0.026 mol) in acetonitrile (20 ml) and the mixture heated at 100 °C for 24 hours. The orange solution was allowed to cool to room temperature and then the reaction quenched with a saturated solution of aqueous sodium bicarbonate (50 ml). The crude product was extracted with DCM and the combined washings dried over magnesium sulfate. The orange solution was isolated from the magnesium sulfate by filtration and the volatile species removed under reduced pressure to yield the crude product as a dark orange oil. The crude oil was purified by column chromatography (silica, 20 : 80, ethyl acetate : hexane, $R_f = 0.4$) to yield 4-*tert*-butyl-2-cyanopyridine as a pale yellow oil (0.949 g, 0.018 mol, 46 %). Spectroscopic data were found to be consistent with those reported in the literature.⁵⁵

¹H NMR (400.1 MHz, CDCl₃): δ (ppm) = 8.61 (1H, dd, $^3J_{\text{HH}} = 5.3$ Hz, $^5J_{\text{HH}} = 0.8$ Hz, CH¹), 7.69 (1H, dd, $^4J_{\text{HH}} = 2.0$ Hz, $^5J_{\text{HH}} = 0.8$ Hz, CH³), 7.49 (1H, dd, $^3J_{\text{HH}} = 5.3$ Hz, $^4J_{\text{HH}} = 2.0$ Hz, CH²), 1.34 (9H, s, (CH₃)₃).

Preparation of **4**



Scheme 34 - 4-*Open* and 4-*Closed* showing NMR spectroscopic assignment numbering scheme.

Phenyllithium (1.9 M in dibutylether, 0.7 ml, 1.148 mmol) was added to a solution of 4-*tert*-butyl-2-cyanopyridine (0.200 g, 1.248 mmol) in DME (30 ml) at $-78\text{ }^{\circ}\text{C}$ and the mixture stirred for 1 hour at this temperature. A solution of $(i\text{Pr}_2\text{N})_2\text{PCl}$ (0.333 g, 1.248 mmol) in DME (20 ml) was added to the deep purple solution at $-78\text{ }^{\circ}\text{C}$. The solution was allowed to attain room temperature and then stirred for 24 hours. The volatile species were removed from the red solution *in vacuo* and the product extracted with hexane (100 ml). The hexane solution was concentrated under reduced pressure and cooled to $-30\text{ }^{\circ}\text{C}$. Red cuboidal crystals suitable for an X-ray crystallographic study were obtained within 12 hours at $-30\text{ }^{\circ}\text{C}$. MS (EI⁺) m/z : 501.3 ([M+{MeOH₂}⁺]).^{††}

³¹P {¹H} NMR (162.0 MHz, CDCl₃): δ (ppm) = +69.9 (**4-Open**), +40.3 (**4-Closed**). **4-Open data:** ¹H NMR (599.6 MHz, C₆D₆): δ (ppm) = 8.45 (1H, d, ³J_{HH} = 5.2 Hz, CH¹), 7.86 (2H, d, ³J_{HH} = 7.6 Hz, CH⁸), 7.15 (2H, dd, ³J_{HH} = 8.3 Hz, ³J_{HH} = 7.0 Hz, CH⁹), 7.12 - 7.10 (1H, m, CH⁴), 7.09 - 9.05 (1H, m, CH¹⁰), 6.80 (1H, dd, ³J_{HH} = 5.3 Hz, ⁴J_{HH} = 2.0 Hz, CH²), 3.88 - 3.78 (4H, m, CH(CH₃)₂), 1.21 (12H, d, ³J_{HH} = 6.8 Hz, CH₃), 1.15 (12H, d, ³J_{HH} = 6.6 Hz, CH₃), 1.09 (9H, s, C(CH₃)₃). ¹³C{¹H} NMR (150.8 MHz, C₆D₆): δ (ppm) = 148.9 (s, C¹), 129.2 (s, C⁴), 128.8 (s, C⁸), 119.8 (s, C²), 45.2 (d, ²J_{CP} = 12.7 Hz, CH(CH₃)₂), 30.0 (s, C(CH₃)₃), 24.2 (d, ³J_{CP} = 6.1 Hz, CH₃), 24.0 (d, ³J_{CP} = 8.9 Hz, CH₃). C⁹ and C¹⁰ are not observed in the ¹³C{¹H} NMR as they are masked by the solvent peak. The quaternary carbons were not observed in the ¹³C{¹H} NMR spectrum due to the long relaxation times associated with quaternary carbon centres. **4-Closed data:** ¹H NMR (599.6 MHz, C₆D₆): δ (ppm) = 8.09 (2H, s, CH⁸), 7.75 (1H, s, CH⁴), 7.29 (2H, s, CH⁹), 7.00 (1H, s, CH¹⁰), 6.18 (1H, s, CH¹), 5.39 (1H, s, CH²), 3.43 - 3.32 (4H, m, CH(CH₃)₂), 1.20-1.1.16 (12H, m, CH₃), 1.04 (9H, s, C(CH₃)₃), 0.96 (12H, d, ³J_{HH} = 6.8 Hz, CHCH₃). ¹³C{¹H} NMR (150.8 MHz, C₆D₆): δ (ppm) = 126.2 (s, C⁸), 105.7 (s, C²), 47.2 (s, CH(CH₃)₂), 29.1 (s, C(CH₃)₃), 22.5 (s, CH₃), 22.0 (s, CH₃). The broad nature of the signals in the ¹H and 2D NMR spectra prevented the assignment of the ¹³C{¹H} NMR spectroscopic signals for C¹, C⁴, C⁹ and C¹⁰. The quaternary carbons were not observed in the ¹³C{¹H} NMR spectrum due to the long relaxation times associated with quaternary carbon centres.

^{††} MeOH consequence of the MS experimental method.

2.7.8 – Synthesis of *N,N,N',N'*-tetraisopropyl-1-((phenyl(4-dimethylamino-2-yl)methylene)amino)phosphanediamine (5-Open) / (5-Closed)

Preparation of 4-dimethylamino-2-pyridinecarboxamide

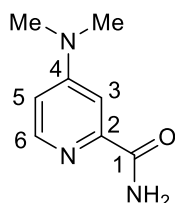


Figure 32 – 4-Dimethylamino-2-pyridinecarboxamide showing NMR spectroscopic assignment numbering scheme.

A mixture of 4-chloro-2-cyanopyridine (0.926 g, 6.68 mmol) and 40 % aqueous dimethylamine (8.5 ml, 66.8 mmol) was heated at 100 °C in a flame-sealed, thick walled Carius tube (sealed in a metal tube) in a dedicated furnace for 20 hours. The reaction mixture was allowed to cool to room temperature then the sealed Carius tube opened. The volatile components were removed under reduced pressure to yield the crude product. The crude product was passed through silica (1 : 9, Et₃N : ethyl acetate, R_f = 0.3), and subsequently, after removal of solvent *in vacuo*, recrystallized from DCM at –30 °C to yield the pure product as colourless crystals suitable for an X-ray crystallographic study (0.1383 g, 0.868 mmol, 13 %). MS (EI⁺) *m/z*: 165.9 (M⁺). See **Appendix 3** for X-ray crystallographic data.

IR (ATR) ν (cm⁻¹): 3365 (w, amide N-H str), 3127 (w, Ar-H str), 2963 (w, Ar-H str), 1606 (s, amide C=O str), 1064 (s, C-N str). ¹H NMR (699.7 MHz, CDCl₃): δ (ppm) = 8.16 (1H, dd, ³J_{HH} = 5.9 Hz, ⁵J_{HH} = 0.5 Hz, CH⁶), 7.93 (1H, s, NH'/NH''), 7.47 (1H, d, ⁴J_{HH} = 2.8 Hz, CH³), 6.57 (1H, dd, ³J_{HH} = 5.9 Hz, ⁴J_{HH} = 2.8 Hz, CH⁵), 5.67 (1H, s, NH'/NH''), 3.06 (6H, s, CH₃' and CH₃''). ¹³C{¹H} NMR (176.0 MHz, CDCl₃): δ (ppm) = 167.4 (s, C¹), 155.2 (s, C⁴), 149.7 (s, C²), 148.4 (s, C⁶), 108.3 (s, C⁵), 105.4 (s, C³), 39.3 (s, CH₃' and CH₃'').

Preparation of 4-dimethylamino-2-cyanopyridine

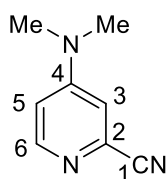
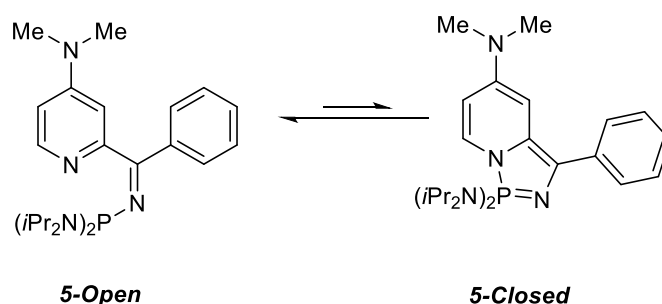


Figure 33 – 4-Dimethylamino-2-cyanopyridine showing NMR spectroscopic assignment numbering scheme.

To a cooled solution (0 °C) of 4-dimethylamino-2-pyridinecarboxamide (0.1383 g, 0.837 mmol) and triethylamine (0.2 ml, 1.67 mmol) in DCM (20 ml), trifluoroacetic anhydride (0.2 ml, 1.088 mmol) was added dropwise. The mixture was allowed to stir at 0 °C for 1 hour then the reaction allowed to attain room temperature. The mixture was stirred at room temperature for 16 hours. The reaction was quenched with a saturated solution of aqueous sodium bicarbonate (30 ml) and the product extracted with DCM (3 x 20 ml) and the combined organic portions dried over magnesium sulfate. The DCM solution was isolated by filtration then concentrated and crystals suitable for an X-ray crystallographic study were obtained at –30 °C (0.100 g, 0.679 mmol, 81 %). MS (EI⁺) *m/z*: 148.9 ([MH]⁺). See **Appendix 4** for X-ray crystallographic data.

¹H NMR (499.6 MHz, CDCl₃): δ (ppm) = 8.24 (1H, d, ³J_{HH} = 6.1 Hz, CH⁶), 6.87 (1H, d, ⁴J_{HH} = 2.7 Hz, CH³), 6.60 (1H, dd, ³J_{HH} = 6.1 Hz, ⁴J_{HH} = 2.7 Hz, CH⁵), 3.05 (6H, s, CH₃' and CH₃''). ¹³C{¹H} NMR (150.8 MHz, CDCl₃): δ (ppm) = 154.1 (s, C⁴), 150.3 (s, C⁶), 133.7 (s, C²), 117.9 (s, C¹), 111.6 (s, C³), 108.7 (s, C⁵).

Preparation of **5**



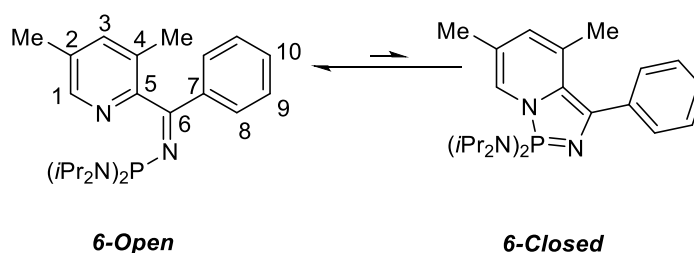
Scheme 35 – **5-Open** and **5-Closed**.

Phenyllithium (1.9 M in dibutyl ether, 0.4 ml, 0.68 mmol) was added dropwise to a stirred solution of 4-dimethylamino-2-cyanopyridine (0.100 g, 0.68 mmol) in DME (20 ml) at –78 °C, then the mixture stirred for 1 hour at –78 °C. A mixture of (iPr₂N)₂PCl (0.181 g, 0.68 mmol) in DME (20 ml) was added and the mixture then allowed to attain room temperature and stirred for 24 hours. Volatile species were removed under reduced pressure, then hexane (40 ml) added to the residue and the resulting mixture filtered. ³¹P{¹H} NMR spectroscopic analysis of the crude reaction product revealed the presence of several phosphorus-containing species including **5-Open** and **5-Closed**. Attempts to isolate **5-Open** and **5-Closed** by recrystallisation (from concentrated solutions of the crude reaction product mixture in hexane and pentane)

and solvent extraction (using DCM (30 ml) and Et₂O (30 ml)) were unsuccessful, this hindered full NMR spectroscopic characterisation of **5-Open** and **5-Closed**.

³¹P{¹H} NMR (162.0 MHz, C₆D₆): δ (ppm) = +70.4 (s, **5-Open**), +44.9 (s, **5-Closed**).

2.7.9 – Synthesis of *N,N,N',N'*-tetraisopropyl-1-((phenyl(3,5-dimethylpyridin-2-yl)methylene)amino)phosphanediamine (**6-Open**) / (**6-Closed**)



Scheme 36 - **6-Open** and **6-Closed** showing NMR spectroscopic assignment numbering scheme.

Phenyllithium (1.9 M in dibutylether, 1.0 ml, 1.89 mmol) was added to a solution of 3,5-dimethyl-2-cyanopyridine (0.25 g, 1.89 mmol) in DME (40 ml) at –78 °C and the mixture stirred for 1 hour at this temperature. A solution of (iPr₂N)₂PCl (0.504 g, 1.89 mmol) in DME (20 ml) was added to the red solution at –78 °C and stirred for 30 minutes at this temperature. The reaction was allowed to attain room temperature and stirred for 24 hours. The volatile species were then removed under reduced pressure from the deep red solution and the red-brown residue washed with hexane (100 ml). The volatile species removed *in vacuo* to give a viscous orange oil. MS (EI⁺) *m/z*: 473.3 ([{M+MeO₂}H]⁺).^{§§}

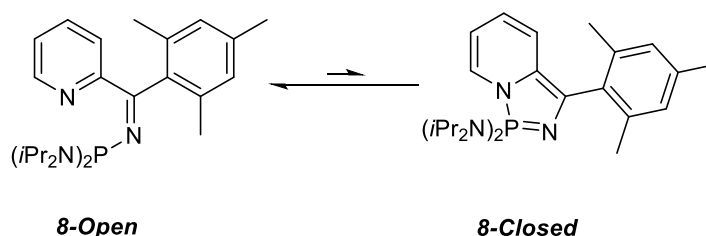
³¹P{¹H} NMR (162.0 MHz, CDCl₃): δ (ppm) = +69.2 (**6-Open**), +39.6 (**6-Closed**). **6-Open data:** ¹H NMR (599.6 MHz, C₆D₆): δ (ppm) = 8.27 (1H, s, CH¹), 7.88-4.84 (2H, m, CH⁸), 7.13-7.09 (2H, m, CH⁹), 7.14-7.10 (1H, m, CH¹⁰), 6.77 (1H, s, CH³), 3.96-3.85 (4H, m, CH(CH₃)₂), 2.07 (3H, s, C⁴CH₃), 1.86 (3H, s, C²CH₃), 1.28 (24H, *pseudo t*, ³J_{HH} = 6.4 Hz, CH₃). ¹³C{¹H} NMR (599.6 MHz, CDCl₃): δ (ppm) = 164.7 (d, ²J_{CP} = 32.2 Hz, C⁶), 155.7 (d, ³J_{CP} = 6.6 Hz, C⁵), 146.9 (s, C¹), 140.2 (d, ³J_{CP} = 7.6 Hz, C⁷), 137.3 (s, C³), 131.6 (s, C²), 129.8 (s, C¹⁰), 129.1 (d, ⁴J_{CP} 2.0 Hz, C⁴), 128.1 (d, ⁴J_{CP} = 5.9 Hz, C⁸), 127.9 (s, C⁹), 45.3 (d, ²J_{CP} = 12.5 Hz, CH(CH₃)₂), 24.4 (d, ³J_{CP} = 6.0 Hz, CH(CH₃)₂), 24.2 (d, ³J_{CP} = 6.0 Hz, CH(CH₃)₂), 18.2 (d, ⁵J_{CP} = 3.3 Hz, C⁴CH₃), 17.5 (s, C²CH₃).

^{§§} MeOH consequence of the MS experimental method.

2.7.10 – Attempted Synthesis of *N,N,N',N'*-tetraisopropyl-1-((phenyl(5-methylpyridin-2-yl)methylene)amino)phosphanediamine (**7-Open**) / (**7-Closed**)

Phenyllithium (1.9 M in dibutylether, 1.1 ml, 2.12 mmol) was added to a solution of 5-methyl-2-cyanopyridine (0.25 g, 2.12 mmol) in DME (20 ml) at $-78\text{ }^{\circ}\text{C}$ and the mixture stirred for 1 hour at this temperature. A solution of $(i\text{Pr}_2\text{N})_2\text{PCl}$ (0.565 g, 2.12 mmol) in DME (20 ml) was added to the deep red solution at $-78\text{ }^{\circ}\text{C}$. The solution was allowed to attain room temperature and stirred for 24 hours. Analysis of the crude reaction mixture by ^{31}P NMR spectroscopy revealed a mixture of phosphorus-containing species, most of which could not be identified. Resonances at +71.0 ppm, +70.5 ppm and +41.1 ppm, +41.0 were seen which could potentially correspond to **7-Open** and **7-Closed**, respectively. All attempts to isolate these species by recrystallisation and extraction with organic solvents were unsuccessful.

2.7.11 – Synthesis of *N,N,N',N'*-tetraisopropyl-1-((mesityl(pyridin-2-yl)methylene)amino)phosphanediamine (**8-Open**) / (**8-Closed**)



Scheme 37 - **8-Open** and **8-Closed**.

Preparation of mesityllithium

Mesityllithium was prepared using a modification of a known procedure.⁵⁶ A solution of *n*-butyllithium (2.5 M in hexane, 16.0 ml, 0.04 moles) was added to a stirred solution of 2-bromomesitylene (6.1 ml, 0.04 moles) in Et_2O (80 ml) at $-78\text{ }^{\circ}\text{C}$ and the mixture stirred at this temperature for 2 hours. The mixture was allowed to attain room temperature and stirred for a further 16 hours. The resulting white precipitate was isolated by filtration, washed with hexane and dried *in vacuo* (3.68 g, 0.029 moles, 73 %).

Preparation of **8**

A solution of mesityllithium (0.200 g, 1.58 mmol) in DME (20 ml) was added dropwise to a cooled ($-78\text{ }^{\circ}\text{C}$) solution of 2-cyanopyridine (0.165 g, 1.58 mmol) in DME (20 ml) and the mixture stirred for 1 hour at $-78\text{ }^{\circ}\text{C}$. A solution of $(i\text{Pr}_2\text{N})_2\text{PCl}$ (0.423 g, 1.58 mmol) in DME (35 ml) was then added to the dark red solution at $-78\text{ }^{\circ}\text{C}$ and the reaction stirred for a further 1 hour at this temperature. The reaction was allowed to attain room temperature and stirred for 48 hours. Volatile species were removed from the dark green solution under reduced pressure and the residue washed with hexane (200 ml). The hexane washings were combined and the volatile components removed *in vacuo* leaving an oily red residue. The oily red residue was found to contain a mixture of phosphorus-containing products, including **8-Open** and **8-Closed**. **8-Open** and **8-Closed** decomposed within hours and all attempts to isolate compounds **8-Open** and **8-Closed** by recrystallization and extraction with organic solvents were unsuccessful, this prevented full NMR spectroscopic characterisation of compound **8**.

$^{31}\text{P}\{^1\text{H}\}$ NMR (162.0 MHz, CDCl_3): δ (ppm) = +67.9 (s, **8-Open**), +39.0 (s, **8-Closed**).

2.7.11.1 – Synthesis of bis(Diisopropylamino)(mesityl)phosphine Selenide

Preparation of bis(diisopropylamino)(mesityl)phosphine

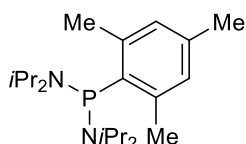


Figure 34 - bis(Diisopropylamino)(mesityl)phosphine.

To a cooled ($-78\text{ }^{\circ}\text{C}$) solution of $(i\text{Pr}_2\text{N})_2\text{PCl}$ (42 mg, 1.87 mmol) in Et_2O (20 ml), mesityllithium (20 mg, 1.87 mmol) in Et_2O (20 ml) was added dropwise. The mixture was stirred at $-78\text{ }^{\circ}\text{C}$ for 2 hours then allowed to attain room temperature and stirred for 16 hours. The volatile species were removed under reduced pressure. The product was extracted with hexane (50 ml) and the volatile components removed *in vacuo* to yield the product as an off white solid (0.360 g, 1.03 mmol, 55 %).

$^{31}\text{P}\{^1\text{H}\}$ (162.0 MHz, C_6D_6): δ (ppm) = +75.0 (s, $\text{P}(\text{Mes})(\text{NiPr}_2)_2$). ^1H NMR (699.7 MHz, C_6D_6): δ (ppm) = 6.80 (2H, d, $^4J_{\text{HP}} = 3.0\text{ Hz}$, CH), 3.61-3.48 (4H, m, $\text{CH}(\text{CH}_3)_2$), 2.81 (6H, s, *o*- CH_3), 2.13 (3H, s, *p*- CH_3), 1.30 (12H, d, $^3J_{\text{HH}} = 6.8\text{ Hz}$, $\text{CH}(\text{CH}_3)_2$), 1.05 (12H, $^3J_{\text{HH}} = 6.7\text{ Hz}$, $\text{CH}(\text{CH}_3)_2$). $^{13}\text{C}\{^1\text{H}\}$

NMR (175.9 MHz, C₆D₆): δ (ppm) = 138.4 (d, $^1J_{CP}$ = 42.5 Hz, CP), 130.2 (s, CH), 47.9 (d, $^3J_{CP}$ = 14.2 Hz, CH(CH₃)₂), 47.1 (d, $^3J_{CP}$ = 13.3 Hz, CH(CH₃)₂), 24.3 (d, $^4J_{CP}$ = 6.1 Hz, CH(CH₃)₂), 23.4 (d, $^4J_{CP}$ = 8.2 Hz, CH(CH₃)₂), 22.6 (d, $^4J_{CP}$ = 11.9 Hz, *o*-CH₃), 20.5 (s, *p*-CH₃). Signals corresponding to the *o*-C and *p*-C were not observed in the $^{13}\text{C}\{^1\text{H}\}$ NMR spectrum as they were masked by a solvent peak.

Preparation of bis(diisopropylamino)(mesityl)phosphine monoselenide

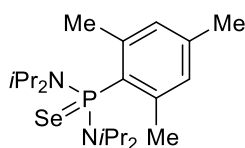


Figure 35 - bis(Diisopropylamino)(mesityl)phosphine monoselenide.

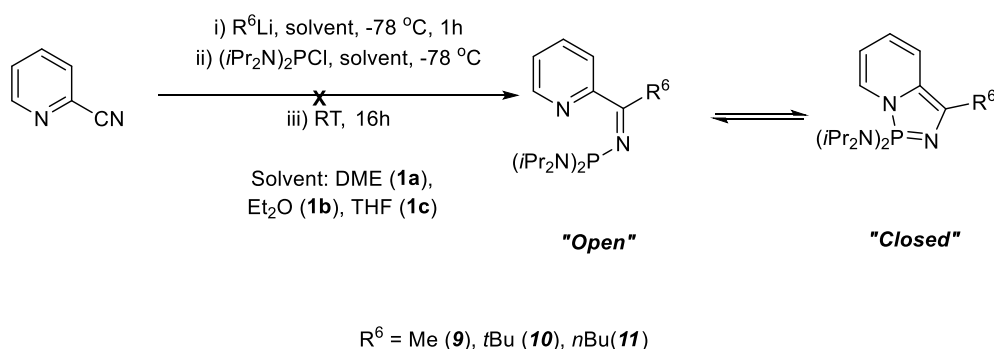
To a solution of MesP(NiPr₂)₂ (20 mg, 0.06 mmol) in CDCl₃ (1 ml) in a Young's NMR tube was added elemental selenium (7.1 mg, 0.09 mmol) and the solution left to stand for 12 hours until full consumption of the starting tertiary phosphine was observed by $^{31}\text{P}\{^1\text{H}\}$ NMR spectroscopic analysis.

$^{31}\text{P}\{^1\text{H}\}$ (162.0 MHz, CDCl₃): δ (ppm) = +76.1 (s, with satellites $^1J_{PSe}$ = 746 Hz, P(NiPr₂)₂(Mes)(Se)). ^1H NMR (400.1 MHz, CDCl₃): δ (ppm) = 6.84 (2H, d, $^4J_{HP}$ = 4.3 Hz, aromatic H), 4.29-4.13 (4H, m, CH(CH₃)₂), 2.82 (6H, d, $^4J_{HP}$ = 1.4 Hz, *o*-CH₃), 2.27 (3H, s, *p*-CH₃), 1.40 (12H, d, $^3J_{HH}$ = 6.9 Hz, CH(CH₃)₂), 1.35 (12H, d, $^3J_{HH}$ = 7.0 Hz, CH(CH₃)₂). $^{13}\text{C}\{^1\text{H}\}$ NMR (150.8 MHz, CDCl₃): δ (ppm) = 143.5 (d, $^1J_{CP}$ = 11.4 Hz, CP), 131.3 (d, $^4J_{CP}$ = 12.6 Hz, CH), 130.6 (s, *o*-C/*p*-C), 129.9 (s, *o*-C/*p*-C), 49.8 (d, $^3J_{CP}$ = 6.3 Hz, CH(CH₃)₂), 25.5 (d, $^3J_{CP}$ = 3.9 Hz, *o*-CH₃), 24.2 (*pseudo t*, $^3J_{CP}$ = 4.6 Hz, CH(CH₃)₂ & CH(CH₃)₂), 20.7 (d, $^5J_{CP}$ = 1.6 Hz, *p*-CH₃).

2.7.12 – Attempted Synthesis of Target Compounds **9**, **10** and **11**

2.7.12.1 – Attempted Preparation of **9**, **10** and **11** Using Alkylolithium Reagents

Route 1



Scheme 38 - Attempted synthesis of target **9**, **10** and **11** using R^6Li species.

General procedure for synthetic **Route 1** (Scheme 38)

R^6Li (1 equiv.) was added to a solution of 2-cyanopyridine (1 equivalent) in solvent at $-78\text{ }^\circ\text{C}$ and the mixture stirred for 1 hour at $-78\text{ }^\circ\text{C}$. A solution of $(iPr_2N)_2PCl$ (1 equiv.) in solvent was added to the solution at $-78\text{ }^\circ\text{C}$. The mixture was allowed to attain room temperature and then stirred for 16 hours. The volatile components were removed *in vacuo* and the product extracted using hexane. The hexane solution was concentrated and cooled to $-30\text{ }^\circ\text{C}$, no individual species were isolated or successfully identified. Table 8 shows the quantities of reagents used for synthetic routes **1a**, **1b** and **1c**, note: greyed out boxes indicate experiments not carried out.

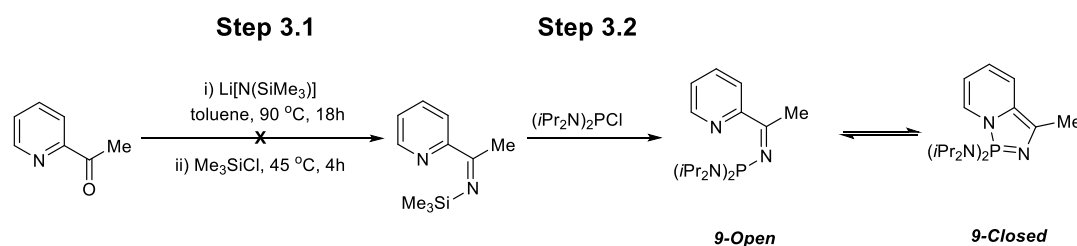
R^6Li		1a Solvent = DME			1b Solvent = Et_2O			1c Solvent = THF		
		2-CN-Py ^a mmol	R^6Li mmol	$(iPr_2N)_2PCl$ mmol	2-CN-Py ^a mmol	R^6Li mmol	$(iPr_2N)_2PCl$ mmol	2-CN-Py ^a mmol	R^6Li mmol	$(iPr_2N)_2PCl$ mmol
9	MeLi	4.8	4.8	4.8	4.8	4.8	4.8			
10	<i>t</i> BuLi	4.8	4.8	4.8	4.8	4.8	4.8	1.55	1.55	1.55
11	<i>n</i> BuLi	2.40	2.40	2.40						

Table 8 – Quantities of reagents used for attempts to prepare **9**, **10** and **11** using R^6Li species. ^a 2-CN-Py = 2-cyanopyridine.

An attempt to prepare target compound **9** using MeLi and LiCl was made. MeLi (1.6 M in diethyl ether, 1.2 ml, 1.87 mmol) was added to a solution of 2-cyanopyridine (0.19 g, 1.87 mmol) and LiCl (0.79 g, 1.87 mmol) in DME (20 ml) at $-78\text{ }^{\circ}\text{C}$ and the mixture stirred for 1 hour at $-78\text{ }^{\circ}\text{C}$. A solution of $(i\text{Pr}_2\text{N})_2\text{PCl}$ (0.50 g, 1.87 mmol) in DME (20 ml) was added to the solution at $-78\text{ }^{\circ}\text{C}$. The mixture was allowed to attain room temperature and then stirred for 22 hours. The volatile components were removed *in vacuo* and the product extracted using hexane. The hexane solution was concentrated and cooled to $-30\text{ }^{\circ}\text{C}$, no individual species were isolated or identified.

2.7.12.2 – Attempted Preparation of **9** Using LiHDMS

Route 3



Scheme 39 - Attempted synthesis of target compound **9** from 2-acetylpyridine.

Step 3.1 (Scheme 39) was carried out using a modified procedure previously reported by Rawson and co-workers.⁴⁶ To a solution 2-acetylpyridine (0.104 g, 0.855 mmol) in toluene (10 ml) was added a solution of $\text{Li}[\text{N}(\text{SiMe}_3)_2]\cdot 0.9\text{Et}_2\text{O}$ (0.200 g, 0.855 mmol of $\text{Li}[\text{N}(\text{SiMe}_3)_2]$) in toluene (15 ml) and the mixture stirred at $90\text{ }^{\circ}\text{C}$ for 18 hours. The orange solution was allowed to cool to $45\text{ }^{\circ}\text{C}$ and Me_3SiCl (0.1 ml, 0.940 mmol) added and the mixture stirred at $45\text{ }^{\circ}\text{C}$ for 2 hours. The volatile species were removed under reduced pressure to yield a yellow solid. ^1H NMR spectroscopic analysis of the yellow solid revealed a complex mixture of compounds which could not be separated by extraction using organic solvents, therefore, **Step 3.2** (Scheme 39) was not pursued.

2.7.12.3 – Attempt to Prepare **9** Using a Grignard Reagent

An attempt to prepare target compound **9** using MeMgBr was made using a modification of a previously reported procedure.⁴⁸ A solution of methyllithium (1.6 M in diethyl ether, 3.0 ml, 4.8 mmol) was added dropwise to a stirred solution of 2-cyanopyridine (0.500 g, 4.8 mmol) in toluene (25 ml) at 0 °C, and then the reaction stirred for 1 hour at 0 °C. A mixture of (*i*Pr₂N)₂PCl (1.28 g, 4.8 mmol) in toluene (35 ml) was subsequently added and the mixture then allowed to attain room temperature and stirred for 22 hours. ³¹P{¹H} NMR spectroscopic analysis of the crude reaction mixture showed a mixture of several (mostly unidentifiable) phosphorus-containing species including a significant proportion of unreacted (*i*Pr₂N)₂PCl. Resonances at $\delta_P = +74.0$ ppm, +66.3 ppm were observed, which lie within the region characteristic of the “open” species prepared in this work and previously. The reaction was left for a further 24 hours at room temperature and reanalysed by ³¹P{¹H} NMR spectroscopy; no further change in the reaction was detected. All attempts to isolate single species were unsuccessful. The reaction was repeated using Et₂O and THF as the reaction solvents (in separate reactions) with no success. This reaction was discontinued.

Chapter 2 References

- ¹ P. W. Dyer, J. Fawcett and M. J. Hanton, *J. Organomet. Chem.*, 2005, **690**, 5264-5281.
- ² R. A. M. Robertson and D. J. Cole-Hamilton, *Coord. Chem. Rev.*, 2002, **225**, 67-90.
- ³ D. A. Smith, A. S. Batsanov, K. Miqueu, J. –M. Sotiropoulos, D. C. Apperley, J. A. K. Howard and P. W. Dyer, *Angew. Chem. Int. Ed.*, 2008, **47**, 8674-8677.
- ⁴ D. A. Smith, PhD Thesis, Durham University, 2009.
- ⁵ A. Maraval, K. Owsianik, D. Arquier, A. Igau, Y. Coppel, B. Donnadiou, M. Zablocka and J. –P. Majoral, *Eur. J. Inorg. Chem.*, 2003, 960-968.
- ⁶ S. J. Geier, A. L. Gille, T. M. Gilbert and D. W. Stephan, *Inorg. Chem.*, 2009, **48**, 10466-10474.
- ⁷ S. J. Geier and D. W. Stephan, *J. Am. Chem. Soc.*, 2009, **131**, 3476-3477.
- ⁸ Y. Cao, J. K. Nagle, M. O. Wolf and B. O. Patrick, *J. Am. Chem. Soc.*, 2015, **137**, 4888–4891.
- ⁹ H. J. Kwon, H. W. Kim and Y. M. Rhee, *Chem. Eur. J.*, 2011, **17**, 6501–6507.
- ¹⁰ D. R. Lide (Ed.), *CRC handbook of chemistry and physics: a ready-reference book of chemical and physical data 87th Edition*, 2006, CRC Press.
- ¹¹ D. A. Smith, A. S. Batsanov, K. Costuas, E. Edge, D. C. Apperley, D. Collison, J. –F. Halet, J. A. K. Howard and P. W. Dyer, *Angew. Chem. Int. Ed.*, 2010, **49**, 7040-7044.
- ¹² R. K. Bansal in *Heterocyclic Chemistry Third Edition*, 2005, New Age International (P) Ltd.
- ¹³ H. Brown and X. Mihm, *J. Am. Chem. Soc.*, 1955, **77**, 1723-1726.
- ¹⁴ H. Brown and B. Kanner, *J. Am. Chem. Soc.*, 1966, **88**, 986-992.
- ¹⁵ J. March in *Advanced Organic Chemistry Fourth Edition*, 1992, Wiley-Interscience.
- ¹⁶ S. Masoud Nabavizadeh and M. Rashidi, *J. Am. Chem. Soc.*, 2006, **128**, 351-357.
- ¹⁷ F. H. Allen, O. Kennard, D. G. Watson, L. Brammer, A. G. Orpen and R. Taylor, *J. Chem. Soc. Perkin Trans. 2*, 1987, S1-S19.
- ¹⁸ J. P. Wibaut and J. W. Hey, *Rec. Trav. Chim.*, 1953, **72**, 513-521.
- ¹⁹ Z. R. Bell, G. R. Motson, J. C. Jeffery J. A. McCleverty and M. D. Ward, *Polyhedron*, 2001, **20**, 2045-2053.
- ²⁰ G. Höfle, W. Steglich and H. Vorbrüggen, *Angew. Chem. Int. Ed. Engl.*, 1978, **17**, 569-583.
- ²¹ E. Busto, V. Gotor-Fernández and V. Gotor, *Tetrahedron: Asymmetry*, 2005, **16**, 3427–3435
- ²² X. Zhang, J. E. Tellew, Z. Luo, M. Moorjani, E. Lin, M. C. Lanier, Y. Chen, J. P. Williams, J. Saunders, S. M. Lechner, S. Markinson, T. Joswig, R. Petroski, J. Piercey, W. Kargo, S. Malany,

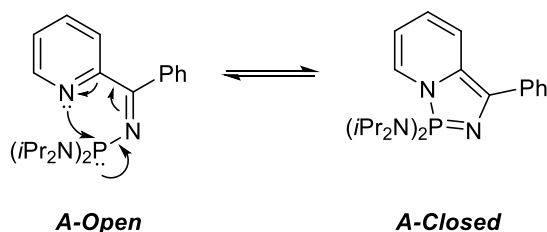
- M. Santos, R. J. Gross, J. Wen, K. Jalali, Z. O'Brien, C. E. Stoz, M. I. Crespo, J. -L. Díaz and D. H. Slee, *J. Med. Chem.*, 2008, **51**, 7099-7110.
- ²³ J. F. King, J. H. Hillhouse and S. Skonieczny, *Can. J. Chem.*, 1984, **62**, 1977-1995.
- ²⁴ I. I. Grandberg, G. K. Faizova and A. N. Kist, *Chem. Heterocycl. Compd.*, 1967, **2**, 421-425.
- ²⁵ A. Hübner, T. Bernert, I. Sängler, E. Alig, M. Bolte, L. Fink, M. Wagner and H. -W. Lerner, *Dalton Trans.*, 2010, **39**, 7528–7533.
- ²⁶ J. McMurray in *Organic Chemistry*, 1984, Brooks/Cole Publishing Company.
- ²⁷ S. Mavel, J. -L. Renou, C. Galtier, H. Allouchi, R. Snoeck, G. Andrei, E. De Clercq, J. Balzarini and A. Gueiffier, *Bioorg. Med. Chem.*, 2002, **10**, 941-946.
- ²⁸ Z. Chen, C. S. Wannere, C. Corminboeuf, R. Puchta and P. von Ragué Schleyer, *Chem. Rev.*, 2005, **105**, 3843-3888.
- ²⁹ P. von Ragué Schleyer, H. Jiao, N. K. R. v. E Hommes, V. G. Malkin, and O. J. Malkina, *J. Am. Chem. Soc.*, 1997, **119**, 12669-12670.
- ³⁰ C. A. Tolman, *J. Am. Chem. Soc.*, 1970, **92**, 2956-2965.
- ³¹ D. W. Allen and B. F. Taylor, *Dalton Trans.*, 1982, 51.
- ³² D. G. Gilheany, *Chem. Rev.*, 1994, **94**, 1339.
- ³³ W. McFarlane and D. S. Rycroft, *Dalton Trans.*, 1973, 2162-2166.
- ³⁴ R. P. Pinnell, C. A. Megerle, S. L. Manatt and P. A. Kroon, *J. Am. Chem. Soc.*, 1973, **95**, 977-978.
- ³⁵ C. A. Tolman, *Chem. Rev.*, 1977, **77**, 313-348.
- ³⁶ A. Katrusiak, M. Podsiadło and A. Budzianowski, *Cryst. Growth Des.*, 2010, **10**, 3461–3465.
- ³⁷ J. Trotter, *Acta Cryst.*, 1961, **14**, 1135-1140.
- ³⁸ Z.A. Starikova, T.M. Shchegoleva, V.K. Trunov, O. B. Lantratova and I. E. Pokrovskaya, *Zh. Strukt. Khim.*, 1980, **21**, 73.
- ³⁹ T. Sakurai, K. Kobayashi, T. Kanari, T. Kawata, I. Higashi and S. Tsuboyama, *Acta Crystallogr., Sect. B: Struct. Sci.*, 1983, **39**, 84.
- ⁴⁰ H. Dietrich, *Acta Crystallogr.*, 1963, **16**, 681-689.
- ⁴¹ H. J. Reich, *Chem. Rev.*, 2013, **113**, 7130–7178.
- ⁴² L. D. McKeever, R. Waack, M. A. Doran and E. B. Baker, *J. Am. Chem. Soc.*, 1969, **91**, 1057-1061.

- ⁴³ T. Kottke and D. Stalke, *Angew. Chem., Int. Ed. Engl.*, 1993, **32**, 580-582.
- ⁴⁴ W. Bauer, W. R. Winchester and P. v. R. Schleyer, *Organometallics*, 1987, **6**, 2371-2379.
- ⁴⁵ D. Seebach, H. Bossler, H. Gründler, S. Shoda and R. Wenger, *Helv. Chim. Acta*, 1991, **74**, 197-224.
- ⁴⁶ C. E. Bacon, D. J. Eisler, R. L. Melen and J. M. Rawson, *Chem. Comm.*, 2008, 4924–4926.
- ⁴⁷ M. Orchin, *J. Chem. Ed.*, 1989, **6**, 586-588.
- ⁴⁸ F. -J. Chen, G. Liao, X. Li, J. Wu and B. -F. Shi, *Org. Lett.*, 2014, **16**, 5644–5647.
- ⁴⁹ R. W. Layer, *Chem. Rev.*, 1963, **63**, 489–510.
- ⁵⁰ G. Schick, A. Loew, M. Nieger, K. Ariola and E. Niecke, *Chem. Ber.*, 1996, **129**, 911-917.
- ⁵¹ P. P. Power and X. Xiaojie, *J. Chem. Soc. Chem. Commun.*, 1984, 358-359.
- ⁵² R. B. King and N. D. Sadanani, *Synth. React. Org. Met. -Org. Chem.*, 1985, **15**, 149-153.
- ⁵³ M. Lagasi and P. Moggi, *J. Mol. Catal. A: Chem.*, 2001, **182-183**, 61-72.
- ⁵⁴ R. S. Edmundson in *CRC Handbook of Phosphorus-31 Nuclear Magnetic Resonance Data*, 1991, CRC Press Inc.
- ⁵⁵ Z. R. Bell, G. R. Motson, J. C. Jeffery, J. A. McCleverty and M. D. Ward, *Polyhedron*, 2001, **20**, 2045–2053.
- ⁵⁶ A. Hubner, T. Bernert, I. Sängler, E. Alig, M. Bolte, L. Fink, M. Wagner and H. -W. Lerner, *Dalton Trans.*, 2010, **39**, 7528–7533.

Chapter 3 - Synthesis of a Novel
Macrocyclic Pyridyl-*N*-
Phosphinoimine and
Intramolecularly Base-Stabilised
Phosphenium Salt

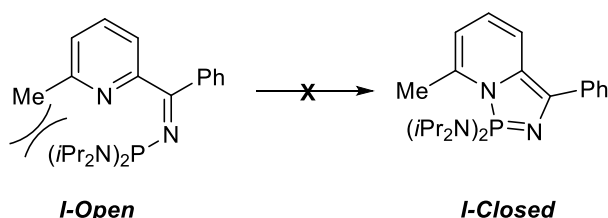
Chapter 3 – Synthesis of a Novel Macrocyclic Pyridyl-*N*-Phosphinoimine and Intramolecularly Base-Stabilised Phosphenium Salt

3.1 – Introduction



Scheme 1 – Pseudo-1,5-electrocyclisation of *A-Open*.

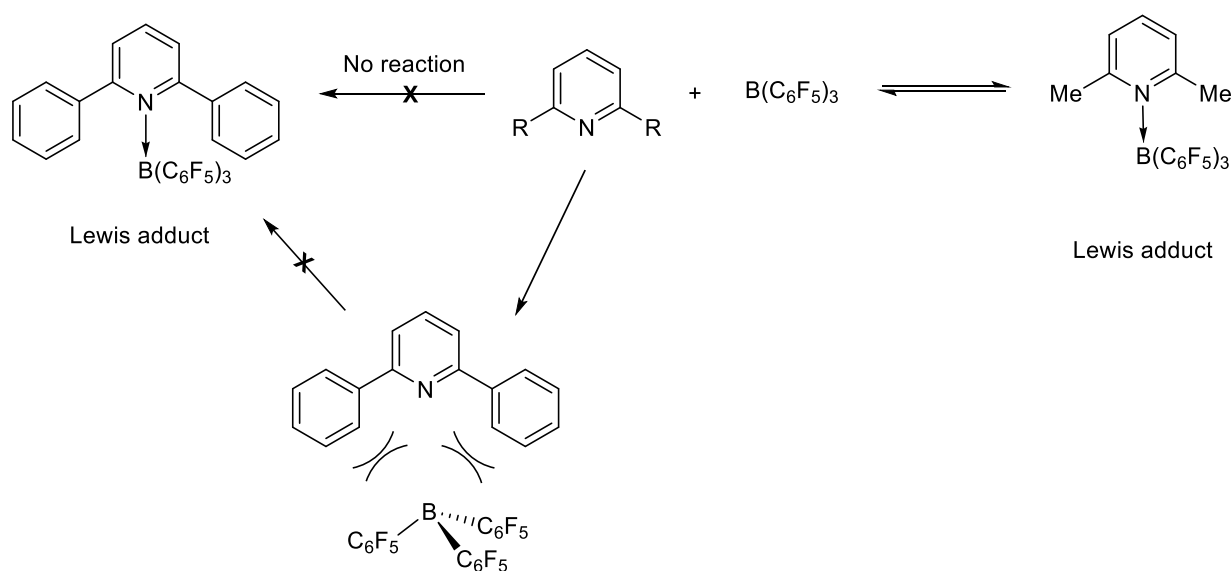
As has been discussed in previous chapters, the cyclisation of the pyridyl-*N*-phosphinoimine (“open”) tautomer to form the bicyclic diazaphosphazole (“closed”) is believed to occur *via* a *pseudo*-1,5-electrocyclisation mechanism (as shown for compound **A** in Scheme 1).¹ In this context, Dyer and co-workers have reported how steric crowding adjacent to the pyridine nitrogen centre precludes the formation of the “closed” tautomer, as is shown for compound **I** in Scheme 2. Computational studies (at the B3LYP/6-31G** level of theory) revealed that **I-Closed** is 20.2 kcal mol⁻¹ higher in energy than **I-Open**, an energy difference too high to overcome, even after prolonged heating at 365 K.¹ The contrasting ratios of the “open”：“closed” tautomers for compounds **I** (Scheme 2, 100:0 in C₆D₆ at 298 K) and **A** (Scheme 1, 5:95 in C₆D₆ at 298 K) demonstrate how the reduction in size of the R² substituent (from Me (**I**) to H (**A**)) allows for the formation of the “closed” tautomer.¹



Scheme 2 - Compound **I-Open** showing the position of the unfavourable steric interaction that prevents ring closure.

Stephan and co-workers have studied the pyridine FLP systems shown in Scheme 3.² The formation of the Lewis adduct in these pyridine-borane systems can be precluded by

increasing the steric bulk of the substituents *ortho* to the pyridine nitrogen centre (R, Scheme 3) from Me to Ph, this steric barrier to Lewis adduct formation is comparable to what is seen for compounds **A** and **I**, where the increase in R² substituent size from compounds **A** (H) to **I** (Me) hinders cyclisation of the pyridyl-*N*-phosphinoimine tautomer to form the diazaphosphazole Lewis adduct. For Stephan's FLP systems, when the *ortho* substituents are Ph, the Lewis adduct cannot form as the phenyl substituents sterically prevent the approach, and subsequent coordination, of the B(C₆F₅)₃ Lewis acid to the Lewis basic pyridine nitrogen centre. When the R substituent is a smaller methyl group, however, no such steric barrier to Lewis adduct formation exists.



Scheme 3 – Pyridine-borane FLP systems reported by Stephan and co-workers.²

As has been seen from the work carried out by both Dyer and co-workers (on compounds **A** (Scheme 1) and **I** (Scheme 2)),¹ and Stephan and co-workers (on the species shown in Scheme 3),² the reduction in size of the substituent(s) *ortho* to a pyridine nitrogen centre can allow for the formation of a classical Lewis adduct. This chapter will probe any changes to the extent of cyclisation/formation of Lewis adduct (“closed”/diazaphosphazole tautomer) for compound **I** (Scheme 2) that may arise as a result of the replacement of the bulky, electron withdrawing (NiPr₂) substituents (at the P centre) with smaller, more electronegative chloro groups. Attempts were made to prepare the species structurally analogous to compound **I** where R¹ = Cl, *i.e.* target compound **11** (Figure 1), using PCl₃ to quench the *N*-lithiopyridylimine intermediate generated from the reaction between 6-methyl-2-cyanopyridine and PhLi.

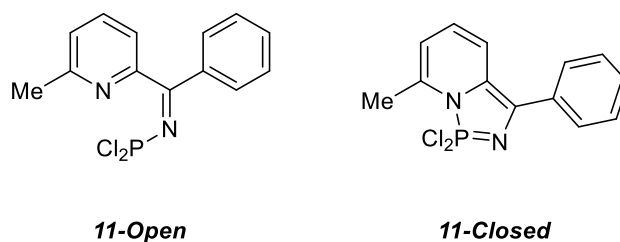


Figure 1 – Target compound **11**.

3.2 – Attempted Preparation of Target Compound Dichlorophosphino-1-((phenyl(6-methyl-pyridin-2-yl)methylene)amino) amine (**11-Open**) / (**11-Closed**)

The reaction between 6-methyl-2-cyanopyridine, PhLi and PCl₃ was carried out in an attempt to prepare target compound **11** (Figure 1). Upon addition of PCl₃ to the *N*-lithiopyridylimine intermediate (generated from the reaction between 6-methyl-2-cyanopyridine and PhLi), the immediate formation of a yellow precipitate from an orange solution was observed. Solution state ³¹P NMR spectroscopic analysis of the liquid component of the crude reaction mixture, after its separation from the yellow precipitate, revealed only one phosphorus-containing species, unreacted PCl₃ (δ_P = +218.6 ppm).

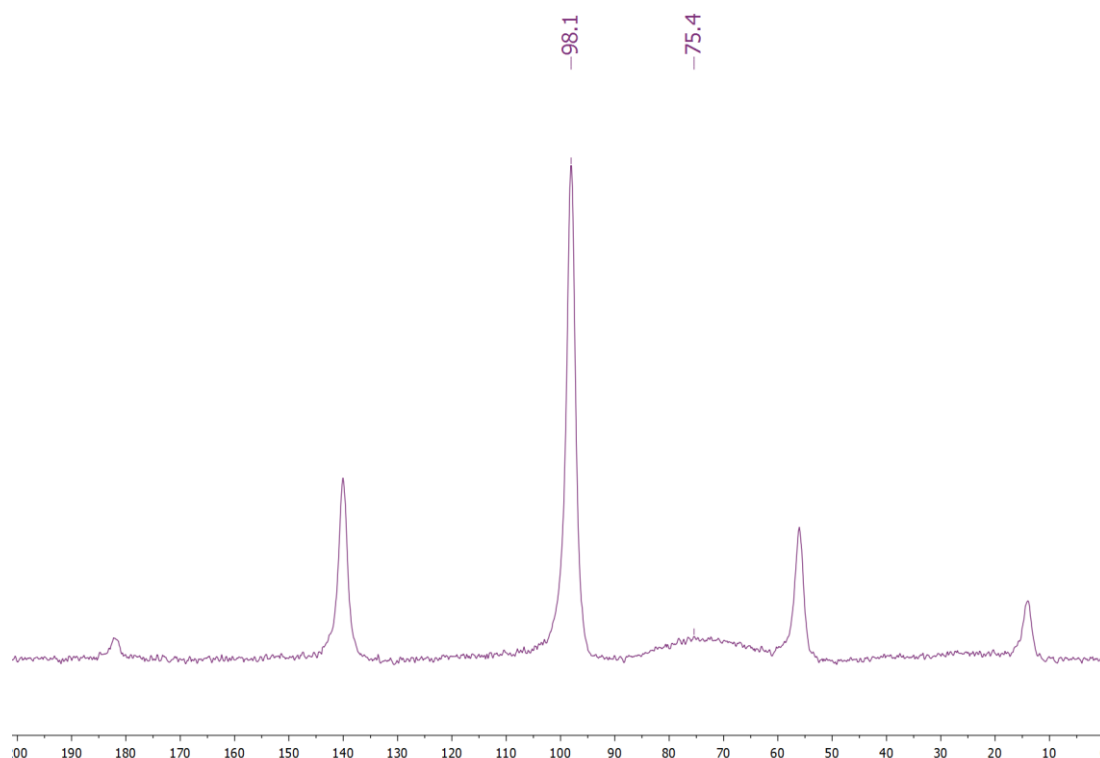


Figure 2 - Solid state ³¹P{¹H} NMR of precipitate isolated from the reaction between 6-methyl-2-cyanopyridine, PhLi and PCl₃, after 16 hours. Frequency = 161.9 MHz, spin rate = 10 kHz.

Solid state $^{31}\text{P}\{^1\text{H}\}$ NMR spectroscopic analysis* was carried out on the yellow precipitate isolated from the reaction between 6-methyl-2-cyanopyridine, PhLi and PCl_3 . This revealed the presence of two phosphorus-containing species, one giving rise to a sharp signal centred at $\delta_{\text{P}} = +98.1$ ppm and one presenting a broad resonance at $\delta_{\text{P}} = +75.4$ ppm (Figure 2), in a ratio of 1:4, respectively† (accounting for the spinning side bands). The bulk yellow precipitate was found to be sparingly soluble in CH_2Cl_2 and insoluble in all other common laboratory solvents, e.g. Et_2O , hexane, pentane, THF, toluene and DME. Solution state $^{31}\text{P}\{^1\text{H}\}$ NMR spectroscopic analysis of the yellow precipitate was carried out in CD_2Cl_2 and revealed only one phosphorus-containing species, presenting a sharp singlet resonance at $\delta_{\text{P}} = +78.4$ ppm, a chemical shift consistent with the resonance observed at $\delta_{\text{P}} = +75.4$ ppm in the solid state $^{31}\text{P}\{^1\text{H}\}$ NMR spectrum of the same material.

The “open” pyridyl-*N*-phosphinoimine and “closed” diazaphosphazole tautomers reported thus far in this work (Chapter 2), and in the literature,^{1,3,4} all present characteristic resonances by solution and solid state $^{31}\text{P}\{^1\text{H}\}$ NMR spectroscopy, at $\delta_{\text{P}} \sim +70$ ppm (“open”) and $\sim +40$ ppm (“closed”). The $^{31}\text{P}\{^1\text{H}\}$ NMR spectroscopic data observed for the products of the reaction between 6-methyl-2-cyanopyridine, PhLi and PCl_3 , hereby referred to as compounds **12** and **13** (Table 1), are not consistent with the characteristic resonances observed for the “open” (iminophosphine) and “closed” (iminophosphorane) species, and therefore with target compounds **11-Open** and **11-Closed** (Figure 1) being the two isolated reaction products. Attempts made to elucidate the structure of compounds **12** and **13** will now be discussed.

Compound	Solid State $^{31}\text{P}\{^1\text{H}\}$	Solution State $^{31}\text{P}\{^1\text{H}\}$
	NMR Chemical Shift ^a (ppm)	NMR Chemical Shift ^b (ppm)
12	+98.1	Not observed
13	+75.4	+78.4

Table 1 – Solid and solution state $^{31}\text{P}\{^1\text{H}\}$ NMR spectroscopic signals for compounds **12** and **13**. ^a Frequency: 161.9 MHz, spin rate: 10 kHz. ^b Frequency = 162.0 MHz, solvent: CD_2Cl_2 .

* Solid-state NMR spectra recorded by Dr D. Apperley and Mr F. Markwell of the EPSRC National Solid-State NMR Research Service at Durham University.

† Ratio of signals determined by Dr D. Apperley and Mr F. Markwell of the EPSRC National Solid-State NMR Research Service at Durham University

3.2.1 – Structural Elucidation of Products **12** and **13**

3.2.1.1 – X-Ray Crystallographic Study of Compound **12**

Upon isolating the liquid component of the reaction between 6-methyl-2-cyanopyridine, PhLi and PCl₃, this solution was left to stand at room temperature for two months. After this time, orange crystals (yield of crystals = 0.100 g, 6 %) suitable for an X-ray crystallographic study were obtained which were isolated by filtration and dried under reduced pressure. The single crystals were found to be insoluble in all laboratory solvents, *e.g.* Et₂O, hexane, pentane, THF, toluene, DME and DCM, and therefore, were unable to be studied by solution state NMR spectroscopy. A sample of the crystals was studied by solid state ³¹P{¹H} NMR spectroscopy,[‡] and found to present a sharp singlet resonance (with spinning side bands) centred at $\delta_P = +97.6$ ppm. This solid state ³¹P{¹H} NMR spectroscopic resonance is consistent with the chemical shift observed at $\delta_P = +98.1$ ppm in the solid state ³¹P{¹H} NMR spectrum recorded for the precipitate isolated from the reaction between 6-methyl-2-cyanopyridine, PhLi and PCl₃, *i.e.* compound **12** (Table 1).

The molecular structure determined by the X-ray crystallographic study of crystals of compound **12** is shown in Figure 3. Two molecules of compound **12** (**12.1** and **12.2** (Figure 3)) co-crystallised, alongside two molecules of disordered DME, with each unit cell containing one molecule of **12.2** and half a molecule of **12.1**. Comparison of the key structural data (dihedral angles (Table 2), bond lengths (Table 3) and bond angles (see **Appendix 5**) reveals that molecule **12.1** and molecule **12.2** are near identical, the conformational similarity between **12.1** and **12.2** can be seen from the overlay of the two molecules shown in Figure 4.⁵ For the purposes of the following discussion of the structural data, the data obtained for molecule **12.2** will be used.

[‡] Solid-state NMR spectra recorded by Dr D. Apperley and Mr F. Markwell of the EPSRC National Solid-State NMR Research Service at Durham University.

Chapter 3 - Synthesis of a Novel Macrocyclic Pyridyl-*N*-Phosphinoimine and Intramolecularly
Base-Stabilised Phosphenium Salt

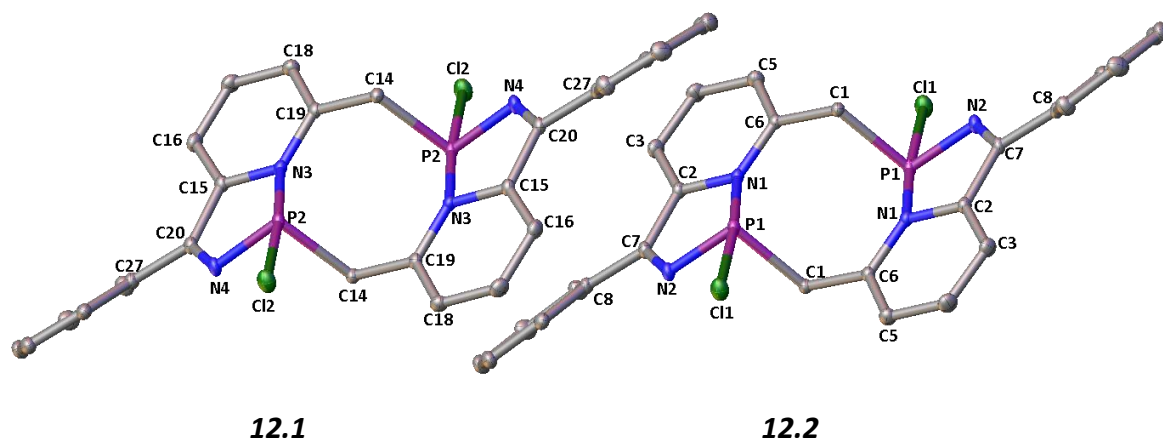


Figure 3 - X-ray molecular structure of compound 12 showing the two molecules which crystallised, 12.1 and 12.2. Selected atoms have been labelled; hydrogen atoms and solvent molecules have been omitted for clarity. Thermal ellipsoids are drawn at the 50% probability level.

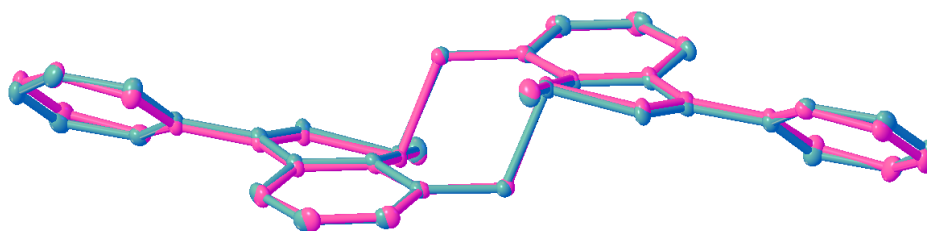


Figure 4 - Overlay of the X-ray molecular structures of molecules 12.1 (blue) and 12.2 (pink). Hydrogen atoms and solvent molecules have been omitted for clarity. Thermal ellipsoids are drawn at the 50% probability level.

Bond Distances (Å)				Dihedral Angles (°)			
12.1		12.2		12.1		12.2	
C7-C8	1.480(2)	C27-C20	1.480(2)	C9-C8...C7-C2	30.6(2)	C22-C27...C20-C15	35.1(2)
C7-C2	1.477(2)	C20-C15	1.479(2)	P1-Cl...C6-N1	76.3(1)	P2-C14...C19-N3	75.5(1)
C2-N1	1.352(2)	C15-N3	1.353(2)	N2-P1...C1-C6	162.6(1)	N4-P2...C14-C19	164.3(1)
N1-C6	1.347(2)	N3-C19	1.349(2)	C7-N2...P1-N1	9.3(1)	N3-P2...N4-C20	10.0(1)
C6-C1	1.491(2)	C19-C14	1.492(2)	C6-N1...P1-C1	88.8(1)	C14-P2...N3-C19	90.5(1)
C7-N2	1.291(2)	C20-N4	1.293(2)	C5-C6...C1-P1	103.4(1)	C18-C19...C14-P2	105.3(1)
N2-P1	1.708(1)	N4-P2	1.712(1)				
P1-Cl1	2.3931(5)	P2-Cl2	2.3233(5)				
P1-C1	1.878(1)	P2-C14	1.876(1)				
N1-P1	2.038(1)	N3-P2	2.109(1)				

Table 3 - Selected bond length data for molecules 12.1 and 12.2. Estimated standard deviations are shown in brackets. See Figure 3 for atom labels.

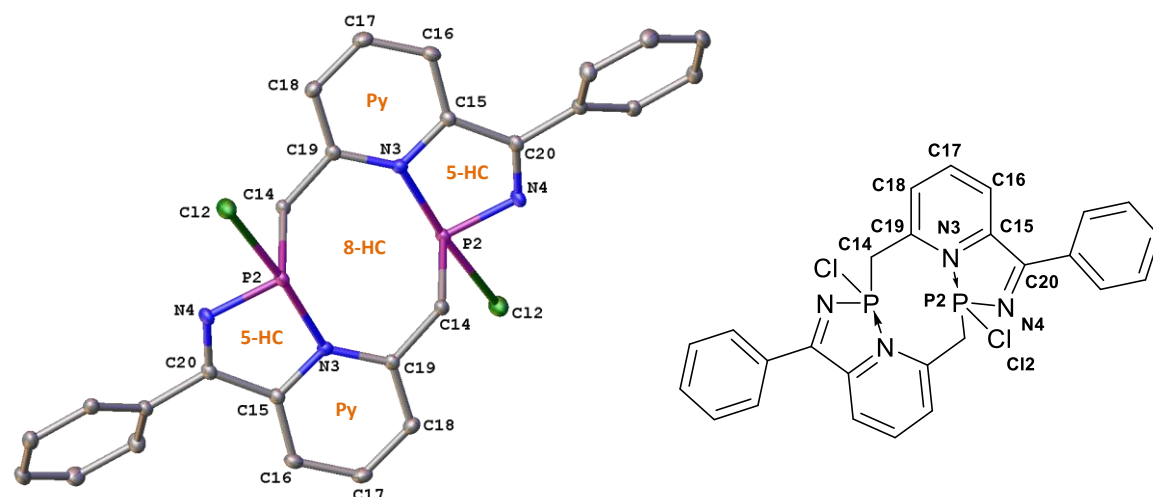


Figure 5 – LHS = X-ray molecular structure of **12.2**. Selected atoms have been labelled; hydrogen atoms and solvent molecules have been omitted for clarity. Thermal ellipsoids are drawn at the 50 % probability level. RHS = numbered pictorial representation of **12**.

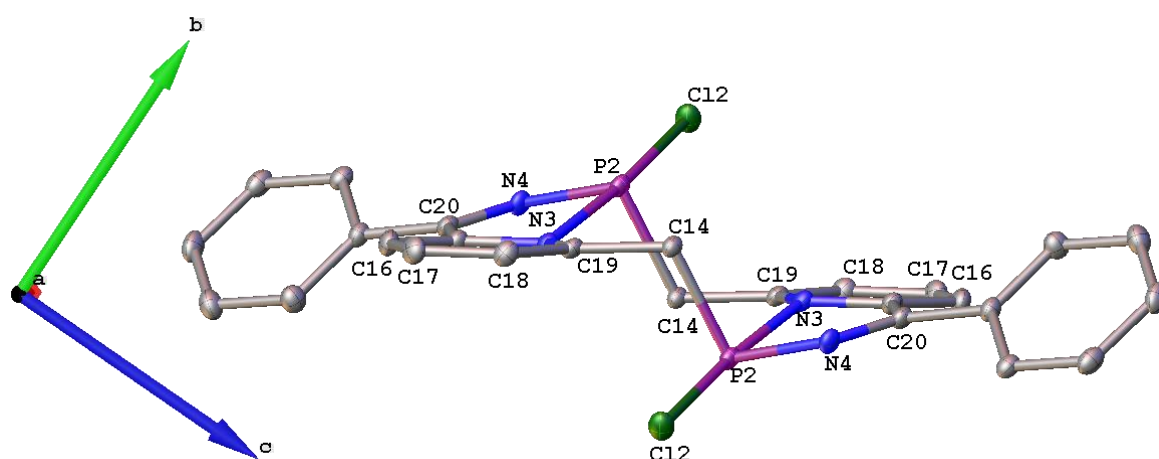


Figure 6 – View along the a axis of the X-ray molecular structure of molecule **12.2**. Select atoms have been labelled; hydrogen atoms and solvent molecules have been omitted for clarity. Thermal ellipsoids are drawn at the 50% probability level.

Compound **12**, which is observed by ASAP mass spectrometric analysis ($M^+ = 521.3$), can be described as consisting of five heterocyclic rings, fused together as shown in Figure 5. The central heterocycle (**8-HC**, Figure 5) can be regarded as an 8-membered macrocycle adopting a chair-type conformation (Figure 6), with two identical “closed” iminophosphorane units (**5-HC**, **Py**, Figure 5) fused to it. The P-Cl bonds are orientated transoidal to **8-HC** ring, *i.e.* above and below the macrocyclic motif. The bond lengths and angles within the **Py** ring are consistent with those observed for pyridine itself, indicating that this heterocycle can be

regarded as a true pyridine ring.⁶ The bicyclic, fused **5-HC – Py** motif adopts a distorted planar geometry, the C19-N3...P2-N4 dihedral angle measures 171.1(1) °. The phenyl rings bound to the imine carbon centres orientate themselves at an angle of 35.1(2) ° with respect to the distorted planar **5-HC – Py** motif. The length of the C20-N4 bond, 1.293(2) Å, is consistent with the average imine bond length.⁷ The N3-P2 distance in **12.2**, 2.109(1) Å, is greater than the covalent N(pyridine)-P^V bond observed for the diazaphosphazole species **A-Closed**, **1-Closed**, **2-Closed** and **4-Closed**, suggesting that the P-N interaction in compound **12** is dative in nature, with the pyridine nitrogen lone pair donating its electron density into the vacant σ^* orbital on the phosphorus centre, *i.e.* N(pyridine) \rightarrow PR₃.

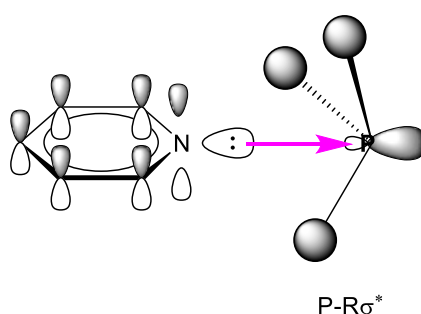


Figure 7 – Interaction of a pyridine nitrogen lone pair with the σ^* LUMO of a PR₃ centre.

For a N(pyridine) \rightarrow PR₃ dative interaction, the pyridine nitrogen lone pair is expected to interact with the phosphorus σ^* LUMO through the base of the trigonal pyramid at the phosphorus centre, as shown in Figure 7. The phosphorus centre in **12.2**, however, adopts a constrained, 4-coordinate geometry, as is highlighted in Figure 8, this geometry is comparable to that observed by Bushuk and co-workers⁸ for bis(2-phenylethynyl)-(8-dimethylaminonaphthalen-1-yl)phosphorus (Figure 9). The constrained 4-coordinate geometry adopted by the phosphorus centres in molecule **12.2**, in preference to the geometry shown in Figure 7, is likely as a result of the geometric constraint imposed by the position of the pyridine nitrogen relative to the phosphorus centre and the N(pyridine) \rightarrow PR₃ interaction that exists within compound **12**.

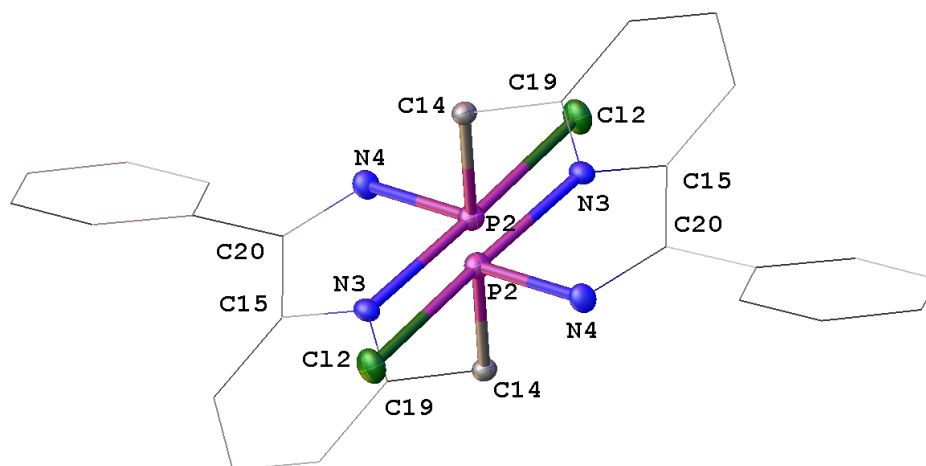


Figure 8 – X-ray molecular structure of molecule **12.2** highlighting the geometry at the phosphorus centres. Hydrogen atoms and solvent molecules have been omitted for clarity. Thermal ellipsoids have been drawn at the 50 % probability level.

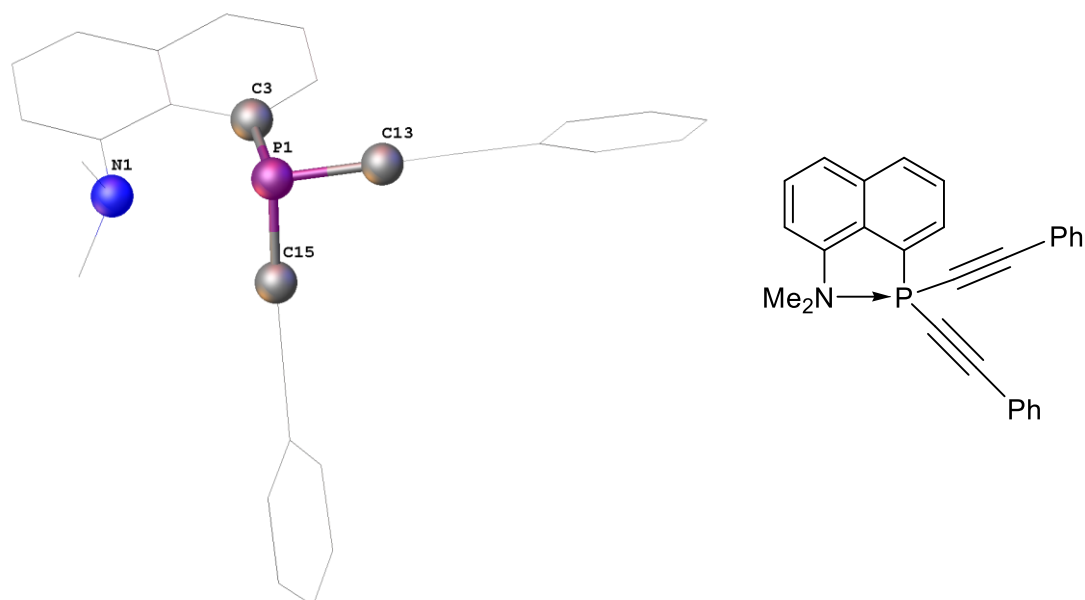


Figure 9 – LHS = X-ray molecular structure of bis(2-phenylethynyl)-(8-dimethylaminonaphthalen-1-yl)phosphorus⁸ highlighting the geometry about the P centre. Hydrogen atoms have been omitted for clarity. RHS = Pictorial representation of bis(2-phenylethynyl)-(8-dimethylaminonaphthalen-1-yl)phosphorus.

The covalent P2-Cl2 (2.3931(5) Å) and P2-N3 (2.109(1) Å) bonds in **12.2** are longer than the average P-Cl (2.03 Å) and P-N (1.77 Å) bond lengths, respectively, whereas the P2-C14 bond length (1.492(2) Å) is shorter than the average P-C bond length (1.85 Å).^{7,9} The elongation of the P2-Cl2 and P2-N3 bonds relative to the average P-Cl and P-N lengths, respectively, is expected as a consequence of the donation of the pyridine nitrogen lone pair into the vacant P-R σ^* orbital at the phosphorus centre. In contrast, the shorter than average P2-C14 bond length is unexpected and is thought to be as a consequence of the geometric constraint

placed upon molecule **12.2** as a whole by the position of the pyridine nitrogen relative to the phosphorus centre and the N(pyridine)→PR₃ dative interaction.

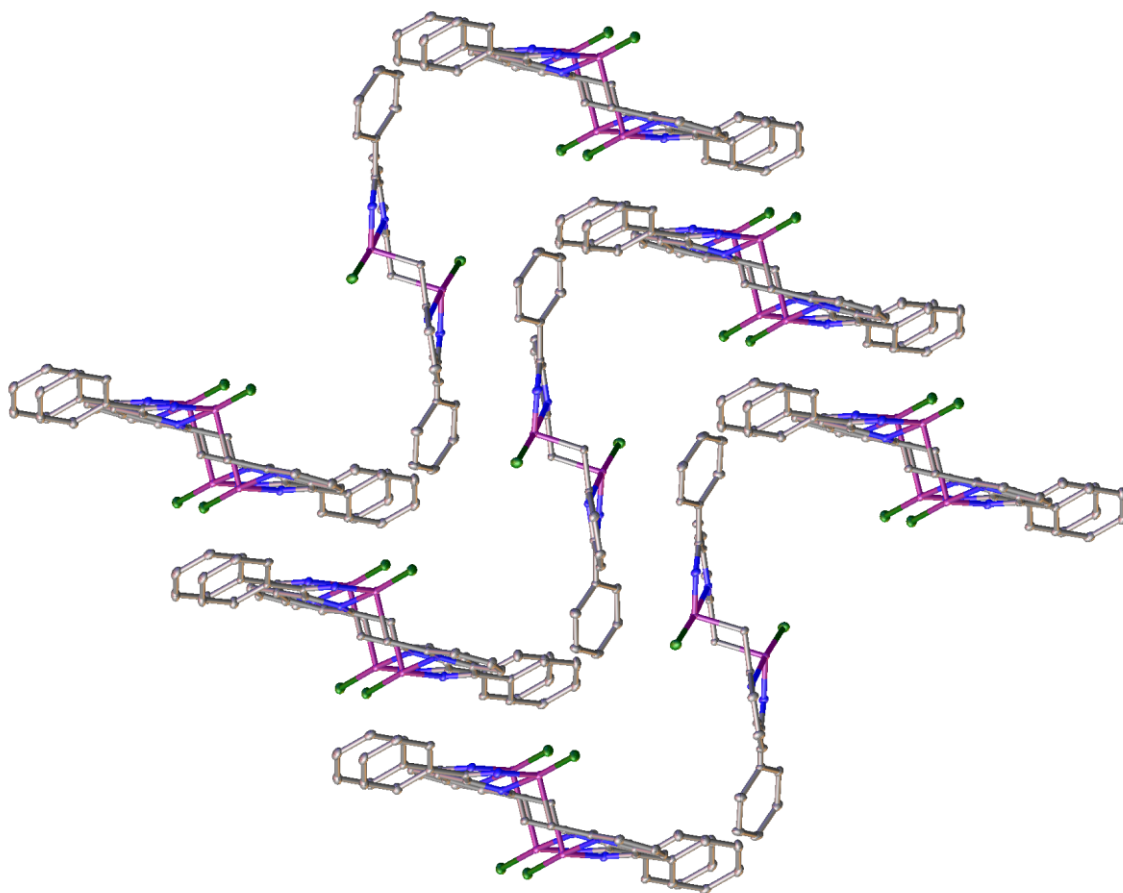
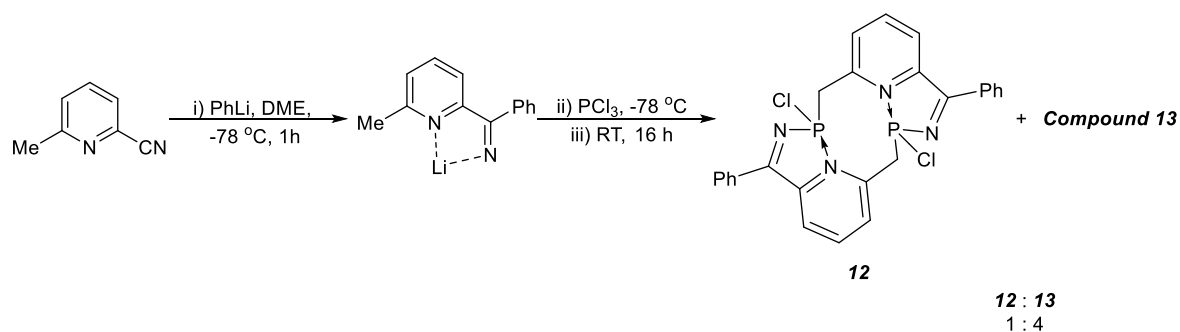


Figure 10 – Solid state packing of compound **12**. Hydrogen atoms and solvent molecules have been omitted for clarity. Thermal ellipsoids have been drawn at the 50 % probability level.

The packing arrangement of compound **12** in the solid state is shown in Figure 10. Molecules of **12.1** and **12.2** arrange themselves in an ordered array with the molecules close enough to experience intermolecular, short contact interactions between proton and chloro groups less than the sum of their Van der Waals radii (Cl = 1.75 Å, H = 1.2 Å).¹⁰ The short contact interactions observed for compound **12** are likely to be responsible for the lack of solubility of **12** in solvents such as DCM, hexane, pentane, Et₂O, THF, benzene, chloroform and toluene.

3.2.1.2 – Computational and Experimental Studies to Identify Compound 13



Scheme 4 – Synthetic procedure used to prepare compounds **12** and **13**.

The reaction between 6-methyl-2-cyanopyridine, PhLi and PCl₃ (Scheme 4) produced a yellow precipitate that was found to comprise of a mixture of two phosphorus-containing species (by solid state ³¹P{¹H} NMR spectroscopic analysis), compounds **12** and **13**, in a 1:4 ratio, respectively. Macrocyclic compound **12** was structurally elucidated by an X-ray crystallographic study (section 3.2.1.1). The identification of compound **13** ($\delta_P = +75.4$ (solid state) and +78.4 ppm (solution state)) will now be discussed.

Upon examination of the solution state ¹³C{¹H} NMR spectrum recorded for compound **13**, doublet signals were observed for the CH₃ and CCH₃ carbon centres: $\delta_C = 21.0$ ppm (d, $J = 3.7$ Hz, CH₃), 156.5 (d, $J = 2.5$ Hz, CCH₃), suggesting the presence of a bonding interaction between the pyridine nitrogen and phosphorus centres. In the ¹³C{¹H} and ¹H NMR spectra recorded for compound **13**, the chemical shifts observed for the pyridyl moiety lie within regions characteristic of aromatic carbon / proton centres, respectively, indicating the presence of an aromatic pyridine motif. The signal corresponding to the quarternary carbon centre adjacent to the pyridine ring lies at $\delta_C = 168.7$ ppm (d, $J = 1.3$ Hz) in the ¹³C{¹H} NMR spectrum, a chemical shift consistent with an imine C=N functionality. These solution state NMR data collected for compound **13** are not consistent with **13** existing as either an “open” pyridyl-*N*-phosphinoimine or a “closed” diazaphosphazole, computational studies (at the B3LYP/6-31G** level of theory)[§] were therefore carried out to aid with the structural elucidation of compound **13**. Two energy minima were identified by a computational study carried out to model the most likely products of the reaction between 6-methyl-2-cyanopyridine, PhLi and

[§] Computational studies carried out by Dr Mark A. Fox, Durham University.

PCl_3 . The species revealed by this computational study are shown in Figure 11: compound **11-Open** (an “open” pyridyl-*N*-phosphinoimine) and an intramolecularly base-stabilised phosphenium salt. The “closed”, diazaphosphazole species was not computed as an energy minimum, suggesting that it is too high in energy to form experimentally.

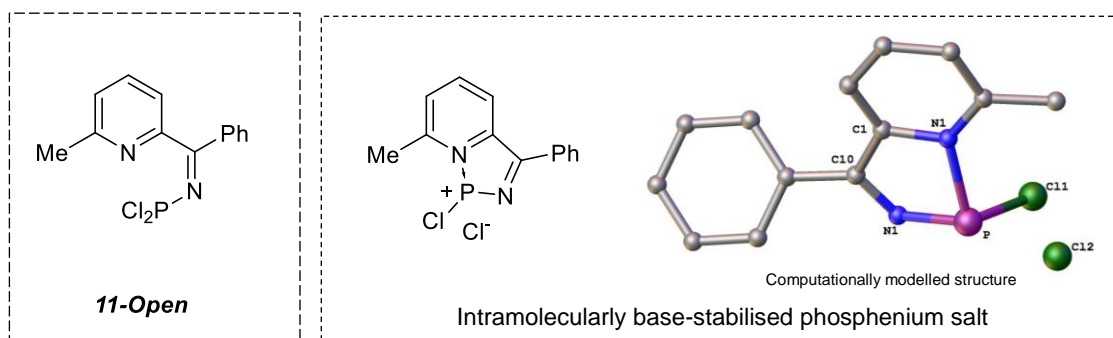
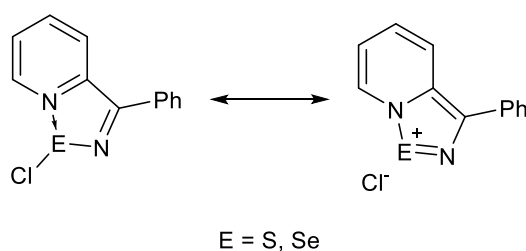


Figure 11 – Computationally identified lowest energy products of the reaction between 6-methyl-2-cyanopyridine, PhLi and PCl_3 .

The computationally proposed compound **11-Open** (Figure 11) is analogous to the other pyridyl-*N*-phosphinoimine, “open” tautomers observed previously, such as **1-Open**, **4-Open** and **5-Open** (see Chapter 2). The intramolecularly base-stabilised phosphenium salt, with a $[\text{:PR}_2]^+$ motif, is comparable to the sulfur- and selenium-containing species reported by Rawson and co-workers, shown in Scheme 5.¹¹ The computed geometry of the phosphenium salt is shown in Figure 11, the unbound chloride anion can be seen to occupy a position in space such that it does not come into close proximity with the phosphorus lone pair.



Scheme 5 - Compounds reported by Rawson and co-workers.¹¹

The solution state $^{13}\text{C}\{^1\text{H}\}$ NMR data obtained for compound **13** indicate a bonding interaction between the pyridine nitrogen centre and the phosphorus centre (as discussed above), and are therefore inconsistent with compound **13** existing as **11-Open** (Figure 11). Further

computational analysis** of the proposed intramolecularly base-stabilised phosphenium salt shown in Figure 11 (which possesses a “closed”-type structure with a dative N→P interaction) was carried out to predict its ^{31}P NMR chemical shift, in order to allow for its comparison with the experimental solution and solid state $^{31}\text{P}\{^1\text{H}\}$ NMR signals observed for **13**. The B3LYP/6-31G** level of theory was first tested, and was found to compute a ^{31}P NMR spectroscopic resonance of $\delta_{\text{P}} = +94.3$ ppm for the experimentally observed compound **12**. This chemical shift is in good agreement with the resonance observed experimentally by solid state $^{31}\text{P}\{^1\text{H}\}$ NMR spectroscopic analysis ($\delta_{\text{P}} = +98.1$ ppm), thus indicating the suitability of this basis set for these ^{31}P NMR spectroscopic predictions. The ^{31}P NMR chemical shift for the phosphenium salt shown in Figure 11 was computed at $\delta_{\text{P}} = +83.4$ ppm. This computed ^{31}P NMR chemical shift is reasonably comparable to that observed experimentally for compound **13**: $\delta_{\text{P}} = +75.4$ ppm (solid state) and $+78.4$ ppm (solution state), suggesting that compound **13** takes the structural form of the intramolecularly base-stabilised phosphenium salt shown in Figure 12. The experimentally obtained multi-nuclear solution state NMR data are consistent with compound **13** existing as an intramolecularly base-stabilised phosphenium salt. The stabilising dative N(pyridine) → $^+\text{P}(\text{R})\text{Cl}$ interaction is consistent with the doublet signals observed for the CH_3 and CCH_3 carbon centres in the $^{13}\text{C}\{^1\text{H}\}$ NMR spectrum. The aromatic pyridine moiety in **13** is consistent with the position of the chemical shifts observed in the solution state ^1H and $^{13}\text{C}\{^1\text{H}\}$ NMR spectra for the pyridyl motif.¹² The chemical shift of the carbon centre adjacent to the pyridine ring ($\delta_{\text{C}} = 168.7$ ppm) in the $^{13}\text{C}\{^1\text{H}\}$ NMR spectrum is consistent with the presence of the imine functionality.

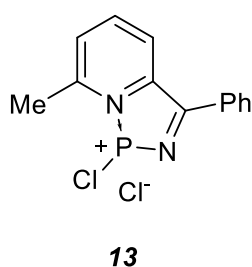
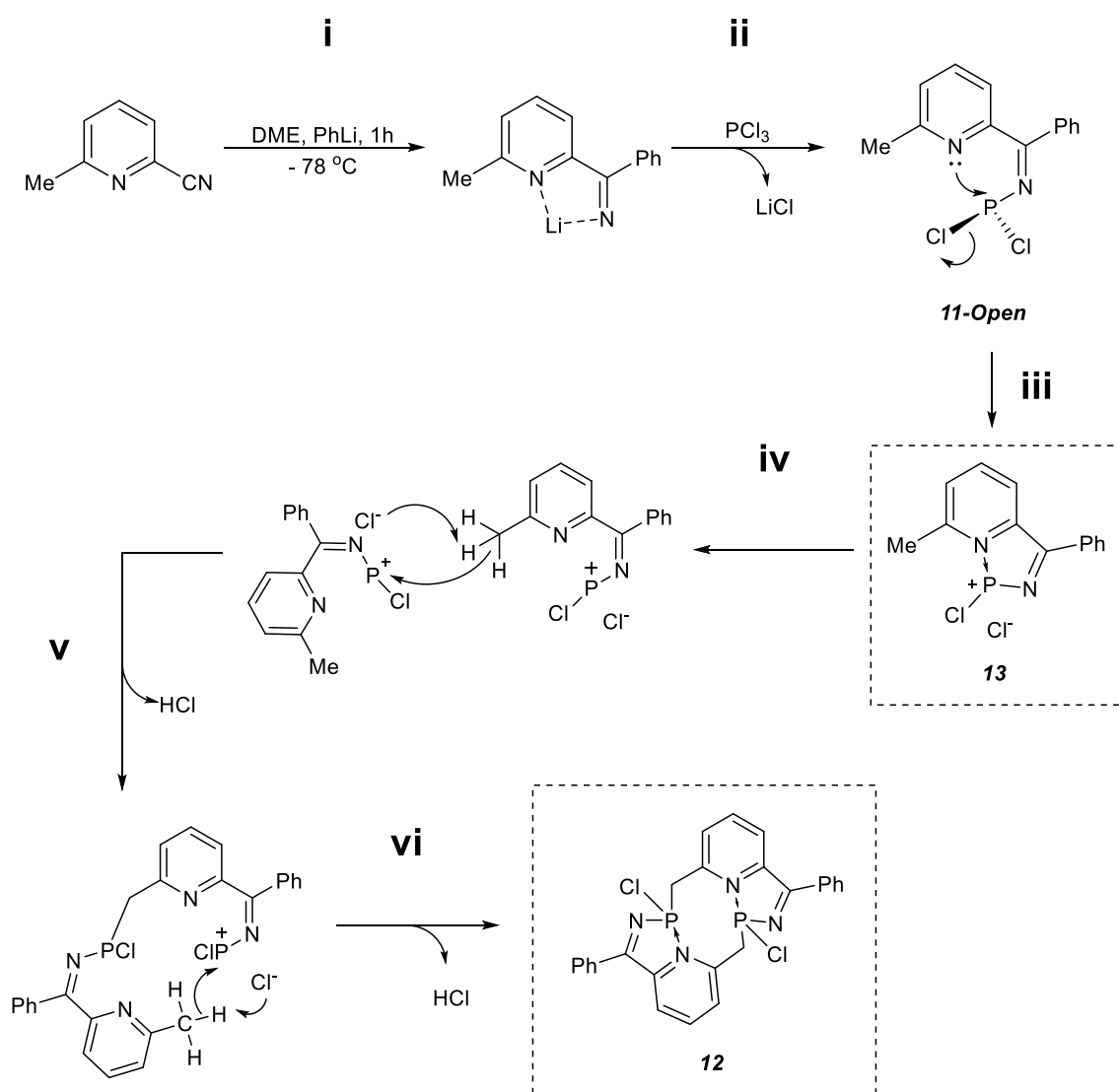


Figure 12 – Structural identity of compound **13**.

** Computational studies carried out by Dr Mark A. Fox, Durham University.

3.2.2 – Proposed Mechanism for the Formation of Compounds **12** and **13**

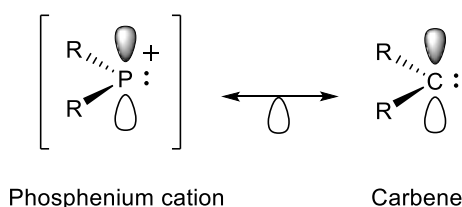
The structural identity of compounds **12** and **13**, products of the reaction between 6-methyl-2-cyanopyridine, PhLi and PCl₃, have been determined by using experimental and computational methods. The proposed mechanism for the formation of compounds **12** and **13** is shown in Scheme 6. It is postulated that the intramolecular phosphenium salt, **13**, is the precursor to macrocyclic compound **12**.



Scheme 6 – Proposed mechanism for the formation of compounds **12** and **13**.

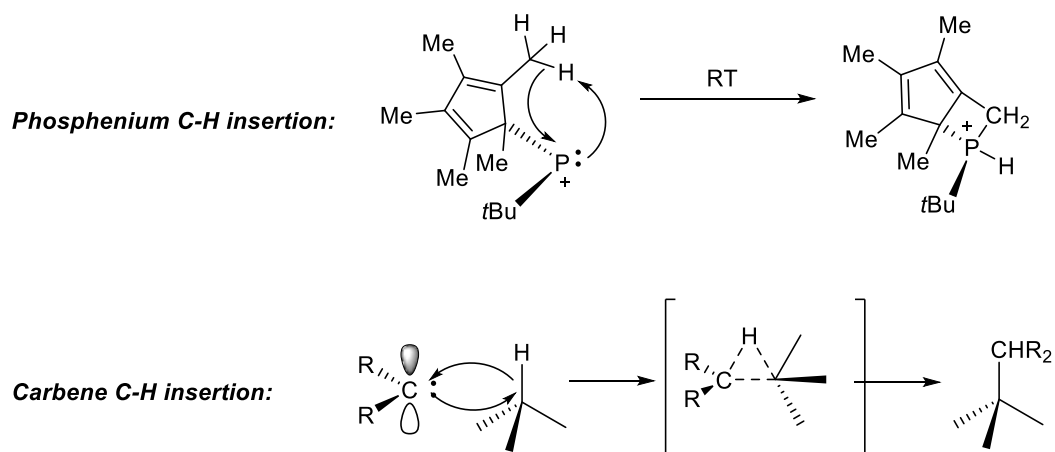
It is postulated that upon the quenching of the *N*-lithiopyridylimine (generated from step **i**, Scheme 6) using PCl₃ (step **ii**), that the “open” pyridyl-*N*-phosphinoimine species **11-Open** is

transiently generated. The difference in electronegativity between P (2.1 on the Pauling scale)¹³ and Cl (3.0 of the Pauling scale)¹³ gives rise to polar P-Cl bonds in **11-Open**, it is suggested that one of the highly electronegative chloro substituents irreversibly dissociates from the phosphorus centre in **11-Open** to form compound **13** which, due to its low solubility, precipitates out of the DME reaction solvent (step **iii**, Scheme 6).



Scheme 7 – Isolobal phosphonium cation and carbene motifs.

The co-ordinately unsaturated, electropositive $[:PR_2]^+$ phosphorus centre in compound **13** can be regarded as an intramolecularly stabilised phosphenium cation, which is isolobal to a carbene (Scheme 7). It is well documented that both phosphenium cations¹⁴ and carbenes¹⁵ readily undergo insertion into C-H bonds, as shown in Scheme 8. It is proposed, therefore, that the cationic phosphenium centre in **13** inserts into one of the C-H bonds of the pyridine methyl substituent on a second molecule of **13** (accompanied by the elimination of HCl) as described in step **v** (Scheme 6), followed by a second C-H insertion-HCl elimination (step **iv**, Scheme 6) to yield compound **12**.



Scheme 8 – Phosphenium cation and carbene C-H insertion reactions.¹⁵

For the conversion of compound **13** to **12** to occur (Scheme 6, steps **iv-vi**), compound **13** must be in solution, therefore the C-H insertion steps **v** and **vi** must occur immediately upon

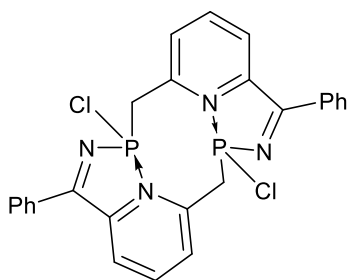
formation of **13**, before it precipitates out of the DME reaction solvent. As a greater proportion of compound **13** than compound **12** is observed (4:1, respectively), it is postulated that the formation of compound **13**, *via* steps **ii** and **iii**, occurs much faster than steps **iv** - **vi** (Scheme 6). This proposition is supported by the experimental observation that the composition of the initial bulk reaction product (containing a 4:1 mixture of compounds **12** and **13**) remained unchanged after extended reaction times and prolonged heating of the reaction mixture at 358 K for 3 weeks.

3.3 – Probing the Chemical Reactivity of Compounds **12** and **13**

Compounds **12** and **13** both possess multiple functionalities, most notably, both species contain imine motifs, dative N→P interactions, and potentially labile chlorides bound to the phosphorus centres. The potential for multifunctional behaviour of compounds **12** and **13**, and the unconfirmed structural identity of compound **13**, made it of interest to study the chemical reactivity of compounds **12** and **13** towards small molecules (such as inorganic salts, elemental selenium, DMF and B(C₆F₅)₃) and their coordination to metal centres.

3.3.1 – Investigating the Lability of the P-Cl Bonds in Compounds **12** and **13**

3.3.1.1 – Attempted Anion Exchange Reactions of Compound **12**



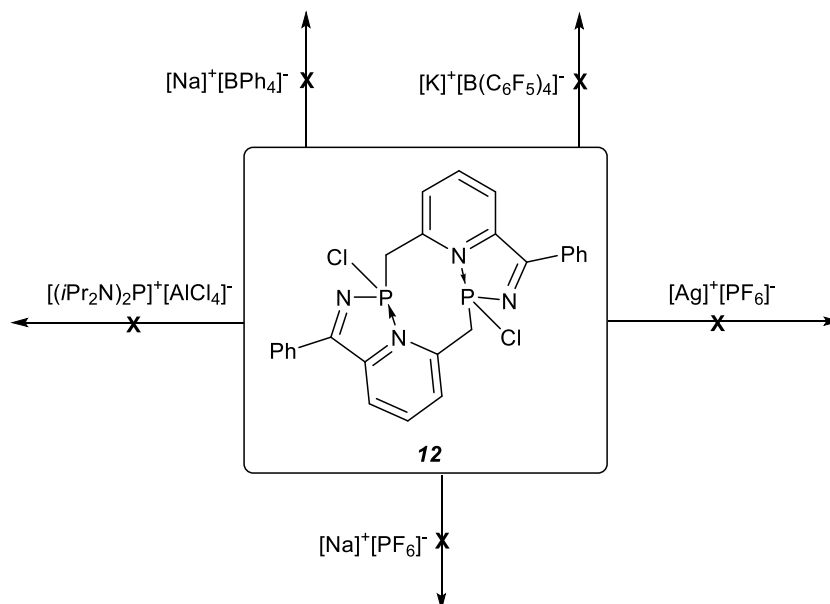
12

Figure 13 – Compound **12**.

Compound **12** possesses two longer than average (2.03 Å)⁹ P-Cl bonds (2.3931(5) Å for **12.2**), suggesting that these bonds could be quite labile. In order to probe the reactivity of the P-Cl bonds in **12**, attempts were made to try and exchange the chloro substituents by the reactions

Chapter 3 - Synthesis of a Novel Macrocyclic Pyridyl-*N*-Phosphinoimine and Intramolecularly
Base-Stabilised Phosphenium Salt

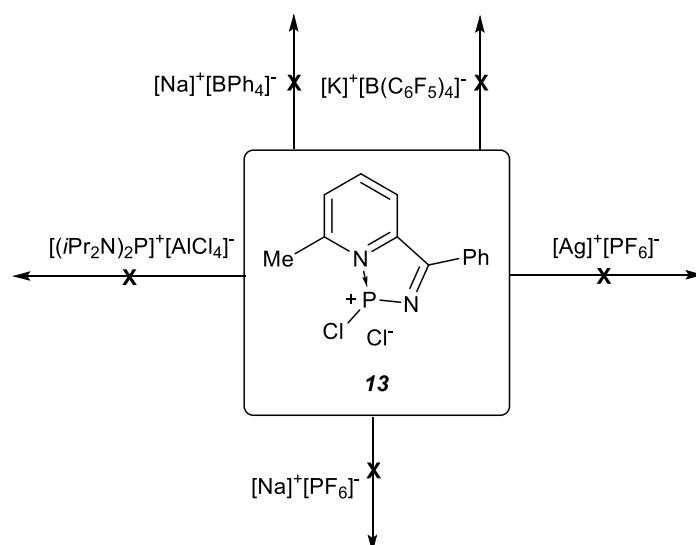
of compound **12** with a range of different inorganic salts (Scheme 9). The attempted anion exchange reactions were carried out on an NMR scale in Young's NMR tubes and are summarised in Scheme 9.



Scheme 9 – Attempted anion exchange reactions of compound **12**. All attempted reactions were carried out in DCM.

The reactions outlined in Scheme 9 were monitored by solution state NMR spectroscopy, it was found that, even after prolonged heating at elevated temperatures, no reaction occurred. This evidence suggests that, despite the anticipated lability of the chloro groups, this is not in fact the case, that the P-Cl bonds in compound **12** are too strong to be disrupted.

3.3.1.2 – Attempted Anion Exchange Reactions of Compound **13**



Scheme 10 - Attempted anion exchange reactions of compound **13**. All attempted reactions were carried out in DCM.

Compound **13** has been proposed, as a result of experimental and computational NMR spectroscopic studies (section **3.2.1.2**), to exist as an intramolecularly base-stabilised phosphenium salt containing a dative N(pyridine)→⁺P(R)Cl interaction, a P-Cl bond and an unbound chloride anion. The lability of the two chlorides in compound **13** was probed by investigating its reactivity towards the inorganic salts shown in Scheme 10 in a medium of DCM, these same five salts were reacted with compound **12** (section **3.3.1.1**). These reactions were carried out on an NMR scale in Young's NMR tubes and monitored by solution state multi-nuclear NMR spectroscopy. Solution state ³¹P NMR and ¹¹B NMR spectroscopic analysis were potentially powerful tools in analysing these reactions *in situ*, as any changes to compound **13** and the phosphorus-containing ions ([PF₆]⁻ and [(iPr₂N)₂P]⁺) could be observed by ³¹P NMR spectroscopy and changes to the boron species ([BPh₄]⁻ and [B(C₆F₅)₄]⁻) by ¹¹B NMR spectroscopy.

Solution state ³¹P{¹H} NMR spectroscopic analysis of all the attempted anion exchange reactions (Scheme 10) showed no change in chemical shift for the signal corresponding to compound **13** (δ_P = +78.4 ppm), suggesting that no displacement of the bonded chloro substituent at the phosphorus centre occurred. This result is attributed to the strength and covalent-nature of the P-Cl bond.

Solution state $^{31}\text{P}\{^1\text{H}\}$ NMR spectroscopic analysis of the reaction between compound **13** and $[(i\text{Pr}_2\text{N})_2\text{P}][\text{AlCl}_4]$ allowed any changes to the $[(i\text{Pr}_2\text{N})_2\text{P}]^+$ cation ($\delta_{\text{P}} = +312.7$ ppm) to be detected, however, no change to the chemical shift of the cation was observed. This observation for the reaction between **13** and $[(i\text{Pr}_2\text{N})_2\text{P}][\text{AlCl}_4]$ suggests that no exchange of a chloro group (either bound or unbound to the phosphorus centre) in **13**, for an $[\text{AlCl}_4]^-$ anion, occurred; the generation of $(i\text{Pr}_2\text{N})_2\text{PCl}$ ($\delta_{\text{P}} = +134.8$ ppm) would have been observed if exchange had taken place. The afore mentioned experimental observation suggests that, in the case of the reaction between **13** and $[(i\text{Pr}_2\text{N})_2\text{P}][\text{AlCl}_4]$, that the disruption of the proposed P-Cl bond and $\text{R}_2\text{P}^+\text{Cl}^-$ interaction in **13**, does not occur. For the other reactions outlined in Scheme 10, no change to the chemical shifts (by $^{31}\text{P}\{^1\text{H}\}$ and ^{11}B NMR spectroscopic analysis) corresponding to the inorganic salt species was observed, it is unclear from these data, however, whether the exchange of any discreetly anionic species in compound **13** has occurred as the exchange of discreet anions would not give rise to notable changes in chemical shift for either component of the ion pair.

3.3.2 – Investigating the ease of Phosphorus(III) Oxidation in Compounds **12** and **13**

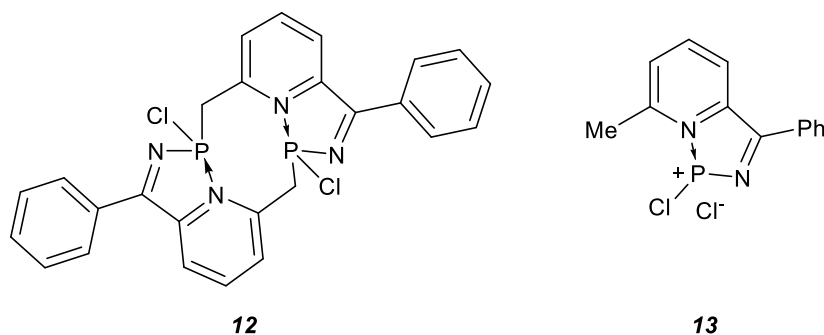


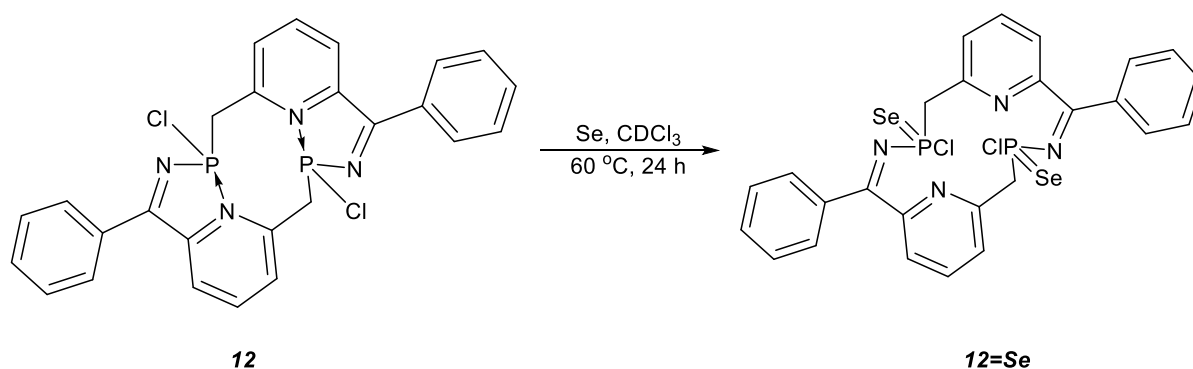
Figure 14 – Compounds **12** and **13** – products of the reaction between 6-methyl-2-cyanopyridine, PhLi and PCl_3 .

Section **3.3.1** demonstrates how the P-Cl interactions in compounds **12** and **13** (Figure 14) are not disrupted by anions, this section will examine reactivity at the phosphorus centres. Compounds **12** and **13** contain formally P^{III} centres which, if the phosphorus lone pair can be accessed, *i.e.* if the dative $\text{N}(\text{pyridine}) \rightarrow \text{P}^{\text{III}}$ interaction can be disrupted, have the potential of being oxidised to P^{V} by oxidising agents, two will be examined here, elemental selenium and DMF.

3.3.2.1 – Oxidation of Compounds **12** and **13** by Elemental Se

The oxidation of a P^{III} centre by elemental Se occurs concurrently with the reduction of the chalcogen and formation of a P=Se bond. Oxidation of compounds **12** and **13** by elemental selenium were attempted on an NMR scale in Young's NMR tubes, the progress of the reactions was monitored *in situ* by solution state ³¹P{¹H} NMR spectroscopy.

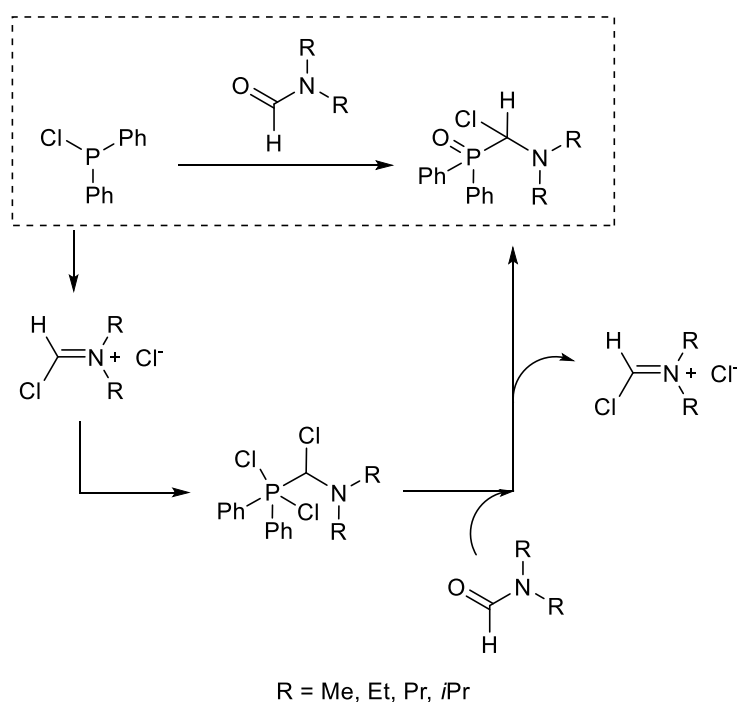
After 24 hours of heating a mixture of compound **12** and excess Se at 60 °C in CDCl₃, a single phosphorus selenium-containing species was observed at δ_P = +60.8 ppm (¹J_{PSe} = 871 Hz) by solution state ³¹P{¹H} NMR spectroscopic analysis – full conversion of compound **12** (which is not observed by solution state NMR due to poor solubility in CDCl₃) is assumed as no residual yellow precipitate of **12** was seen in the NMR tube after heating for 24 hours. The chemical shift of this resonance, and the |¹J_{PSe}| value (as determined from the satellites) are both comparable to those observed for (R₂N)₃PSe species: (Me₂N)₃PSe: δ_P = +83.2 ppm, |¹J_{PSe}| = 805 Hz; (Et₂N)₃PSe: δ_P = +77.1 ppm, |¹J_{PSe}| = 794 Hz,¹⁶ and in reasonable agreement with *t*BuP(Se)(Cl)NEt₂: δ_P = +118.0 ppm, |¹J_{PSe}| = 874 Hz,¹⁷ suggesting that the oxidation of both P^{III} centres in compound **12** has occurred, leading to the formation of the bis-tertiary phosphine selenide, **12=Se** (Scheme 11). The ¹H and ¹³C{¹H} NMR spectroscopic data are in agreement with the structure of **12=Se**: the CH₂ protons are observed as two doublets in the ¹H NMR spectrum (δ_H = 6.12 ppm (d, ²J_{HH} = 13.5 Hz), 6.09 ppm (d, ²J_{HH} = 13.5 Hz)) indicating a diastereotopic relationship, the quarternary imine carbon adjacent to the pyridine ring is observed as a doublet at δ_C = 181.8 ppm in the ¹³C{¹H} NMR spectrum (consistent with the imine carbon resonances observed for **A=Se** and **I=Se**).¹



Scheme 11 – Formation of **12=Se**.

In contrast to the reactivity observed for compound **12**, compound **13** undergoes no reaction with elemental selenium, even after heating the mixture in CDCl_3 at 60°C for 5 days. For a concerted reaction to occur between compound **13** and selenium, selenium would need to approach the phosphorus lone pair. The phosphorus lone pair is likely sterically blocked by crowding at the phosphonium centre. These steric constraints at the phosphorus centre are imposed by the close proximity of the pyridine moiety (as a result of the stabilising $\text{N}(\text{pyridine})\rightarrow\text{P}^+$ interaction) and the presence of a bulky, unbound chloride anion. To enable a reaction at the phosphonium centre, disruption of the dative $\text{N}\rightarrow\text{P}$ interaction must occur in order to reduce steric crowding at the phosphorus centre, and therefore increase the accessibility of the phosphorus lone pair. The differing reactivity of elemental Se with compounds **12** and **13** has been attributed to the differing strengths of the dative $\text{N}\rightarrow\text{P}$ interactions, this interaction is weaker within compound **12** than for compound **13**, and the energy required to disrupt this interaction must be compensated for by the formation of the $\text{R}_3\text{P}=\text{Se}$ double bond.

3.3.2.2 – Oxidation of Compounds **12** and **13** by DMF



Scheme 12 - Reaction between $\text{Ph}_2\text{P}(\text{Ph})\text{Cl}$ and N,N -dialkylformamides.¹⁸

N,N-Dialkylformamides, including DMF, are known to react with diphenylchlorophosphine to give a (diphenylphosphoryl)-*N,N*-dialkylaminochloromethane, as shown in Scheme 12.¹⁸ The reaction presented in Scheme 12, reported by Strelkova,¹⁸ requires the presence of the active species, $[R_2N=C(H)Cl]^+[X]^-$ ($X = Cl, I$), to trigger the reaction. This active species can either be generated during the reaction by addition of NaI, or prepared separately, then added to the Ph_2PCl and DMF mixture. The reactions of diphenylchlorophosphine with *N,N*-dialkylformamides leads to the formation of a phosphine oxide.

To probe the behaviour of compounds **12** and **13** towards DMF, **12/13** were added to an excess of dried and degassed DMF, the reactions were monitored by solution state $^{31}P\{^1H\}$ NMR spectroscopic analysis. After 3 days at room temperature, solution state $^{31}P\{^1H\}$ NMR spectroscopic analysis of the reaction between compound **12** and DMF revealed a singlet resonance at $\delta_P = +25.7$ ppm, a chemical shift in moderate agreement with $R_2C=N-P(O)R_2$ species (*e.g.* $Me(tBu)C=N-P(O)Ph_2$, $\delta_P = +17.3$ ppm). Excess DMF was unable to be removed from the reaction mixture, this hindered further NMR spectroscopic analysis. Based on position of the $^{31}P\{^1H\}$ NMR chemical shift observed for the phosphorus-containing product of the reaction between **12** and DMF, it is speculated that a phosphine oxide species may have been formed. If the product of the reaction between **12** and DMF is indeed a phosphine oxide, compound **12** may have undergone a reaction with DMF similar that of Ph_2PCl as reported by Strelkova and co-workers, to generate the species shown in Figure 15, compound **14**.¹⁸

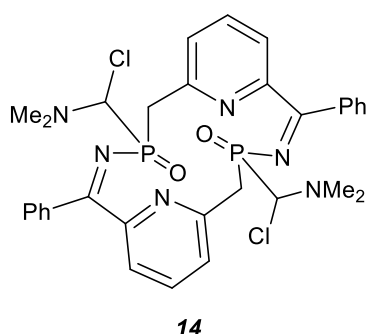


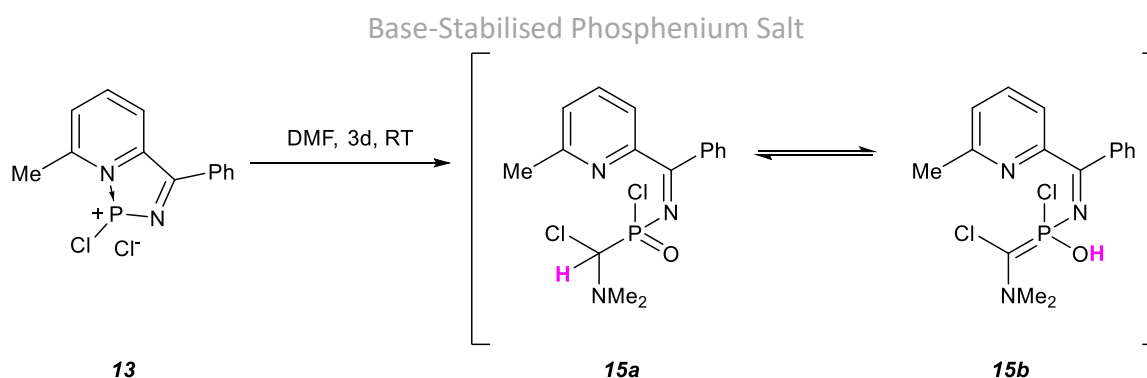
Figure 15 – Postulated product of the reaction between **12** and DMF.

The reaction between compound **13** and (excess) DMF was carried out and full consumption of **13** was observed by solution state $^{31}P\{^1H\}$ NMR spectroscopic analysis of the reaction mixture after 3 days at room temperature. Excess DMF was removed from the reaction

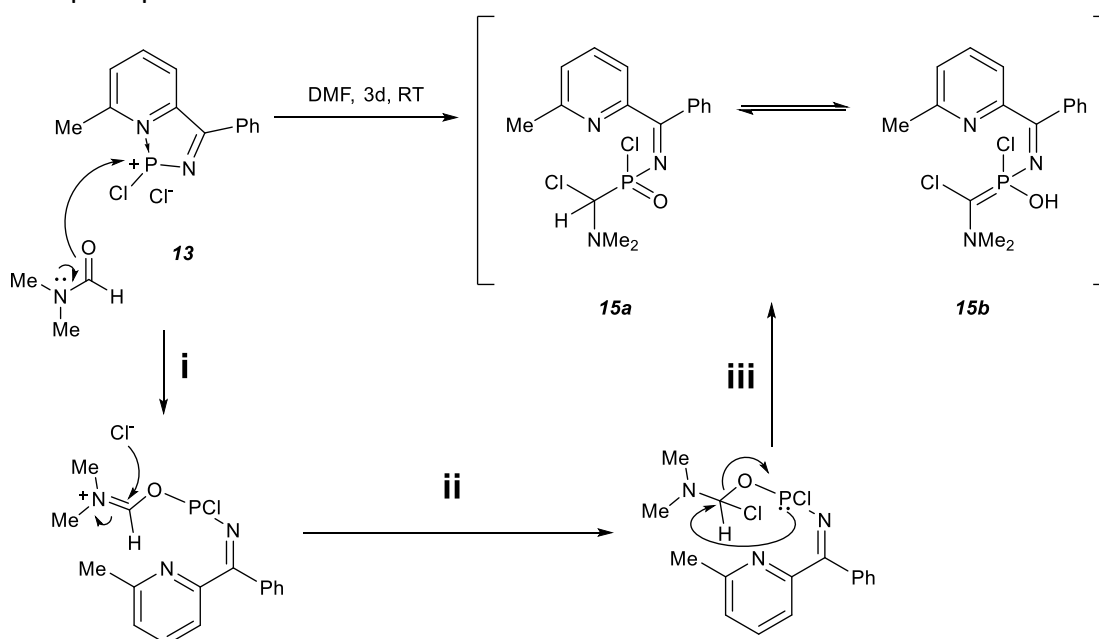
mixture, the residue dissolved in CDCl_3 and subsequently analysed by $^{31}\text{P}\{^1\text{H}\}$ NMR spectroscopy; a single phosphorus-containing species, presenting a broad singlet resonance ($\nu_{1/2} = 121$ Hz) at $\delta_{\text{P}} = -25.4$ ppm in the $^{31}\text{P}\{^1\text{H}\}$ NMR spectrum, was seen.

Solution state ^1H and $^{13}\text{C}\{^1\text{H}\}$ NMR spectroscopic analyses of the product of the reaction between compound **13** and DMF revealed that the pyridyl motif had retained its aromaticity. The $\text{N}(\text{CH}_3)_2$ protons which, in free DMF are inequivalent,¹⁹ are seen as equivalent by ^1H ($\delta_{\text{H}} = 3.07$ ppm, s) and $^{13}\text{C}\{^1\text{H}\}$ NMR ($\delta_{\text{C}} = 44.8$ ppm, s) spectroscopic analysis after its reaction with **13**. The *HCO* proton from DMF is observed at a lower frequency¹⁹ than in free DMF, as a weak, broad signal by ^1H NMR spectroscopic analysis ($\delta_{\text{H}} = 7.92$ ppm, $\nu_{1/2} = 6$ Hz), the broadness of this signal is suggestive that this proton is labile. Examination of the $^{13}\text{C}\{^1\text{H}\}$ NMR spectrum recorded for the reaction product shows that the CH_3 and CCH_3 carbon centres (corresponding to the methyl substituent *ortho* to the pyridine nitrogen centre) now present sharp singlets ($\delta_{\text{C}} = 19.4$ ppm and 134.1 ppm, respectively), as opposed to the doublet signals seen for compound **13**, indicating that the $\text{N} \rightarrow \text{P}$ dative interaction in compound **13** has been disrupted. Mass spectrometric analysis of the reaction product saw a peak at $m/z = 300.1$, this is consistent with the Na^+ adduct of a compound with the molecular formula $\text{C}_{13}\text{H}_{11}\text{ClN}_2\text{OP}$. These various spectroscopic data suggest that the product of the reaction between compound **13** and DMF exists in two structural forms, **15a** and **15b** (Scheme 13).

Compounds **15a** and **15b** are proposed to be in a prototropic equilibrium with each other (the labile proton, which gives rise to a broad signal ($\nu_{1/2} = 6$ Hz) at $\delta_{\text{H}} = 7.92$ ppm, by ^1H NMR spectroscopic analysis, is highlighted in Scheme 13), as other $\text{R}_2\text{P}(=\text{X})\text{H}$ species are reported to exist in.²⁰ The phosphorus centres in compounds **15a** and **15b** are magnetically and chemically inequivalent, the dynamic, tautomeric equilibrium proposed to exist between **15a** and **15b** is consistent with the broad nature of the signal observed in the $^{31}\text{P}\{^1\text{H}\}$ NMR spectrum, $\nu_{1/2} = 121$ Hz. The chemical shift observed for **15a** and **15b** in the $^{31}\text{P}\{^1\text{H}\}$ NMR spectrum, $\delta_{\text{P}} = -25.4$ ppm, is in reasonable agreement with that observed for an analogous species, $\text{PhP}(\text{O})(\text{Cl})\text{NEt}_2$, $\delta_{\text{P}} = -18.0$ ppm.²¹ No coupling between the labile proton (highlighted in Scheme 13) and the phosphorus centre is observed due to the broad nature of their resonances in the ^1H and ^{31}P NMR spectra, respectively.

Scheme 13 – Proposed products of the reaction between **13** and DMF.

The formation of compounds **15a** and **15b** is proposed to occur in the absence of any active species, unlike the reactions reported by Strelkova and co-workers,¹⁸ due to the electron deficient nature of the phosphorus centre in **13**. The proposed mechanism for the formation of **15a** and **15b** from compound **13** and DMF is shown in Scheme 14, namely a Vilsmeier-Haack-type mechanism.²² The C=O bond in DMF is proposed to attack the phosphonium centre in compound **13**, leading to a disruption of the N(pyridine)→P⁺ interaction, and formation of an iminium-chloride ion pair (step i, Scheme 14). The unbound chloride anion is then thought to attack at the iminium carbon to generate a neutral species (step ii, Scheme 14). This neutral Me₂N-C(H)(Cl)-O-PR₂ species then undergoes a rearrangement (step iii, Scheme 14), whereby a P=O bond is created and the CHCl(NMe₂) group migrates onto the phosphorus centre to create a P-C bond, giving rise to compound **15a**, which can exist in a prototropic equilibrium with **15b**.

Scheme 14 – Proposed mechanism of the reaction between compound **13** and DMF to form **15a** and **15b**.

As described above, compound **13** was found to undergo a reaction with (excess) DMF (to form compounds **15a** and **15b**, Scheme 13), but not to react with elemental selenium (section 3.3.2.1). The differing reactivity of compound **13** towards DMF and Se is attributed to the high-energy requirement for the disruption of the N→P⁺ interaction. The disruption of the dative N→P⁺ interaction is required in order to unblock the phosphorus lone pair so it can interact with an oxidising agent, and therefore allow for oxidation of the P^{III} centre. The oxidation of the P^{III} centre in compound **13** can occur with DMF as a strong P=O is formed, this energetically favourable bond formation compensates for the energy required to disrupt the N→P⁺ interaction in **13**, whereas, with Se, the formation of a (weaker) P=Se bond²³ would not compensate for the energy required to disrupt the dative N→P⁺ interaction.

3.3.3 – Investigating the Coordination of B(C₆F₅)₃ to Compounds **12** and **13**

It has been reported by Dyer and co-workers that a tautomeric mixture of **A-Open** and **A-Closed** coordinates to a hard aluminium centre, *via* the hard nitrogen centre of the iminophosphorane motif in **A-Closed**, to yield a single species with a N→Al interaction, **A-AlMe₃** (Figure 16).¹ The coordination behaviour of compounds **12** and **13** in the presence of a hard, Lewis acidic group XIII centre was of interest to probe as both species possess two different hard nitrogen centres (*i.e.* a pyridine and an imine nitrogen), which could form a N→Z interaction with the group XIII centre (Z). The reactivity of compounds **12** and **13** towards Lewis acidic boron centre in B(C₆F₅)₃ will now be discussed.

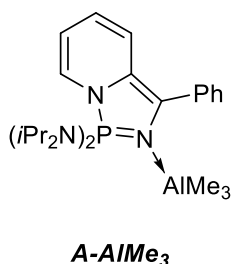
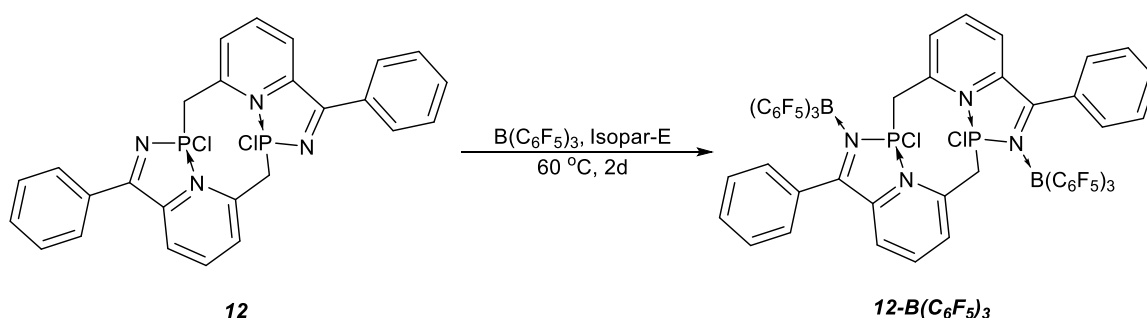


Figure 16 – Coordination compound **A-AlMe₃**.

Diphosphine compound **12** was added to a solution containing two equivalents of B(C₆F₅)₃ in isopar-E, and the mixture heated at 60 °C for 2 days. After 2 days at 60 °C, attempts were made to fully remove the volatile species under reduced pressure (at elevated temperatures), but were not successful, nevertheless, the residue was then dissolved in C₆D₆ and analysed

by solution state NMR spectroscopy. ^1H and $^{13}\text{C}\{^1\text{H}\}$ NMR spectroscopic analysis revealed that residual isopar-E was present in the reaction residue in greater quantities than any other species. Consequently, the NMR signals corresponding to isopar-E “swamped” the ^1H and $^{13}\text{C}\{^1\text{H}\}$ NMR spectra, hindering the observation of any other species. Solution state $^{31}\text{P}\{^1\text{H}\}$ and ^{11}B NMR spectroscopic analysis of the reaction mixture, however, revealed single singlet resonances at $\delta_{\text{P}} = +41.9$ ppm and $\delta_{\text{B}} = -8.6$ ppm, respectively – chemical shifts consistent with those observed for analogous pyridyl-*N*-phosphinoimine species that coordinate to $\text{B}(\text{C}_6\text{F}_5)_3$ *via* their imine nitrogen centre (see **Chapter 4**). These NMR spectroscopic data are suggestive of **12-B(C₆F₅)₃** (Scheme 15) being the product of the reaction between **12** and $\text{B}(\text{C}_6\text{F}_5)_3$, where each imine nitrogen lone pair coordinates to a Lewis acidic boron centre. Mass spectrometric analysis (by ASAP at various temperatures and by ESI) of the product of the reaction between **12** and $\text{B}(\text{C}_6\text{F}_5)_3$ did not identify any fragments consistent with **12-B(C₆F₅)₃**. If **12-B(C₆F₅)₃** is the product of the reaction between **12** and $\text{B}(\text{C}_6\text{F}_5)_3$, its high molecular mass is likely to result in low volatility of the species, and therefore making **12-B(C₆F₅)₃** unlikely to be observed by mass spectrometric methods.



Scheme 15 – Proposed product of the reaction between **12** and $\text{B}(\text{C}_6\text{F}_5)_3$, **12-B(C₆F₅)₃**.

The intramolecularly base-stabilised phosphenium salt, **13**, was added to a solution containing one equivalent of $\text{B}(\text{C}_6\text{F}_5)_3$ in isopar-E, and the mixture heated at $60\text{ }^\circ\text{C}$ for 7 days. Even after prolonged heating at $60\text{ }^\circ\text{C}$, solution state $^{31}\text{P}\{^1\text{H}\}$, ^{11}B and ^{19}F NMR spectroscopic analyses of the reaction mixture showed no change to the starting materials, indicating that **13** does not coordinate to the Lewis acidic boron centre in $\text{B}(\text{C}_6\text{F}_5)_3$. Sections **3.3.2.1** and **3.3.2.2** suggest that the stabilising $\text{N}(\text{pyridine}) \rightarrow ^+\text{PR}_2$ interaction in **13** is strong, and not easily disrupted. The high energy required to interrupt this dative interaction, and to therefore “free” the pyridine nitrogen lone pair to allow for $\text{N} \rightarrow \text{B}$ coordination, evidently cannot be provided by the coordination of $\text{B}(\text{C}_6\text{F}_5)_3$ to the pyridine nitrogen centre. The imine nitrogen

lone pair is likely sterically prevented from coordinating to the Lewis acidic boron centre in $B(C_6F_5)_3$ as a result of the close proximity of the bulky, unbound chloride anion which sterically precludes the approach of $B(C_6F_5)_3$ to the imine nitrogen centre (Figure 17). Somewhat surprisingly, there appears to be no reaction between the proposed unbound chloride anion in **13** with $B(C_6F_5)_3$ to afford the known $[ClB(C_6F_5)_3]^-$ anion,²⁴ suggesting that the unbound chloride anion within **13** is much more strongly associated with the phosphorus centre than expected.

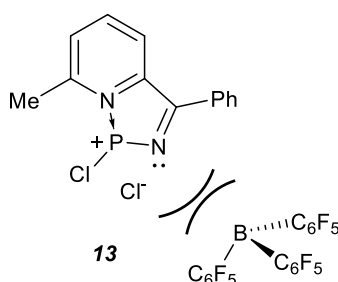
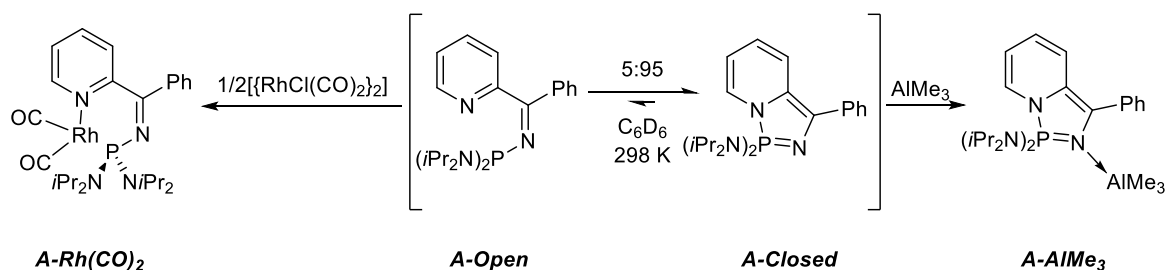


Figure 17 – Steric hindrance between **13** and $B(C_6F_5)_3$ preventing coordination.

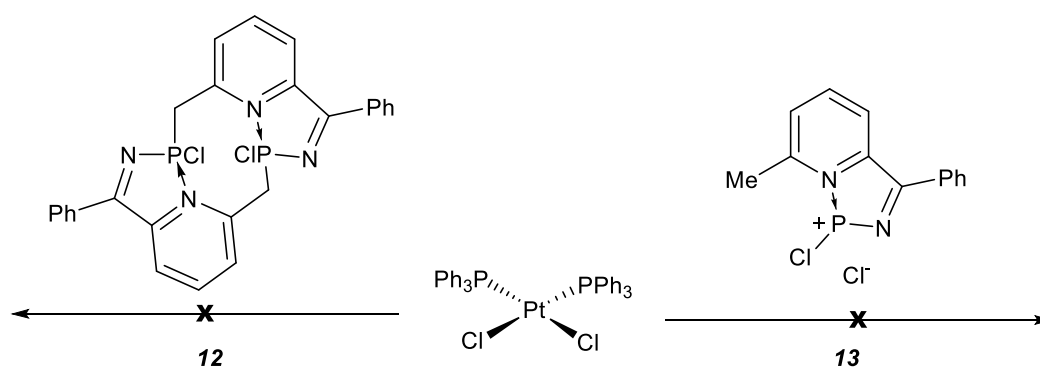
3.4 – Probing the Coordination of Novel Compounds **12** and **13** to Platinum Centres



Scheme 16 – Previously reported coordination behaviour of compound **A**.¹

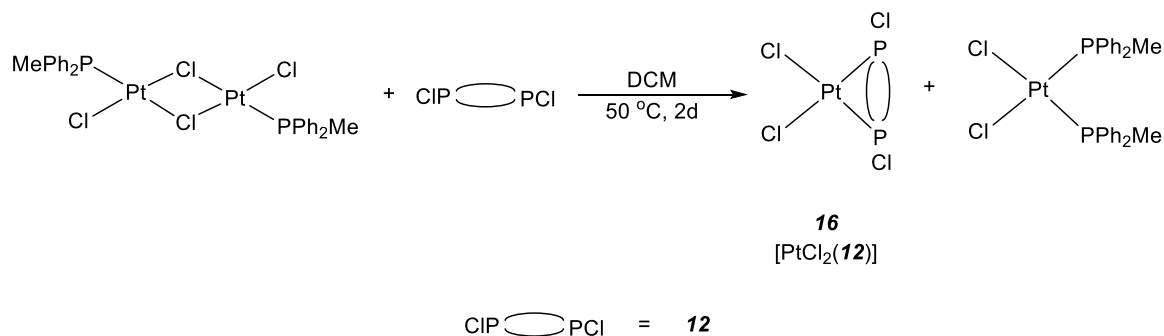
The ability of the pyridyl-*N*-phosphinoimine – diazaphosphazole tautomeric pairs to switch coordination modes, depending on whether they are presented with a soft metal centre (κ^2 -*N,P* coordination, *e.g.* to Rh)¹ or a hard metal centre (κ^1 -*N* coordination, *e.g.* to Al),¹ is shown in Scheme 16 for compound **A**. The coordination of compounds **12** and **13** to the Lewis acidic boron centre of $B(C_6F_5)_3$ has already been discussed in section 3.3.2.2, macrocyclic compound **12** is proposed to form compound **12- $B(C_6F_5)_3$** , whereas the phosphenium salt, **13**, was found not to coordinate.

To extend this reactivity, it was of interest to explore the behaviour of compounds **12** and **13** with a soft Lewis acid, *e.g.* Pt^{II}. To this end, the coordination of compounds **12** and **13** to soft platinum centres has been probed. Platinum was chosen due to the 33.7 % abundance of the NMR active spin ½ ¹⁹⁵Pt nucleus, and therefore the ability to observe ³¹P-¹⁹⁵Pt coupling, the magnitude of which is indicative of a *cis* (¹J_{Pt} > 3000 Hz) or *trans* (¹J_{Pt} = 2400 Hz – 3000 Hz) coordination geometry about a square planar platinum centre.²⁵ Separately, compounds **12** and **13** were added to a solution of *cis*-[PtCl₂(PPh₃)₂] in DCM (Scheme 17), however no reaction was observed to take place in either case.



Scheme 17 – Unsuccessful reactions between **12/13** and *cis*-[PtCl₂(PPh₃)₂].

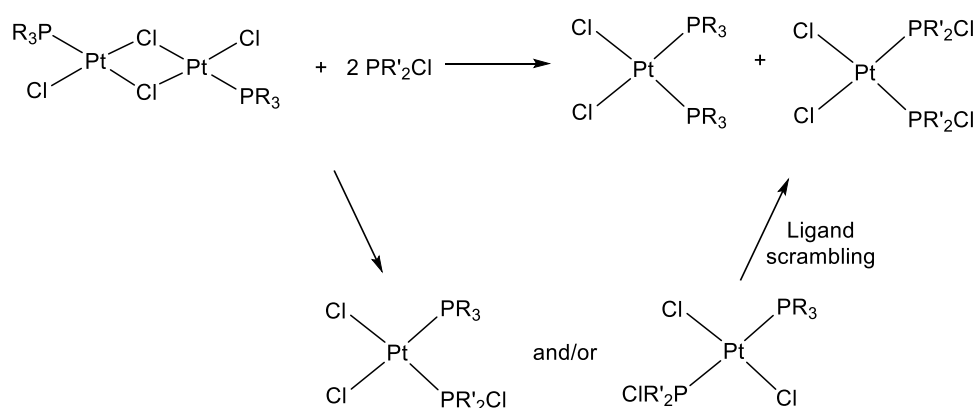
Since no reactivity was observed between compounds **12** / **13** and *cis*-[PtCl₂(PPh₃)₂], these species were subsequently added to a solution of the dimeric platinum complex *trans*-[Pt(PPh₂Me)Cl(μ-Cl)]₂ in DCM. *trans*-[Pt(PPh₂Me)Cl(μ-Cl)]₂ was chosen as it differs from *cis*-[PtCl₂(PPh₃)₂] in that it possesses labile sites on each platinum centre, making it more reactive than the monomeric platinum complex.²⁶ Here, both compounds **12** and **13** were found to undergo a reaction with this more reactive *trans*-[Pt(PPh₂Me)Cl(μ-Cl)]₂ complex.



Scheme 18 – Proposed products of the reaction between **12** and *trans*-[Pt(PPh₂Me)Cl(μ-Cl)]₂.

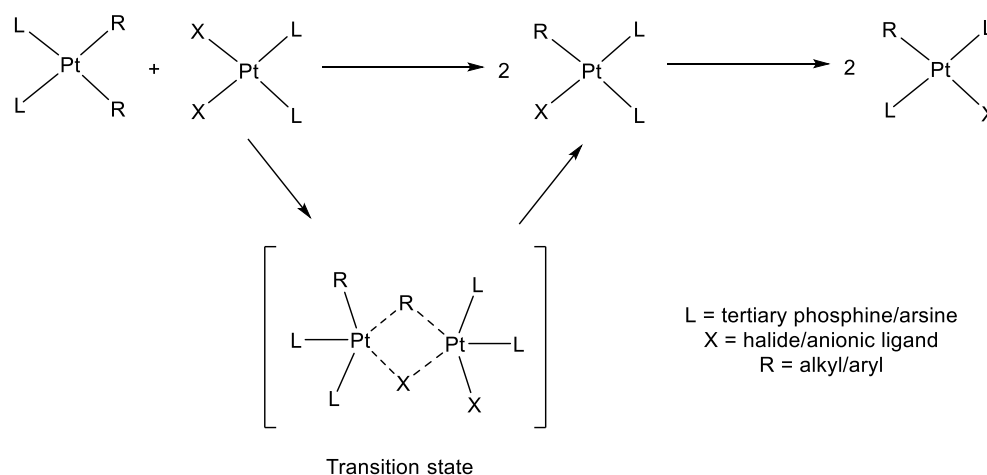
Compound **12** and $trans\text{-[Pt(PPh}_2\text{Me)Cl}(\mu\text{-Cl})_2]$ were reacted in a 1:1 ratio, and a mixture of several phosphorus-containing products were observed by solution state $^{31}\text{P}\{^1\text{H}\}$ NMR spectroscopic analysis of the resulting reaction mixture. No single species could be isolated (by recrystallization or solvent extraction) and individual species could not be distinguished from one another by ^1H and $^{13}\text{C}\{^1\text{H}\}$ NMR spectroscopic analysis.

The identity of the two-major phosphorus-containing species (which account for $\sim 70\%$ of the phosphorus-containing compounds observed by solution state $^{31}\text{P}\{^1\text{H}\}$ NMR spectroscopy), namely compound **16** and $cis\text{-[PtCl}_2\text{(PPh}_2\text{Me)}_2]$ (Scheme 18), has been speculated based on chemical shifts observed by solution state $^{31}\text{P}\{^1\text{H}\}$ NMR spectroscopic analysis. The complex $cis\text{-[PtCl}_2\text{(PPh}_2\text{Me)}_2]$ is proposed to form from the reaction between **12** and $trans\text{-[Pt(PPh}_2\text{Me)Cl}(\mu\text{-Cl})_2]$ as the signal at $\delta_{\text{P}} = -0.9$ ppm (s, with satellites $^1J_{\text{PPt}} = 3616$ Hz) in the solution state $^{31}\text{P}\{^1\text{H}\}$ NMR spectrum is consistent with the data for this complex that has been previously reported in the literature ($\delta_{\text{P}} = +0.1$ ppm, s, $^1J_{\text{PPt}} = 3600$ Hz).²⁶ The formation of compound **16** is speculated as, by $^{31}\text{P}\{^1\text{H}\}$ NMR spectroscopic analysis, a broad ($\nu_{1/2} = 42$ Hz) singlet resonance at $\delta_{\text{P}} = +73.8$ ppm (with satellites $^1J_{\text{PPt}} = 3868$ Hz) is observed. This chemical shift is consistent with that of the structurally analogous complex, $cis\text{-[PtCl}_2\text{(PPh}_2\text{Cl)}]$ ($\delta_{\text{P}} = +73.2$ ppm, s, $^1J_{\text{PPt}} = 3780$ Hz).²⁷ At this time, the proposed formation of compound **16** from the reaction between **12** and $trans\text{-[Pt(PPh}_2\text{Me)Cl}(\mu\text{-Cl})_2]$ is not corroborated by full multi-nuclear NMR spectroscopic data (see above), however, its formation, alongside the previously reported complex $cis\text{-[PtCl}_2\text{(PPh}_2\text{Me)}_2]$, is consistent with the products observed by Dillon and co-workers for reactions between $\text{R}'_2\text{PCl}$ species and $trans\text{-[Pt(PR}_3\text{)Cl}(\mu\text{-Cl})_2]$ complexes (Scheme 19).^{26,27}



Scheme 19 – General reaction between $trans\text{-[Pt(PR}_3\text{)Cl}(\mu\text{-Cl})_2]$ and $\text{R}'_2\text{PCl}$ compounds seen by Dillon and co-workers.^{26,27}

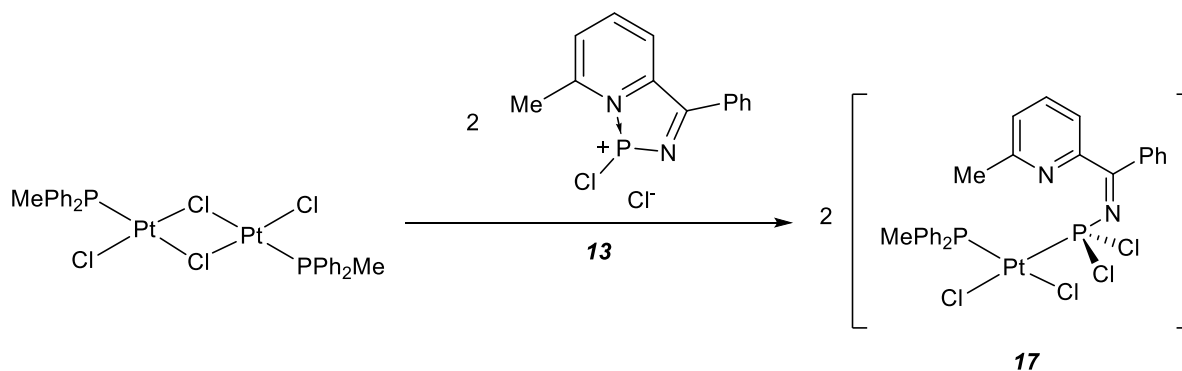
If compounds **16** and *cis*-[PtCl₂(PPh₂Me)₂] are the products of the reaction between compound **12** and *trans*-[Pt(PPh₂Me)Cl(μ-Cl)]₂, they are likely to result from a ligand scrambling process analogous to that shown in Scheme 19 (which has been previously observed by Dillon and co-workers for analogous reactions between R'₂PCl and *trans*-[Pt(PR₃)Cl(μ-Cl)]₂ species).^{26,27} Such ligand scrambling processes have been previously reported by Puddephatt and Thompson^{28,29} for pairs of platinum complexes, like those shown in Scheme 20, and is likely to proceed by an associative pathway (*via* a five-coordinate intermediate) giving rise to the more thermodynamically stable *cis*-isomers.³⁰ The cleavage of dimeric *trans*-[Pt(PPh₂Me)Cl(μ-Cl)]₂ by its reaction with compound **12** is postulated to give rise to the thermodynamically favourable *cis* isomers of both [PtCl₂(**12**)] (compound **16**) and *cis*-[PtCl₂(PPh₂Me)₂].



Scheme 20 – Ligand scrambling observed by Puddephatt and Thompson.^{28,29}

The reaction of *trans*-[Pt(PPh₂Me)Cl(μ-Cl)]₂ and compound **13** (which can be regarded as a dichlorophosphine) led to the cleavage of the platinum dimer and full consumption of the starting materials to give a single reaction product by ³¹P{¹H} NMR spectroscopic analysis ($\delta_P = +57.0$ (d, ²J_{PP} = 645 Hz, with satellites ¹J_{PtP} = 3053 Hz), +4.7 (d, ²J_{PP} = 645 Hz, with satellites ¹J_{PtP} = 2948 Hz)). These solution state ³¹P{¹H} NMR spectroscopic data are suggestive of the formation of a square planar platinum complex possessing two inequivalent phosphine ligands coordinated *cis* to one another (as indicated by the magnitude of the ¹J_{PtP} coupling constants). The formation of complex **17** (Scheme 21) from the reaction between **13** and *trans*-[Pt(PPh₂Me)Cl(μ-Cl)]₂ is proposed. The formation of complex **17** from the reaction between **13** and *trans*-[Pt(PPh₂Me)Cl(μ-Cl)]₂ is consistent with ¹³C{¹H} NMR spectroscopic

data which show the CCH₃ and CH₃ carbon centres as singlet resonances at $\delta_c = 144.0$ and 22.8 ppm, respectively, indicating the disruption of the N \rightarrow P⁺ interaction in the starting phosphenium salt, **13**. Mass spectrometric analysis (by ESI) of compound **17** gave rise to fragments consistent with the two phosphine ligands, at $m/z = 335.1$ ([C₁₃H₁₁ClN₂PK]⁺) and 201.1 ([Ph₂MePH]⁺).

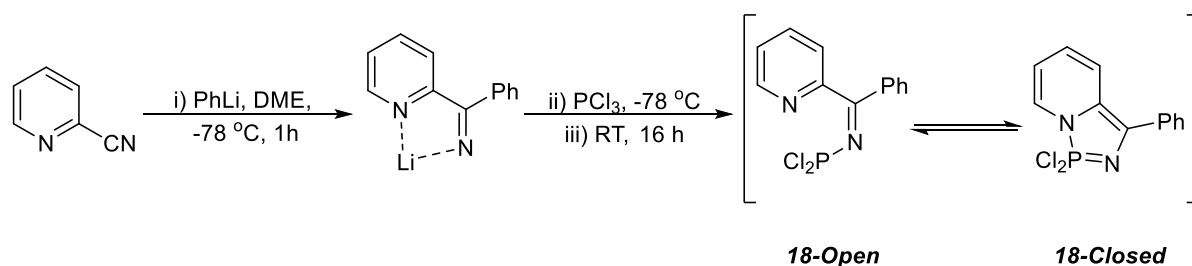


Scheme 21 – Proposed reaction between **13** and *trans*-[Pt(PPh₂Me)Cl(μ-Cl)]₂.

3.5 – Attempted Preparation of Dichlorophosphino-1-((phenyl(pyridin-2-yl)methylene)amino) amine (**18-Open**) / (**18-Closed**)

The unprecedented formation of compounds **12** and **13** from the reaction between 6-methyl-2-cyanopyridine, phenyllithium and PCl₃ led to the question of how the reaction between 2-cyanopyridine, phenyllithium and PCl₃ would proceed. The synthetic procedure outlined in Scheme 22 was used to explore this reaction, and to investigate whether or not compound **18-Open** and/or **18-Closed** would be generated as product(s). Upon addition of PCl₃ to quench the intermediate lithium species, the immediate formation of a pale green precipitate in a dark orange solution was observed. Solution state ³¹P{¹H} NMR spectroscopic analysis of the liquid portion of the reaction mixture, after 16 hours at room temperature, revealed only unreacted PCl₃. The pale green precipitate was isolated from the reaction mixture by filtration and dried under reduced pressure. All attempts to dissolve the precipitate (in, for example, hexane, pentane, Et₂O, THF, toluene, chloroform and DCM) were unsuccessful, therefore the solid was analysed by solid state ³¹P{¹H} NMR spectroscopy.^{††}

^{††} Solid-state NMR spectra recorded by Dr D. Apperley and Mr F. Markwell of the EPSRC National Solid-State NMR Research Service at Durham University.



Scheme 22 – Attempted preparation of target compounds **18-Open**/**18-Closed**.

Solid state $^{31}\text{P}\{^1\text{H}\}$ NMR spectroscopic analysis of the precipitate isolated from the reaction mixture after 16 hours showed the presence of only one phosphorus-containing species, giving rise to a sharp resonance at $\delta_{\text{P}} = -120.4$ ppm. This resonance observed by solid state $^{31}\text{P}\{^1\text{H}\}$ NMR spectroscopic analysis of the precipitate isolated from the reaction mixture lies in the region characteristic of primary phosphines and PR_5 compounds,³¹ it is, however, not consistent with either the solution or solid state $^{31}\text{P}\{^1\text{H}\}$ NMR signals seen previously for either “open” pyridyl-*N*-phosphinoimines ($\delta_{\text{P}} \sim +70$ ppm) or “closed” diazaphosphazoles ($\delta_{\text{P}} \sim +40$ ppm), nor with those for compounds **12** and **13**. The bulk reaction product was found to be unreactive towards inorganic salts ($[(i\text{Pr}_2\text{N})_2\text{P}][\text{AlCl}_4]$, NaBPh_4 , $\text{KB}(\text{C}_6\text{F}_5)_4$, AgPF_6 and NaPF_6) and elemental selenium. The ^{31}P NMR shifts for several different potential reaction products were predicted computationally (at the B3LYP/6-31G** level of theory)^{††} and are shown in Figure 18 – none of these chemical shifts are comparable to the resonance observed by solid state $^{31}\text{P}\{^1\text{H}\}$ NMR spectroscopy at $\delta_{\text{P}} = -120.4$ ppm for the product of the reaction between 2-cyanopyridine, PhLi and PCl_3 . To date there has been no success at elucidating the structural identity of the reaction product.

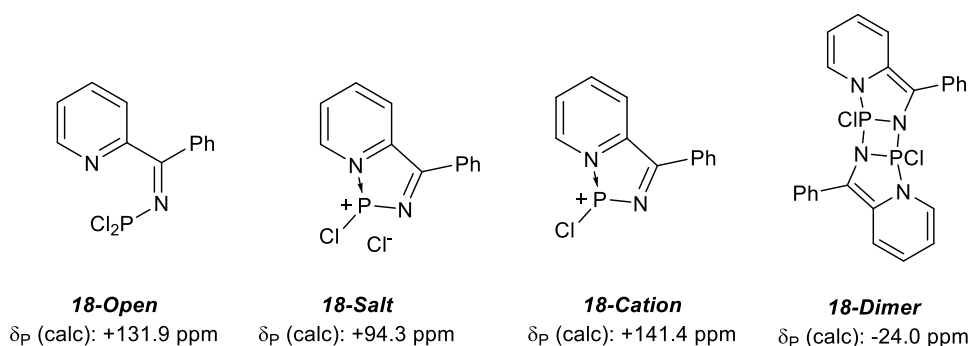


Figure 18 – Computationally predicted ^{31}P NMR shifts.

^{††} Computational studies carried out by Dr Mark A. Fox, Durham University.

3.6 – Probing the Product(s) of the Reactions Between 2-Cyanopyridine/6-Methyl-2-Cyanopyridine, PhLi and PCl₅

To further extend the chemistry described thus far in this chapter, and to try and gain insight into the structural identity of the product of the reaction between 2-cyanopyridine, PhLi and PCl₃ (section 3.5), the reactions between 6-methyl-2-cyanopyridine/2-cyanopyridine, PhLi and PCl₅ were explored. The reactions between 6-methyl-2-cyanopyridine (reaction a)/2-cyanopyridine (reaction b), PhLi and PCl₅ were first studied computationally (at the B3LYP/6-31G** level of theory),^{§§} and the lowest energy products revealed are shown in Figure 19 (**19-Open**, **19-SO**, **20-Open** and **20-SO**). Dizaphosphazole “closed” species (analogous to e.g. **A-Closed**) could not be identified on the PE surface. For reversible conversion between **19-Open/20-Open** and their respective “closed” tautomers, there would be the requirement for reversible dissociation of a chloro substituent from the phosphorus centre, something that is unlikely to occur in the absence of any species to “trap” the chloride anion.

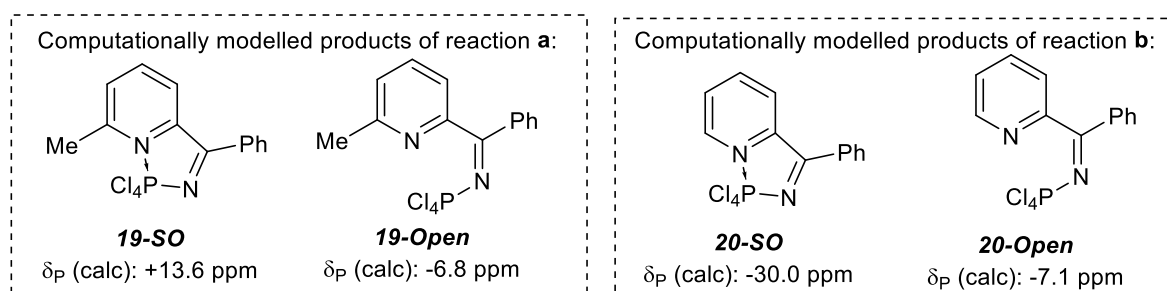


Figure 19 – Computationally modelled possible products of reactions a and b.

For both reactions **a** and **b**, computational studies revealed an “open” pyridyl-*N*-phosphinoimine form, **19-Open** and **20-Open**. **19-Open** and **20-Open** are comparable to the other “open” compounds previously observed experimentally, such as **A-Open**, **I-Open**, **6-Open** and **8-Open**. The second computed product for reactions **a** and **b**, **18-SO** and **19-SO**, are intramolecularly stabilised “open” species with a λ^6 -phosphorus centre. Neutral, hexacoordinate compounds **18-SO** and **19-SO**, where the electrophilic phosphorus(V) centre makes four covalent bonds (four P-Cl bonds, one P-N(imine)) and is stabilised by a dative interaction with the pyridine nitrogen (N(pyridine) \rightarrow P), are comparable to the neutral species

^{§§} Computational studies carried out by Dr Mark A. Fox, Durham University.

reported by Cavell and co-workers³² shown in Figure 20. Cavell and co-workers were able to isolate and characterise a series of neutral $X_4P[(N)-(E)]$ species (including those shown in Figure 20) where $X = Cl, F$ and CF_3 and $[(N)-(E)]$ is a chelating ligand with $E = N, O$ and S .³² The hexacoordinate geometry of the species reported by Cavell is attributed to the electrophilic nature of the X substituents and the presence of a chelating ligand, both of which compounds **19-SO** and **20-SO** possess. The predicted ^{31}P NMR spectroscopic chemical shifts (at the B3LYP/6-31G** level of theory)^{***} of the computationally modelled compounds **19-Open**, **20-Open**, **19-SO** and **20-SO** are shown in Figure 19.

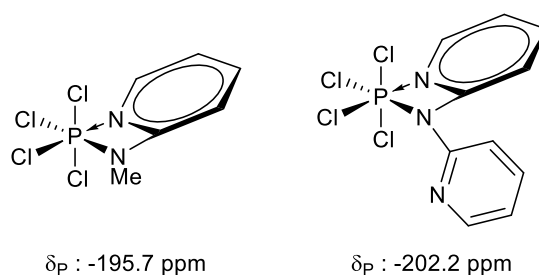


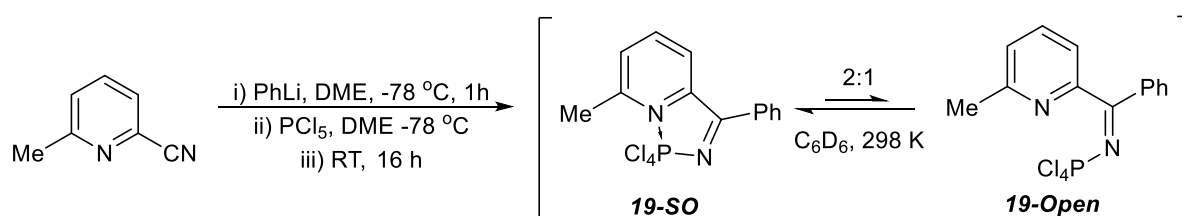
Figure 20 – Neutral hexacoordinate phosphorus species reported by Cavell and co-workers.³²

With these computational observations in hand, the reactions of 6-methyl-2-cyanopyridine (reaction **a**)/2-cyanopyridine (reaction **b**) with PhLi and PCl_5 were carried out. After 16 hours at room temperature, a pale brown precipitate in a dark solution was observed for both reactions **a** and **b**. The solid and liquid components of the reaction mixtures were separated by filtration and volatile species removed under reduced pressure. The dried solid component of each reaction mixture was analysed by solid state $^{31}P\{^1H\}$ NMR spectroscopic analysis and, for both reactions, found to comprise of only one phosphorus-containing species, unreacted PCl_5 .^{†††} The residue from the liquid portion of reactions **a** and **b** was washed with THF, the volatile species removed and the resulting residue analysed by solution state $^{31}P\{^1H\}$ spectroscopy. This solution state $^{31}P\{^1H\}$ NMR spectroscopic analysis of the dark brown residue obtained by THF extraction from the residue of the reaction between 6-methyl-2-cyanopyridine, PhLi and PCl_5 (reaction **a**, Scheme 23) revealed multiple phosphorus-containing species. The two major resonances were seen in the solution state $^{31}P\{^1H\}$ NMR spectrum at $\delta_P = +8.3 \text{ ppm}$ and -2.7 ppm , in a 2:1 ratio (which account for 70 % of the

^{***} Computational studies carried out by Dr Mark A. Fox, Durham University.

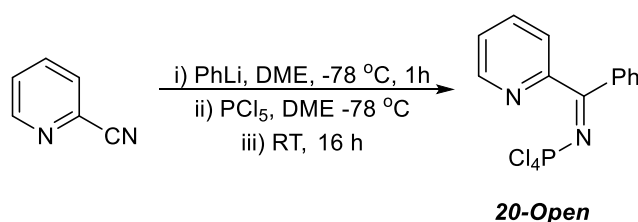
^{†††} Solid-state NMR spectra recorded by Dr D. Apperley and Mr F. Markwell of the EPSRC National Solid-State NMR Research Service at Durham University.

phosphorus-containing species), which lie within the same range as for the computationally predicted chemical shifts for **19-SO** and **19-Open**, respectively (Figure 19), suggesting that both these species may have formed. Attempts to purify the product from reaction **a**, and to isolate individual species, by recrystallization from THF, for full spectroscopic analysis were unsuccessful. If compounds **19-SO** and **19-Open** have indeed formed from the reaction between 6-methyl-2-cyanopyridine, PhLi and PCl_5 , these species are likely to exist in a dynamic equilibrium with each other, with **19-SO** being favoured at 298 K due to the stabilisation of the electrophilic phosphorus centre by the donation of the pyridine nitrogen lone pair in the $\text{N}(\text{pyridine}) \rightarrow \text{P}$ interaction.



Scheme 23 – Proposed productions of reaction b.

The solution state $^{31}\text{P}\{^1\text{H}\}$ NMR spectroscopic analysis of the dark brown residue isolated by THF extraction from the reaction between 2-cyanopyridine, PhLi and PCl_5 (reaction **b**, Scheme 24) revealed one major phosphorus-containing species (which accounts 86 % of the total phosphorus-containing species observed by solution state $^{31}\text{P}\{^1\text{H}\}$ NMR spectroscopic analysis) presenting a singlet resonance at $\delta_{\text{P}} = -4.4$ ppm. This $^{31}\text{P}\{^1\text{H}\}$ NMR spectroscopic resonance at $\delta_{\text{P}} = -4.4$ ppm is in reasonable agreement with the chemical shift predicted for compound **20-Open**. The ^1H and $^{13}\text{C}\{^1\text{H}\}$ NMR spectroscopic data collected are in agreement with the product of reaction **b** being **20-Open** (Scheme 24), notably no coupling between the CH carbon atom ($\delta_{\text{C}} = 151.0$ ppm, s) *ortho* to the pyridine nitrogen centre and the phosphorus centre is observed.



Scheme 24 – Reaction a.

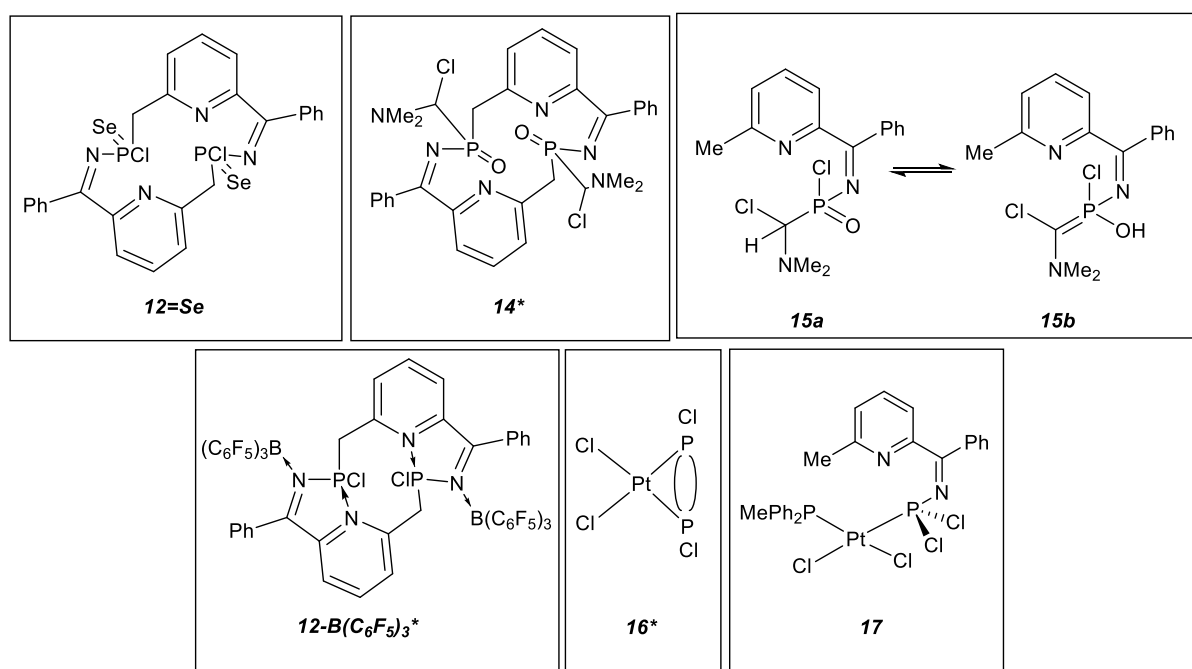
The formation of a λ^6 -phosphorus species vs the formation of a λ^5 -phosphorus compound is intimately linked to the Lewis acidic character of the phosphorus centre itself, whereby the formation of the hexacoordinate phosphorus is more likely to occur the more electrophilic a phosphorus centre is.³² The electronic nature of the phosphorus(V) centres in **19-Open** and **20-Open** (Scheme 23 and Scheme 24) are very similar, yet compound **19-Open** is postulated to form its hexacoordinate analogue, **19-SO**, whereas the λ^5 -P species **20-Open** is not seen to form the λ^6 -P compound, **20-SO**. The inability to isolate proposed compounds **19-Open** and **19-SO**, in order to unambiguously assign their structure and probe their proposed interconversion, means that no explanation for the apparent inability of **20-Open** to form **20-SO** can be given at this time.

3.7 – Summary

Whilst attempting to prepare dichlorophosphino-1-((phenyl(6-methyl-pyridin-2-yl)methylene)amino) amine from 6-methyl-2-cyanopyridine, PhLi and PCl₃, two unprecedented species were observed, compounds **12** and **13** (in a 1:4 ratio), which were identified using a combination of experimental and computational spectroscopic techniques. The structure of macrocyclic compound **12** was identified by an X-ray crystallographic study. The structural identity of compound **13**, an intramolecularly base-stabilised phosphenium salt, was determined by experimental and computational ³¹P NMR spectroscopic studies. Compound **13** is proposed to form after the quenching of the intermediate lithium species generated from the reaction between 6-methyl-2-cyanopyridine and PhLi, with PCl₃ via the irreversible dissociation of a labile chloride from transiently-generated **11-Open**. Upon formation of **13**, two equivalents of the phosphenium salt are proposed to undergo two sequential C-H insertion reactions (akin to reactions previously reported for phosphenium cations and their isolobal analogues, carbene) to yield compound **12**.

The reactivity of compounds **12** and **13** was probed in order to investigate the chemistry of their various functionalities and to gain further structural information of compound **13**. The lability of the chloro substituents in compound **12** and **13** was investigated. Attempts to exchange the chloro substituents with other anions, by the reactions of **12** and **13** with

NaBPh₄, KB(C₆F₅)₄, XPF₆ (X = Ag, Na) and [(*i*Pr₂N)₂P][AlCl₄], proved unsuccessful, indicating that the covalent P-Cl interactions in **12** and **13** are too strong to be disrupted. It is unclear whether the proposed R₂P⁺Cl⁻ interaction in **13** was interrupted, if the unbound chloride anion in **13** is indeed a discreet anion, anion exchange would not lead to notable changes in chemical shift for either component of the ion pair.



* The structural identity of this species has not been unambiguously determined.

Figure 21 - Proposed products of the reactions of **12/13** with Se, DMF, B(C₆F₅)₃ and *trans*-[Pt(PPh₂Me)Cl(μ-Cl)]₂.

The ease of oxidation of the formally P^{III} centres in **12** and **13** by elemental selenium and DMF was examined. Macrocyclic compound **12** was found to react with two equivalents of elemental selenium to form the bis-selenide (**12=Se**, Figure 21), suggesting that the N(pyridine)→P dative interaction in **12** is readily disrupted to allow for a reaction at the phosphorus centre. Compound **13**, however, was not able to be oxidised by selenium, this has been attributed to the strength of intramolecular the N(pyridine)→P⁺ dative interaction being too great to overcome – this interaction must be broken in order to unblock the phosphorus lone pair and therefore allow for a reaction to occur at the P^{III} centre in **13**. Both compounds **12** and **13**, however, are proposed to have undergone a reaction with an excess of DMF to give R₃P=O species (**14** (the structural identity of this species has not been unambiguously assigned) and **15a/15b**, respectively, Figure 21). The differing reactivity of compound **13**

towards DMF and Se is attributed to the high-energy requirement for the disruption of the N(pyridine)→P⁺ interaction in compound **13** to allow for oxidation of the P^{III} centre.

The coordination behaviour of compounds **12** and **13** towards Lewis acidic B(C₆F₅)₃ (hard) and Pt^{II} complexes (soft) was explored. Macrocyclic compound **12** is proposed to coordinate to the Lewis acidic boron *via* the imine nitrogen centre (**12**-B(C₆F₅)₃, Figure 21). No reaction between compound **13** and B(C₆F₅)₃ was observed. The proposed unbound chloride anion in compound **13** is thought to sterically preclude the approach, and subsequent coordination, of B(C₆F₅)₃ to the imine nitrogen centre. The N(pyridine)→⁺PR₂ interaction in **13** is too strong to overcome and allow for coordination of B(C₆F₅)₃ at the pyridine nitrogen centre. Surprisingly, no reaction between B(C₆F₅)₃ and the unbound chloride in **13** is seen, suggesting that the anion is strongly associated with the phosphenium centre. Compounds **12** and **13** were found to behave in the same manner as the R₂PCl and R'PCl₂ species reported by Dillon and co-workers,^{26,27} respectively, in the presence of *trans*-[Pt(PPh₂Me)Cl(μ-Cl)]₂. Compound **12**, which can be regarded as an R₂PCl compound, is proposed to cleave the dimeric platinum complex to yield two platinum containing species: compound **16**, *cis*-[PtCl₂(**12**)] (where **12** behaves as a κ²-*P,P* ligand, Figure 21, the structural identity of this species has not been unambiguously assigned) and *cis*-[PtCl₂(PPh₂Me)₂]. Compound **13** was found also to cleave the platinum dimer, *trans*-[Pt(PPh₂Me)Cl(μ-Cl)]₂, and gave two equivalents of compound **17**, *cis*-[PtCl₂(PPh₂Me)(**13**)], where **13** behaves as a κ¹-*P* ligand (Figure 21). Whilst compounds **12** and **13** readily cleave *trans*-[Pt(PPh₂Me)Cl(μ-Cl)]₂, no reaction is observed between **12/13** and [PtCl₂(PPh₃)₂], as the platinum centre in the latter, in contrast to *trans*-[Pt(PPh₂Me)Cl(μ-Cl)]₂, does not possess any labile sites

The reaction between 2-cyanopyridine, PhLi and PCl₃ was carried out to explore the nature of the reaction product(s). The bulk reaction product was isolated as an insoluble, pale green solid. Solid state ³¹P{¹H} NMR spectroscopic analysis revealed a single phosphorus-containing species, presenting a signal at -120.4 ppm. Computational studies were carried out to model the lowest energy products of the reaction, and to predict their respective ³¹P NMR shifts. However, no species identified computationally were consistent with the chemical shift

observed by solid state $^{31}\text{P}\{^1\text{H}\}$ NMR spectroscopic analysis. Structural elucidation of the reaction product has not been achieved to date.

The reactions of 6-methyl-2-cyanopyridine (reaction **a**) and 2-cyanopyridine (reaction **b**) with PhLi and PCl_5 were carried out, and have been proposed to generate the “*open*” pyridyl-*N*-phosphinoimine species, **19-Open** and **20-Open**, respectively. Reaction **a** is proposed to have also formed a second product, compound **19-SO**, a neutral, hexacoordinate phosphorus species with a dative $\text{N}\rightarrow\text{P}$ interaction between the pyridine nitrogen lone pair and the electrophilic phosphorus centre.

3.8 – Chapter 3 Experimental Details

Standard preparative methods were used throughout, see **Appendix 1** for general experimental considerations.

3.8.1 – Synthesis of Novel Macrocyclic Compound **12** and Novel Phosphenium Salt **13**

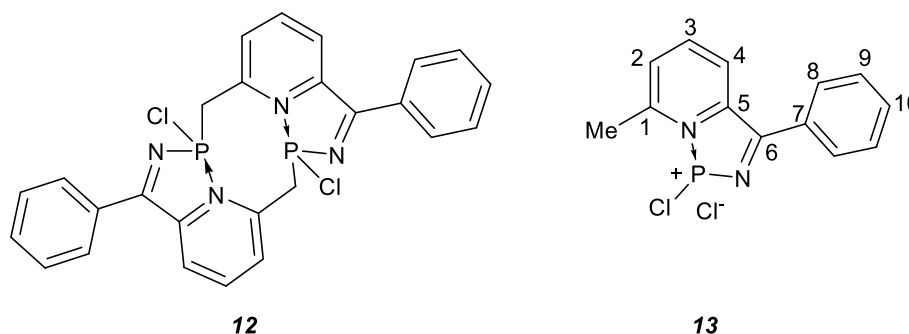


Figure 22 – Compounds **12** and **13** showing NMR spectroscopic assignment numbering scheme for **13**.

A solution of phenyllithium (2.4 ml, 1.8 M, 4.23 mmol) was added dropwise to a stirred solution of 6-methyl-2-cyanopyridine (0.500 g, 4.23 mmol) in DME (25 ml) at $-78\text{ }^{\circ}\text{C}$, and the mixture then stirred for 1 hour at $-78\text{ }^{\circ}\text{C}$. A solution of PCl_3 (0.4 ml, 4.23 mmol) in DME (35 ml) was subsequently added and the reaction mixture then allowed to attain room temperature. On warming to room temperature, a yellow precipitate in a red/orange solution began to form. The mixture was stirred for 16 hours at room temperature. The yellow precipitate was isolated by filtration and dried *in vacuo* and was found to comprise a mixture of compounds **12** and **13** in a 1:4 ratio (0.503 g) by solid state $^{31}\text{P}\{^1\text{H}\}$ NMR spectroscopic analysis. Orange crystals of **12** (yield of crystals = 0.100 g, 6 %) suitable for an X-ray crystallographic study were obtained from the liquid component of the reaction mixture after it was left to stand at room temperature for two months. Compound **13** was isolated from the bulk reaction product by extraction with several portions of DCM (5 x 15 ml), the volatile species were removed from the washings under reduced pressure to give compound **13** as a dark orange solid.

$^{31}\text{P}\{^1\text{H}\}$ CP MAS NMR (162.0 MHz): δ (ppm) = +98.1 (**12**), +75.4 (**13**).

12 Data: Anal. Found C, 58.24 %; H, 4.44 %; N, 7.09 %. Calc. C, 59.90 %; H, 3.87 %; N 10.75 %.

MS (ASAP) m/z : 521.3 (M^+). Solid state ^1H and $^{13}\text{C}\{^1\text{H}\}$ NMR spectroscopic analysis gave rise to

spectra that could not be interpreted due to the broad nature of the resonances that arises as a result of chemical shift anisotropy. The insolubility of compound **12** prevented the collection of solution state NMR spectroscopic data.

13 Data: $^{31}\text{P}\{^1\text{H}\}$ NMR (283.3 MHz, CD_2Cl_2): δ (ppm) = +78.6 (s, **13**). ^1H NMR (699.7 MHz, CD_2Cl_2): δ (ppm) = 8.39 (1H, dt, $^3J_{\text{HH}} = 7.8$ Hz, $^5J_{\text{HH}} = 1.8$ Hz, CH^3), 8.12 (1H, ddd, $^3J_{\text{HH}} = 7.8$ Hz, $J_{\text{HH}} = 1.0$ Hz, $J_{\text{HH}} = 0.6$ Hz, CH^4), 7.90 (1H, ddt, $^3J_{\text{HH}} = 7.7$ Hz, $J_{\text{HH}} = 1.1$ Hz, $J_{\text{HH}} = 0.6$ Hz, CH^2), 7.86-7.81 (2H, m, CH^8), 7.68-7.62 (1H, m, CH^{10}), 7.62-7.57 (2H, m, CH^9), 3.15 (3H, dd, $J_{\text{HH}} = 1.2$ Hz, $J_{\text{HH}} = 0.7$ Hz, CH_3). $^{13}\text{C}\{^1\text{H}\}$ NMR (176.0 MHz, CD_2Cl_2): δ (ppm) = 168.7 (d, $^2J_{\text{CP}} = 1.3$ Hz, C^6), 156.5 (d, $^2J_{\text{CP}} = 2.5$ Hz, C^1), 144.0 (d, $^2J_{\text{CP}} = 6.2$ Hz, C^5), 143.0 (d, $^4J_{\text{CP}} = 3.0$ Hz, C^3), 133.7 (d, $^3J_{\text{CP}} = 5.7$ Hz, C^7), 132.2, (s, C^{10}), 129.1 (s, C^9), 128.9 (d, $^4J_{\text{CP}} = 4.5$ Hz, C^8), 128.4 (d, $^3J_{\text{CP}} = 3.5$ Hz, C^2), 123.2 (d, $^3J_{\text{CP}} = 4.7$ Hz, C^4), 21.0 (d, $^3J_{\text{CP}} = 3.7$ Hz, CH_3). Mass spectrometric analysis of compound **13** as a solid (at various temperatures by ASAP) was found to be unsuitable due to the high energy required to vaporise the salt, analysis by ESI (as a DCM solution) was also unsuitable as the charged species gave rise to a complex fragmentation pattern that could not be interpreted.

3.8.2 – Attempted Anion Exchange Reactions of Compounds **12** and **13**

The following general procedure was used in an attempt to carry out anion exchange reactions with compounds **12** and **13**. To a solution of **12** (20 mg, 0.038 mmol) / **13** (20 mg, 0.067 mmol) in DCM (1 ml) in a Young's NMR tube was added a salt (2 equivalents for reactions with **12** / 1 equivalent for reactions with **13**, see Table 4 for masses). The reaction mixtures were heated at 50 °C and monitored by solution state $^{31}\text{P}\{^1\text{H}\}$ NMR spectroscopic analysis. For each reaction, no change to the starting material was observed by solution state $^{31}\text{P}\{^1\text{H}\}$ NMR spectroscopic analysis.

	Salt				
	NaBPh ₄	KB(C ₆ F ₅) ₄	AgPF ₆	NaPF ₆	(iPr ₂ N) ₂ PAICl ₄
Mass (g) of salt used in reaction with 11	0.026	0.055	0.019	0.013	0.031
Mass (g) of salt used in reaction 12	0.023	0.048	0.017	0.011	0.027

Table 4 – Masses of salts used in the attempted anion exchange reactions with **12** and **13**.

3.8.3 – Synthesis of the Diselenide Derivative of Compound **12**, **12=Se**

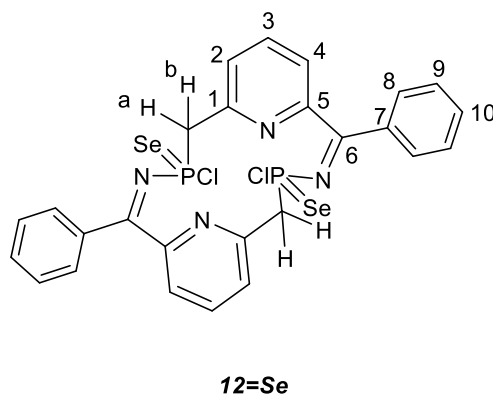


Figure 23 – Compound **12=Se** showing NMR spectroscopic assignment numbering scheme.

To a Young's NMR tube, compound **12** (0.040 g, 0.077 mmol), elemental selenium (0.018 g, 0.230 mmol) and CDCl_3 (0.8 ml) was added. The mixture was heated at 60 °C for 24 hours, after which time no further change to the reaction mixture was observed by solution state $^{31}\text{P}\{^1\text{H}\}$ NMR spectroscopic. **12=Se** was not isolated from the reaction mixture, and was subsequently analysed *in situ*. MS (ESI) m/z : 341.0 ($[\text{C}_{13}\text{H}_{11}\text{N}_2\text{PClSe}]^+$).

$^{31}\text{P}\{^1\text{H}\}$ NMR (283.3 MHz, CDCl_3): δ (ppm) = + 60.8 (s, with satellites $^1J_{\text{PSe}} = 872$ Hz, **12=Se**). ^1H NMR (699.7 MHz, CDCl_3): δ (ppm) = 7.87 (2H, *pseudo t*, $J_{\text{HH}} = 7.8$ Hz, CH^3), 7.80-7.86 (4H, m, CH^8), 7.64-7.59 (2H, m, CH^2), 7.58-7.52 (4H, m, CH^9), 7.50-7.45 (2H, m, CH^{10}), 7.36 (2H, d, $^3J_{\text{HH}} = 7.1$ Hz, CH^4), 6.12 (2H, d, $^2J_{\text{HH}} = 13.6$ Hz, CH^a/CH^b), 6.09 (2H, d, $^2J_{\text{HH}} = 13.6$ Hz, CH^a/CH^b). $^{13}\text{C}\{^1\text{H}\}$ NMR (176.0 MHz, CDCl_3): δ (ppm) = 181.8 (d, $^2J_{\text{CP}} = 14.3$ Hz, C^6), 169.0 (s, C^7), 154.6 (d, $^2J_{\text{CP}} = 9.8$ Hz, C^1), 152.9 (d, $^3J_{\text{CP}} = 24.4$ Hz, C^5), 138.9 (s, C^3), 131.1 (d, $^3J_{\text{CP}} = 7.2$ Hz, C^2), 129.0 (s, C^8), 128.2 (s, C^4), 53.5 (d, $^1J_{\text{CP}} = 77.5$ Hz, CH_2).

3.8.4 – Attempted Synthesis of the Mono-Selenide Derivative of Compound **13**

To a Young's NMR tube, compound **13** (0.040 g, 0.135 mmol), elemental selenium (0.021 g, 0.270 mmol) and CDCl_3 (0.8 ml) was added and the mixture heated at 60 °C. After 5 days heating at 60 °C, solution state $^{31}\text{P}\{^1\text{H}\}$ NMR spectroscopic analysis showed no change to the reaction mixture. This reaction was discontinued.

3.8.5 – Synthesis of the Proposed Product, **14**, from the Reaction of **12** with DMF

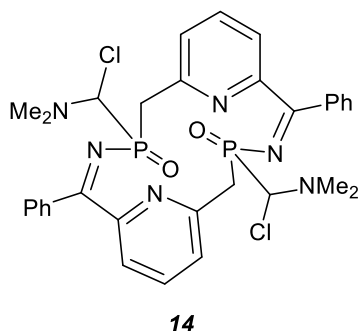
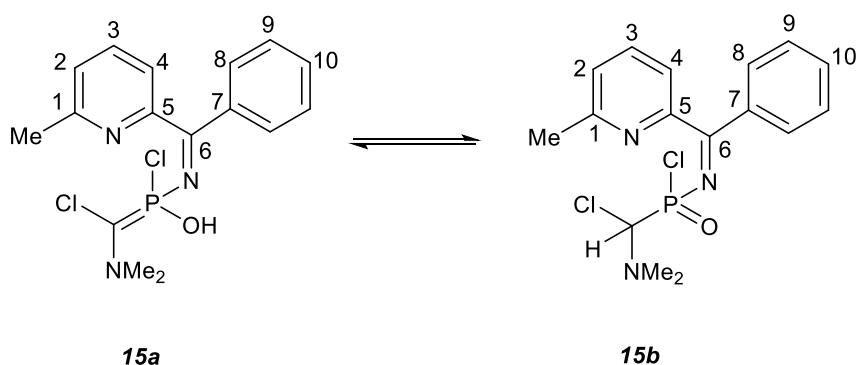


Figure 24 – Proposed compound **14**.

To compound **12** (0.040 g, 0.077 mmol) in a Young's NMR tube, DMF (1 ml) was added and the reaction left to stand at room temperature for three days, when no further change to the reaction mixture was observed by solution state $^{31}\text{P}\{^1\text{H}\}$ NMR spectroscopic analysis. Attempts to fully remove excess DMF from the reaction product were unsuccessful, hindering full spectroscopic characterisation by NMR and mass spectrometry (ESI was attempted but was unsuccessful, this has been attributed to the viscosity of the residual DMF). The structural identity of compound **14** has not been determined unambiguously.

$^{31}\text{P}\{^1\text{H}\}$ NMR (162.0 MHz, C_6D_6): δ (ppm) = +25.7 (s, **14**).

3.8.6 – Synthesis of the Oxidation Products, **15a** and **15b**, from the Reaction Between **13** and DMF



Scheme 25 – Compounds **15a** and **15b** showing NMR spectroscopic assignment numbering scheme.

To compound **13** (0.040 g, 0.013 mmol) in a Young's NMR tube, DMF (1 ml) was added and the reaction left to stand at room temperature for 3 days, after which time full consumption of the starting material was observed by solution state $^{31}\text{P}\{^1\text{H}\}$ NMR spectroscopic analysis.

Excess DMF was removed from the reaction mixture under reduced pressure, followed by the addition of CDCl₃ (0.8 ml) to the residue and multi-nuclear NMR spectroscopic analysis undertaken. MS (ESI) *m/z*: 300.1 ([C₁₃H₁₁ClN₂OPNa]⁺).

³¹P{¹H} NMR (283.3 MHz, CDCl₃): δ (ppm) = -25.4 (broad s, *v*_{1/2} = 121 Hz, **15a/15b**). ¹H NMR (699.7 MHz, CDCl₃): δ (ppm) = 7.92 (1H, broad s, *v*_{1/2} = 6 Hz, CHClNMe₂), 7.86 (2H, d, ³*J*_{HH} = 7.7 Hz, CH⁸), 7.56 (1H, d, ³*J*_{HH} = 9.4 Hz, CH²), 7.41 (2H, *pseudo t*, ³*J*_{HH} = 7.7 Hz, CH⁹), 7.29 (1H, s, CH¹⁰), 6.84 (1H, s, CH³), 6.54 (1H, s, CH⁴), 3.07 (6H, s, N(CH₃)₂), 2.78 (3H, s, CH₃). ¹³C{¹H} NMR (176.0 MHz, CDCl₃): δ (ppm) = 162.4 (s, PC), 141.2 (s, C⁶), 134.1 (s, C¹), 129.1 (s, C⁹), 128.9 (s, C¹⁰), 128.7 (s, C⁷), 128.2 (s, C⁸), 124.7 (s, C⁵), 123.5 (s, C³), 118.0 (s, C⁴), 116.7 (s, C²), 44.8 (s, N(CH₃)₂), 19.4 (s, CH₃).

3.8.7 – Synthesis of the Proposed Adduct from the reaction between B(C₆F₅)₃ and Compound **12**, **12-B(C₆F₅)₃**

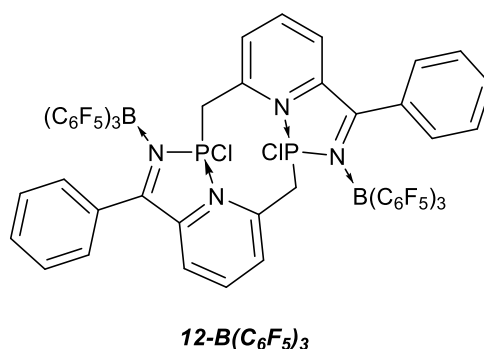


Figure 25 – Proposed compound **12-B(C₆F₅)₃**.

To a Young's NMR tube charged with **12** (0.020 g, 0.038 mmol), B(C₆F₅)₃ (1.000 g, 3.9% in isopar-E, 0.077 mmol) was added. The mixture was heated at 60 °C for 2 days, after which time full conversion of starting material was observed by ³¹P NMR spectroscopic analysis. The volatile species were removed under reduced pressure at 60 °C. Mass spectrometric analysis (by ASAP at various temperatures, and by ESI) of the reaction product proved uninformative, likely as the result of its low volatility. The full removal of isopar-E was not successful, even after 3 days under reduced pressure at 60 °C. ¹H and ¹³C{¹H} NMR spectroscopic analysis revealed residual isopar-E in far greater quantities than the product meaning that these spectra could not be assigned for the product species. The structural identity of compound **12-B(C₆F₅)₃** has not been determined unambiguously.

$^{31}\text{P}\{^1\text{H}\}$ NMR (242.7 MHz, C_6D_6): δ (ppm) = +41.9 (s, **12-B(C₆F₅)₃**). ^{11}B NMR (128.4 MHz, C_6D_6): δ (ppm) = -8.6 (s). ^{19}F NMR (376.4 MHz, C_6D_6): δ (ppm) = -163.8 (*pseudo* t, $^3J_{\text{FF}} = 21$ Hz, *m*-F), -156.3 (t, $^3J_{\text{FF}} = 21$ Hz, *p*-F), -133.1 (d, $^3J_{\text{FF}} = 26$ Hz, *o*-F).

3.8.8 – Attempted Reaction between Compound 13 and B(C₆F₅)₃

To a Young's NMR tube charged with **13** (0.020 g, 0.067 mmol), B(C₆F₅)₃ (0.884 g, 3.9% in isopar-E, 0.067 mmol) was added and the mixture was heated at 60 °C. After heating the reaction at 60 °C for 7 days, solution state $^{31}\text{P}\{^1\text{H}\}$ NMR spectroscopic analysis showed no change to the starting materials. This reaction was discontinued.

3.8.9 – Attempted Coordination of Compounds 12 and 13 to *cis*-[PtCl₂(PPh₃)₂]

The same general procedure was used for the attempted reactions of both compounds **12** and **13** with *cis*-[PtCl₂(PPh₃)₂]. To a Young's NMR tube charged with compound **12/13** in CDCl₃ (1 ml) was added *cis*-[PtCl₂(PPh₃)₂] – see Table 5 for quantities used. All reactions were heated at 60 °C. After heating the reactions for 5 days at 60 °C, no change to starting materials was observed by solution state $^{31}\text{P}\{^1\text{H}\}$ NMR spectroscopic analysis. The reactions were discontinued.

Reaction	Compound 12		Compound 13		<i>cis</i> -[PtCl ₂ (PPh ₃) ₂]	
	Moles	Mass (g)	Moles	Mass (g)	Moles	Mass (g)
a	0.038	0.020			0.038	0.030
b	0.038	0.028			0.076	0.061
c			0.047	0.020	0.067	0.053

Table 5 – Quantities of reagents used whilst probing the reactions between compounds 12 and 13 with *cis*-[PtCl₂(PPh₃)₂].

3.8.10 – Synthesis of *cis*-[PtCl₂(PPh₂Me)₂] and Proposed Complex *cis*-[PtCl₂(12**)]
(Compound **16**) from the Reaction Between **12** and *trans*-[Pt(PPh₂Me)Cl(μ-Cl)]₂**

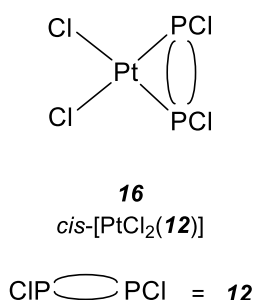


Figure 26 – Proposed compound **16**.

To a Young's NMR tube containing a suspension of **12** (0.020 g, 0.038 mmol) in CD₂Cl₂ (0.8 ml), *trans*-[Pt(PPh₂Me)Cl(μ-Cl)]₂^{†††} (0.036 g, 0.038 mmol) was added. The reaction mixture was heated at 50 °C for 2 days, after which no further change to the reaction composition was observed by solution state ³¹P{¹H} NMR spectroscopy. Solution state ³¹P{¹H} NMR spectroscopic analysis of the reaction mixture revealed several phosphorus-containing species including unreacted *trans*-[Pt(PPh₂Me)Cl(μ-Cl)]₂, compound **16** and *cis*-[PtCl₂(PPh₂Me)₂]. No single species could be isolated for the purposes of full characterisation, either by recrystallization or solvent extraction (using hexane, pentane, THF, toluene, chloroform). The structural identity of compound **16** has not been determined unambiguously.

³¹P{¹H} NMR (162.0 MHz, CD₂Cl₂): δ (ppm) = +73.8 (broad s, *v*_{1/2} = 42 Hz, with satellites ¹*J*_{PtP} = 3868 Hz, **16**), -0.9 (s, with satellites ¹*J*_{PtP} = 3616 Hz, *cis*-[PtCl₂(PPh₂Me)₂]).²⁶

3.8.11 – Synthesis of *cis*-[PtCl₂(PPh₂Me)(13**)] (Compound **17**)**

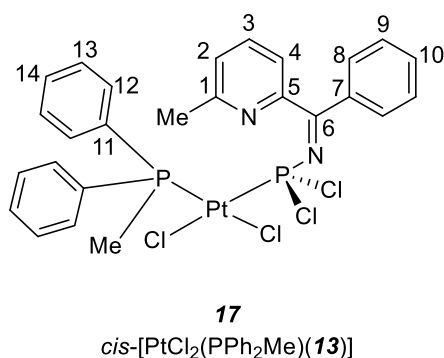


Figure 27 – Compound **17** showing NMR spectroscopic assignment numbering scheme.

^{†††}Sample of *trans*-[Pt(PPh₂Me)Cl(μ-Cl)]₂ used was prepared by Dr P. K. Coffey (née Monks).^{26,27}

To a Young's NMR tube containing a solution of **13** (0.020 g, 0.067 mmol) in CD₂Cl₂ (0.8 ml), *trans*-[Pt(PPh₂Me)Cl(μ-Cl)]₂^{§§§} (0.031 g, 0.034 mmol) was added. The reaction mixture was heated at 50 °C for 2 days, after which no further change to the reaction composition was observed by solution state ³¹P{¹H} NMR spectroscopic analysis. Compound **17** was not isolated and was analysed *in situ*. MS (ESI) *m/z*: 335.1 ([C₁₃H₁₁ClN₂PK]⁺), 201.1 ([Ph₂MePH]⁺). ³¹P{¹H} NMR (283.3 MHz, CD₂Cl₂): δ (ppm) = +57.0 (d, ²J_{PP} = 644.8 Hz, with satellites ¹J_{PPt} = 3053 Hz, PRC₂), +4.7 (d, ²J_{PP} = 644.7 Hz, with satellites ¹J_{PPt} = 2948 Hz, PPh₂Me). ¹H NMR (699.7 MHz, CD₂Cl₂): δ (ppm) = 8.43 (1H, *pseudo t*, ³J_{HH} = 7.7 Hz, CH³), 8.06 (1H, d, ³J_{HH} = 7.7 Hz, CH⁴), 7.96 (1H, d, ³J_{HH} = 7.9 Hz, CH²), 7.92-7.89 (2H, m, CH⁸), 7.71-7.74 (1H, m, CH¹⁰), 7.54-7.46 (2H, m, CH¹³), 7.45-7.39 (2H, m, CH¹²), 7.33-7.29 (1H, m, CH¹⁴), 3.57 (3H, s, CCH₃), 1.99 (3H, d, ²J_{HP} = 11.4 Hz, PCH₃). ¹³C{¹H} NMR (176.0 MHz, CD₂Cl₂): δ (ppm) = 177.2 (d, ²J_{CP} = 16.2 Hz, C⁶), 157.5 (s, C⁵), 144.0 (s, C¹), 133.1 (s, C¹⁰), 132.7 (d, ³J_{CP} = 2.3 Hz, C⁷), 132.4 (d, ¹J_{CP} = 5.8 Hz, C¹¹), 131.4 (d, ³J_{CP} = 2.7 Hz, C¹³), 131.1 (d, ²J_{CP} = 2.9 Hz, C¹²), 130.9 (d, ⁴J_{CP} = 2.6 Hz, C⁴), 129.6 (s, C⁸), 129.3 (s, C⁹), 127.8 (s, C¹⁴), 122.0 (s, C²), 22.8 (s, C¹CH₃), 12.8 (d, ¹J_{CP} = 45.1 Hz, PCH₃).

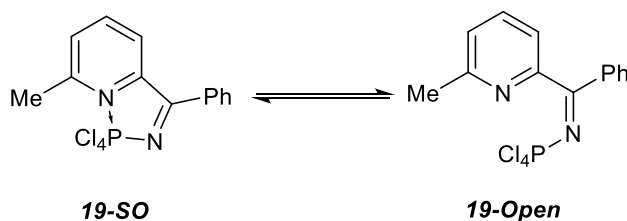
3.8.12 – Attempted Synthesis of *N*-(dichlorophosphanyl)-1-phenyl-1-(pyridin-2-yl)methanimine

A solution of PhLi (2.7 ml, 1.8 M in dibutyl ether, 4.8 mmol) was added dropwise to a stirred solution of 2-cyanopyridine (0.500 g, 4.8 mmol) in DME (25 ml) at -78 °C, and the mixture then stirred for 1 hour at -78 °C. A solution of PCl₃ (2.7 ml, 4.8 mmol) in DME (35 ml) was added and the mixture then allowed to attain room temperature; on warming to room temperature a pale green precipitate began to form from a red/orange solution. The mixture was stirred for 16 hours at room temperature to give an olive-green precipitate in an orange/red solution. The red/orange solution was removed by filtration and the olive green solid dried *in vacuo*. The green solid was found to be insoluble in all common solvents. Despite applying a variety of techniques, the structural identity of the reaction product has not been determined.

³¹P{¹H} CP MAS NMR (162.0 MHz): δ (ppm) = -120.8 (s).

^{§§§}Sample of *trans*-[Pt(PPh₂Me)Cl(μ-Cl)]₂ used was prepared by Dr P. K. Coffey (née Monks).^{26,27}

3.8.13 – Synthesis of Proposed Compounds **19-Open**/**19-SO** (Tetrachlorophosphino-1-((phenyl(6-methyl-pyridin-2-yl)methylene)amino) amine)



Scheme 26 – Proposed compounds **19-SO** and **19-Open**.

A solution of PhLi (1.1 ml, 1.9 M in dibutyl ether, 2.1 mmol) was added dropwise to a stirred solution of 6-methyl-2-cyanopyridine (0.250 g, 2.1 mmol) in DME (25 ml) at $-78\text{ }^{\circ}\text{C}$ and the mixture then stirred for 1 hour at $-78\text{ }^{\circ}\text{C}$. A solution of PCl_5 (0.440 g, 2.1 mmol) in DME (15 ml) was added and the mixture then allowed to attain room temperature; on warming to room temperature a pale brown precipitate began to form in a brown/orange solution. The mixture was stirred for 16 hours at room temperature, the dark brown solution isolated by filtration and the volatile species removed under reduced pressure. The pale brown residue was washed with THF (2 x 20 ml) then the volatile species removed from the washings *in vacuo* to give a dark brown residue which, when analysed by solution state $^{31}\text{P}\{^1\text{H}\}$ NMR spectroscopy, was found to contain several species, including proposed compounds **19-SO** and **19-Open**. No single species were isolated by solvent extraction or recrystallization from THF. The structural identity of compounds **19-Open** and **19-SO** has not been determined unambiguously.

$^{31}\text{P}\{^1\text{H}\}$ NMR (162.0 MHz, $\text{C}_4\text{D}_8\text{O}$): δ (ppm) = +8.3 (s, **19-SO**), -2.7 (s, **19-Open**).

3.8.14 – Synthesis of Compound **20-Open** (Tetrachlorophosphino-1-((phenyl(pyridin-2-yl)methylene)amino) amine)

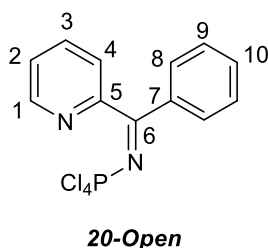


Figure 28 – Compound **20-Open** showing NMR spectroscopic assignment numbering scheme.

A solution of PhLi (1.23 ml, 1.9 M in dibutyl ether, 2.4 mmol) was added dropwise to a stirred solution of 2-cyanopyridine (0.250 g, 2.4 mmol) in DME (25 ml) at $-78\text{ }^{\circ}\text{C}$, and the mixture then stirred for 1 hour at $-78\text{ }^{\circ}\text{C}$. A solution of PCl_5 (0.500 g, 2.4 mmol) in DME (15 ml) was added and the mixture then allowed to attain room temperature; on warming to room temperature a brown precipitate began to form from a green solution. The mixture was stirred for 16 hours at room temperature then the dark liquid component isolated by filtration. The volatile species were removed from the liquid portion of the reaction mixture and the residue washed with THF (40 ml). The volatile species were removed from the washings *in vacuo* to yield **20-Open** as a brown oily residue (0.132 g, 0.373 mmol, 16 %).

$^{31}\text{P}\{^1\text{H}\}$ NMR (283.3 MHz, $\text{C}_4\text{D}_8\text{O}$): δ (ppm) = -4.4 (s, **20-Open**). ^1H NMR (699.7 MHz, $\text{C}_4\text{D}_8\text{O}$): δ (ppm) = 8.68 (1H, d, $^3J_{\text{HH}} = 4.7$ Hz, CH^1), 7.95 (1H, dd, $^3J_{\text{HH}} = 7.8$ Hz, $^3J_{\text{HH}} = 7.7$ Hz, CH^3), 7.82 (1H, d, $^3J_{\text{HH}} = 7.7$ Hz, CH^4), 7.61 (1H, dd, $^3J_{\text{HH}} = 7.8$ Hz, $^3J_{\text{HH}} = 4.6$ Hz, CH^2), 7.58 (2H, d, $^3J_{\text{HH}} = 7.8$ Hz, CH^8), 7.41-7.36 (2H, m, CH^9), 7.28 (1H, t, $^3J_{\text{HH}} = 7.4$ Hz, CH^{10}). $^{13}\text{C}\{^1\text{H}\}$ NMR (176.0 MHz, $\text{C}_4\text{D}_8\text{O}$): δ (ppm) = 151.1 (s, C^1), 137.2 (s, C^3), 132.5 (s, C^2), 129.0 (s, C^9), 128.5 (s, C^4), 126.9 (s, C^8), 126.7 (s, C^{10}). The quaternary carbons were not observed in the $^{13}\text{C}\{^1\text{H}\}$ NMR spectrum due to the long relaxation times associated with quaternary carbon centres.

Chapter 3 References

- ¹ D. A. Smith, A. S. Batsanov, K. Miqueu, J. –M. Sotiropoulos, D. C. Apperley, J. A. K. Howard and P. W. Dyer, *Angew. Chem. Int. Ed.*, 2008, **47**, 8674-8677.
- ² S. J. Geier, A. L. Gille, T. M. Gilbert and D. W. Stephan, *Inorg. Chem.*, 2009, **48**, 10466–1047.
- ³ D. A. Smith, PhD Thesis, Durham University, 2009.
- ⁴ D. A. Smith, A. S. Batsanov, K. Costuas, E. Edge, D. C. Apperley, D. Collison, J. –F. Halet, J. A. K. Howard and P. W. Dyer, *Angew. Chem. Int. Ed.*, 2010, **49**, 7040-7044.
- ⁵ O. V. Dolomanov, L. J. Bourhis, R. J. Gildea, J. A. K. Howard and H. Puschmann, *J. Appl. Cryst.*, 2009, **42**, 339-341.
- ⁶ C. Sandofry in *The Chemistry of Functional Groups: The Chemistry of the Carbon-Nitrogen Double Bond*, 1970, Interscience Publishers.
- ⁷ J. March in *Advanced Organic Chemistry Fourth Edition*, 1992, Wiley-Interscience.
- ⁸ S. B. Bushuk, F. H. Carre, D. M. H. Guy, W. E. Douglas, Y. A. Kalvinkovskya, L. G. Klapshina, A. N. Rubinov, A. P. Stupak and B. A. Bushuk, *Polyhedron*, 2004, **23**, 2615-2623.
- ⁹ J. E. Huheey, E. A. Keiter, and R. L. Keiter in *Inorganic Chemistry 4th ed.*, 1993, Harper Collins.
B. de B. Darwent in National Standard Reference Data Series, 1970, National Bureau of Standards. S. W. Benson, *J. Chem. Ed.*, 1965, **42**, 502-518.
- ¹⁰ A. Bondi, *J. Phys. Chem.*, 1965, **68**, 441-451.
- ¹¹ C. E. Bacon, D. J. Eisler, R. L. Melen and J. M. Rawson, *Chem. Comm.*, 2008, 4924–4926.
- ¹² F. A. L. Anet and I. Yavari, *J. Org. Chem.*, 1976, **41**, 3589-3591.
- ¹³ L. Pauling in *The Nature of the Chemical Bond 3rd Edition*, 1960, Cornell University Press.
- ¹⁴ A. H. Cowley and R. A. Kemp, *Chem. Rev.*, 1985, **85**, 367-382.
- ¹⁵ M. P. Doyle, R. Duffy, M. Ratnikov and Lei Zhou, *Chem. Rev.*, 2010, **110**, 704–724.
- ¹⁶ S. M. Godfrey, S. L. Jackson, C. A. McAuliffe and R. G. Pritchard, *J. Chem. Soc. Dalton Trans.*, 1997, 4499–4502.
- ¹⁷ D. Dakternieks and R. Di Giacomo, *Phosphorus and Sulfur*, 1985, **24**, 217-224.
- ¹⁸ V. P. Morgalyuk and T. V. Strelkova, *Russ. J. Gen. Chem.*, 2011, **81**, 2096-2102.
- ¹⁹ H. E. Gottlieb, V. Kotlyar, and A. Nudelman, *J. Org. Chem.*, 1997, **62**, 7512-7515.
- ²⁰ R. S. Edmundson in *The Chemistry of Phosphorus Compounds Volume 2: Phosphine Oxides, Sulphides, Selenides and Tellurides*, 1992, John Wiley & Sons.

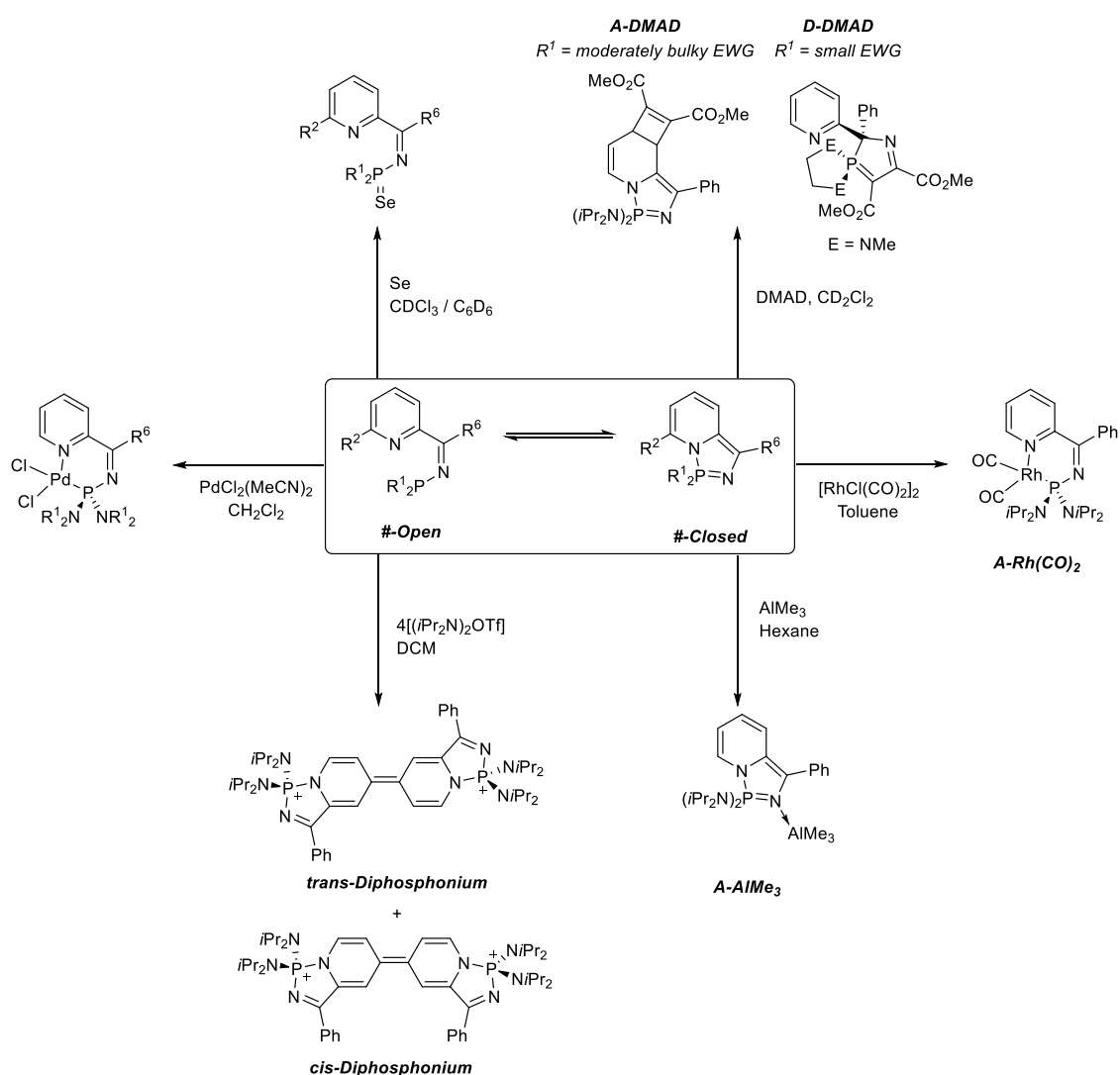
- ²¹ W. Haubold and E. Fluck, *Z. Anorg. Allg. Chem.*, 1972, **392**, 69-61.
- ²² C. Boudou, M. Bergès, C. Sagnes, J. Sopková-de Oliveira Santos, S. Perrio and P. Metzner, *J. Org. Chem.*, 2007, **72**, 5403–5406.
- ²³ D. G. Gilheany in *The Chemistry of Phosphorus Compounds Volume 2: Phosphine Oxides, Sulphides, Selenides and Tellurides*, 1992, John Wiley & Sons.
- ²⁴ B. E. Bosch, G. Erker, R. Fröhlich and O. Meyer, *Organometallics*, 1997, **16**, 5449-5456.
- ²⁵ P. S. Pregosin, *Coord. Chem. Rev.*, 1982, **44**, 247-291.
- ²⁶ K. B. Dillon, A. E. Goeta, P. K. Monks and H. J. Shepherd, *Polyhedron*, 2010, **29**, 606-612.
- ²⁷ P. K. Monks, PhD Thesis, Durham University, 2008.
- ²⁸ R. J. Puddephatt and P. J. Thompson, *J. Chem. Soc. Dalton Trans.*, 1975, 1810-1814.
- ²⁹ R. J. Puddephatt, *J. Chem. Soc. Dalton Trans.*, 1977, 1219-1223.
- ³⁰ D. Minniti, *Inorg. Chem.*, 1994, **33**, 2631-2634
- ³¹ S. Berger, S. Braun and H. -O. Kalinowski in *NMR-Spektroskopie von Nichtmetallen Band 3 ³¹P-NMR Spektroskopie*, 1993, Georg Thieme Verlag.
- ³² D. K. Kennepohl, A. A. Pinkerton, Y. F. Lee and R. G. Cavell, *Inorg. Chem.*, 1989, **29**, 5088-5096.

Chapter 4 – Probing the Reactivity of
the Interconverting Pyridyl-*N*-
Phosphinoimine – Diazaphosphazole
Tautomers

Chapter 4 – Probing the Reactivity of the Interconverting Pyridyl-*N*-Phosphinoimine – Diazaphosphazole Tautomers

4.1 – Introduction

The multifunctional behaviour of the interconverting bulky pyridyl-*N*-phosphinoimine – diazaphosphazole tautomers has already been discussed in **Chapter 1**, a summary of the reactions discussed is illustrated in Scheme 1.^{1,2,3,4,5} These reactions all demonstrate preferential reactivity of one tautomer of # (general “open”-“closed” species) over the other.



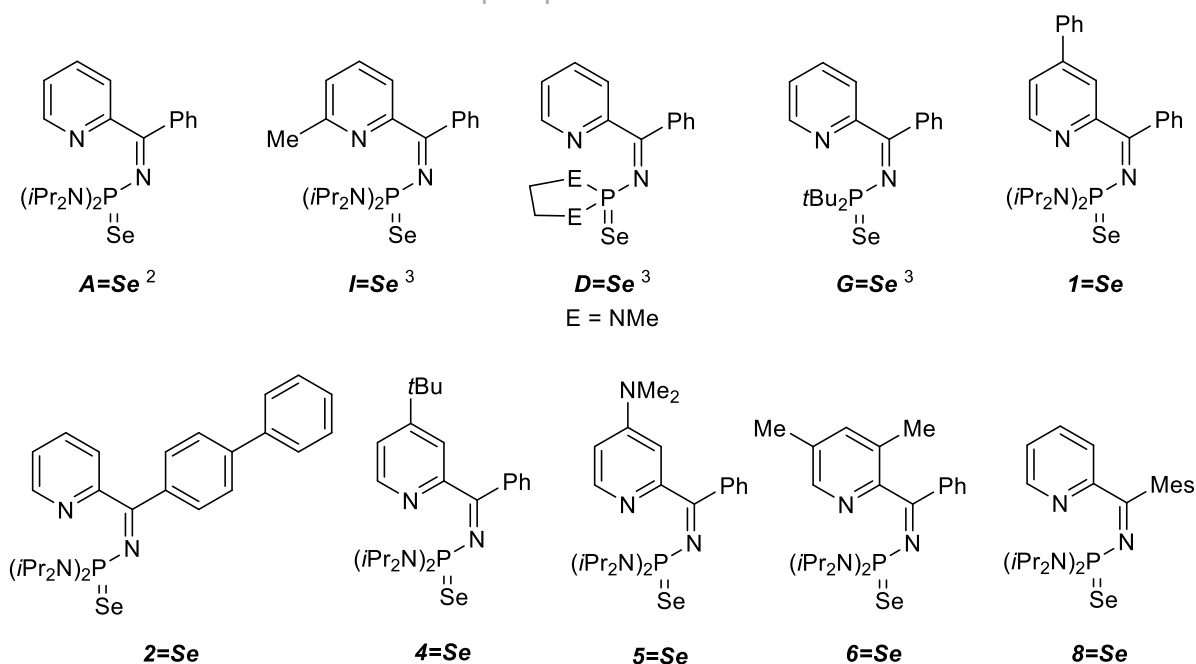
Scheme 1 – Selected, previously reported reactions of the “open” and “closed” tautomers.^{1,2,3,4}

The cyclisation of the “open” tautomer to form the “closed” species, as discussed in **Chapter 1**, can be regarded as initially comprising of a Lewis adduct forming reaction. The extent of Lewis adduct (“closed”) formation, from what can be regarded as a weak intramolecular FLP (“open”), is intimately linked to variations in the stereoelectronic nature of the substituents bound to the central pyridyl-phosphinoimine scaffold of the “open” tautomer, as well as to changes in temperature and solvent polarity (**Chapter 2**). **Chapter 1** (section **1.8**) described some of the wide and varied chemistry of FLPs and the value of FLP mediated processes, from both a synthetic and environmental standpoint, makes the potential FLP character of the “open” pyridyl-*N*-phosphinoimines of interest to explore. This chapter will outline a study of the behaviour of these pyridyl-*N*-phosphinoimine – diazaphosphazole tautomers towards commercially accessible small molecules that literature FLP systems are known to react with.

4.2 – Reactivity of the Pyridyl-*N*-Phosphinoimines Towards Elemental Selenium

The oxidation of a P^{III} centre to P^V *via* the reaction with a chalcogen, such as selenium, is well documented for R₃P species - the oxidation of the P^{III} centre occurs concurrently with the reduction of the chalcogen and formation of a R₃P=Se bond, which is more accurately represented in the zwitterionic form, [R₃P⁺-Se⁻].⁶ The magnitude of the ¹J_{PSe} coupling constant (*i.e.* |¹J_{PSe}|) for [R₃P=Se ↔ R₃P⁺-Se⁻] species is indicative of the donor-acceptor character of the phosphorus centre; when a phosphine is a poor σ-donor, the phosphorus-selenium bond is primarily *s* in character, this gives rise to higher |¹J_{PSe}| values than are observed for good σ-donor phosphines.^{7,8} In the case of the pyridyl-*N*-phosphinoimine - diazaphosphazole tautomers, the nucleophilic P^{III} centre in the “open” tautomer is highly reactive and susceptible to oxidation to form a P^V centre. The phosphorus(V) monoselenide derivatives (Figure 1) of the “open” pyridyl-*N*-phosphinoimines reported in **Chapter 2** have been prepared in order to probe the electronic character and ease of oxidation of the phosphorus centres in the starting pyridyl-*N*-phosphinoimine – diazaphosphazole species.

Diazaphosphazole Tautomers

Figure 1 – Tertiary phosphine monoselenides of the “open” pyridyl-*N*-phosphinoimines.

Compound	δ_P (ppm) (298 K, C_6D_6) Starting “Open”/“Closed”	Starting “Open”：“Closed” (298 K, C_6D_6)	T (°C)	Time (h)	$R_3P=Se$ δ_P (ppm)	$ ^1J_{PSe} $ (Hz)
A=Se	+71.0 / +42.3	5:95	50	80	+55.5	821 ^b
I=Se	+71.3 / N/O ^a	100:0	50	15	+54.3	824 ^c
D=Se	N/O ^a / +40.6	0:100	50	96	+66.7	842 ^c
G=Se	+81.2 / N/O ^a	100:0	25	1	+91.5	746 ^c
1=Se	+70.3 / +41.0	1:99	50	92	+43.3	800 ^c
2=Se	+70.4 / +41.2	4:96	50	84	+76.1	746 ^c
4=Se	+69.9 / +40.3	28:72	50	72	+52.8	797 ^c
5=Se	+70.4 / +44.9	90:10	50	5	+54.9	828 ^b
6=Se	+69.2 / +39.6	98:2	50	12	+58.3	798 ^c
8=Se	+67.9 / +39.0	85:15	50	16	+58.4	820 ^c

Table 1 - Experimental data for the “open” monoselenides derivatives. ^a N/O = not observed at 298 K. Time refers to time taken for full conversion to monoselenide to occur. ^b Recorded in C_6D_6 . ^c Recorded in $CDCl_3$.

The ^{31}P NMR spectroscopic chemical shifts and $|^1J_{PSe}|$ values observed for compounds **1=Se**, **2=Se**, **4=Se**, **5=Se**, **6=Se** and **8=Se** (Table 1) are in good agreement with the data previously reported for their structural analogues, **A=Se**, **I=Se**, **D=Se** and **G=Se** (Table 1),^{1,3} as well as other related compounds: $(Me_2N)_3PSe$, $\delta_P = +83.2$ ppm, $|^1J_{PSe}| = 805$ Hz; $(Et_2N)_3PSe$, $\delta_P = +77.1$

ppm, $|^1J_{PSe}| = 794$ Hz; $(Me_2N)_2(Ph)PSe$, $\delta_P = +84.0$ ppm, $|^1J_{PSe}| = 790$ Hz; $(Me_2N)_2(Me)PSe$, $\delta_P = +80.5$ ppm, $|^1J_{PSe}| = 767$ Hz.^{9,10,11} From the data presented in Table 1, it can be seen that when there are electron donating substituents bound to the phosphorus centre, *e.g.* *t*Bu in **G=Se**, the $|^1J_{PSe}|$ values are, in general, notably smaller than the tertiary monochalcogenide species that possess electrophilic groups at the phosphorus centre, *e.g.* (NiPr₂) in **1=Se** and **4=Se** and (MeNC₂H₄NMe) in **D=Se**. The larger $|^1J_{PSe}|$ values for species containing electron withdrawing substituents at the phosphorus centre is attributed to the greater *s* character of the phosphorus-selenium bond.^{7,8} Compounds **A=Se**, **I=Se**, **1=Se**, **4=Se**, **5=Se** and **6=Se**, which differ from each other in the identity and position of the substituents bound to the pyridine ring, all give rise to $|^1J_{PSe}|$ values in a similar region, 800 – 830 Hz, indicating that the pyridine substituents have only a small impact upon the electronic character of the phosphorus centre.

Compounds **2=Se**, **A=Se** and **8=Se** differ from each other in their imine carbon substituent; 4,4'-biphenyl, Ph and Mes, respectively. The $|^1J_{PSe}|$ value for compound **2=Se** measures 746 Hz, a value that is notably smaller than those recorded for structurally analogous compounds **A=Se** (821 Hz) and **8=Se** (820 Hz). The aromatic carbocyclic substituent bound to the imine carbon centre is able to enter into conjugation with the imine C=N bond when their respective π -systems lie coplanar to each other. The conjugated π -system within compound **2=Se** is more electron rich than the π -systems in **A=Se** and **8=Se**, as a consequence of the greater extent of aromaticity of the 4,4'-biphenyl substituent (**2=Se**) compared to the Ph and Mes groups in **A=Se** and **8=Se**. The more electron rich conjugated π -system in **2=Se**, compared to that in **A=Se** and **8=Se**, increases electron density at the electronegative phosphorus centre leading to a decrease in *s* character of the phosphorus-selenium bond, and therefore a decrease in $|^1J_{PSe}|$ value.

The relative ease of oxidation of the pyridyl-*N*-phosphinoimine species (“*open*” tautomer) by elemental selenium is judged by the time taken for a given reaction to reach completion (Table 1), *i.e.* the shorter the reaction time, the easier the oxidation of the “*open*” species by elemental selenium, and *vice versa*. Examination of the time taken for quantitative formation of tertiary phosphine chalcogenide and the relative percentage of “*open*” tautomer present in the corresponding starting tautomeric pair shows that the reaction time increases as the

percentage of “*open*” observed decreases. This observation is attributed to the fact that the N(pyridine)-P bond in the “*closed*” diazaphosphazole must be disrupted in order for a reaction between the phosphorus centre and selenium to occur.

4.3 – Reactivity of Dynamic “*Open*”-“*Closed*” Tautomers Towards Small Molecules

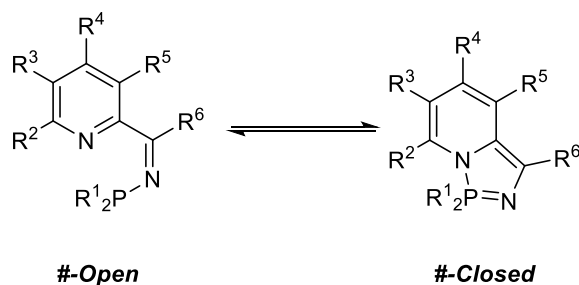


Figure 2 – Dynamic “*open*”-“*closed*” valence tautomers.

The reactions of species that take the general form of # (Figure 2), both described here in this chapter and reported previously (see Scheme 1 or **Chapter 1**),^{1,2,3,4,5} demonstrate their capability of reacting at different positions on the “*open*”/“*closed*” framework as well as their ability to react solely as one tautomeric form, irrespective of the position of the “*open*”-“*closed*” equilibrium. The next section of this chapter further examines the reactivity of interconverting pyridyl-*N*-phosphinoimine – diazaphosphazole systems (of general form #, Figure 2), specifically the reactions of two tautomeric systems, **A** and **I** (Figure 3), with B(C₆F₅)₃, MeNO₂ and TMSN₃. Compounds **A** and **I** have been chosen due to the differing positions of their tautomeric equilibria. Compound **A** exists in a dynamic equilibrium between **A-Open** and **A-Closed** (5:95, C₆D₆ at 298 K), and can therefore react as either tautomeric form. Compound **I**, however, exists solely in its “*open*” form (even after prolonged heating at elevated temperatures),² and can therefore only react as a pyridyl-*N*-phosphinoimine.

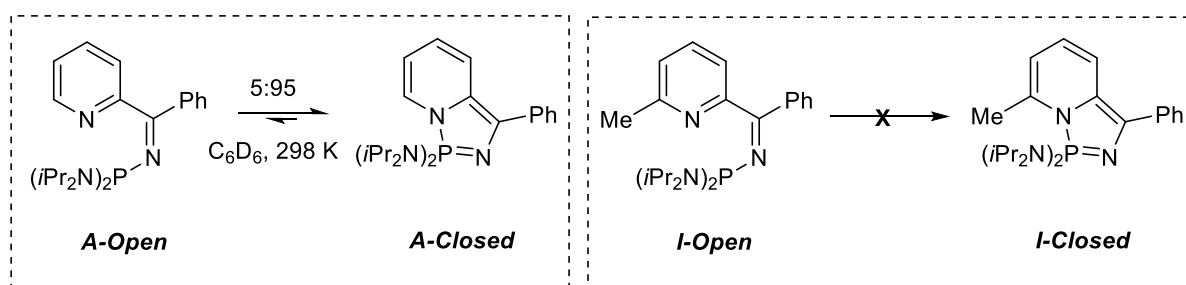
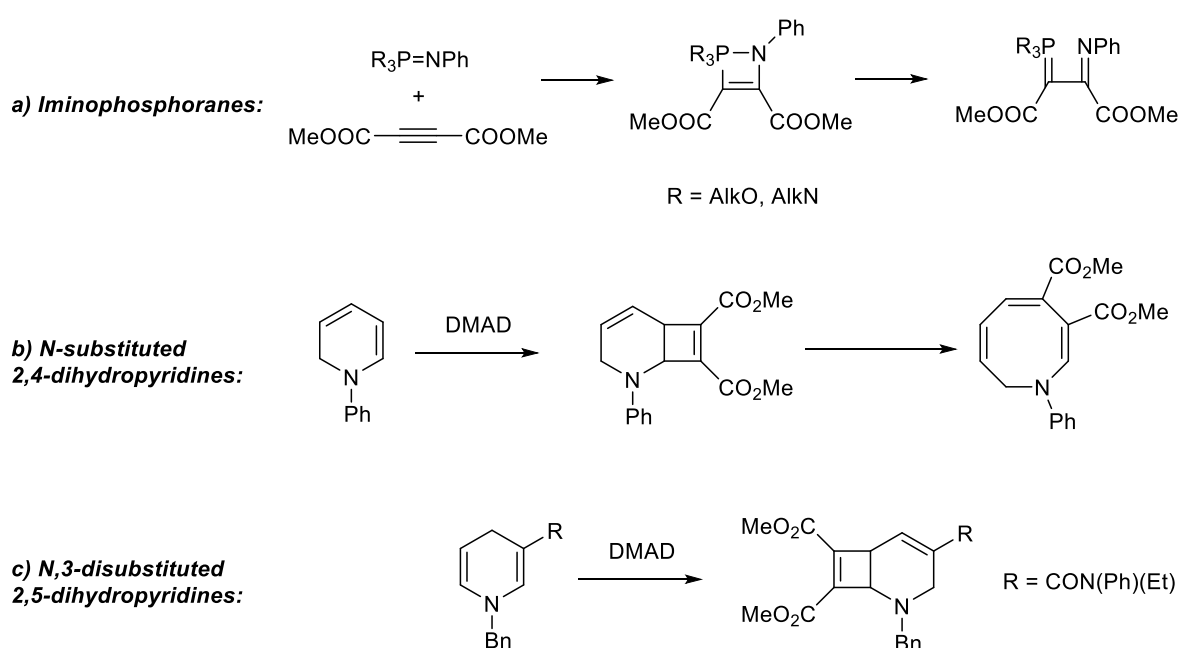


Figure 3 – Compounds **A** and **I**.²

4.3.1 – Reactivity of the Dynamic “Open”-“Closed” Tautomers Towards DMAD

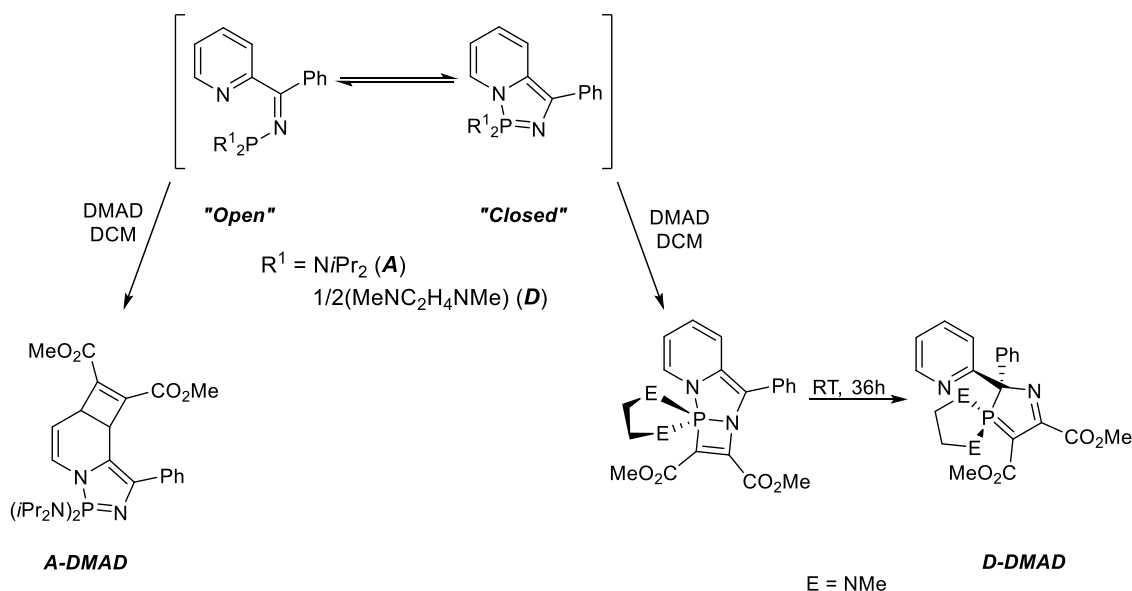
Iminophosphoranes ($R_3P=NR'$) are known to readily undergo *pseudo* [2+2] cycloaddition reactions with DMAD, such as the reaction shown in Scheme 2 (a), whereby a four-membered heterocycle is first formed, which can then undergo a rearrangement to form a less strained species.^{12,13} *N*-substituted 2,4- and 2,5-dihydropyridines are also known to undergo *pseudo* [2+2] cycloaddition reactions with DMAD, these cycloaddition reactions are always seen to occur at the least hindered double bond as shown in Scheme 2 (b and c).^{14,15}



Scheme 2 – *Pseudo* [2+2] cycloaddition reactions of iminophosphoranes (a) and dihydropyridines (b and c) with DMAD.^{12,13,14,15}

Compounds **A** and **D** (Scheme 3), which exist primarily in their “closed” forms at 298 K (“open”：“closed” = 5:95 (**A**) and 0:100 (**D**) in C_6D_6), possess multiple unsaturated functional groups. These unsaturated groups have the potential to undergo reactions with DMAD, notably dearomatized C=C bonds in the dihydropyridine ring, iminophosphorane P=N bonds and imine C=N bonds. The differing reactivity of compounds **A** and **D** towards the electron deficient alkyne DMAD has been reported previously, the products of these reactions are shown in Scheme 3.³ Compound **A**, which possesses bulky phosphorus substituents that sterically crowd the iminophosphorane functionality, undergoes a *pseudo* [2+2] cycloaddition reaction at one of the accessible, dearomatized C=C bonds in the dihydropyridine motif of **A**-

Closed, reminiscent of the reactions of 2,4- and 2,5-dihydropyridines with DMAD studied by Acheson and co-workers (Scheme 2).^{14,15} Compound **D**, which possesses less bulky substituents at the phosphorus, is able to undergo a *pseudo* [2+2] cycloaddition with DMAD at the iminophosphorane P=N bond in **D-Closed** to form the tricyclic fused *pseudo* [2+2] cycloaddition product that subsequently undergoes a ring expansion and rearrangement to form **D-DMAD**.³ In light of the reactivity observed for compounds **A** and **D** towards DMAD, it was of interest to examine the reactivity of a pyridyl-*N*-phosphinoimine – diazaphosphazole tautomeric pair that possesses relatively bulky substituents at both the 4-position on the pyridine ring (which will block one of the C=C bonds on the dihydropyridine) and at the phosphorus centre (to block the P=N bond) in order to probe the effect of these blocking groups.



Scheme 3 – Products of the reactions of **A** and **D** with DMAD.³

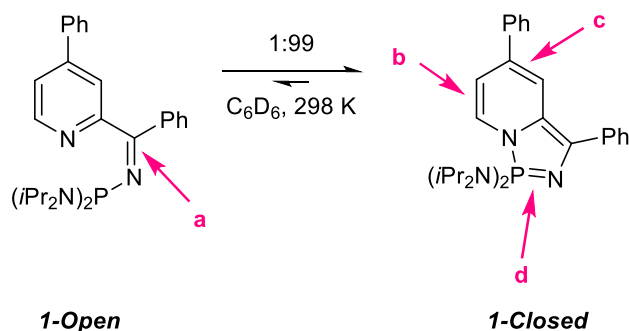
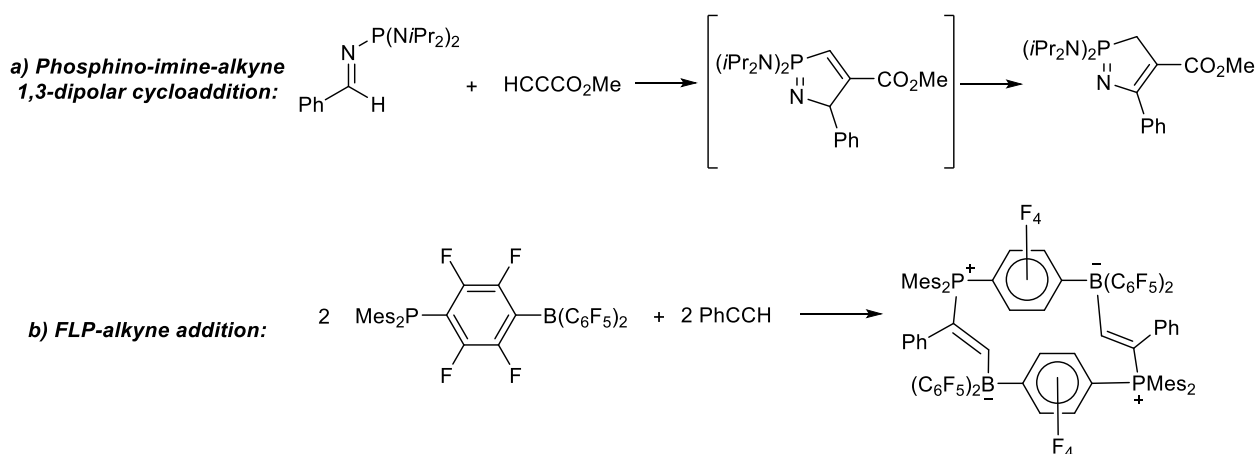


Figure 4 – Potential positions for attack on **1** by DMAD.

Compound **1** (“open”：“closed”, 1:99 in C₆D₆ at 298 K, Figure 4) was chosen for this study as, in contrast to compounds **A** and **D**, it possesses a phenyl substituent *para* to the pyridine nitrogen centre and, similarly to **A**, bulky (N*i*Pr₂) groups bound to the phosphorus centre. These substituents in compound **1** sterically block the reaction of **1** with DMAD at the **c** and **d** positions (Figure 4). There are two sterically accessible positions in compound **1** at which DMAD could attack, the unhindered dearomatized C=C bond in the dihydropyridine moiety in **1-Closed** (**b**, Figure 4) and the phosphino-imine motif in **1-Open** (**a**, Figure 4). The reactions of phosphino-imines with alkynes have been previously reported in the literature by Baceiredo and co-workers, the example shown in Scheme 4 (**a**) gives rise to the formation of a five-membered heterocycle.¹⁶ Furthermore, **1-Open** has the potential ability to behave as an FLP when reacted with an alkyne, an example which demonstrates the addition of the alkyne across sterically crowded P and B centres (reported by Stephan and co-workers) is shown in Scheme 4 (**b**).¹⁷

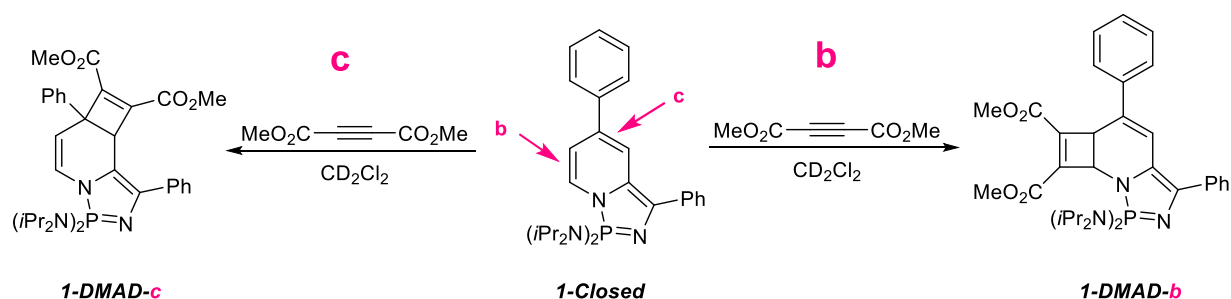


Scheme 4 – Reactions of alkynes with phosphino-imines (**a**)¹⁶ and FLPs (**b**).¹⁷

The reaction between compound **1** and a stoichiometric amount of DMAD was carried out. Solution state ³¹P{¹H} NMR spectroscopic analysis of the reaction mixture revealed the presence of several phosphorus-containing species. Two majority products (accounting for 73 % of the total phosphorus-containing species observed by ³¹P NMR spectroscopy), presenting singlet resonances at δ_P = +90.8 and +54.0 ppm (in a 55:45 ratio) were observed by ³¹P NMR spectroscopic analysis. Attempts to purify the reaction mixture by recrystallization and solvent extraction were unsuccessful, something that hindered further NMR spectroscopic

analysis. The following is a discussion of the possible identity of these two majority phosphorus-containing species based on their solution state $^{31}\text{P}\{^1\text{H}\}$ NMR resonances ($\delta_{\text{P}} = +90.8$ and $+54.0$ ppm).

The reaction between compound **1** and DMAD gave rise to a singlet resonance in the $^{31}\text{P}\{^1\text{H}\}$ NMR spectrum at $\delta_{\text{P}} = +53.2$ ppm, a chemical shift that lies in a similar region to that observed for previously-described compound **A-DMAD** ($\delta_{\text{P}} = +46.6$ ppm, Scheme 3).³ This chemical shift suggests that **1-Closed** may possibly have undergone a similar *pseudo* [2+2] cycloaddition reaction with DMAD as has been observed for **A-Closed**. The reaction between **A** and DMAD proceeds *via* a *pseudo* [2+2] cycloaddition of the alkyne at one of the dearomatized C=C bonds in the dihydropyridine motif of **A-Closed**, at a position far removed from the phosphorus centre as indicated by the small $\Delta\delta_{\text{P}}$ between the chemical shifts for **A-Closed** and **A-DMAD** (~ 4 ppm). For the reaction between **1** and DMAD, the singlet resonance observed at $\delta_{\text{P}} = +53.2$ ppm in the ^{31}P NMR spectrum is ~ 11 ppm to higher frequency than the resonance for **1-Closed** ($+41.0$ ppm), a greater value of $\Delta\delta_{\text{P}}$ than that observed for **A-Closed** and **A-DMAD**. This is something that could be indicative of a *pseudo* [2+2] cycloaddition occurring closer to the phosphorus centre in **1-Closed**, *i.e.* at the accessible C=C bond at the **b** position to give **1-DMAD-b**, instead of at the sterically encumbered C=C bond at the **c** position (Scheme 5). The *pseudo* [2+2] cycloaddition of DMAD at the least sterically encumbered C=C bond of a dihydropyridine motif is entirely consistent with the observations made by Acheson and co-workers (Scheme 2, **c**).^{14,15} In the absence of further spectroscopic data, however, the structural identity of the species formed from reaction of DMAD with **1**, that presents the chemical shift at $\delta_{\text{P}} = +53.2$ ppm, cannot be unambiguously assigned.



Scheme 5 – Two possible reaction pathways for the reaction between DMAD and **1-Closed**.

The second phosphorus-containing majority product of the reaction between compound **1** and DMAD presented a singlet resonance at $\delta_P = +90.8$ ppm, a chemical shift in a similar region as that observed for previously-described compound **D-DMAD** (Scheme 3, $\delta_P = +84.3$ ppm),³ this is suggestive that a similar product may have been formed from the reaction between **1** and DMAD. The formation of **D-DMAD** from the reaction of **D** with DMAD is proposed to proceed *via* the initial *pseudo* [2+2] cycloaddition of DMAD to the P=N bond in **D-Closed**, followed by the rearrangement of the cycloadduct to form **D-DMAD**.³ The reaction of compound **1-Closed** with DMAD at the P=N bond, however, is likely to be sterically prevented by the presence of bulky (N*i*Pr₂) substituents at the phosphorus centre (as is seen for the reaction of compound **A** with DMAD). **1-Closed**, however, can undergo a 1,3-dipolar cycloaddition with DMAD at the phosphino-imine motif (as reported for the phosphino-imine species shown in Scheme 4),¹⁶ to form a bicyclic compound with 5- and 6-membered heterocycles joined by a C-C bond, **1-DMAD-a** (Figure 5). In the absence of further spectroscopic data, however, the structural identity of the species formed from the reaction between DMAD and compound **1**, that presents the chemical shift at $\delta_P = +90.8$ ppm, cannot be confidently assigned.

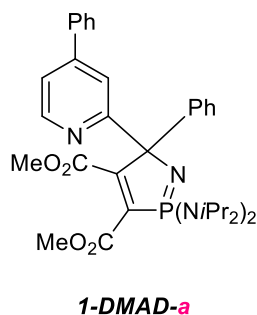
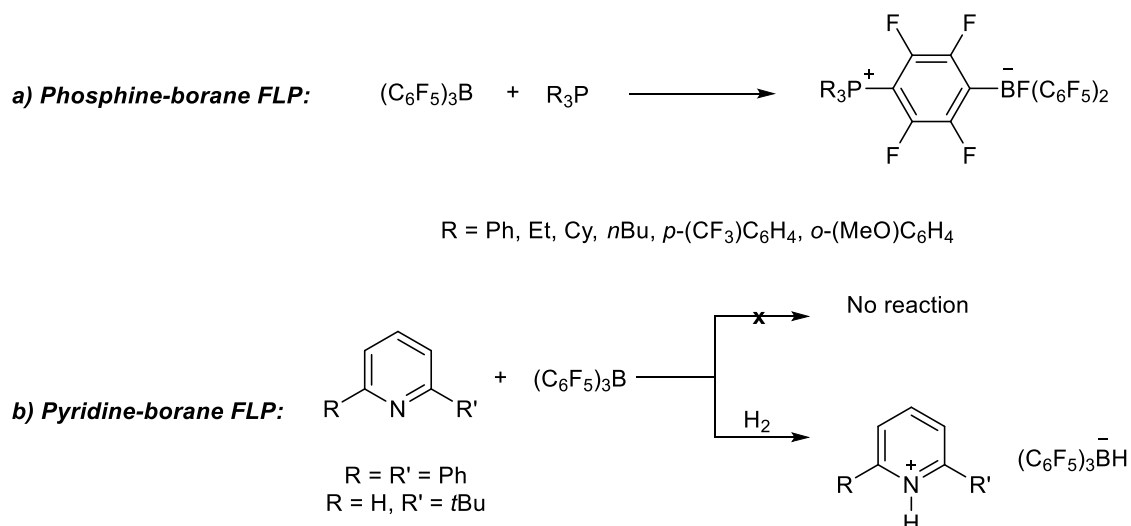


Figure 5 – Proposed product of the reaction between **1** and DMAD.

4.3.2 – Reaction of Compounds **A** and **I** with Tris(pentafluorophenyl)borane

It is well documented that that the sterically crowded boron centre in B(C₆F₅)₃ is unable to form classical Lewis adducts with sterically hindered phosphines (**a**, Scheme 6) and pyridines (**b**, Scheme 6), and exhibit FLP behaviour instead (Scheme 6).^{18,19,20}



Scheme 6 – Phosphine-borane FLPs (a) and pyridine-borane FLPs (b).^{18,19,20}

The interconverting tautomeric mixture of **A-Open** and **A-Closed** has been reported to react with $AlMe_3$ to form a single species, **A- $AlMe_3$** (Figure 6),² whereby preferential coordination of the “closed” tautomer to the hard aluminium centre, *via* an N(iminophosphorane) \rightarrow Al interaction, is observed. This coordination behaviour of compound **A** is reminiscent of other iminophosphoranes towards sterically unencumbered hard metal centres.²¹ The reactivity of compound **A** towards sterically crowded group XIII elements has not yet been explored and is of interest to study in order to probe potential FLP behaviour of **A-Open**.

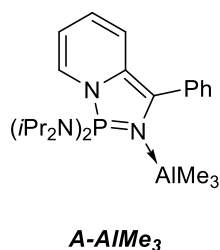
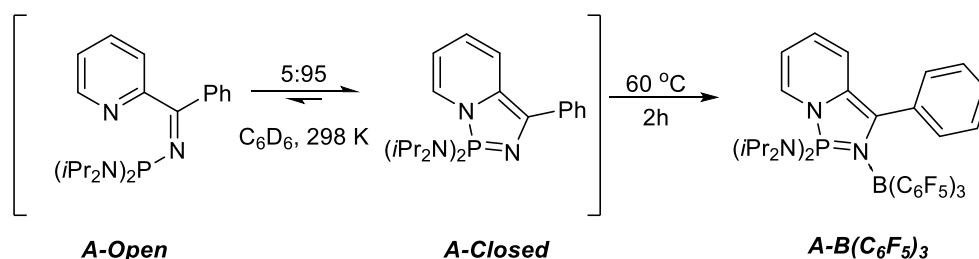


Figure 6 – Product of the reaction of **A** with $AlMe_3$.²

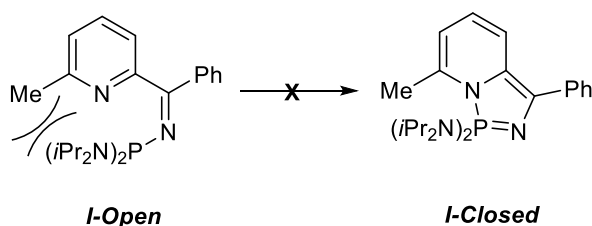
To further explore the coordination behaviour of compound **A**, the reaction of compound **A** with the Lewis acidic, non-metallic, sterically crowded boron centre in $B(C_6F_5)_3$ was probed. Compound **A** was mixed with a stoichiometric amount of $B(C_6F_5)_3$ and the mixture heated at 60 °C for 2 hours. Subsequent solution state ^{31}P NMR spectroscopic analysis of the heated reaction mixture revealed the formation of a single phosphorus-containing species that presented a sharp singlet resonance at $\delta_p = +50.5$ ppm, a shift comparable to that observed for **A- $AlMe_3$** .² In the ^{11}B NMR spectrum recorded for the reaction mixture, a broad singlet

resonance at $\delta_B = -7.7$ ppm ($\nu_{1/2} = 314$ Hz) was observed, a chemical shift characteristic of $R_3B \leftarrow L$ compounds *e.g.* $Me_3B \leftarrow NEt_3$, $\delta_B = -13.7$ ppm.²² These ^{31}P and ^{11}B NMR spectroscopic data are suggestive of the formation of **A-B(C₆F₅)₃** (Scheme 7) from the reaction between **A** and $B(C_6F_5)_3$.



Scheme 7 – Proposed product of the reaction between **A** and $B(C_6F_5)_3$.

To probe the reactivity of the “open” tautomer towards $B(C_6F_5)_3$, the reaction between compound **I** (Scheme 8), which exists solely in its “open” form, and $B(C_6F_5)_3$ was carried out to investigate whether a classical Lewis adduct between **I-Open** and $B(C_6F_5)_3$ could form, and, if so, at which nitrogen centre **I-Open** would coordinate to the Lewis acidic boron centre. Tris(pentafluorophenyl)borane is well documented to form adducts with imines and pyridines, both of these functionalities are present in **I-Open** and therefore open the possibility of this pyridyl-*N*-phosphinoimine species to form a classical Lewis adduct with $B(C_6F_5)_3$.^{18,20,23} The hard Lewis acidic boron centre in $B(C_6F_5)_3$ also has the potential of forming an FLP with either the sterically crowded pyridine nitrogen or phosphorus centres in **I-Open**, as is seen for FLPs **b** and **a** (Scheme 6).

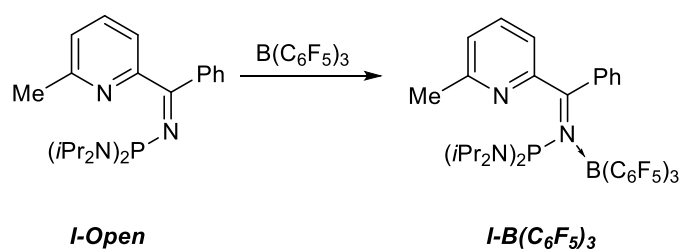


Scheme 8 – Steric barrier to the cyclisation of **I-Open**.

Compound **I** was reacted with a stoichiometric amount of $B(C_6F_5)_3$. Subsequent ^{31}P and ^{11}B NMR spectroscopic analysis of the reaction mixture revealed singlet resonances at $\delta_P = +53.3$ ppm (sharp) and $\delta_B = -8.4$ ppm (broad, $\nu_{1/2} = 168$ Hz), respectively, chemical shifts that are in good agreement with those observed for **A-B(C₆F₅)₃** ($\delta_P = +50.3$ ppm, $\delta_B = -7.7$ ppm) and the

^{11}B NMR chemical shift reported for $\text{Me}_3\text{B} \leftarrow \text{NEt}_3$ ($\delta_{\text{B}} = -7.7$ ppm).²² These spectroscopic data are suggestive of the formation of a classical Lewis adduct from the reaction between *I-Open* and $\text{B}(\text{C}_6\text{F}_5)_3$.

It is unlikely that the phosphorus centre in *I-Open* coordinates to the Lewis acidic boron centre as the bulky, electrophilic (NiPr_2) phosphorus substituents block, and decrease the availability of, the phosphorus lone pair. It is concluded, therefore, that the Lewis adduct formed from the reaction between *I* and $\text{B}(\text{C}_6\text{F}_5)_3$ takes the form of *I-B(C₆F₅)₃* (Scheme 9), whereby the unhindered, Lewis basic sp^2 -hybridised imine nitrogen centre coordinates to the boron centre. The ^1H and $^{13}\text{C}\{^1\text{H}\}$ NMR spectroscopic data are consistent with compound *I-B(C₆F₅)₃* being the product of the reaction between *I* and $\text{B}(\text{C}_6\text{F}_5)_3$, these data are comparable to those reported for compound *I*.

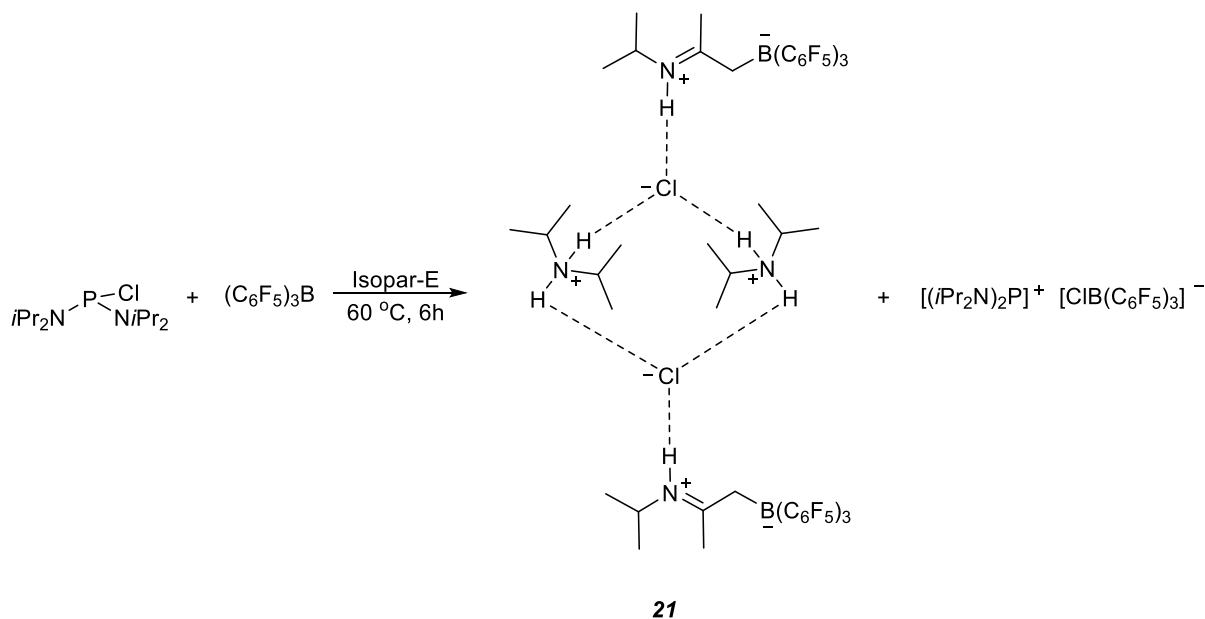


Scheme 9 – Proposed reaction between *I-Open* and $\text{B}(\text{C}_6\text{F}_5)_3$.

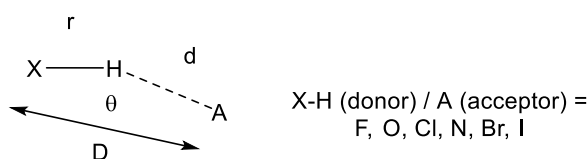
4.3.3 – Reaction of $(i\text{Pr}_2\text{N})_2\text{P}(\text{Cl})$ with $\text{B}(\text{C}_6\text{F}_5)_3$

Whilst attempting to probe the identity of the products from the reactions of compounds **A** and *I* with $\text{B}(\text{C}_6\text{F}_5)_3$, the reaction between $(i\text{Pr}_2\text{N})_2\text{P}(\text{Cl})$ and $\text{B}(\text{C}_6\text{F}_5)_3$ was carried out. Solution state ^{31}P NMR spectroscopic analysis of the reaction residue revealed the presence of one majority phosphorus-containing product, $[(i\text{Pr}_2\text{N})_2\text{P}][\text{ClB}(\text{C}_6\text{F}_5)_3]$ ($\delta_{\text{P}} = +245.2$ ppm). A second product, compound **21**, was identified by an X-ray crystallographic study of crystals obtained by slow evaporation of C_6D_6 . In the solid state, compound **21** is best represented as shown in Scheme 10, where the dashed lines represent hydrogen bonds.

Diazaphosphazole Tautomers

Scheme 10 – Reaction between $(iPr_2N)_2P-Cl$ and $B(C_6F_5)_3$ showing identified products.

The solid state molecular structure for compound **21** is shown in Figure 8, and selected structural data are shown in Table 2. Compound **21** can be regarded as a dimeric species comprising of four components (two identical ammonium cations and two identical iminium borate zwitterions) held together by hydrogen bonds (2 x H1--Cl1, 2 x H2A--Cl1, 2 x H2B--Cl1) to two central bridging chloride anions, 2 x Cl1 (Figure 8 and Scheme 10). By the definitions and parameters laid out by Desiraju and Steiner regarding the components of hydrogen bonds (Figure 7), the N1-H1, N2-H2A and N2-H2B components in compound **21** (Figure 8) can be regarded as donors (X-H, Figure 7) and the chloride anions as acceptors (A, Figure 7). Each chloride anion acceptor contributes three sterically accessible pairs of electrons to the hydrogen bonds within compound **21**.²⁴ Each chloride anion in **21** makes three hydrogen bonds (Cl1--H1, Cl2--H2A and Cl2--H2B), and can therefore be described as a trifurcated acceptor.²⁴ Whilst the interaction of an acceptor with three donor groups is possible, as has been demonstrated here for compound **21**, no examples can be found in the current literature.

Figure 7 – Geometrical parameters for a hydrogen bond as defined by Desiraju and Steiner.²⁴

Desiraju and Steiner categorize hydrogen bonds as being “very strong”, “strong” or “weak”, and the distinction between these classifications is made based on a series of properties, including those shown in Table 3.²⁴ From examination of the geometric parameters *D*, *d* and θ (as defined in Figure 7) for compound **21**, and the comparison of the H--A and X-H distances, it can be seen that the values found for **21** are consistent with those typical of “weak” hydrogen bonds.²⁴

Parameter	“Very strong” hydrogen bond	“Strong” hydrogen bond	“Weak” hydrogen bond	Compound 21 ^a
Bond lengths	H–A \approx X–H	H–A > X–H	H–A \gg X–H	H–A \gg X–H
D(X...A) (Å)	2.2–2.5	2.5–3.2	3.0–4.0	3.160(2) – 3.208(2)
d(H...A) (Å)	1.2–1.5	1.5–2.2	2.0–3.0	2.24(2) – 2.31(2)
θ(X–H...A) (°)	175–180	130–180	90–180	167(2)–174(2)

Table 3 – Selected properties of “very strong”, “strong” and “weak” hydrogen bonds as outlined by Desiraju and Steiner.²⁴ ^a X = N1/N2, A = Cl1, H = H1/H2A/H2B, see Figure 8 for atom labels.

For compound **21**, the B1-C19 (1.654(2) Å), B1-C13 (1.660(3) Å) and B1-C7 (1.648(2) Å) bond distances (*i.e.* the B-*sp*²C lengths) are comparable to those observed for analogous species, such as that shown in Figure 9 (1.657(2), 1.655(2) and 1.667(2) Å).²⁵ The B-*sp*³C bond distance in **21** (B1-C1 = 1.694(3) Å) is greater than those observed for the B-*sp*²C bonds, which is consistent with that observed for the compound in Figure 9, however, the exact bond length in **21** is smaller than for the compound in Figure 9. The variation in B-C bond lengths within compound **21** is in agreement with the differing strengths of B-*sp*²C and B-*sp*³C bonds. The N1-C2 bond length is characteristic of a carbon-nitrogen double bond (average = 1.28 Å).²⁶

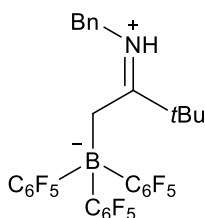
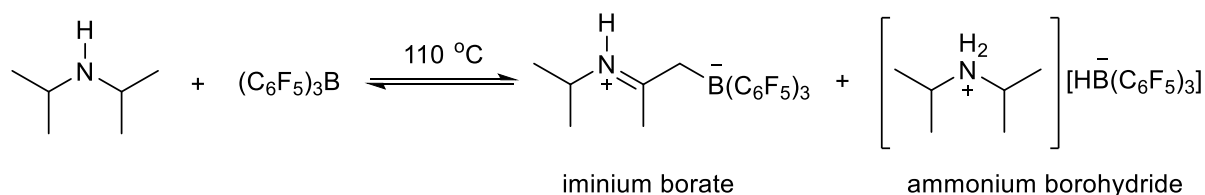


Figure 9 - ((2-Benzyliminium)-3,3-dimethylbutyl)-tris(pentafluorophenyl)borate reported by McDonald.²⁵

The extraction of the protons from an isopropyl substituent of diisopropylamine by tris(pentafluorophenyl) borane has been previously observed, and found to generate a

mixture of iminium borate and ammonium borohydride species as shown in Scheme 11.²⁷ The iminium borate components in **21**, the product of the reaction between $(iPr_2N)_2PCl$ and $B(C_6F_5)_3$, are comparable to the iminium borate species generated by the reaction shown in Scheme 11. The mechanism for the formation of compound **21** is not known at this time.



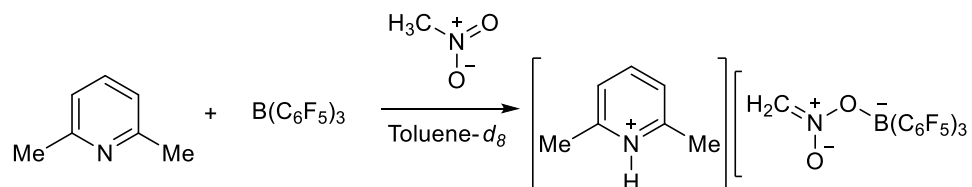
Scheme 11 – Reaction between $B(C_6F_5)_3$ and diisopropylamine.²⁷

Solution state $^{31}P\{^1H\}$ NMR spectroscopic analysis of the residue from the reaction between $(iPr_2N)_2PCl$ and $B(C_6F_5)_3$ revealed the presence of only one phosphorus-containing species, presenting a resonance at $\delta_P = +242.6$ ppm, a chemical shift characteristic of the stable $[(iPr_2N)_2P]^+$ cation.²⁸ ^{11}B NMR spectroscopic analysis of the phosphonium salt revealed a single resonance at $\delta_B = -4.5$ ppm, which is consistent with the reported chemical shift for the $[ClB(C_6F_5)_3]^-$ anion.²⁹ These solution state ^{31}P and ^{11}B NMR spectroscopic data are suggestive of the formation of the phosphonium salt $[(iPr_2N)_2P]^+ [ClB(C_6F_5)_3]^-$, likely as a result of halide abstraction from $(iPr_2N)_2PCl$ by $B(C_6F_5)_3$, a process that the heavier group XIII congener aluminium, as Al_2Cl_6 , is known to do with $(R_2N)_2PCl$ compounds.²⁸

4.3.4 – Reaction of Compounds A and I with Nitromethane

The activation and reduction of NO_2 has been described as a problem that has not yet been solved, but one that has importance in physiological processes and the environmental remediation of NO_x ,³⁰ and one that has much potential for O-atom activation and transfer.³¹ Only a few examples have been reported in the literature that demonstrate the activation of nitro-methane/-ethane molecules (which possess a NO_2 functionality) by FLPs, one example is the 2,2-lutidine-borane FLP that activates $MeNO_2/EtNO_2$ via a C-H activation process (Scheme 12).³¹ As a consequence of the potential synthetic value of the activation of nitroalkanes, and the limited number of examples reported in the literature for nitroalkane

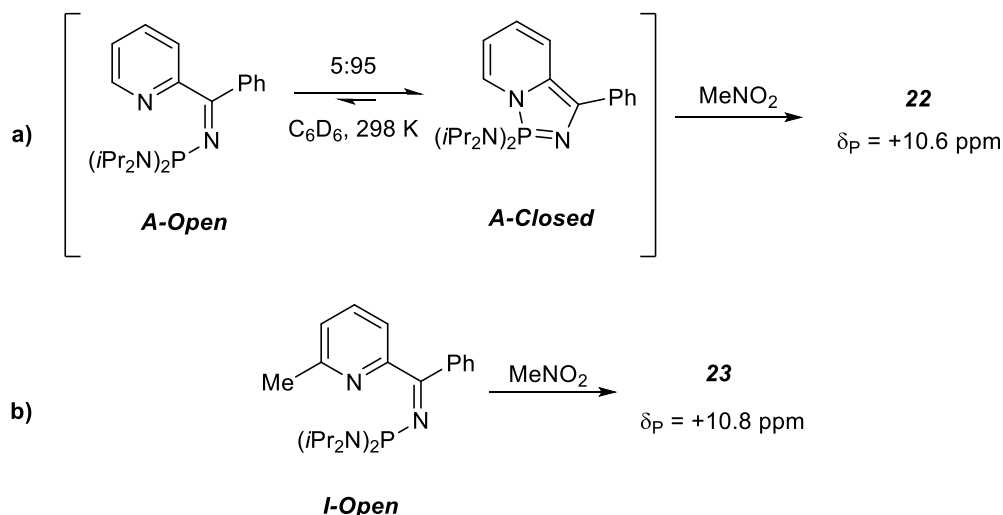
activation by FLPs, it was of interest to probe the behaviour of the air- and moisture-sensitive pyridyl-*N*-phosphinoimine – diazaphosphazole tautomeric system towards anhydrous nitromethane as the “*open*” tautomer has the potential to exhibit FLP behaviour.



Scheme 12 – MeNO₂ activation by a pyridine-borane FLP.³¹

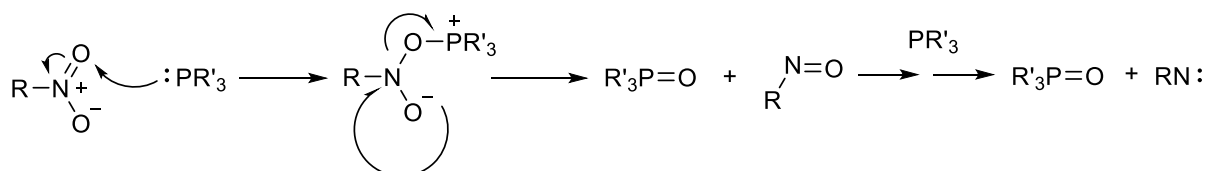
In order to examine the behaviour of the “*open*”-“*closed*” tautomers towards anhydrous nitromethane, compounds **A** and **I** were each reacted with an excess of nitromethane. Compounds **A** and **I** were selected because **A** has the potential to undergo reactions as either **A-Open** or **A-Closed** (5:95, C₆D₆ at 298 K), whereas **I** can only exist, and therefore react, as **I-Open**. Compounds **A** (reaction **a**, Scheme 13) and **I** (reaction **b**, Scheme 13) were each added to an excess of nitromethane and the reactions monitored by solution state ³¹P NMR spectroscopy; full conversion of the starting materials was observed after 1 hour at room temperature, after which time the volatile species were removed from the reaction mixtures under reduced pressure. The residues obtained from reactions **a** and **b** (Scheme 13) were dissolved in CDCl₃, and subsequently analysed by solution state ³¹P NMR spectroscopy. The reaction between compound **A** and MeNO₂ (**a**, Scheme 13) was found to present two major resonances in the ³¹P NMR spectrum, at δ_p = +10.6 ppm (**22**) and +5.1 ppm (chemical shift characteristic of (iPr₂N)₂P(OH))³² in a ratio of 99:1, these species account for ~ 50 % of the total phosphorus-containing species observed by ³¹P NMR spectroscopic analysis. Solution state ³¹P NMR spectroscopic analysis of the residue from the reaction between compound **I** and MeNO₂ (**b**, Scheme 13) revealed two phosphorus-containing species, presenting resonances at δ_p = +10.8 ppm (**23**) and +5.1 ppm ((iPr₂N)₂P(OH)) in a 19:81 ratio. The resonances observed at δ_p = +10.6 ppm and +10.8 ppm for reactions **a** and **b**, respectively, are identical (within experimental error), suggesting that both compounds **A** and **I** undergo similar reactions with MeNO₂. All attempts to isolate individual species by recrystallization and solvent extraction were unsuccessful, which hindered the full characterisation of the major phosphorus-containing species observed by ³¹P NMR spectroscopy.

Diazaphosphazole Tautomers



Scheme 13 – $^{31}\text{P}\{^1\text{H}\}$ NMR spectroscopic chemical shifts of the phosphorus-containing products from the reaction between compounds **A** (a) and **I** (b) with MeNO_2 .

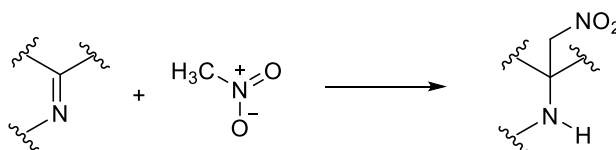
The singlet resonances observed for products **22** and **23** by solution state ^{31}P NMR spectroscopic analysis, at $\delta_{\text{P}} = +10.6$ and $+10.8$ ppm, respectively, appear in a region characteristic of $(\text{R}_2\text{N})_3\text{P}=\text{O}$ species.³³ IR spectroscopic analysis confirmed the presence of $(\text{R}_2\text{N})_3\text{P}=\text{O}$ motifs in both **22** and **23**, which show absorptions at 1021 cm^{-1} and 1160 cm^{-1} , respectively, these absorptions are consistent with $\text{P}=\text{O}$ stretches.³⁴ Phosphorus(III) species are known to deoxygenate nitro (and nitroso) compounds *via* the attack of phosphorus at the $\text{N}=\text{O}$ oxygen centre, followed by the elimination of a phosphine oxide, to give two equivalents of phosphine oxide and a nitrene as shown in Scheme 14.³⁵ The highly reactive nitrene generated is likely to dimerise or undergo a rearrangement to form more stable species.³⁶ A mechanism similar to that shown in Scheme 14 occurring between **A-Open/I-Open** and MeNO_2 would account for the oxidation of the trialkylamino P^{III} centres in **A-Open/I-Open** during its reaction with an excess of MeNO_2 .



Scheme 14 – Generalised reaction pathway for the deoxygenation of organo-nitrates by P^{III} species.³⁵

Analysis of the ^1H NMR spectra recorded for products **22** and **23** revealed broad singlet resonances at $\delta_{\text{H}} = 2.82$ ($\nu_{1/2} = 42$ Hz) and 2.83 ($\nu_{1/2} = 26$ Hz) ppm, respectively, these chemical

shifts are consistent with the signals observed for amine protons, *e.g.* in $(\text{CH}_3\text{CH}_2)_2\text{NH}$ ($\delta_{\text{H}} = 2.68$ ppm, NH),³⁷ and are therefore suggestive of the presence of a R_2NH motif in compounds **22** and **23**. The presence of an N-H bond in **22** and **23** is further confirmed by IR spectroscopic analysis, which shows absorptions in the N-H bending region ($1580 - 1660 \text{ cm}^{-1}$)³⁸ at 1618 cm^{-1} and 1618 cm^{-1} , respectively. Resonances observed for compound **22** at $\delta_{\text{H}} = 4.65$ ppm (d, $J_{\text{HH}} = 13.6$ Hz) and compound **23** at $\delta_{\text{H}} = 4.60$ ppm (d, $J_{\text{HH}} = 13.5$ Hz) present as doublets, the 2D NMR spectra show that these protons couple to the NH proton. The chemical shift of the doublet signals observed for compounds **22** (at $\delta_{\text{H}} = 4.65$ ppm) and **23** (at $\delta_{\text{H}} = 4.60$ ppm), each of which corresponds to two protons (by integration), are consistent with the chemical shift observed for the CH_2 protons in $\text{CH}_3\text{CH}_2\text{NO}_2$ ($\delta_{\text{H}} = 4.45$ ppm, CH_2). These ^1H NMR spectroscopic data suggest that the addition of a molecule of MeNO_2 across the imine bond of the “*open*” tautomers has potentially occurred, as shown in Scheme 15. The addition of nitromethane across an imine bond to generate amine in the manner shown in Scheme 15 is a well-established process.³⁹



Scheme 15 – Generalised MeNO_2 addition across an imine bond.

The NMR spectroscopic data described above suggest that MeNO_2 reacts with compounds **A-Open** and **I-Open** at two positions: one molecule of MeNO_2 is proposed to have added across the $\text{C}=\text{N}$ imine bond, and a second molecule to have been deoxygenated by the phosphorus(III) centre. Based on these spectroscopic data, the products of reactions **a** and **b** (Scheme 13), compounds **22** and **23** (which present singlet resonances at $\delta_{\text{P}} = +10.6$ and $+10.8$ ppm, respectively, by ^{31}P NMR spectroscopic analysis), are proposed to take the forms shown in Figure 10. Mass spectrometric analysis of compounds **22** and **23** revealed fragmentation patterns consistent with the proposed structures of **22** and **23** (two cationic fragments observed are shown in Figure 10).

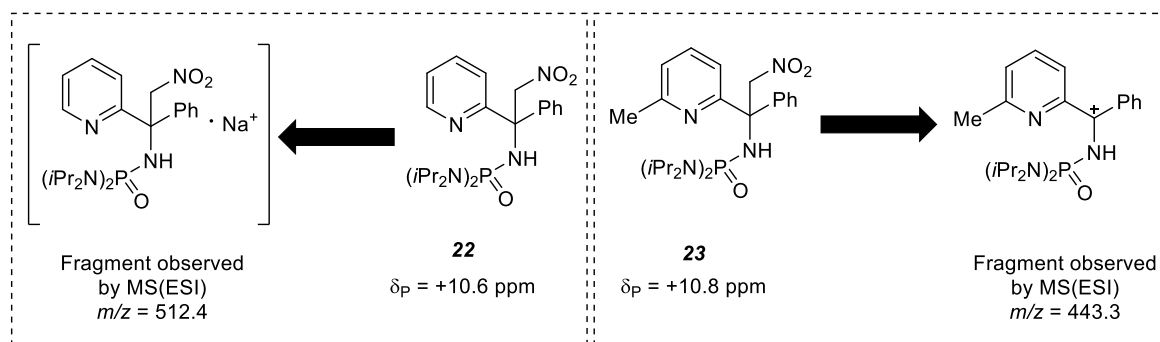
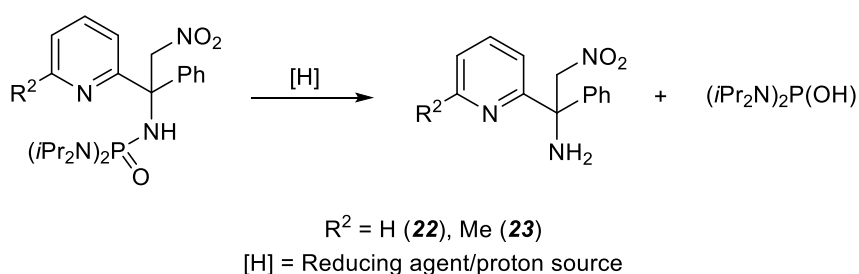


Figure 10 – Compounds **22** and **23** and cationic fragments observed by positive ion electron impact support mass spectrometry.

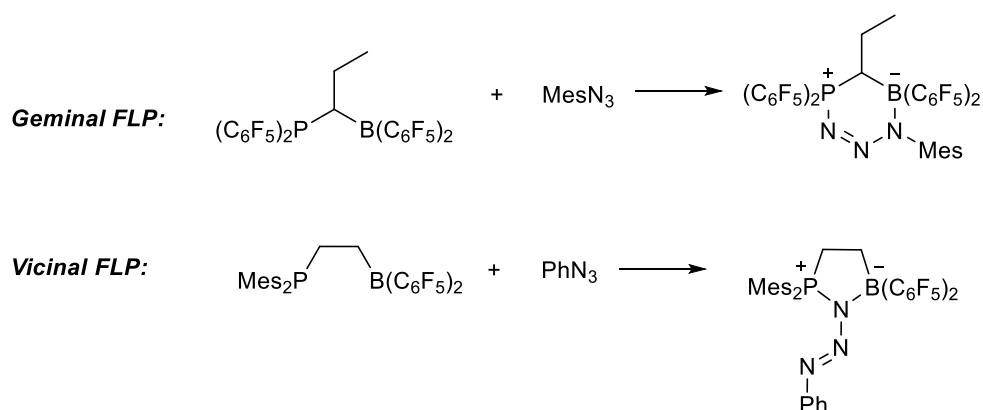
The reactions of *A-Open* and *I-Open* with MeNO₂ are proposed to generate (iPr₂N)₂P(OH) alongside compounds **22** and **23**, respectively. Indeed, (iPr₂N)₂P(OH) was identified as a doublet resonance at δ_P = +5.1 ppm (d, ²J_{PH} = 544.3 Hz) in the ³¹P NMR spectroscopic analysis of the bulk products obtained from reactions **a** and **b** (Scheme 13); this chemical shift is consistent with that reported for (iPr₂N)₂P(OH) in the literature (δ_P = +5.3 ppm, ²J_{PH} = 540.7 Hz).²⁸ Mass spectrometric analysis of the reaction mixtures from both reactions **a** and **b** (Scheme 13) revealed the presence of the H⁺ adduct of (iPr₂N)₂P(OH), as well as the H⁺ adduct of the amine shown in Scheme 16, something that suggests compounds **22** and **23** are somehow broken down into (iPr₂N)₂P(OH) and a primary amine. The nitromethane used in reactions **a** and **b** was dried and distilled prior to use (in accordance with standard literature procedure) in order to remove the small quantities of water, aldehydes and alcohols that commercial nitromethane is known to contain (residual by-products generated during the preparation of MeNO₂ by the gas phase nitration of methane).⁴⁰ If any of the afore mentioned impurities were not fully removed during the MeNO₂ purification process, these would react with compounds **22** and **23** and feasibly give rise to the hydrolysis product observed here, *i.e.* (iPr₂N)₂P(OH).



Scheme 16 – Proposed break up of *A-MeNO*₂ and *I-MeNO*₂.

4.3.5 – Reaction of Compounds **A** and **I** with Trimethylsilylazide

Organoazides are readily transformed into *e.g.* amines, imines and triazoles, and it is possible to incorporate other functionalities within the organic component.⁴¹ These properties of organoazides make them versatile synthetic reagents, “click chemistry” in particular makes extensive use of organoazides, notably for the preparation of pharmaceuticals.^{42,43} Investigations into the reactions of azides with FLPs have the potential of unearthing novel organoazide chemistry that could be of significant value in organic synthesis.

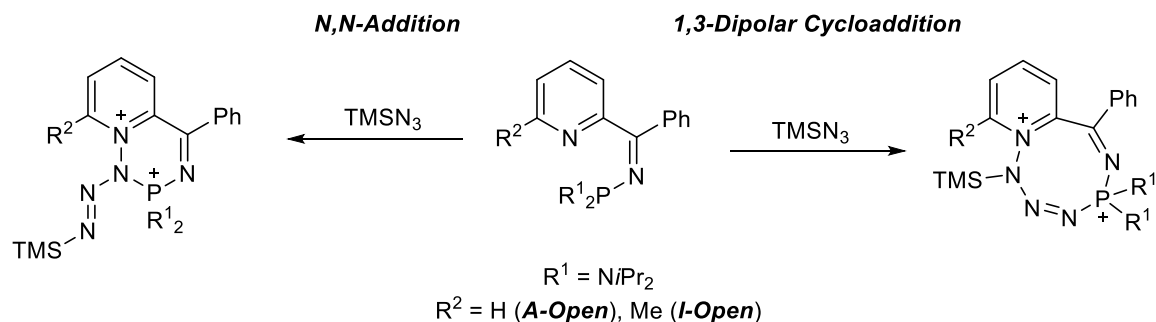


Scheme 17 – 1,3-Addition reactions of organo-azides with FLPs.^{44,45}

Geminal FLPs are known to react cleanly with organo-azides to form six-membered ring compounds, *via* a 1,3-dipolar cycloaddition, which formally results in the insertion of the N₃ motif between the Lewis acid and base centres (Scheme 17).⁴⁴ Vicinal FLPs, however, undergo an *N,N*-addition to organo-azides, to insert just the terminal nitrogen of the azide between the Lewis acid and base centres (Scheme 17).⁴⁵ The different outcomes of the addition reactions shown in Scheme 17 is as a consequence of the preferential formation of the heterocycle with the least ring strain.⁴⁶

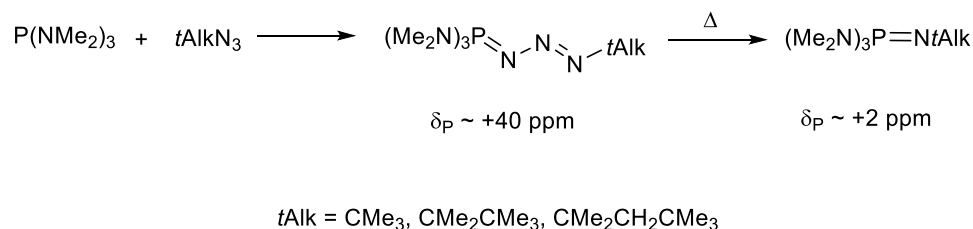
As suggested previously, compounds **A-Open** and **I-Open** have the potential to exhibit FLP character, similar to that described in Scheme 17, and thus could insert an organo-azide molecule, *e.g.* TMSN₃, between the sterically hindered Lewis acidic and Lewis basic centres to form one or other of the fused bicyclic species shown in Scheme 18. If compounds **A-Open** and **I-Open** were to exhibit FLP behaviour, it is most likely that the insertion reaction would

proceed *via* the *N,N*-addition pathway, in preference to the 1,3-dipolar cycloaddition, as the former would generate a less strained fused bicyclic species.



Scheme 18 – Potential *N,N*-addition and 1,3-dipolar cycloaddition of $TMSN_3$ across the Lewis acidic and basic centres of **A-Open** and **I-Open**.

The phosphorus(III) centres in $P(NR_2)_{3-x}(R')_x$ species are known to undergo a Staudinger reaction to form iminophosphorane-amines, as shown in Scheme 19.⁴⁷ Consequently, the presence of P^{III} centres in **A-Open** and **I-Open** raises the possibility of such Staudinger reactions occurring in the presence of an organo-azide.



Scheme 19 – Staudinger reaction between P^{III} centres and bulky organo-azides.⁴⁷

In order to probe the reactivity of multi-functional compounds **A** and **I** with an organo-azide, each species was added to a stoichiometric amount of $TMSN_3$. Solution state ^{31}P NMR spectroscopic analysis of the reaction mixtures revealed several phosphorus-containing species, suggesting that compounds **A** and **I** do not react cleanly with the organo-azide, something likely to result from the presence of more than one functional group in the *P,N*-species. Separation of the phosphorus-containing species by recrystallization and solvent extraction was unsuccessful, and attempts to identify the phosphorus-containing compounds by mass spectrometric analysis was inconclusive. For the reactions of both **A** and **I** with $TMSN_3$, singlet resonances in the $^{31}P\{^1H\}$ NMR spectra were observed at $\delta_P = +5.3$ and $+7.1$ ppm, respectively, which lie broadly in the region characteristic of $(R_2N)_3P=NR'$ species ($\delta_P \sim$

+2 ppm, e.g. $(\text{Me}_2\text{N})_3\text{P}=\text{NtBu}$, $\delta_{\text{P}} = +1.3$ ppm and $(\text{Me}_2\text{N})_3\text{P}=\text{N}(\text{CMe}_2\text{CMe}_3)$, $\delta_{\text{P}} = +1.7$ ppm).⁴⁷ These chemical shifts could potentially correspond the products of a Staudinger reaction between compounds **A-Open**/**I-Open** and TMSN_3 , compounds **24** and **25**, respectively (Figure 11).⁴⁷

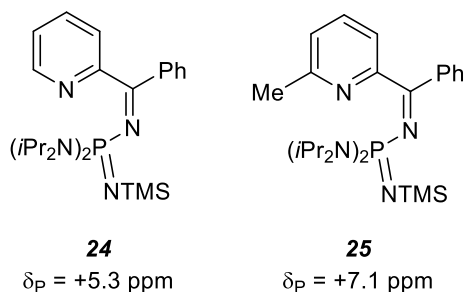
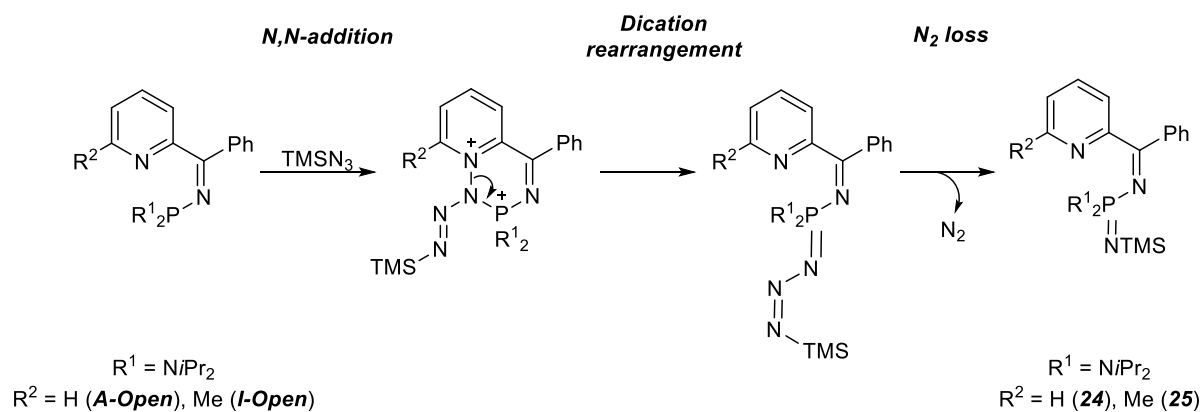


Figure 11 – Proposed Staudinger products of the reactions between **A** / **I** and TMSN_3 .

If compounds **24** and **25** are indeed products of the reactions between **A**/**I** and TMSN_3 , their formation would not necessarily occur *via* a Staudinger-type reaction (Scheme 19). If the “open” tautomers, **A-Open** and **I-Open**, can behave as FLPs and form the dicationic fused bicyclic species shown in Scheme 20, it is unlikely that this dication would be stable. The dicationic species could undergo a rearrangement to form a neutral intermediate, reminiscent of those generated during a Staudinger reaction, which could subsequently lose nitrogen, N_2 , to form **24**/**25** (Scheme 20).



Scheme 20 – Proposed *N,N*-addition of TMSN_3 to “open” and subsequent dication rearrangement and N_2 loss.

4.4 – Summary

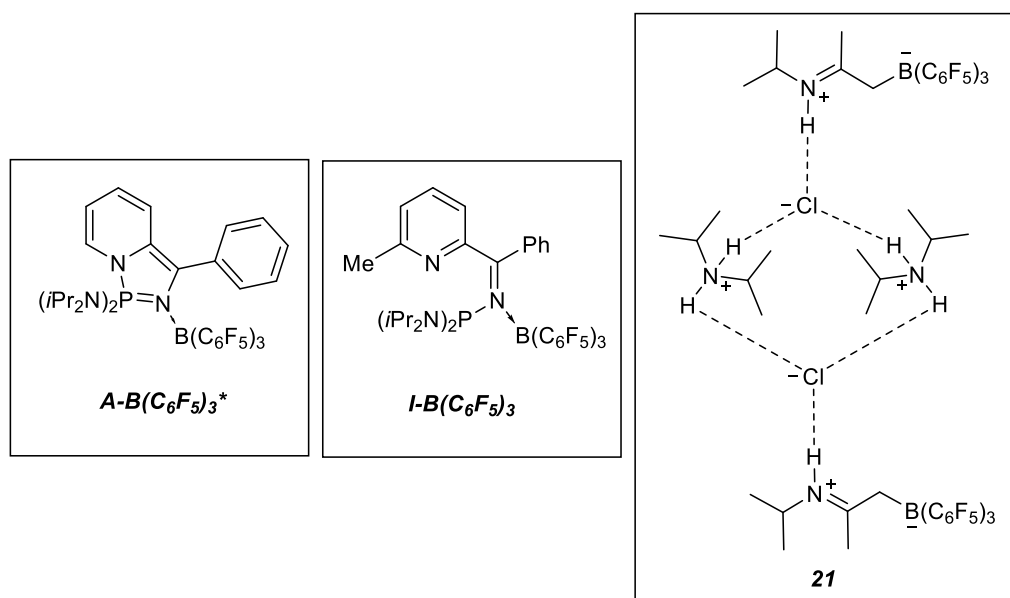
The attempted reactions of compounds **1**, **2**, **4**, **5**, **6** and **8** with elemental selenium were carried out, and all found to yield the tertiary monoselenide of the “open” tautomer. It was found that time taken for full conversion of the starting species to the monoselenide *decreased* with an *increase* in the percentage of “open” pyridyl-*N*-phosphinoimine observed in the starting tautomeric pair; P^{III} oxidation is slowed as the P-N bond in the “closed” tautomer, this bond must be disrupted in order for the reaction between the P^{III} centre and selenium to occur. Compounds **A=Se**,² **I=Se**,² **1=Se**, **4=Se**, **5=Se** and **6=Se**, which differ from each other in the identity and position of the substituents bound to the pyridine ring, all give rise to $|^1J_{PSe}|$ values in within a similar region, 800 – 830 Hz, indicating that the pyridine substituents have only a small impact upon the electronic character of the phosphorus centre. The $|^1J_{PSe}|$ value for compound **2=Se** is notably smaller than those recorded for structural analogues **A=Se** and **8=Se**, this has been attributed to the greater electron density at the P centre arising from the more electron rich conjugated π -system in **2=Se**.

The steric impact of bulky substituents at the phosphorus centre upon the reactions of the interconverting “open”-“closed” tautomeric species with DMAD has been previously studied by Dyer and co-workers. The reaction of compound **1** (with bulky (N*i*Pr₂) phosphorus substituents and a bulky phenyl group at the 4-position on the pyridine moiety) with DMAD was carried out and found to yield two major phosphorus-containing products. It has been proposed that one product of the reaction between **1** and DMAD corresponds to the *pseudo* [2+2] cycloaddition product from the reaction of DMAD at the unhindered C=C bond in the dihydropyridine motif of **1-Closed**. The second major phosphorus-containing product is thought to correspond to the product from the 1,3-dipolar cycloaddition of DMAD at the phosphino-imine motif in **1-Closed**.

The potential FLP character of the pyridyl-*N*-phosphinoimine “open” tautomers of **A** and **I** was probed by investigating their reactivity towards B(C₆F₅)₃, MeNO₂ and TMSN₃, small molecules which are known to react cleanly with previously reported FLP systems. The wealth of reactive positions within compounds **A** and **I**, however, has resulted in the pyridyl-*N*-phosphinoimine

– diazaphosphazole tautomers not exhibiting FLP-type behaviour towards small molecules, but rather the chemistry of their individual components (*i.e.* P^{III}, imine, P=N and dihydropyridine).

Compound **A** is proposed to coordinate to the Lewis acidic boron centre in B(C₆F₅)₃ *via* its iminophosphorane nitrogen (**A-B(C₆F₅)₃**, Figure 12) – a coordination analogous to that previously reported between **A** and AlMe₃. Compound **I-Open**, which cannot cyclise to form the “closed” tautomer as **A-Open** can, was observed to coordinate to the Lewis acidic boron centre in B(C₆F₅)₃ *via* its exocyclic imine nitrogen (**I-B(C₆F₅)₃**, Figure 12). (*i*Pr₂N)₂PCl was also reacted with B(C₆F₅)₃, the reaction was found to yield a complex mixture of products including [(*i*Pr₂N)₂P]⁺ [ClB(C₆F₅)₃]⁻ and compound **21** (Figure 12). Compound **21** is described as comprising of two zwitterionic iminium borate components and two ammonium cations which are held together by weak hydrogen bonds to two bridging chloride anions.



* The structural identity of this species has not been unambiguously determined.

Figure 12 – Compounds **A-B(C₆F₅)₃**, **I-B(C₆F₅)₃** and **21**, products of the reactions of **A**, **I** and (*i*Pr₂N)₂PCl (respectively) with B(C₆F₅)₃.

A-Open and **I-Open** are proposed to have reacted with an excess of MeNO₂ at two positions; at the P^{III} centre and the imine bond, to give compounds **22** and **23**, respectively. Addition of one molecule of MeNO₂ across the exocyclic C=N bond was observed, a reaction characteristic of imines. Oxidation of the P^{III} centre to a P^V phosphine oxide centre was also observed, and

is proposed to have occurred as a result of the deoxygenation of MeNO₂. The breakdown of compounds **22** and **23** to an amine and (*i*Pr₂N)₂P(OH) was seen, this has been attributed to reactions of **22** and **23** with inherent impurities found in MeNO₂ (alcohols, aldehydes and water) that were not successfully removed during the purification process.

Based on ³¹P NMR spectroscopic analysis, TMSN₃ is postulated to react with **A-Open** and **I-Open** to give the (*i*Pr₂N)₂P(NTMS)(NR) species **24** and **25**, respectively. The mechanism for formation of proposed products **24** and **25** is not known – the reaction could proceed *via* a Staudinger-type reaction or *via* the *N,N*-addition of TMSN₃ to **A-Open** / **I-Open** (as FLPs are known to do), followed by the rearrangement of an unstable dicationic intermediate and loss of N₂.

4.5 – Chapter 4 Experimental Details

Standard preparative methods were used throughout, see **Appendix 1** for general experimental considerations.

4.5.1 – Synthesis of the “Open” *P^V* Monoselenides

The following general procedure, a modification of that reported by Dyer and co-workers for the preparation of compounds **A=Se**, **D=Se**, **G=Se** and **I=Se**,^{2,3,4} was used to make compounds **1=Se**, **2=Se**, **4=Se**, **5=Se**, **6=Se** and **8=Se** - variations in temperature, reaction time and solvent are detailed in Table 4. A Young’s NMR tube was charged with starting *P,N*-species (20 mg), elemental selenium (1 equivalent) and solvent (0.8 ml). The reaction mixture was left until full conversion of starting material was observed by ³¹P NMR spectroscopic analysis (Table 4).

	Starting <i>P,N</i> -Species	T (°C)	t (h)	³¹ P{ ¹ H} δ (ppm)	¹ J _{PSe} (Hz)
A=Se	A	50	80	+55.5 ^{a,b}	821
I=Se	I	50	15	+54.3 ^{a,b}	824
D=Se	D	50	96	+66.7 ^{a,d}	842
G=Se	G	25	1	+91.5 ^{c,d}	746
1=Se	1	50	92	+43.3 ^{c,d}	800
2=Se	2	50	84	+76.06 ^{c,d}	746
4=Se	4	50	72	+ 52.8 ^{c,d}	797
5=Se	5	50	5	+54.9 ^{b,d}	828
6=Se	6	50	12	+58.3 ^{c,d}	798
8=Se	8	50	16	+58.4 ^{c,d}	820

Table 4 – Details of experimental procedure for the preparation of the “open” *P^V* monoselenides and the corresponding ³¹P{¹H} NMR data. ^a Measured at 80.9 MHz. ^b Measured in C₆D₆. ^c Measured at 161.9 MHz. ^d Measured in CDCl₃.

4.5.2 – Reaction of Compound **1** with DMAD

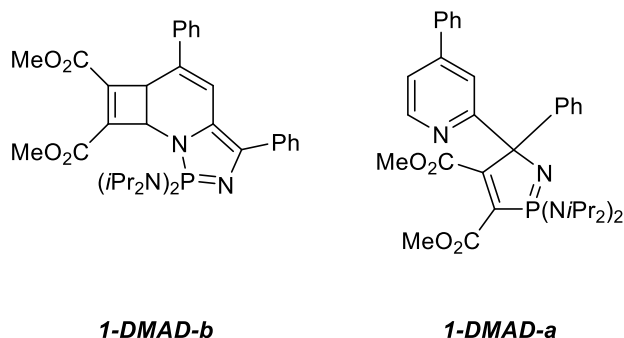


Figure 13 – Proposed products of the reaction between **1** and DMAD, compounds **1-DMAD-a** and **1-DMAD-b**.

A Young's NMR tube was charged with compound **1** (0.040 g, 0.008 mmol), DMAD (0.012 g, 0.008 mmol) and CD₂Cl₂ (0.8 ml). The reaction mixture was heated at 60 °C; full conversion of the starting material was observed by ³¹P{¹H} NMR spectroscopy after 2 days. All attempts at separating the major reaction products were unsuccessful. This reaction was repeated on a larger scale and the same result observed, the phosphorus-containing products were unable to be separated. Compounds **1-DMAD-a** and **1-DMAD-b** have been proposed as possible reaction products (section 4.3.1).

³¹P{¹H} NMR (283.3 MHz, CDCl₃): δ (ppm) = +53.2 (s, **1-DMAD-b**), +90.8 (s, **1-DMAD-a**).

4.5.3 – Synthesis of the B(C₆F₅)₃ Coordination Complexes of Compounds **A**, **I** and (iPr₂N)₂PCI

4.5.3.1 – Proposed Compound **A-B(C₆F₅)₃**

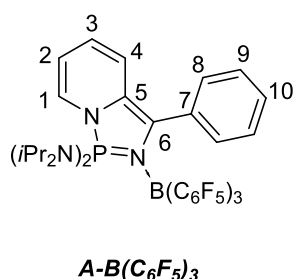


Figure 14 – Proposed product of the reaction between **A** and B(C₆F₅)₃, compound **A-B(C₆F₅)₃**, showing NMR spectroscopic assignment numbering scheme.

To a Young's NMR tube charged with **A** (0.020 g, 0.048 mmol) and a C₆D₆ lock tube, B(C₆F₅)₃ (0.615 g, 3.9% in isopar-E, 0.048 mmol) was added. The mixture was heated at 60 °C; full

conversion of starting material was observed by ^{31}P NMR spectroscopy after 2 hours. The volatile species were removed under reduced pressure at 60 °C.*†

$^{31}\text{P}\{^1\text{H}\}$ NMR (242.7 MHz, C_6D_6): δ (ppm) = +50.5 (s, **A-B(C₆F₅)₃**). ^1H NMR (599.6 MHz, C_6D_6): δ (ppm) = 8.01 (2H, d, $^3J_{\text{HH}} = 5.7$ Hz, CH^8), 7.64 (2H, *pseudo* d, $J_{\text{HH}} = 7.6$ Hz, CH^9), 7.31-7.26 (1H, m, CH^4), 6.91-6.84 (1H, m, CH^{10}), 6.33 (1H, d, $^3J_{\text{HH}} = 8.8$ Hz, CH^1), 5.35-5.29 (1H, m, CH^3), 5.24 (1H, *pseudo* d, $J_{\text{HH}} = 8.77$ Hz, CH^2), 2.94-2.98 (4H, m, $\text{CH}(\text{CH}_3)_2$), 0.70 (12H, d, $^3J_{\text{HH}} = 6.7$ Hz, CH_3), 0.59 (12H, d, $^3J_{\text{HH}} = 6.7$ Hz, CH_3). ^{11}B NMR (128.4 MHz, C_6D_6): δ (ppm) = -7.8 (s). ^{19}F NMR (376.4 MHz, C_6D_6): δ (ppm) = -133.0 (d, $^3J_{\text{FF}} = 27$ Hz, *o*-F), -157.6 (t, $^3J_{\text{FF}} = 22$ Hz, *p*-F), -163.7 (dt, $^3J_{\text{FF}} = 22$ Hz, $^3J_{\text{FF}} = 27$ Hz, *m*-F).

4.5.3.2 – Compound **I-B(C₆F₅)₃**

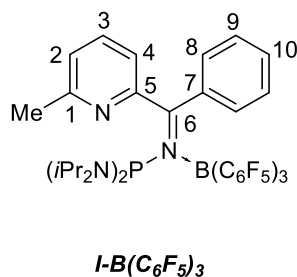


Figure 15 – Proposed product of the reaction between **I** and $\text{B}(\text{C}_6\text{F}_5)_3$, compound **I-B(C₆F₅)₃**, showing NMR spectroscopic assignment numbering scheme.

To a Young's NMR tube charged with **I** (0.020 g, 0.047 mmol) and a C_6D_6 lock tube, $\text{B}(\text{C}_6\text{F}_5)_3$ (0.615 g, 3.9% in isopar-E, 0.047 mmol) was added. The mixture was heated at 60 °C, full conversion of starting material was observed (by ^{31}P NMR spectroscopy) after 2 hours. The volatile species were removed under reduced pressure at 60 °C.‡

$^{31}\text{P}\{^1\text{H}\}$ NMR (242.7 MHz, C_6D_6): δ (ppm) = +52.7 (s, **I-B(C₆F₅)₃**). ^1H NMR (599.6 MHz, C_6D_6): δ (ppm) = 7.93 (2H, d, $^3J_{\text{HH}} = 7.6$ Hz, CH^8), 7.64 (2H, *pseudo* t, $J_{\text{HH}} = 7.6$ Hz, CH^9), 7.15 (1H, t, $^3J_{\text{HH}} = 1.3$ Hz, CH^{10}), 6.69 (1H, t, $^3J_{\text{HH}} = 7.8$ Hz, CH^4), 6.56 (1H, *pseudo* t, $^3J_{\text{HH}} = 7.8$ Hz, CH^3), 6.30 (1H, d, $^3J_{\text{HH}} = 7.4$ Hz, CH^2), 3.90-3.80 (4H, m, $\text{CH}(\text{CH}_3)_2$), 2.13 (3H, s, C^1CH_3), 0.86-0.82 (24H, m,

* The full removal of isopar-E could not be achieved. $^{13}\text{C}\{^1\text{H}\}$ NMR spectroscopic analysis revealed residual isopar-E in far greater quantities than the product meaning that this spectrum could not be assigned. Upon repeating the reaction on a larger scale, isopar-E still could not be fully removed.

† Mass spectrometric analysis by electron impact and ASAP were found to be unsuitable for this species.

‡ Mass spectrometric analysis by electron impact and ASAP were found to be unsuitable for this species.

CHCH₃). ¹³C{¹H} NMR (150.8 MHz, C₆D₆): δ (ppm) = 175.7 (d, ²J_{CP} = 26.9 Hz, C⁶), 160.0 (s, C¹), 149.0 (s, C⁵/C⁷), 146.4 (s, C⁵/C⁷), 129.8 (s, C⁹), 128.5 (s, C¹⁰), 128.3 (d, ⁴J_{CP} = 5 Hz, C⁸), 128.0 (s, C³), 127.9 (d, ⁴J_{CP} = 7 Hz, C⁴), 124.2 (s, C²), 41.8 (s, CHCH₃), 23.6 (s, C¹CH₃), 23.3 (s, CHCH₃), 22.5 (s, CHCH₃). ¹¹B NMR (128.4 MHz, C₆D₆): δ (ppm) = -8.3 (s). ¹⁹F NMR (376.4 MHz, C₆D₆): δ (ppm) = -133.4 (d, ³J_{FF} = 31 Hz, *o*-F), -156.9 (t, ³J_{FF} = 22 Hz, *p*-F), -163.78 (dt, ³J_{FF} = 22 Hz, ³J_{FF} = 31 Hz, *m*-F).

4.5.3.3 – Reaction of (iPr₂N)₂PCl with B(C₆F₅)₃

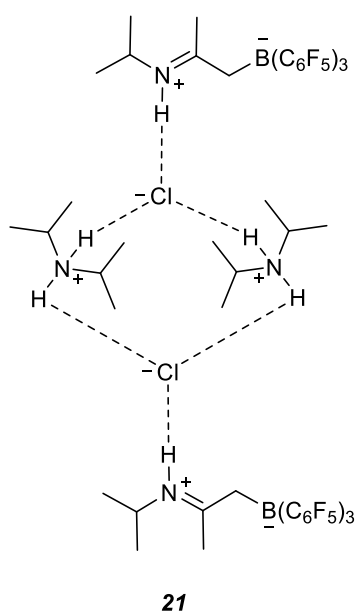


Figure 16 – Compound 21.

To (iPr₂N)₂PCl (0.100 g, 0.375 mmol), a solution of B(C₆F₅)₃ (4.921 g, 3.9% in isopar-E, 0.375 mmol) was added. The mixture was stirred at room temperature for 6 hours then the volatile species removed under reduced pressure at 60 °C. Orange crystals of compound **21** suitable for an X-ray diffraction study were obtained from slow evaporation of C₆D₆ from an NMR sample of the reaction residue (0.095 g, 0.0638 moles, 17 %).

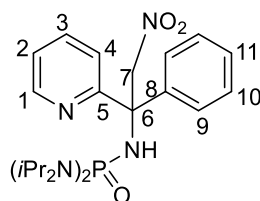
21 Data: ¹¹B NMR (128.4 MHz, C₆D₆): δ (ppm) = -13.0 (s). ¹⁹F NMR (376.4 MHz, C₆D₆): δ (ppm) = -132.1 (d, ¹J_{FF} = 30 Hz, *o*-F), -160.70 (t, ³J_{FF} = 21 Hz, *p*-F), -165.2 (dt, ³J_{FF} = 21 Hz, ³J_{FF} = 30 Hz, *m*-F). MS (EI⁺) *m/z*: 170.1 ([C₆H₁₆NH]⁺+MeOH).

[(iPr₂N)₂P]⁺ [ClB(C₆F₅)₃]⁻ data: ³¹P{¹H} NMR (283.3 MHz, C₆D₆): δ (ppm) = +245.2 (s), +243.5 (s). ¹¹B NMR (128.4 MHz, C₆D₆): δ (ppm) = -11.0 (s). ¹⁹F NMR (376.4 MHz, C₆D₆): δ (ppm) =

-132.1 (d, $^3J_{FF} = 30$ Hz, *o*-F), -160.7 (t, $^3J_{FF} = 21$ Hz, *p*-F), -165.2 (dt, $^3J_{FF} = 21$ Hz, $^3J_{FF} = 30$ Hz, *m*-F). MS (EI⁺) *m/z*: 249.5 ([C₁₂H₂₈N₂PH]+NH₄⁺).

4.5.4 – Reactions of Compounds A and I with Nitromethane

4.5.4.1 – Reaction of Compound A with MeNO₂



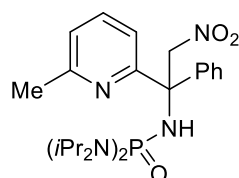
22

Figure 17 – Proposed product of the reaction between A and MeNO₂, compound 22, showing NMR spectroscopic assignment numbering scheme.

To a Young's NMR tube charged with A (0.040 g, 0.097 mmol) and a C₆D₆ lock tube, MeNO₂ (1.0 ml) was added. The reaction mixture was allowed to stand at room temperature for 24 hours; full consumption of starting material was observed by ³¹P NMR spectroscopic analysis after this time. The volatile species were removed under reduced pressure, CDCl₃ (0.8 ml) added to the residue and the sample subsequently analysed. MS (EI⁺) *m/z*: 512.4 ([C₂₅H₄₀N₅O₃PNa]⁺).

IR (ATR) ν (cm⁻¹): 2932 (w, Ar-H str), 2279 (m, Ar-H str), 1618 (w, N-H str), 1453 (w, N-O str), 1021 (w, P=O str). ³¹P{¹H} NMR (283.3 MHz, CDCl₃): δ (ppm) = +10.6 (s, **22**). ¹H NMR (699.7 MHz, CDCl₃): δ (ppm) = 8.58 (1H, d, $^3J_{HH} = 4.9$ Hz, CH¹), 7.91-7.88 (2H, m, CH⁹), 7.61 (1H, d, $^3J_{HH} = 7.8$ Hz, CH⁴), 7.25-7.22 (1H, m, CH³), 7.18-7.12 (3H, m, CH¹⁰ & CH¹¹), 6.80 (1H, dd, $^3J_{HH} = 7.7$ Hz, $^3J_{HH} = 4.8$ Hz, CH²), 4.65 (2H, d, $^4J_{HH} = 13.6$ Hz, CH⁷₂), 3.80-3.71 (4H, m, CHCH₃), 2.82 (1H, broad s, $\nu_{1/2} = 42$ Hz, NH), 1.41 (12H, d, $^3J_{HH} = 6.8$ Hz, CH₃), 1.36 (12H, d, $^3J_{HH} = 6.8$ Hz, CH₃). ¹³C{¹H} NMR (176.0 MHz, CDCl₃): δ (ppm) = 148.2 (s, C¹), 134.2 (s, C³), 129.9 (s, C⁹), 124.2 (s, C⁴), 123.0 (s, C²), 45.9 (d, $^1J_{CP} = 4.8$ Hz, CHCH₃), 22.8 (s, CH₃), 22.8 (s, CH₃), 22.5 (s, C⁷). Quaternary carbons were not observed in the ¹³C{¹H} NMR due to the long relaxation times associated with quaternary carbon centres.

4.5.4.2 – Reaction of Compound *I* with MeNO₂



23

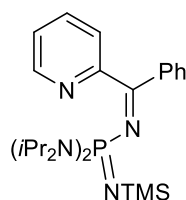
Figure 18 – Proposed product of the reaction between *I* and MeNO₂, compound **23**.

To a Young's NMR tube charged with *I* (0.040 g, 0.094 mmol) and a C₆D₆ lock tube, MeNO₂ (0.8 ml) was added. The reaction mixture was left for 24 hours at room temperature; complete consumption of starting material was observed by ³¹P NMR spectroscopic analysis after this time. The volatile species were removed under reduced pressure, CDCl₃ (0.8 ml) added to the residue and the sample analysed using solution state spectroscopic methods. MS (EI⁺) *m/z*: 443.3 ([C₂₅H₄₀N₄OP]⁺), 258.1 ([C₁₄H₁₆N₃O₂]⁺).

IR (ATR) ν (cm⁻¹): 2279 (m, Ar-H str), 1617 (w, N-H str), 1329 (m, N-O str), 1160 (w, P=O str). ³¹P{¹H} NMR (283.3 MHz, C₆D₆): δ (ppm) = +10.8 (s, **23**), +5.1 (s, (iPr₂N)₂P(OH)). Separation of the phosphorus-containing species by recrystallization and solvent extraction was unsuccessful (even upon repeating the reaction on a larger scale), the small proportion of **23** observed in contrast to (iPr₂N)₂P(OH) (19:81, respectively) meant that the ¹H and ¹³C{¹H} NMR spectra for compound **23** could not be assigned.

4.5.5 – Reactions of Compounds *A* and *I* with TMSN₃

4.5.5.1 – Reaction of *A* with TMSN₃



24

Figure 19 – Proposed product of the reaction between *A* and TMSN₃, compound **24**.

To a solution of *A* (0.020 g, 0.049 mmol) in CDCl₃ (0.8 ml) in a Young's NMR tube, TMSN₃ (0.006 g, 0.049 mmol) was added. The reaction was found to reach completion after 3 hours

at room temperature (by ^{31}P NMR spectroscopic analysis). ^{31}P NMR spectroscopic analysis of the reaction mixture revealed a complex mixture of phosphorus-containing products which (even upon repeating the reaction on a larger scale) were unable to be separated and fully characterised. Compound **24** has been proposed as a possible product (see section 4.3.5 for full discussion).

$^{31}\text{P}\{^1\text{H}\}$ NMR (283.3 MHz, CDCl_3): δ (ppm) = +5.3 (s, **24**).

4.5.5.2 – Reaction of *I* with TMSN_3

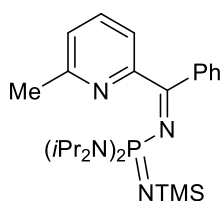


Figure 20 - Proposed product of the reaction between *I* and TMSN_3 , compound **25**.

To a solution of *I* (0.020 g, 0.047 mmol) in CDCl_3 (0.8 ml) in a Young's NMR tube, TMSN_3 (0.005 g, 0.047 mmol) was added. The mixture was found to reach completion after 3 hours at room temperature (by ^{31}P NMR spectroscopic analysis). ^{31}P NMR spectroscopic analysis of the reaction revealed a complex mixture of phosphorus-containing products which (even upon repeating the reaction on a larger scale) were unable to be separated. Compound **25** has been proposed as a possible product (see section 4.3.5 for full discussion).

$^{31}\text{P}\{^1\text{H}\}$ NMR (283.3 MHz, CDCl_3): δ (ppm) = +7.1 (s, **25**).

Chapter 4 References

- ¹ P. W. Dyer, J. Fawcett and M. J. Hanton, *J. Organomet. Chem.*, 2005, **690**, 5264-5281.
- ² D. A. Smith, A. S. Batsanov, K. Miqueu, J. –M. Sotiropoulos, D. C. Apperley, J. A. K. Howard and P. W. Dyer, *Angew. Chem. Int. Ed.*, 2008, **47**, 8674-8677.
- ³ D. A. Smith, PhD Thesis, Durham University, 2009.
- ⁴ D. A. Smith, A. S. Batsanov, K. Costuas, E. Edge, D. C. Apperley, D. Collision, J. –F. Halet, J. A. K. Howard and P. W. Dyer, *Angew. Chem. Int. Ed.*, 2010, **49**, 7040-7044.
- ⁵ D. A. Smith, A. S. Batsanov, M. A. Fox, A. Beeby, D. C. Apperley, J. A. K. Howard and P. W. Dyer, *Angew. Chem.*, 2009, **121**, 9273-9277.
- ⁶ R. Davies in *Handbook of Chalcogen Chemistry: New Perspectives in Sulfur, Selenium and Tellurium*, 2007, RSC Publishing.
- ⁷ D. G. Gilheany, *Chem. Rev.*, 1994, **94**, 1339-1374.
- ⁸ W. McFarlane and D. S. Rycroft, *Dalton Trans.*, 1973, 2162-2166.
- ⁹ S. M. Godfrey, S. L. Jackson, C. A. McAuliffe and R. G. Pritchard, *J. Chem. Soc. Dalton Trans.*, 1997, 4499-4502.
- ¹⁰ S. M. Godfrey, S. L. Jackson, C. A. McAuliffe and R. G. Pritchard, *J. Chem. Soc. Dalton Trans.*, 1998, 4201-4204.
- ¹¹ W. McFarlane and D. S. Rycroft, *J. Chem. Soc. Dalton Trans.*, 1973, 2162-2166.
- ¹² J. Bellan, M. R. Marre, M. Sanchez and R. Wolf, *Phosphorus and Sulfur*, 1981, **12**, 11-18.
- ¹³ J. Bellan, M. Sanchez, M. R. Marre-Mazières and A. Murillo Beltran, *Bull. Soc. Chim. Fr.*, 1985, 491-495.
- ¹⁴ R. M. Acheson, G. Paglietti and P. A. Tasker, *J. Chem. Soc. Perkin Trans.*, 1974, **1**, 2496-2500.
- ¹⁵ R. M. Acheson, *Chem. Heterocycl. Compd.*, 1976, **12**, 837-845.
- ¹⁶ F. Lavigne, A. El Kazzi, Y. Escudié, E. Maerten, T. Kato, N. Saffon-Merceron, V. Branchadell, F. P. Cossío and A. Baceiredo, *Chem. Eur. J.*, 2014, **20**, 12528-12536.
- ¹⁷ M. A. Dureen and D. W. Stephan, *Organometallics*, 2010, **29**, 6594.
- ¹⁸ G. C. Welch, T. Holtrichter-Roessmann and D. W. Stephan, *Inorg. Chem.*, 2008, **47**, 1904-1906.
- ¹⁹ G. C. Welch, R. Prieto, M. A. Dureen, A. J. Lough, O. A. Labeodan, T. Holtrichter-Roessmann and D. W. Stephan, *Dalton Trans.*, 2009, 1559-1570.

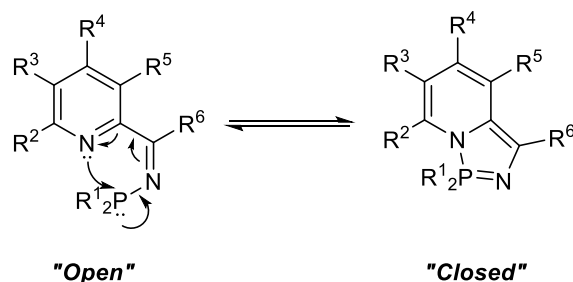
- ²⁰ S. J. Geier, A. L. Gille, T. M. Gilbert and D. W. Stephan, *Inorg. Chem.*, 2009, **48**, 10466-10474.
- ²¹ N. Burford, R. E. v H. Spence and J. F. Richardson, *J. Chem. Soc. Dalton Trans.*, 1991, 1615-1619.
- ²² C. W. Heitsch, *Inorg. Chem.*, 1965, **4**, 1019-1024
- ²³ F. Focante, P. Mercandelli, A. Sironi and L. Resconi, *Coord. Chem. Rev.*, 2006, **250**, 170-188.
- ²⁴ G. Desiraju and T. Steiner in *The Weak Hydrogen Bond: In Structural Chemistry and Biology*, 2001, Oxford University Press.
- ²⁵ J.M. Blackwell, W.E. Piers, M. Parvez and R. McDonald; *Organometallics*, 2002, **21**, 1400-1407.
- ²⁶ J. March in *Advanced Organic Chemistry Fourth Edition*, 1992, Wiley-Interscience.
- ²⁷ V. Sumerin, F. Schulz, M. Nieger, M. Leskel, T. Repo and B. Rieger, *Angew. Chem. Int. Ed.*, 2008, **47**, 6001-6003.
- ²⁸ A. H. Cowley and R. A. Kemp, *Chem. Rev.*, 1985, **85**, 367-382.
- ²⁹ B. E. Bosch, G. Erker, R. Fröhlich and O. Meyer, *Organometallics*, 1997, **16**, 5449-5456.
- ³⁰ B. C. Sanders, S. M. Hassan and T. C. Harrop, *J. Am. Chem. Soc.*, 2014, **136**, 10230-10233.
- ³¹ T. H. Warren and G. Erker, *Top. Curr. Chem.*, 2013, **334**, 219–238.
- ³² E. H. Wong, M. M. Turnbull, K. D. Hutchinson, C. Valdez, E. J. Gabe, F. L. Lee and Y. Le Paget, *J. Am. Chem. Soc.*, 1988, **110**, 8422-8428.
- ³³ R. S. Edmundson in *CRC Handbook of Phosphorus-31 Nuclear Magnetic Resonance Data*, 1991, CRC Press Inc.
- ³⁴ D. G. Gilheany in *The Chemistry of Organophosphorus Compounds Volume 2, Phosphine oxides, sulphides selenides and tellurides*, 1992, John Wiley & Sons.
- ³⁵ J. I. G. Cadogan, *Q. Rev. Chem. Soc.*, 1968, **22**, 222-251. J. I. G. Cadogan, M. Cameron-Wood, R. K. Mackie and R. J. G. Searle, *J. Am. Chem. Soc.*, 1965, 4831-4837. J. I. G. Cadogan and A. Cooper, *J. Chem. Soc. B*, 1969, 883-885.
- ³⁶ B. A. Shainyan, A. V. Kuzmin and M. Y. Moskalik, *Computational and Theoretical Chemistry*, 2013, **1006**, 52-61.
- ³⁷ C. Altona, J. H. Ippel, A. J. A. Westra Hoekzema, C. Erkelens, M. Groesbeek and L. A. Donder, *MRC*, 1989, **27**, 564-576.
- ³⁸ G. Socrates in *Infrared and Raman Characteristic Group Frequencies: Tables and Charts*, 2001, John Wiley & Sons.

- ³⁹ H. Erlenmeyer and V. Oberlin, *Helv. Chim. Acta.*, 1947, **30**, 1329-1335.
- ⁴⁰ W. L. F. Armarego and C. L. L. Chai in *Purification of Laboratory Chemicals Sixth Edition*, 2009, Elsevier Inc.
- ⁴¹ S. Brase, C. Gil, K. Knepper and V. Zimmermann, *Angew. Chem., Int. Ed.* 2005, **44**, 5188–5240.
- ⁴² M. Kohn and R. Breinbauer, *Angew. Chem. Int. Ed.*, 2004, **43**, 3106–3116.
- ⁴³ X. Huang and J. T. Groves, *ACS Catal.*, 2016, **6**, 751–759.
- ⁴⁴ A. Stute, G. Kehr, R. Fröhlich and G. Erker, *Chem. Comm.*, 2011, **47**, 4288-4290.
- ⁴⁵ C. M. Mömning, G. Kehr, B. Wibbeling, R. Fröhlich and G. Erker, *Dalton Trans.*, 2010, **39**, 7556-7564.
- ⁴⁶ E. V. Anslyn and D. A. Dougherty in *Modern Physical Organic Chemistry*, 2006, University Science.
- ⁴⁷ A. V. Alexandrova, T. Mašek, S. M. Polyakova, I. Císařová, J. Saame, I. Leito and I. M. Lyapkalo, *Eur. J. Org. Chem.*, 2013, 1811–1823.

Chapter 5 – Summary, Conclusions and Project Outlook

Chapter 5 – Summary, Conclusions and Project Outlook

5.1 – Thesis Summary

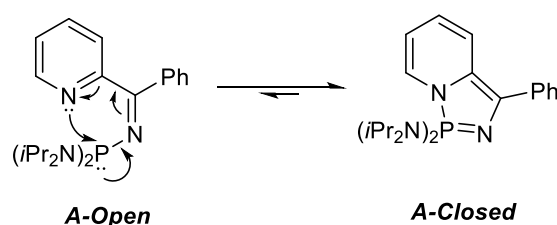
Scheme 1 – Reversible *pseudo*-1,5-electrocyclisation of the interconverting "open" and "closed" tautomers.

Dyer and co-workers have previously reported that the "open" pyridyl-*N*-phosphinoimine and "closed" diazaphosphazole species shown in Scheme 2 exist in a dynamic equilibrium. The cyclisation of the "open" tautomer has been proposed to proceed *via* a *pseudo*-1,5-electrocyclisation (Scheme 2).^{1,2} The extent of cyclisation observed is intimately linked to the nature of the R¹-R⁶ substituents (Scheme 1), as a consequence of their electronic and steric impact upon the interaction between the pyridine nitrogen and phosphorus centres, an interaction that is required for cyclisation to occur.

This thesis has reported a fundamental study into how the modification of the central pyridyl-imine scaffold and solvent polarity impact upon the extent of Lewis adduct ("closed") formation. The "open" pyridyl-*N*-phosphinoimine tautomer can be regarded as an intramolecular FLP whereby the formation of the Lewis adduct ("closed" diazaphosphazole) can be precluded by modification of the R¹-R⁶ substituents (Scheme 2). FLPs have been extensively studied over the past decade and have been shown to be of extreme value for small molecule capture and activation. This thesis has presented preliminary studies that have been carried out to probe the reactivity of the "open" and "closed" tautomers and their potential FLP character.

5.1.1 – Synthetic, Reactivity and Structural Studies of Novel Pyridyl-*N*-Phosphinoimine – Diazaphosphazole Tautomers

This thesis has built upon the work previously carried out by Dyer and co-workers into the factors which impact upon the position of the “open”-“closed” equilibrium shown in Scheme 2. Compound **A** (Scheme 2), previously reported by Dyer and co-workers,¹ was prepared, and the ratio of **A-Open**:**A-Closed** as a function of solvent polarity was probed at 298 K by ³¹P NMR spectroscopy. It was found that as the polarity of the solvent was increased, that the proportion of the more polar tautomer, **A-Closed**, observed (relative to **A-Open**) by ³¹P{¹H} NMR spectroscopic analysis, increased.



Scheme 2 – Interconverting tautomers **A-Open** and **A-Closed** showing reversible *pseudo*-1,5-electrocyclisation of the dynamic “open” and “closed” tautomers.

This thesis has reported the successful preparation and characterisation of the series of structurally analogous pyridyl-*N*-phosphinoimine - diazaphosphazole tautomeric systems shown in Figure 1. These compounds have been prepared in order investigate the stereoelectronic impact of the R³-R⁶ substituents (Scheme 1) upon the position of the “open”-“closed” equilibrium. Suitable crystals of compounds **1-Closed**, **2-Closed** and **4-Closed** were studied by X-ray crystallographic methods and found to be structurally comparable to one another (with respect to key bond lengths and bond angles) as well as structurally analogous species previously reported in the literature (*e.g.* **A-Closed**).¹ Compounds **1-Closed**, **2-Closed** and **4-Closed** can be regarded as comprising of a planar central fused bicyclic motif made up of a dihydropyridine ring and a five-membered heterocycle containing alternating single and double bonds.

The differing “open”-“closed” equilibrium positions observed for compounds **1**, **2**, **4**, **5**,* **6** and **8**[†] (Figure 1) was examined alongside their structural differences. Substitution of groups \neq H at the R³-R⁵ positions (Scheme 1) on the pyridine scaffold has been demonstrated to have a marked impact upon the percentage of the “closed” tautomer observed. Electron donating substituents at the 4-position (R⁴), such as Ph (**1**), favour cyclisation. When R⁵ \neq H (R⁵ = Me, **6**) and the R⁴ substituent is bulky (*t*Bu, **4**), however, the steric impact of these groups precludes cyclisation. It is proposed that the introduction of a conjugating R⁴ group (R⁴ = NMe₂, **5**^{*}) highly disfavours cyclisation of the pyridyl-*N*-phosphinoimine, however, the reason behind this observation remains elusive. The modification of the R⁶ substituent (phenyl (**A**),¹ anthracenyl (**B**),² 4,4'-biphenyl (**2**) and mesityl (**8**[†])) was found to have a noticeable impact upon the position of the “open”-“closed” equilibrium position as a result of a combination of steric and electronic factors.

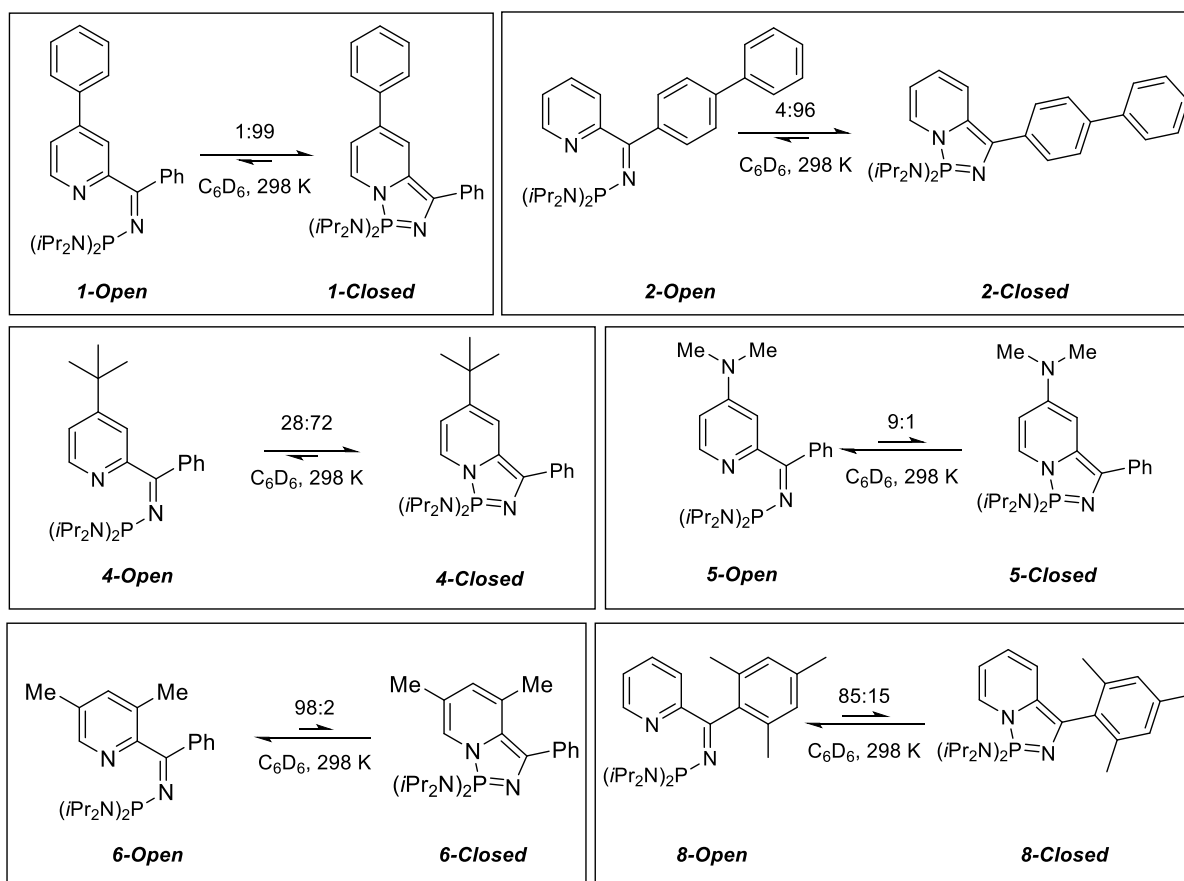


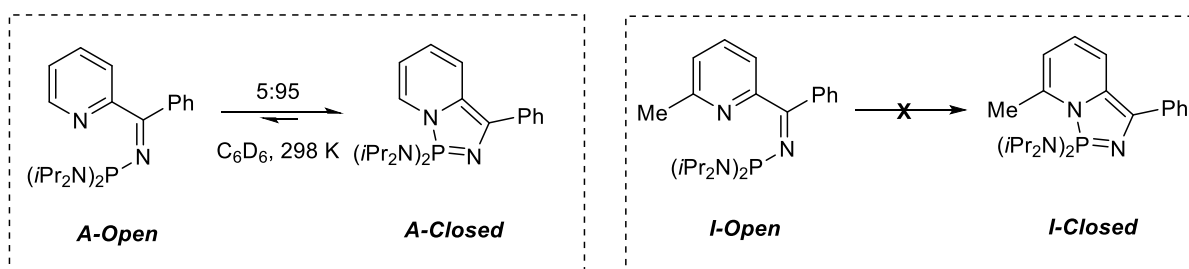
Figure 1 – Novel pyridyl-*N*-phosphinoimine-diazaphosphazole tautomeric species reported in this thesis.*[†]

* Compound **5** was found to readily decompose. Isolation of a pure sample of **5** was unsuccessful which prevented full spectroscopic analysis and unambiguous assignment of compounds **5-Open** and **5-Closed**.

[†] Compound **8** was found to readily decompose, both as a solution in hexane and as a solid, when stored under N₂. Isolation of a pure sample of **8** was unsuccessful which prevented full spectroscopic analysis and unambiguous assignment of compounds **8-Open** and **8-Closed**.

5.1.1.1 – Chemical Reactivity of Pyridyl-*N*-Phosphinoimine – Diazaphosphazole Tautomeric Pairs

The chemical reactivity of the novel pyridyl-*N*-phosphinoimine – diazaphosphazole tautomeric pairs reported in this work (Figure 1) towards elemental selenium has been demonstrated. As has been reported previously by Dyer and co-workers for structurally analogous species,^{1,2} the formation of the P^V-monoselenide of the “open” tautomer was observed for novel compounds **1**, **2**, **4**, **5**,* **6** and **8**[†]. Compounds **A=Se**, **I=Se**, **1=Se**, **4=Se**, **5=Se** and **6=Se**, which differ from each other in the identity and position of the substituents bound to the pyridine ring, were found to exhibit $|^1J_{PSe}|$ values in a similar region (800-830 Hz), indicating that the pyridine substituents have only a small impact upon the electronic character of the phosphorus centre. The $|^1J_{PSe}|$ value for compound **2=Se** (746 Hz) is notably smaller than those for structural analogues **A=Se** (821 Hz) and **8=Se** (820 Hz), this has been attributed to the greater electron density at the phosphorus centre arising from the more electron rich conjugated π -system in **2=Se**. It was also found that time taken for full conversion of the starting species to form the monoselenide *decreased* with an *increase* in the percentage of the “open” tautomer observed for the starting *P,N*-system; P^{III} oxidation is slowed as the P-N bond in the “closed” tautomer must be disrupted in order for a reaction between the phosphorus centre and selenium to occur.



Scheme 3 – Compounds A and I.¹

The chemical reactivity of compounds **A** (**A-Open:A-Closed** 5:95, C₆D₆ at 298 K) and **I** (**I-Open** 100 %, C₆D₆ at 298 K), Scheme 3, as well as their potential FLP character, has been investigated with respect to their behaviour towards B(C₆F₅)₃, nitromethane and trimethylsilylazide. Compounds **A** and **I** were found not to exhibit any FLP behaviour, but instead to display chemical reactivity characteristic on their various functionalities, *i.e.* the iminophosphorane, imine and P^{III} components:

- *Iminophosphorane reactivity of A-Closed*: The iminophosphorane functionality in compound **A-Closed** was found to coordinate to the Lewis acidic boron centre of $B(C_6F_5)_3$ (**A-B(C₆F₅)₃**,[‡] Figure 2).
- *Imine reactivity of A-Open and I-Open*: In the presence of an excess of $MeNO_2$, addition across the imine C=N bonds in **A-Open** and **I-Open** is proposed to be accompanied by the deoxygenation of $MeNO_2$ to yield the amine-phosphine oxide species **22** and **23**[§], respectively (Figure 2). Compound **I-Open** was also found to coordinate *via* its exocyclic imine nitrogen centre to the Lewis acidic boron centre in $B(C_6F_5)_3$ (**I-B(C₆F₅)₃**, Figure 2).
- *P^{III} reactivity of A-Open and I-Open*: $TMSN_3$ is proposed to react with the P^{III} centres in **A-Open** and **I-Open** in a Staudinger-type reaction, to give *N,N*-addition of $TMSN_3$, followed by a rearrangement reaction and loss of N_2 to form $(iPr_2N)_2P(NTMS)(NR)$ species, **24** and **25**,^{**} respectively (Figure 2).

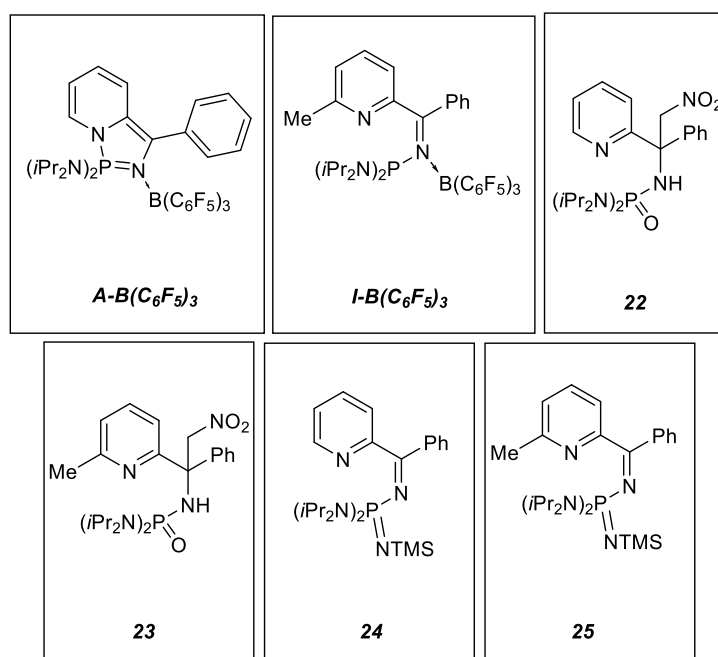


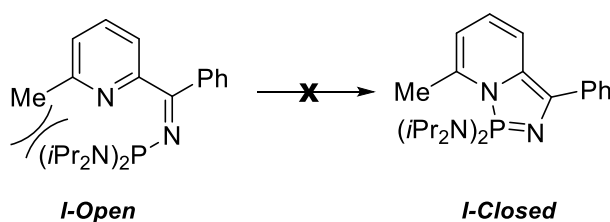
Figure 2 – Proposed products of the reactions of **A** and **I** with $B(C_6F_5)_3$, $MeNO_2$ and $TMSN_3$.^{‡,§,**}

[‡] Residual isopar-E solvent dominated the $^{13}C\{^1H\}$ NMR spectrum, resonances corresponding to proposed compound **A-B(C₆F₅)₃** were not observed. Mass spectrometric analysis of the product of the reaction between **A** and $B(C_6F_5)_3$ did not identify any fragments consistent with proposed compound **A-B(C₆F₅)₃**, this could be a result of the low volatility of **A-B(C₆F₅)₃**.

[§] Isolation of a pure sample of proposed compound **23** was unsuccessful which prevented full spectroscopic analysis and unambiguous assignment of compound **23**.

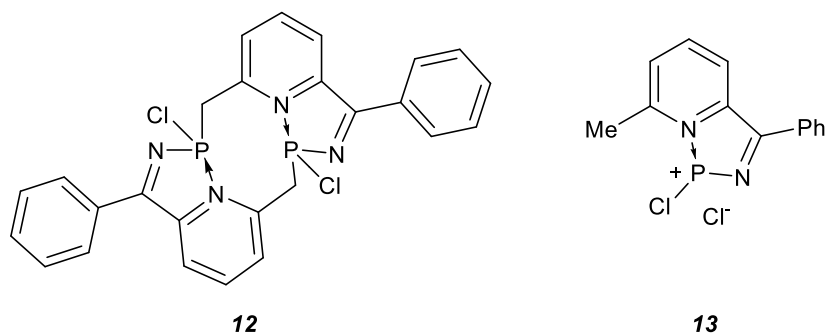
^{**} Isolation of a pure sample of proposed compounds **24** and **25** was unsuccessful which prevented full spectroscopic analysis and unambiguous assignment of these species.

5.1.2 – Synthetic, Reactivity and Structural Studies of Macrocycle, **12** and Phosphenium Salt, **13**

Scheme 4 – Compound *I*.¹

Dyer and co-workers have previously demonstrated the electronic (and steric) impact of the phosphorus substituents (R^1 , Scheme 1) upon the extent of Lewis adduct formation, *i.e.* electron withdrawing groups promote cyclisation.¹ It has been previously reported that compound *I-Open* is unable to undergo cyclisation to form *I-Closed* as a result of an unfavourable steric interaction imposed by the methyl substituent at the R^2 position (Scheme 3).¹ As an extension of the fundamental study into the factors affecting the extent of Lewis adduct formation (section 5.1.1), this thesis has described attempts to prepare the structural analogue of compound *I*, where $R^1 = \text{Cl}$, in order probe whether formation of the Lewis adduct could occur if the bulk of the electrophilic phosphorus substituents was reduced (compared to the (NiPr_2) groups in *I*).

Upon carrying out the reaction between 6-methyl-2-cyanopyridine, PhLi and PCl_3 , a novel reactivity was unearthed. The formation of an intramolecularly base-stabilised phosphenium salt, **13** (Figure 3, identified by experimental and computational NMR spectroscopic studies), was seen by solution- and solid-state ^{31}P NMR spectroscopic studies. It has been postulated that two equivalents of the salt species, **13**, undergo two sequential C-H insertion reactions, reminiscent of those observed for phosphenium cations,³ to yield compound **12**, a novel macrocyclic species (Figure 3), which was identified by an X-ray crystallographic study.

Figure 3 – Compounds **12** and **13**.

5.1.2.1 – Chemical Reactivity of Macrocyclic, **12** and Phosphenium Salt, **13**

The emergence of the unprecedented products **12** and **13** (Figure 3) from the reaction between 6-methyl-2-cyanopyridine, PhLi and PCl_3 prompted an investigation into their chemical reactivity. The chloride substituents in both species were found to be unreactive, and unable to be substituted by other anions ($[\text{BPh}_4]^-$, $[\text{B}(\text{C}_6\text{F}_5)_4]^-$, $[\text{PF}_6]^-$, $[\text{AlCl}_4]^-$), indicating their strong association to the phosphorus centres. The ease of oxidation of the P^{III} centres in **12** and **13** was found to be dependent on the nature of the oxidant. Both compounds **12** and **13** possess an intramolecular $\text{N} \rightarrow \text{P}$ dative interaction, this interaction must be disrupted in order for oxidation of the P^{III} centres to occur. This dative interaction in compound **13** is much stronger than in **12**, as the pyridine nitrogen acts to stabilise a cationic phosphenium centre. The $\text{N} \rightarrow \text{P}^+$ interaction in **13** therefore requires higher energy to disrupt than the $\text{N} \rightarrow \text{P}$ interaction in **12**. Both compounds **12** and **13** were oxidised by an excess of DMF, the oxidation process is proposed to yield $\text{R}_3\text{P}=\text{O}$ species (compounds **14**^{††} and **15a/15b**, Figure 4) *via* a Vilsmeier-Haack-type mechanism. Whilst macrocyclic compound **12** was found to react with two equivalents of elemental selenium to form the diselenide **12=Se** (Figure 4), the phosphenium species, **13**, was unreactive towards selenium as the formation of the $\text{P}=\text{Se}$ bond is thought not to compensate for the energy required to disrupt the strong $\text{N} \rightarrow \text{P}^+$ interaction.

^{††} Isolation of a pure sample of proposed compound **14** was unsuccessful which prevented full spectroscopic analysis and unambiguous assignment of the product of the reaction between **12** and DMF. The presence of residual, highly viscous DMF in the crude reaction product is thought to have prevented meaningful mass spectrometric analysis.

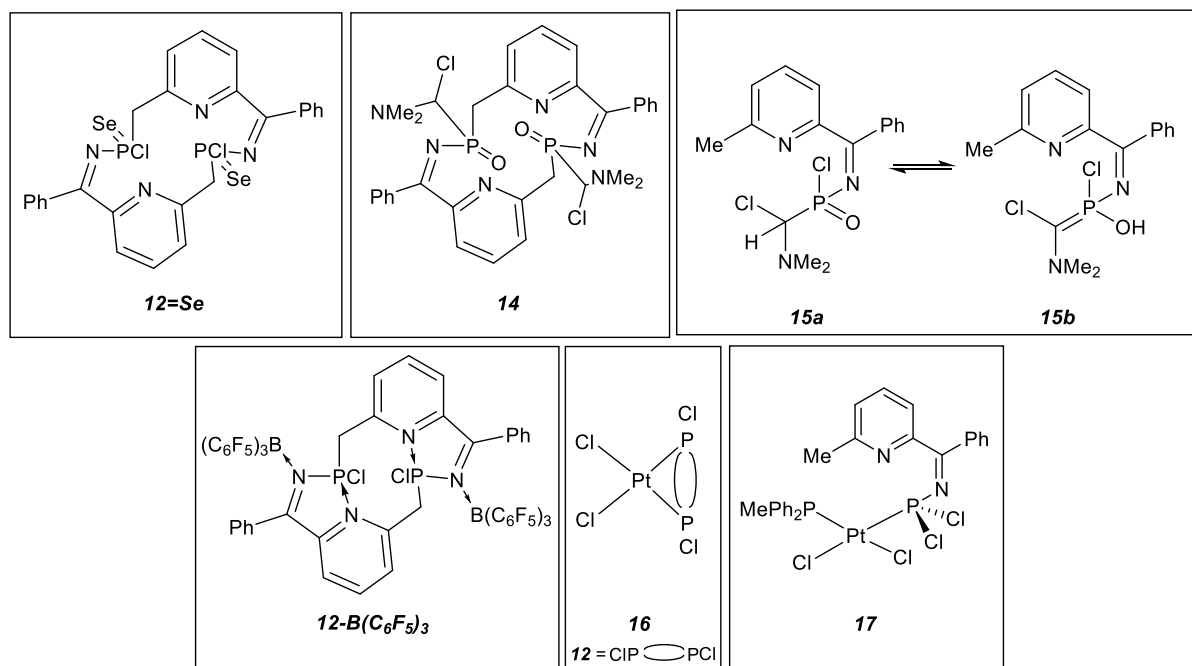


Figure 4 - Proposed products of the reactions of **12** and **13** with Se, DMF, B(C₆F₅)₃ and *trans*-[Pt(PPh₂Me)Cl(μ-Cl)]₂.^{††,§§}

The presence of a strongly associated, unbound chloride anion in compound **13** is thought to sterically preclude the ability of **13** to coordinate to the Lewis acidic boron centre in B(C₆F₅)₃, whereas for compound **12**, there is no such steric barrier, and N→B coordination is seen between the imine nitrogen centre in **12** and the boron centre of B(C₆F₅)₃ (**12-B(C₆F₅)₃**),^{††} Figure 4). In the presence of *trans*-[Pt(PPh₂Me)Cl(μ-Cl)]₂, both compounds **12** and **13** are proposed to have cleaved the platinum dimer and form new platinum complexes. Compound **12** is proposed to act as a R₂PCl species in the presence of *trans*-[Pt(PPh₂Me)Cl(μ-Cl)]₂, to form proposed compound **16**^{§§} (*cis*-[PtCl₂(**12**)], Figure 4, where **12** behaves as a κ²-P,P ligand) and *cis*-[PtCl₂(PPh₂Me)₂]. Compound **13** was found also to cleave the platinum dimer, *trans*-[Pt(PPh₂Me)Cl(μ-Cl)]₂, to give two equivalents of compound **17** (Figure 4), *cis*-[PtCl₂(PPh₂Me)(**13**)], where **13** behaves as a κ¹-P ligand. In both cases, the reactions of **12** and **13** with *trans*-[Pt(PPh₂Me)Cl(μ-Cl)]₂ yielded the more thermodynamically stable *cis* complexes.

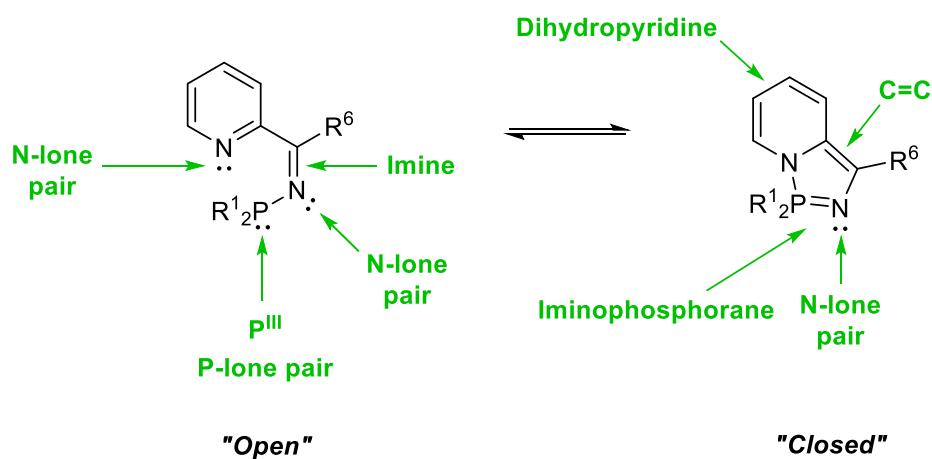
^{††} The inability to fully remove residual isopar-E and the low solubility of proposed compound **12-B(C₆F₅)₃** prevented full spectroscopic characterisation and unambiguous assignment of the identity of the product of the reaction between **12** and B(C₆F₅)₃.

^{§§} Isolation of a pure sample of proposed compound **16** was unsuccessful which prevented its full spectroscopic characterisation and unambiguous assignment.

5.2 – Conclusions

A series of pyridyl-*N*-phosphinoimines and diazaphosphazoles have been successfully prepared, and the external (*e.g.* solvent) and structural factors that impact upon the position of the dynamic “open”-“closed” tautomeric equilibrium investigated. The reactivity of the “open” and “closed” tautomers has been investigated in the hope of unearthing FLP-type behaviour of the “open” species. It was found, however, that the wealth of reactive positions within these dynamic valence tautomers has resulted in their not exhibiting FLP-type behaviour towards small molecules, but rather some of the rich and diverse chemistry characteristic of its individual components (*i.e.* P^{III}, imine, P=N and C=C bonds).

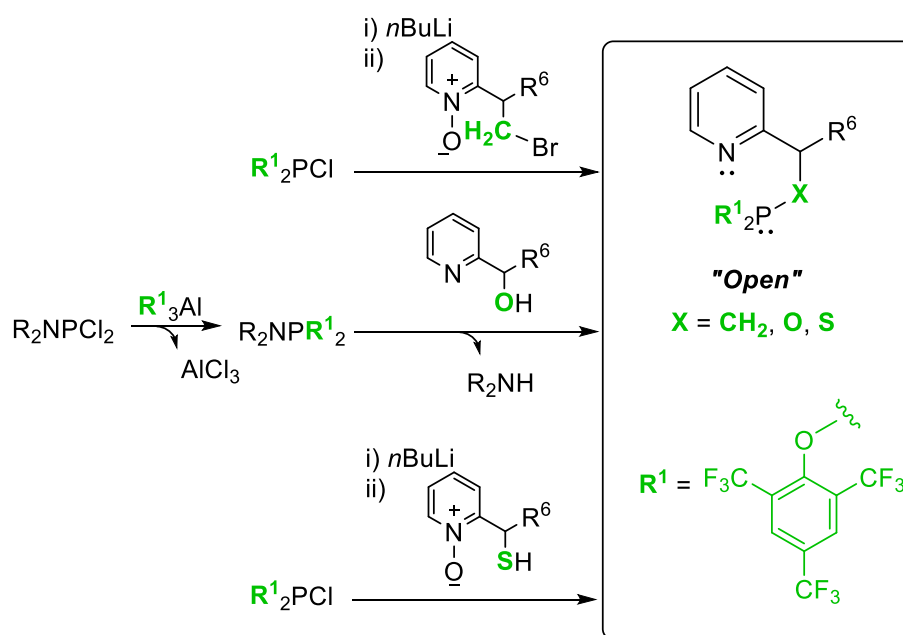
5.3 – Future Project Outlook



Scheme 5 – Multi-functionality of the “open” and “closed” tautomers.

The “open” pyridyl-*N*-phosphinoimine (Scheme 5) has the potential to act as an FLP when cyclisation to form the “closed” species is precluded (either sterically or electronically), as the Lewis basic character of the pyridine nitrogen and Lewis acidic nature of the phosphorus centre (when R¹ is electron withdrawing) is retained. The various functionalities of the “open” and “closed” tautomers are highlighted in Scheme 5, and this work has demonstrated how these functional groups dominate the chemistry of these dynamic tautomers. Looking to the future, in order to encourage FLP behaviour of the pyridyl-*N*-phosphinoimines, modifications should be made to the exocyclic component (remote to the Lewis acid and base centres) to

eliminate the possibility for reactions to occur at the imine or the P^{III} centre, or for coordination *via* an exocyclic heteroatom possessing a lone pair to take place.



Scheme 6 - Proposed modification of the pyridyl-*N*-phosphinoimine "open" species.

Two proposed structural modifications to the previously studied pyridyl-*N*-phosphinoimines are shown in Scheme 6, alongside possible synthetic approaches for the preparation of the target compounds. The removal of the imine functionality, and its replacement with a group/substituent (**X**, Scheme 6) bound to the carbon centre α to the pyridine ring by a *single* bond is proposed. The replacement of the imine C=N double bond with a C-X single bond removes a potential reaction position remote to the Lewis basic and acidic centres. The **X** substituent must be able to form stable bonds to both sp^3 carbon and P^{III} centres, and be unable to expand its valence shell. With a chemically stable **X** substituent, the possibility for a *pseudo*-1,5-electrocyclisation process to form a "closed" species (Scheme 1) is eliminated, and therefore allows for the retention of the Lewis acid-base character of the phosphorus and pyridine nitrogen centres. **X** = **CH₂**, **O** and **S** are proposed, however, the introduction of the chalcogens, which possess a lone pair, opens up the possibility of coordination *via* the **X** centre to Lewis acidic centres (such as boron in B(C₆F₅)₃). The strongly electron withdrawing, bulky **R¹** substituent shown in Scheme 6 has been chosen because its bulk should act to sterically block the lone pair on the P^{III} centre from reacting, as well as disfavour interaction between the electrophilic P^{III} centre and the nucleophilic pyridine nitrogen. The removal of

the imine functionality and blocking of the electrophilic phosphorus centre are proposed with the aim of ensuring that the Lewis acid and base centres retain their acceptor-donor character, and are the most reactive positions within the molecule to maximise the potential for the species to exhibit FLP behaviour.

Chapter 5 References

- ¹ D. A. Smith, A. S. Batsanov, K. Miqueu, J. –M. Sotiropoulos, D. C. Apperly, J. A. K. Howard and P. W. Dyer, *Angew. Chem. Int. Ed.*, 2008, **47**, 8674-8677.
- ² D. A. Smith, PhD Thesis, Durham University, 2009.
- ³ A. H. Cowley and R. A. Kemp, *Chem. Rev.*, 1985, **85**, 367-382.

Appendices

Appendix 1 – General Experimental Considerations

Laboratory coat, safety spectacles and appropriate gloves were worn at all times during experimental work. COSHH and hazard assessments were carried out prior to all experimental work and experiments were carried out in a fume-hood. Waste was separated and disposed of in the appropriate manner (in accordance with the rules set out in Appendix F of Durham University's Department of Chemistry health and safety policy).

Due to the sensitive nature of materials used, all experiments and manipulations were carried out either using standard Schlenk and cannula techniques (and glassware) or using a glove box (Saffron Scientific), both under an atmosphere of dry oxygen-free nitrogen and ambient laboratory lighting, unless otherwise stated. Reagents were purchased from Sigma Aldrich, Alfa Aesar and TCI Europe. Solid reagents, where necessary, were recrystallized and dried under vacuum prior to use. All gases were passed over a drying column (silica/CaCO₃/P₂O₅) prior to use. Liquid reagents were dried, distilled and degassed prior to use. Solvents were dried and purified using an Innovative Technologies SPS facility and degassed before use. 1,2-Dimethoxyethane was distilled from sodium, benzophenone and degassed before use. Pentane was dried over calcium hydride and distilled and degassed prior to use.

Samples for solid- and solution-state NMR spectroscopic analysis were prepared under an atmosphere of dry, oxygen-free nitrogen using either standard NMR tubes or tubes fitted with J. Young's tap valves. C₆D₆, CD₂Cl₂, C₆D₅CD₃ and C₄D₈O were dried over calcium hydride, distilled and degassed prior to use. CDCl₃ was dried over P₂O₅, passed over an alumina column and degassed before use. Solution phase NMR spectra were run on a Varian Mercury 400, Bruker Advance 400, Varian Inova 500, Varian VNMR5-600 and Varian VNMR5-700 at temperatures of 298 K, unless stated otherwise. All chemical shifts were referenced with respect to the ¹³C shift of the solvent (¹³C NMR), the protio impurities in the deuterated solvent (for ¹H NMR) or to an external aqueous standard of 85% H₃PO₄ (for ³¹P NMR). The residual protio impurities of the deuterated solvents are as follows (ppm): C₆D₆ 7.15 (s); CD₂Cl₂ 5.32 (t); C₆D₅CD₃ 2.08 (quintet), 6.97 (quintet), 7.01 (s), 7.09 (m); C₄D₈O 1.72 (s), 5.38 (s); CDCl₃

7.26 (s). The ^{13}C chemical shifts for deuterated NMR solvents are as follows (ppm): C_6D_6 128.6 (s); CD_2Cl_2 54.0 (quintet); $\text{C}_6\text{D}_5\text{CD}_3$ 137.9 (s), 129.2 (t), 128.3 (t), 125.5 (t), 20.4 (sept); $\text{C}_4\text{D}_8\text{O}$ 67.7 (quintet), 25.5 (quintet); CDCl_3 77.4 (t). ^1H and ^{13}C NMR spectra were, when necessary, assigned with the aid of COSY, HMBC, HSQC and NOESY experiments. All spectra are reported with chemical shifts in ppm and coupling constants in Hz.

Variable temperature NMR experiments were carried out by Dr A. Kenwright, Dr J. A. Aguilar Malavia, Ms R. Belda-Vidal and Mrs C. F. Heffernan. Solid-state NMR spectra were recorded by Dr D. Apperley and Mr F. Markwell of the EPSRC National Solid-State NMR Research Service at Durham University on a Varian VNMRS instrument and chemical shifts referenced to H_3PO_4 (^{31}P). Computational calculations were carried out by Dr M. A. Fox from the Chemistry Department of Durham University. Mass spectra were recorded by the Durham University Mass Spectrometry Service. ASAP mass spectra were recorded using a Waters LCT Premier XE mass spectrometer equipped with an ASAP ionisation source and reported as m/z . Elemental analyses were carried out by Dr E. Unsworth of the Analytical Services Department of the Chemistry Department of Durham University. Single crystal X-ray analyses were performed by Dr A. Batsanov of the Durham University X-ray crystallography service.

Where appropriate, the progress of reactions was monitored by solution state ^{31}P and $^{31}\text{P}\{^1\text{H}\}$ NMR spectroscopy. Relative ratios of phosphorus-containing species were determined by the integration of corresponding resonances in the $^{31}\text{P}\{^1\text{H}\}$ NMR spectrum

Appendix 2 – Key NMR Spectra for Chapter 2

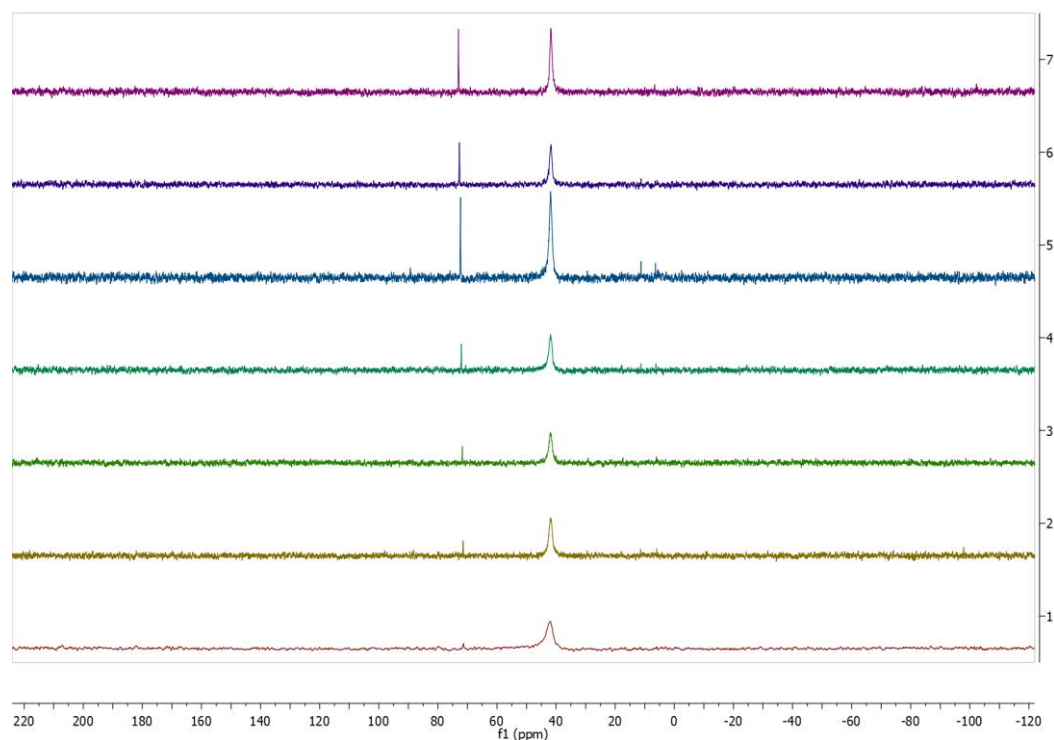


Figure 1 - Stacked $^{31}\text{P}\{^1\text{H}\}$ VT NMR spectra recorded for compound 1 (in $\text{C}_6\text{D}_5\text{CD}_3$ at 202.3 MHz) at: 25 °C (1), 30 °C (2), 40 °C (3), 50 °C (4), 60 °C (5), 70 °C (6) and 80 °C (7).

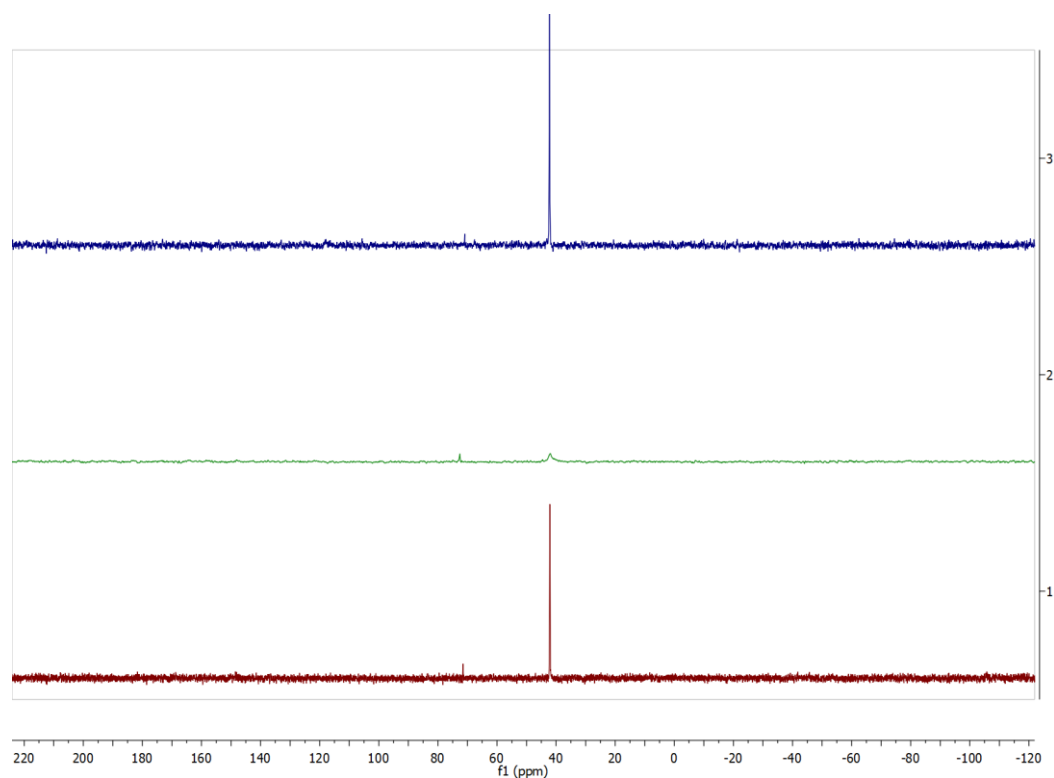


Figure 2 - Stacked $^{31}\text{P}\{^1\text{H}\}$ VT NMR spectra recorded for compound 2 (in $\text{C}_6\text{D}_5\text{CD}_3$ at 202.3 MHz) at: 25 °C (1), 60 °C (2) and 0 °C (3).

Appendix 2 – Key NMR Spectra for Chapter 2

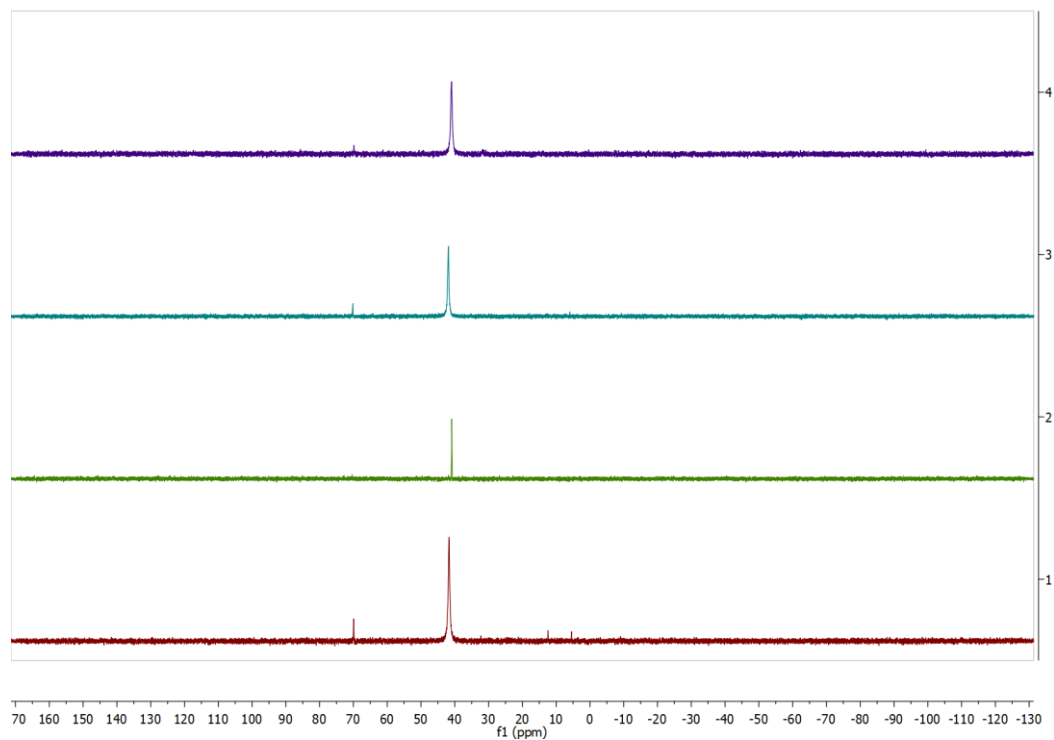


Figure 3 - Stacked $^{31}\text{P}\{^1\text{H}\}$ NMR spectra recorded for compound A (298 K at 162.0 MHz) in: 1,2-DCE (1), hexane (2), DCM (3) and PhBr (4).

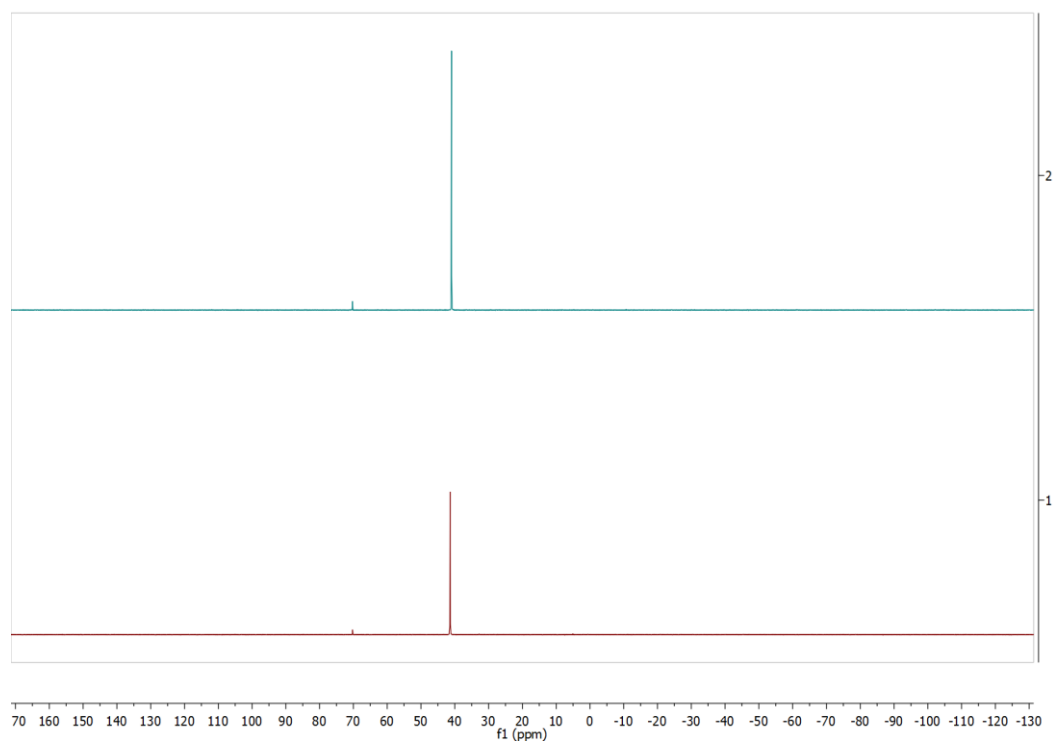


Figure 4 - Stacked $^{31}\text{P}\{^1\text{H}\}$ NMR spectra recorded for compound A (298 K at 162.0 MHz) in: THF (1) and toluene (2).

Appendix 3 – X-Ray Crystallographic Study of 4-Dimethylamino-2-Pyridinecarboxamide

4-Dimethylamino-2-pyridinecarboxamide was prepared as outlined in section 2.7.8. Crystals suitable for an X-ray crystallographic study were grown from a DCM solution at $-30\text{ }^{\circ}\text{C}$. The X-ray molecular structure of 4-dimethylamino-2-pyridinecarboxamide is shown in Figure 1 and selected structural data are shown in Table 1.

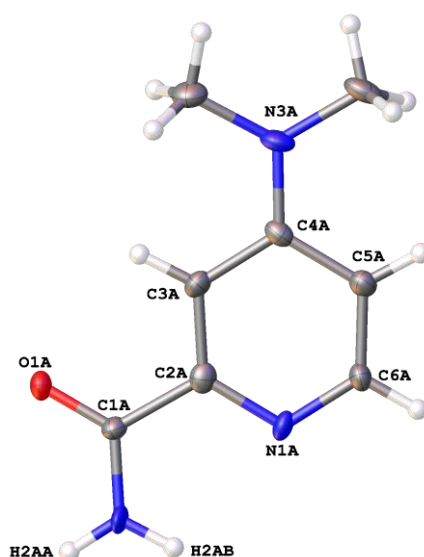


Figure 1 - X-ray molecular structure of 4-dimethylamino-2-pyridinecarboxamide. Thermal ellipsoids are drawn at the 50% probability level.

Bond Distances (Å)		Bond Angles (°)	
N3A-C4A	1.3631	N3A-C4A-C3A	121.89
C4A-C3A	1.4052	N3A-C4A-C5A	122.00
C3A-C2A	1.3825	C5A-C4A-C3A	116.08
C2A-N1A	1.3487	C4A-C3A-C2A	119.82
N1A-C6A	1.3371	C3A-C2A-N1A	123.97
C6A-C5A	1.3788	C2A-N1A-C6A	115.99
C5A-C4A	1.4115	N1A-C6A-C5A	124.70
C2A-C1A	1.5005	C6A-C5A-C4A	119.42
C1A-O1A	1.2267	C2A-C1A-N2A	117.00
C1A-N2A	1.3319	C2A-C1A-O1A	120.11
N2A-H2AB	0.8800	O1A-C1A-N2A	122.88
N2A-H2AA	0.8800	H2AB-H2A-H2AA	120.00

Table 1 - Selected bond length and angle data for 4-dimethylamino-2-pyridinecarboxamide. See Figure 1 for atom labels.

The bond lengths and angles observed for the pyridine motif in 4-dimethylamino-2-pyridinecarboxamide are consistent with those observed for pyridine itself,^{*} indicating that this heterocyclic moiety can be regarded as a true pyridine ring. The length of the amide C1A-O1A double bond is consistent with the average C=O double bond length (1.21 Å).[†] Examination of the long-range packing of 4-dimethylamino-2-pyridinecarboxamide in the solid state shows that pairs of molecules hydrogen bond with each other as shown in Figure . The hydrogen bonding between molecules of 4-dimethylamino-2-pyridinecarboxamide is consistent with the experimental solution state NMR spectroscopic data, notably the inequivalence of the amide NH₂ protons and the through space interaction between all protons in the NOESY NMR spectrum.

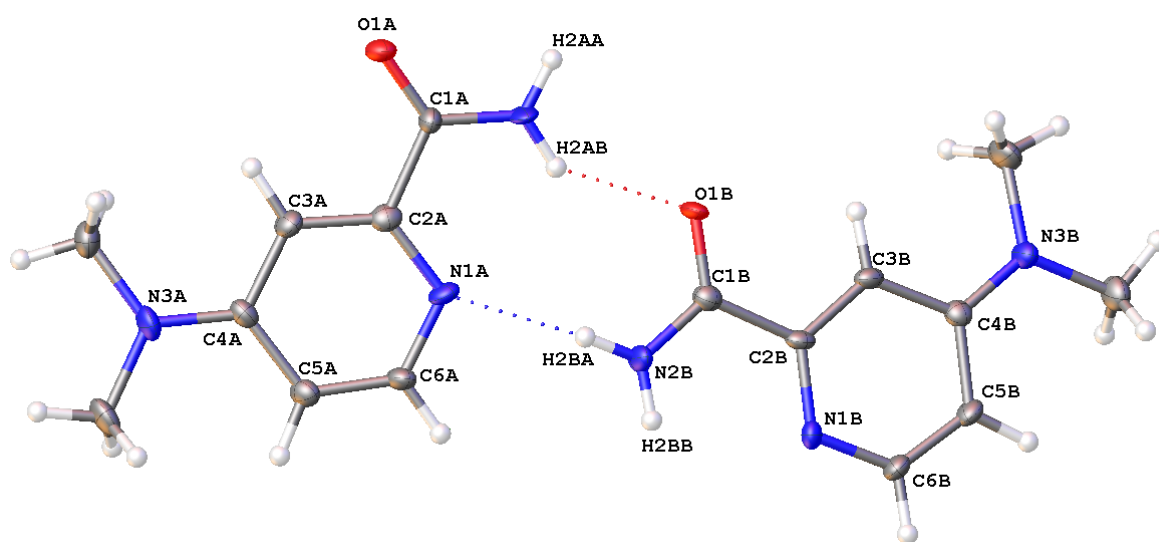


Figure 2 - X-ray molecular structure of two molecules of 4-dimethylamino-pyridinecarboxamide. Thermal ellipsoids are drawn at the 50% probability level.

^{*} C. Sandofry in *The Chemistry of Functional Groups: The Chemistry of the Carbon-Nitrogen Double Bond*, 1970, Interscience Publishers.

[†] J. March in *Advanced Organic Chemistry Fourth Edition*, 1992, Wiley-Interscience.

Appendix 4 – X-Ray Crystallographic Study of 4-Dimethylamino-2-Cyanopyridine

4-Dimethylamino-2-cyanopyridine was prepared as outlined in section 2.7.8. Crystals suitable for an X-ray crystallographic study were grown from a DCM solution at $-30\text{ }^{\circ}\text{C}$. The X-ray molecular structure of 4-dimethylamino-2-cyanopyridine is shown in Figure and selected structural data are shown in Table 1.

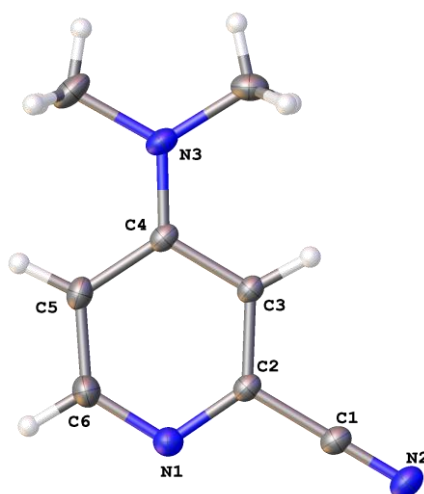


Figure 1 - X-ray molecular structure of 4-dimethylamino-2-cyanopyridine. Thermal ellipsoids are drawn at the 50% probability level.

Bond Distances (Å)		Bond Angles (°)	
C4-C5	1.416	N3-C4-C5	122.17
N3-C4	1.350	C4-C5-C6	119.58
C5-C6	1.378	C5-C6-N1	125.68
C6-N1	1.349	C6-N1-C2	113.68
N1-C2	1.344	N1-C2-C3	126.55
C2-C3	1.381	C2-C3-C4	118.77
C3-C4	1.414	C3-C4-C5	115.74
C2-C1	1.449	N3-C4-C3	122.09
C1-N2	1.153	N2-C1-C2	179.9
C4-C5	1.416	N1-C2-C1	114.69
N3-C4	1.350	C3-C2-C1	118.76

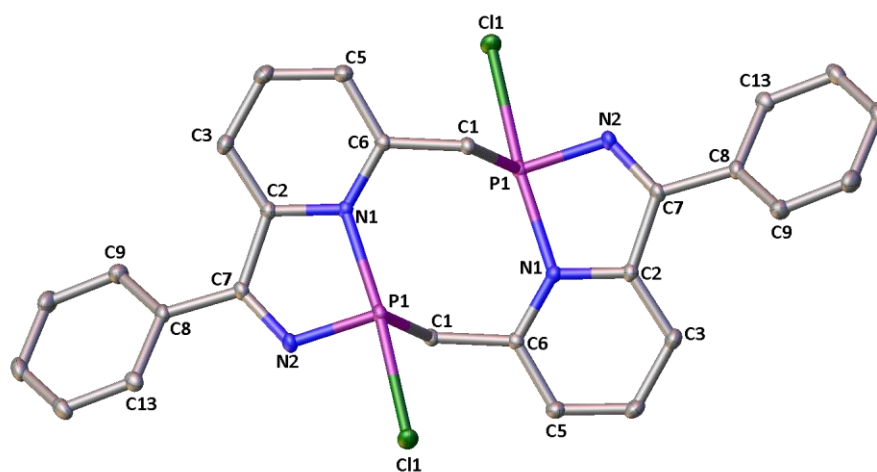
Table 2 - Selected bond length and angle data for 4-dimethylamino-2-cyanopyridine. See Figure 1 for atom labels.

The bond lengths and angles observed for pyridine motif in 4-dimethylamino-2-cyanopyridine are consistent with those observed for pyridine itself,[‡] indicating that this heterocyclic moiety can be regarded as a true pyridine ring. The length of the carbon-nitrogen triple bond of the cyano group is comparable to the average length of a carbon-nitrogen triple bond (1.16 Å).[§]

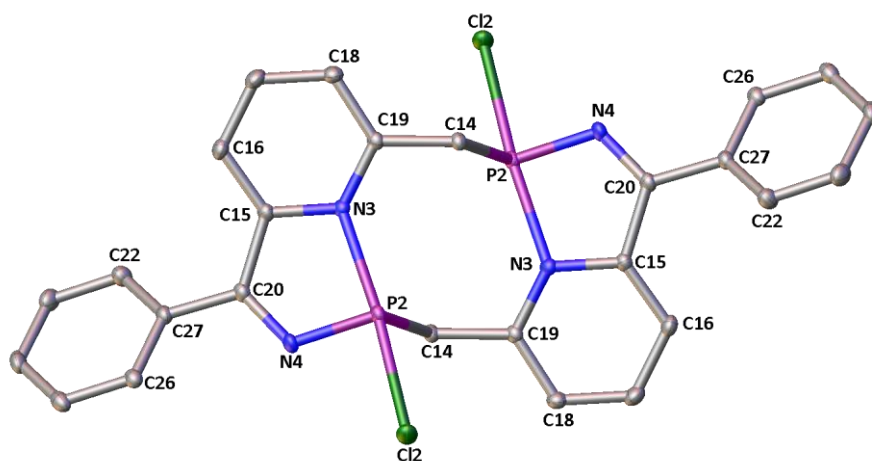
[‡] C. Sandofry in *The Chemistry of Functional Groups: The Chemistry of the Carbon-Nitrogen Double Bond*, 1970, Interscience Publishers.

[§] J. March in *Advanced Organic Chemistry Fourth Edition*, 1992, Wiley-Interscience.

Appendix 5 – Structural Data for the Macrocyclic Pyridyl-*N*-Phosphinoimine, Compound **12**



12.1



12.2

Figure 1 - X-Ray molecular structures of molecules **12.1** and **12.2**, shown separately for clarity. Select atoms have been labelled; hydrogen atoms and solvent molecules have been omitted for clarity. Thermal ellipsoids are drawn at the 50% probability level.

Bond Distances (Å)

12.1		12.2	
C7-C8	1.480(2)	C27-C20	1.480(2)
C7-C2	1.477(2)	C20-C15	1.479(2)
C2-N1	1.352(2)	C15-N3	1.353(2)
N1-C6	1.347(2)	N3-C19	1.349(2)
C6-C1	1.491(2)	C19-C14	1.492(2)
C7-N2	1.291(2)	C20-N4	1.293(2)
N2-P1	1.708(1)	N4-P2	1.712(1)
P1-Cl1	2.3931(5)	P2-Cl2	2.3233(5)
P1-C1	1.878(1)	P2-C14	1.876(1)
N1-P1	2.038(1)	N3-P2	2.109(1)

Table 3 - Selected bond length data for molecules **12.1** and **12.2**. Estimated standard deviations are shown in brackets. See Figure 1 for atom labels.

Bond Angles (°)

12.1		12.2	
C8-C7-C2	123.5(1)	C27-C20-C15	122.1(1)
C8-C7-N2	119.3(1)	C27-C20-N4	119.9(1)
C7-N2-P1	117.8(1)	C20-N4-P2	118.5(1)
N2-P1-Cl1	90.63(5)	N4-P2-Cl2	91.88(5)
N2-P1-C1	98.68(6)	N4-P2-C14	98.69(6)
P1-N1-C2	107.97(9)	P2-N3-C15	106.57(9)
C7-C2-N1	109.7(1)	C20-C15-N3	110.2(1)
C2-N1-C6	121.0(1)	C15-N3-C19	120.7(1)
C6-N1-P1	127.4(1)	C19-N3-P2	128.1(1)
Cl1-P1-C1	89.51(5)	Cl2-P2-C14	90.59(5)
P1-C1-C6	112.5(1)	P2-C14-C19	112.6(1)
N1-C6-C1	117.4(1)	N3-C19-C14	116.9(1)
C9-C8-C7	112.7(1)	C22-C27-C26	119.4(1)
C7-C8-C13	117.9(1)	C20-C27-C26	118.4(1)
C7-C2-C3	128.4(1)	C20-C15-C16	127.7(1)
C5-C6-C1	122.7(1)	C18-C19-C14	123.1(1)
N1-P1-N2	84.74(6)	N3-P2-N4	83.72(6)
N1-P1-C1	93.28(6)	N3-P2-C14	92.39(6)
N1-P1-Cl1	174.91(4)	N3-P2-Cl2	175.01(4)

Table 4 - Selected bond angle data for molecules **12.1** and **12.2**. Estimated standard deviations are shown in brackets. See Figure 1 for atom labels.

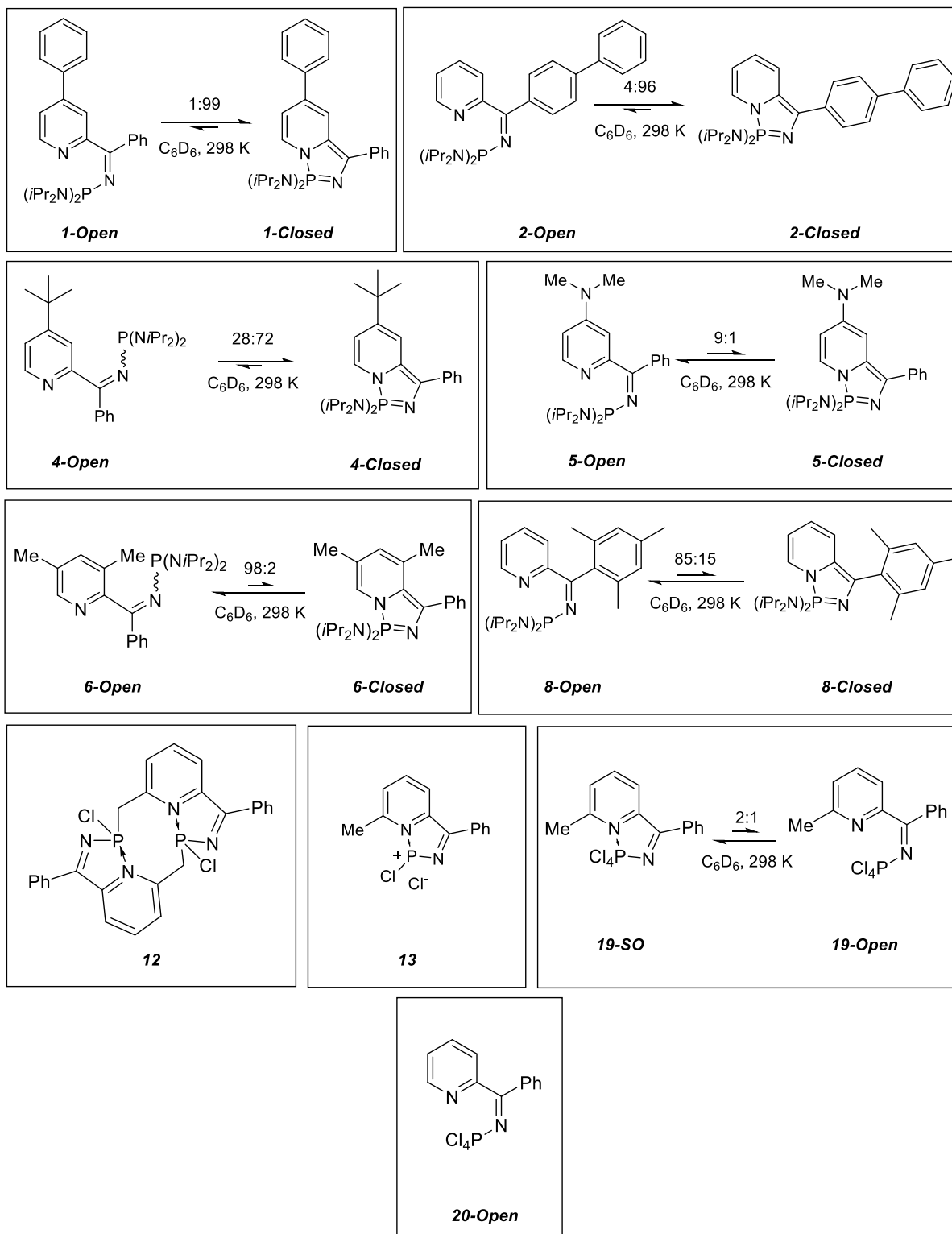
Dihedral Angles (°)

12.1		12.2	
C9-C8···C7-C2	30.6(2)	C22-C27···C20-C15	35.1(2)
P1-Cl···C6-N1	76.3(1)	P2-C14···C19-N3	75.5(1)
N2-P1···C1-C6	162.6(1)	N4-P2···C14-C19	164.3(1)
C7-N2···P1-N1	9.3(1)	N3-P2···N4-C20	10.0(1)
C6-N1···P1-C1	88.8(1)	C14-P2···N3-C19	90.5(1)
C5-C6···C1-P1	103.4(1)	C18-C19···C14-P2	105.3(1)

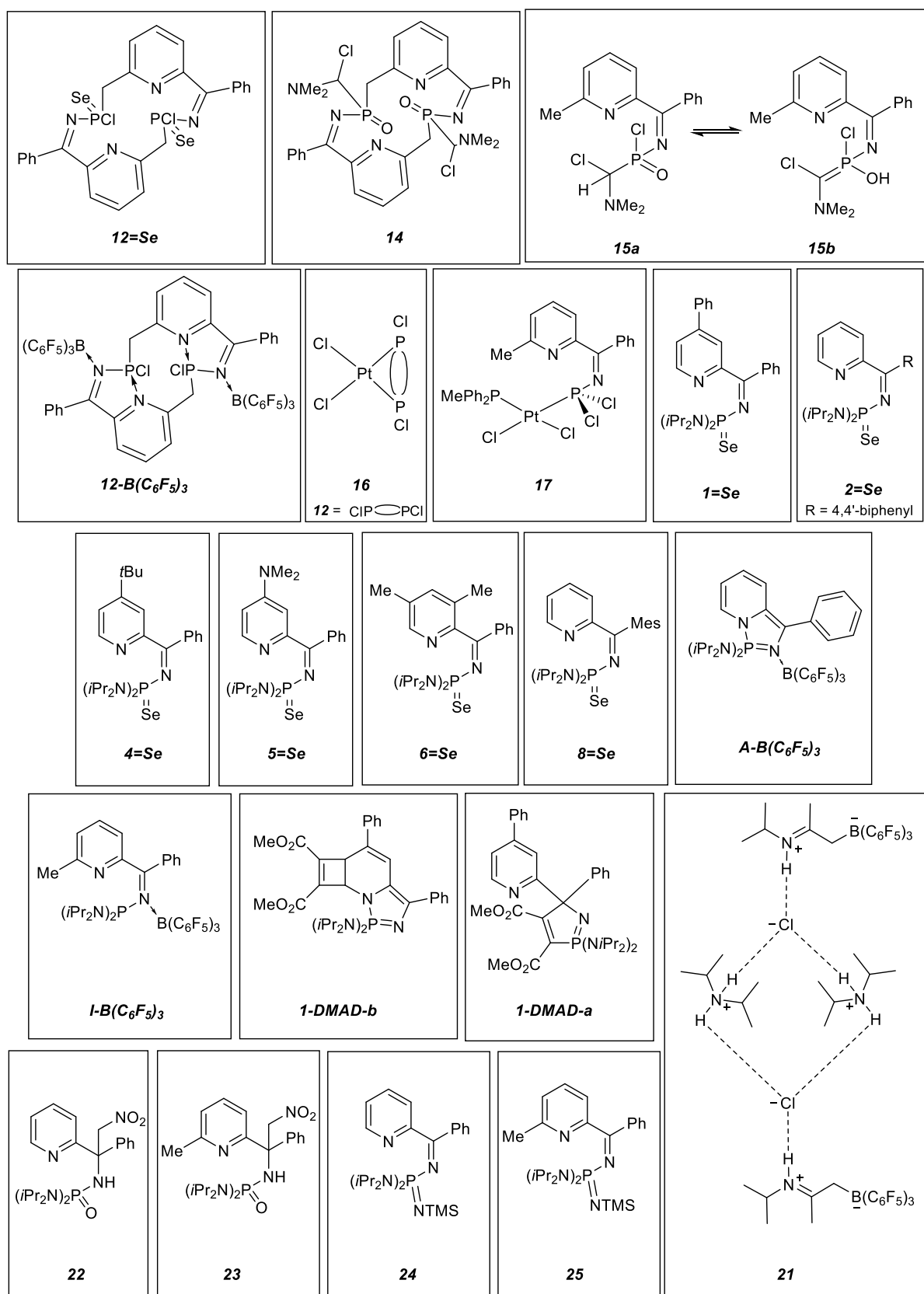
Table 5 - Select dihedral angles for molecules **12.1** and **12.2**. Estimated standard deviations are shown in brackets. See Figure 1 for atom labels.

Appendix 6 – List of Novel Compounds Reported in this Work

A6.1 – Novel Pyridyl-N-Phosphinoimine – Diazaphosphazole Species



A6.2 - Novel Species Prepared from the Reactions the Pyridyl-N-Phosphinoimine - Diazaphosphazole Tautomers with Small Molecules



Appendix 7 - X-Ray Crystallographic Parameters

A7.1 – X-Ray Crystallographic Parameters for Compound 1

Parameter	
Empirical formula	C ₃₀ H ₄₁ N ₄ P
Formula weight	488.64
Temperature/K	120.0
Crystal system	triclinic
Space group	P-1
a/Å	9.3610(6)
b/Å	10.8701(6)
c/Å	13.5108(8)
α/°	98.648(2)
β/°	91.869(2)
γ/°	90.976(2)
Volume/Å ³	1358.10(14)
Z	2
ρ _{calc} /mm ³	1.195
m/mm ⁻¹	0.126
F(000)	528.0
Crystal size/mm ³	0.205 × 0.175 × 0.072
2θ range for data collection	4.494 to 50°
Index ranges	-11 ≤ h ≤ 11, -12 ≤ k ≤ 12, -16 ≤ l ≤ 16
Reflections collected	14945
Independent reflections	4749[R(int) = 0.0689]
Data/restraints/parameters	4749/0/332
Goodness-of-fit on F ²	1.024
Final R indexes [I ≥ 2σ(I)]	R ₁ = 0.0581, wR ₂ = 0.1481
Final R indexes [all data]	R ₁ = 0.0715, wR ₂ = 0.1586
Largest diff. peak/hole / e Å ⁻³	0.39/-0.31

A7.2 – X-Ray Crystallographic Parameters for Compound 2

Parameter	
Empirical formula	C ₃₀ H ₄₁ N ₄ P
Formula weight	488.64
Temperature/K	120
Crystal system	triclinic
Space group	P-1
a/Å	9.5302(3)
b/Å	11.0544(4)
c/Å	13.8558(5)
α/°	88.3900(15)
β/°	70.2419(14)
γ/°	84.0851(14)
Volume/Å ³	1366.43(8)
Z	2
ρ _{calc} /cm ³	1.188
μ/mm ⁻¹	0.126
F(000)	528.0
Crystal size/mm ³	0.332 × 0.243 × 0.106
Radiation	MoKα (λ = 0.71073)
2θ range for data collection/°	4.564 to 60.186
Index ranges	-13 ≤ h ≤ 13, -15 ≤ k ≤ 15, -18 ≤ l ≤ 19
Reflections collected	25700
Independent reflections	8051 [R _{int} = 0.0346, R _{sigma} = 0.0464]
Data/restraints/parameters	8051/0/332
Goodness-of-fit on F ²	1.021
Final R indexes [I ≥ 2σ (I)]	R ₁ = 0.0466, wR ₂ = 0.1118
Final R indexes [all data]	R ₁ = 0.0724, wR ₂ = 0.1232
Largest diff. peak/hole / e Å ⁻³	0.47/-0.34

A7.3 – X-Ray Crystallographic Parameters for Compound 4

Parameter	
Empirical formula	C ₂₇ H ₄₃ N ₄ P
Formula weight	454.62
Temperature/K	120
Crystal system	monoclinic
Space group	C2/c
a/Å	24.8627(11)
b/Å	9.2747(4)
c/Å	25.1947(11)
α/°	90
β/°	110.6439(15)
γ/°	90
Volume/Å ³	5436.7(4)
Z	8
ρ _{calc} /cm ³	1.111
μ/mm ⁻¹	0.122
F(000)	1984.0
Crystal size/mm ³	0.238 × 0.235 × 0.218
Radiation	MoKα (λ = 0.71073)
2θ range for data collection/°	4.728 to 60.312
Index ranges	-35 ≤ h ≤ 34, -13 ≤ k ≤ 13, -35 ≤ l ≤ 35
Reflections collected	58568
Independent reflections	8027 [R _{int} = 0.0460, R _{sigma} = 0.0316]
Data/restraints/parameters	8027/0/320
Goodness-of-fit on F ²	1.049
Final R indexes [I >= 2σ (I)]	R ₁ = 0.0430, wR ₂ = 0.1035
Final R indexes [all data]	R ₁ = 0.0588, wR ₂ = 0.1110
Largest diff. peak/hole / e Å ⁻³	0.44/-0.34

A7.4 – X-Ray Crystallographic Parameters for Compound 12

Parameter	
Empirical formula	C ₃₀ H ₃₀ Cl ₂ N ₄ O ₂ P ₂
Formula weight	611.42
Temperature/K	120
Crystal system	monoclinic
Space group	P2 ₁ /n
a/Å	8.5770(6)
b/Å	18.4771(13)
c/Å	17.9413(13)
α/°	90
β/°	100.438(2)
γ/°	90
Volume/Å ³	2796.3(3)
Z	4
ρ _{calc} /cm ³	1.452
μ/mm ⁻¹	0.384
F(000)	1272.0
Crystal size/mm ³	0.364 × 0.268 × 0.086
Radiation	MoKα (λ = 0.71073)
2θ range for data collection/°	4.618 to 60
Index ranges	-12 ≤ h ≤ 12, -25 ≤ k ≤ 25, -25 ≤ l ≤ 25
Reflections collected	60245
Independent reflections	8128 [R _{int} = 0.0361, R _{sigma} = 0.0230]
Data/restraints/parameters	8128/6/387
Goodness-of-fit on F ²	1.071
Final R indexes [I >= 2σ (I)]	R ₁ = 0.0390, wR ₂ = 0.1035
Final R indexes [all data]	R ₁ = 0.0500, wR ₂ = 0.1103
Largest diff. peak/hole / e Å ⁻³	0.55/-0.29

A7.5 – X-Ray Crystallographic Parameters for Compound 21

Parameter	
Empirical formula	C ₃₆ H ₃₅ BClF ₁₅ N ₂
Formula weight	826.92
Temperature/K	120.0
Crystal system	triclinic
Space group	P-1
a/Å	11.8076(11)
b/Å	11.9474(11)
c/Å	13.6967(13)
α/°	93.264(4)
β/°	99.151(4)
γ/°	99.959(4)
Volume/Å ³	1871.8(3)
Z	2
ρ _{calc} /cm ³	1.467
μ/mm ⁻¹	0.206
F(000)	844.0
Crystal size/mm ³	0.4 × 0.36 × 0.15
Radiation	MoKα (λ = 0.71073)
2θ range for data collection/°	4.404 to 57.998
Index ranges	-16 ≤ h ≤ 16, -16 ≤ k ≤ 16, -18 ≤ l ≤ 18
Reflections collected	39004
Independent reflections	9954 [R _{int} = 0.0510, R _{sigma} = 0.0524]
Data/restraints/parameters	9954/0/609
Goodness-of-fit on F ²	1.007
Final R indexes [I >= 2σ (I)]	R ₁ = 0.0486, wR ₂ = 0.1020
Final R indexes [all data]	R ₁ = 0.0816, wR ₂ = 0.1152
Largest diff. peak/hole / e Å ⁻³	0.41/-0.42

A7.6 – X-Ray Crystallographic Parameters for 4-Dimethylamino-2-Pyridinecarboxamide

Parameter	
Empirical formula	C ₈ H ₁₁ N ₃ O
Formula weight	165.20
Temperature/K	120
Crystal system	monoclinic
Space group	P2 ₁ /n
a/Å	7.6315(5)
b/Å	16.9683(10)
c/Å	26.1099(16)
α/°	90
β/°	91.747(2)
γ/°	90
Volume/Å ³	3379.5(4)
Z	16
ρ _{calc} /cm ³	1.299
μ/mm ⁻¹	0.090
F(000)	1408.0
Crystal size/mm ³	0.159 × 0.141 × 0.058
Radiation	MoKα (λ = 0.71073)
2θ range for data collection/°	3.938 to 50.154
Index ranges	-9 ≤ h ≤ 9, -20 ≤ k ≤ 20, -31 ≤ l ≤ 31
Reflections collected	42270
Independent reflections	5976 [R _{int} = 0.0764, R _{sigma} = 0.0588]
Data/restraints/parameters	5976/0/449
Goodness-of-fit on F ²	1.076
Final R indexes [I >= 2σ (I)]	R ₁ = 0.0790, wR ₂ = 0.1854
Final R indexes [all data]	R ₁ = 0.1414, wR ₂ = 0.2137
Largest diff. peak/hole / e Å ⁻³	0.59/-0.38

A7.7 – X-Ray Crystallographic Parameters for 4-Dimethylamino-2-Cyanopyridine

Parameter	
Empirical formula	C ₈ H ₉ N ₃
Formula weight	147.18
Temperature/K	120
Crystal system	orthorhombic
Space group	Pnma
a/Å	10.5874(4)
b/Å	6.6852(3)
c/Å	10.9744(4)
α/°	90
β/°	90
γ/°	90
Volume/Å ³	776.76(5)
Z	4
ρ _{calc} /cm ³	1.259
μ/mm ⁻¹	0.081
F(000)	312.0
Crystal size/mm ³	0.439 × 0.31 × 0.194
Radiation	MoKα (λ = 0.71073)
2θ range for data collection/°	5.346 to 65.56
Index ranges	-16 ≤ h ≤ 16, -10 ≤ k ≤ 10, -16 ≤ l ≤ 16
Reflections collected	18939
Independent reflections	1542 [R _{int} = 0.0326, R _{sigma} = 0.0170]
Data/restraints/parameters	1542/0/81
Goodness-of-fit on F ²	1.077
Final R indexes [I ≥ 2σ (I)]	R ₁ = 0.0428, wR ₂ = 0.1266
Final R indexes [all data]	R ₁ = 0.0506, wR ₂ = 0.1331
Largest diff. peak/hole / e Å ⁻³	0.45/-0.30

Appendix 8 – Seminars, Conferences and Symposia Attended

A8.1 - Seminars Attended

Date	Speaker	Institution	Seminar Title
22 nd January 2014	Dr Maria Paz Munoz- Herranz	University of East Anglia	Different Metals = Different Products: Gold versus Platinum in the Reaction of Allenenes with Nucleophiles
12 th February 2014	Professor Guy Lloyd- Jones	University of Edinburgh	Cats and Dogma
19 th February 2014	Professor Polly Arnold	University of Edinburgh	Redox and Functionalisation Reactions of the Uranyl Ion; in Pursuit of Transition Metal Oxo Chemistry
14 th April 2014	Professor Christopher Cummins	Massachusetts Institute of Technology	Group 15 Element Triple Bonds and Reactive Intermediates (RSC Ludwig Mond Award Lecture)
24 th April 2014	Dr Rebecca Melen	University of Toronto	Activation of Alkynes with B(C ₆ F ₅) ₃ : Intramolecular Cyclisation Reaction and Rearrangements (RSC Dalton Young Researcher Award Lecture)

Appendix 8 – Seminars and Conferences Attended

16 th May 2014	Professor Robert Grubbs	California Institute of Technology	Controlled Polymer Synthesis with Olefin Metathesis Catalysts
27 th July 2014	Professor Ken Waugh	Emeritus Professor, University of Manchester	The Physical Chemistry of Heterogeneous Catalysis – The Oxidation of Ethylene to Ethylene Oxide
24 th September 2014	Professor Rob Tooze	Sasol Technology UK	Catalysis on the Edge
24 th September 2014	Professor Graham Sandford	Durham University	Durham Fluorine Meets Industry
24 th September 2014	Dr Simon Beaumont	Durham University	Nanoparticles and in situ Spectroscopy for Understanding Syngas Conversion Catalysis
24 th September 2014	Professor David Cole-Hamilton	University of St Andrews	Chemicals from Waste Bio-Oils
15 th December 2015	Professor Catherine Housecroft	University of Basel	From Wadean Clusters to Functional Materials
15 th December 2014	Dr Andrew Hughes	Durham University	Bond Length and Bond Enthalpy Relationships in Metal Carbonyl Clusters

Appendix 8 – Seminars and Conferences Attended

15 th December 2014	Professor Michael Mingos	Oxford University	Bonding in Gold Clusters
15 th December 2014	Dr Alan Welch	Herriot-Watt University	Recent Aspects of the Structural Chemistry of Heterocarboranes
15 th December 2014	Professor Robert Mulvey	University of Strathclyde	Structural Rules for Boron
13 th January 2015	Professor Declan Gilheany	University College Dublin	Useful New Reactions in Organophosphorus Chemistry
28 th January 2015	Professor Chris Hardacre	Queen's University Belfast	Development of In-Situ Methods to Study Gas and Ligand Phase Heterogeneously Catalysed Reactions
24 th February 2015	Dr Christian Bruneau	Université de Rennes	Ruthenium and Iridium Catalysts Equipped with a Phosphinesulfate Ligand Overview of Research: Carbon
19 th May 2015	Professor James Tour	Rice University	Materials, Devices, Medicine and Nanocars
20 th May 2015	Professor James Tour	Rice University	Graphene
21 st May 2015	Professor James Tour	Rice University	Nanomedicines for Stroke, Traumatic Brain Injury, Autoimmune Diseases and Drug Delivery

Appendix 8 – Seminars and Conferences Attended

4 th November 2015	John Hayler	GSK	Sustainability in Industrial Chemistry
4 th November 2015	Katherine Wheelhouse	GSK	Transition Metal Catalysis
4 th November 2015	Keith Mulholland	Astra Zeneca	Biocatalysis
4 th November 2015	Jeroen ten Dam	Johnson Matthey	Biorenewable Feedstocks and Chemicals
5 th November 2015	Helen Sneddon	GSK	Sustainability, Green Chemistry, Solvent Guide
5 th November 2015	George Hodges	Syngenta	Sustainable Agrochemical Manufacturing
5 th November 2015	Matt Grist	Astra Zeneca	Sustainability in Research and Development
18 th November 2015	Eva Hevia	University of Strathclyde	New Main Group Metal Mediated Strategies for Ring Functionalisation
27 January 2016	Patrick McGowan	University of Leeds	Using organometallics as catalysts: from drug precursors to little black dresses
1 st February 2015	Todd Marder	Julius-Maximilians- Universität Würzburg	RSC Organometallic Chemistry Award - Transition Metal Catalyzed Borylation of C-H

Appendix 8 – Seminars and Conferences Attended

			and C-X Bonds: Synthesis of Aryl and Alkyl Boronates
17 February 2016	Pat Guiry,	University College Dublin	Recent Developments in Asymmetric Catalysis and Total Synthesis
11 April 2016	Prof Yi Lu	University of Illinois	RSC Applied Inorganic Chemistry Award
18 th May 2016	Steven Ley	University of Cambridge	Challenges and Opportunities in Natural Product Synthesis
18 th November 2016	Dominikus Heift	Durham University	PG Seminar Series - Inorganic Chemistry
23 November 2016	Dr Ai-Lan Lee	Heriot Watt University	Development of gold and palladium catalysed reactions
25 January 2017	Richard Winpenny	University of Manchester	RSC Ludwig Mond Award Lecture

A8.2 - Conferences and Symposia Attended

Date(s)	Meeting Title	Location	Participation
15 th – 17 th April 2014	Dalton 2014	Warwick University	Attendee
24 th September 2014	CSCP Half-Day Symposium	Durham University	Attendee
15 th December 2014	Ken Wade Celebration Symposium	Durham University	Attendee
11 th September 2015	RSC Main Group Meeting	Burlington House	Poster Presentation
4 th – 5 th November 2015	Sustainability in Industrial Chemistry Symposium and Workshop	Durham University	Poster Presentation
7 th – 9 th March 2016	13 th European Workshop on Phosphorus Chemistry	The Freie Universität Berlin	Poster Presentation
9 th -10 th March 2016	2 nd International Conference on Sustainable Phosphorus Chemistry	The Freie Universität Berlin	Attendee
15 th June 2016	Postgraduate Gala Symposium 2016	Durham University	Oral Presentation
23 rd – 24 th June 2016	4 th Early Career Symposium	University of Strathclyde	Oral Presentation